

Development-dependent changes in the synaptic proteome

Dissertation

zur Erlangung des akademischen Grades

**doctor rerum naturalium
(Dr. rer. nat.)**

genehmigt durch die Fakultät für Naturwissenschaften
der Otto-von-Guericke-Universität Magdeburg

von M.Sc. Elmer Antileo Ibarra

geb. am 28.01.1981 in Nacimiento, Chile

Gutachter: Prof. Dr. rer. nat. Daniela C. Dieterich

Prof. Dr. rer. nat., Dr. med. Sven Meuth

eingereicht am: 22.09.2016

verteidigt am: 23.05.2017

**Development-dependent changes in the synaptic
proteome**

Dissertation

**Der Fakultät für Naturwissenschaften
der Otto-von-Guericke-Universität Magdeburg
zur Erlangung des akademischen Grades**

**Doctor rerum naturalium
(Dr. rer. nat.)**

vorgelegt von: M.Sc. Elmer Antileo Ibarra

Acknowledgement

This thesis work was carried out during the years 2009-2015 at the Leibniz Institute for Neurobiology (LIN) and Institute for Pharmacology and Toxicology (IPT), Magdeburg, Germany.

First, I would like to express my gratitude to Prof. Dr. Daniela Dieterich for the opportunity to do my doctoral thesis under her supervision and constant support during my Ph.D. thesis.

I would like also to thank Dr. Peter Landgraf, my second supervisor at IPT, for his guidance in the lab and encouraging discussions, especially during my thesis writing.

Many thanks also to Prof. Eckart D Gundelfinger for employed me as a Ph.D. student and support my scientific career.

Thanks to my colleagues Anne, Paula, Anke, Ines, Julia, José, Kathrin, Nicole, Regina, Laura, and Karina for a great time, I had with them at coffee klatches, experiment discussion, and nice atmosphere in the lab.

I would like to thank Anke Müller, Kathrin Marter, Vesna Lazarevic and Artur Bikbaev for reviewing my thesis and giving valuable suggestions.

Many thanks to Dr. Rainer Pielot, Dr. Thilo Kähne, and Yvonne Ducho for their help in my proteomic analysis.

Thanks to all my friends and former colleagues from the LIN (Stefano, Stefan, Juan Carlos, Jeet, Jose, Maru, Carolina, Nicole, Sujoy, Rahul, Paramesh, Gilbert, Chris, Rodrigo, Diana, Torsten, Daniela, and Claudia) for the nice time that we spend together.

Many thanks to Dr. Werner Zuschratter, Oliver Kobler, and Dr. Ulrich Thomas, for introducing us the high-resolution imaging and image analysis.

I would like to thank Dr. Karl-Heinz Smalla for the introduction in the subcellular fractionation and his friendly attitude towards foreign people.

I am particularly grateful to Evi for the positive and friendly atmosphere she creates while working next to her, but also for taking care of our everyday lab work. Many thanks to my former colleagues from the LIN: Kathi, Heidi, Sabine, Moni, Corina, Janina, Kathrin and Stefi for their technical support in the lab work while I was working at the LIN.

Finally, I would like to thank my family and friends for their love and support they constantly give me, I am very grateful. Muchas Gracias!

TABLE OF CONTENTS

1. INTRODUCTION	1
1.1. Decentralization of gene expression	2
1.1.1. Control of dendritic protein translation	3
1.1.2. Dendritic protein synthesis and synaptic function	5
1.1.3. Local protein synthesis in axons	7
1.2. Visualization of protein synthesis in neuronal compartments	9
1.3. Neuroproteomics of the synapse	12
1.3.1. Targeting of proteins to pre and postsynaptic sites	13
1.4. Proteome profiling	15
1.4.1. Bio-Orthogonal Non-Canonical Amino acid Tagging (BONCAT)	16
1.4.2. BONCAT applied to cellular systems	18
1.4.3. FUNCAT applied to visualize <i>de novo</i> protein synthesis	19
1.5. Cell-selective metabolic labeling	19
1.6. Objectives	22
2. MATERIALS AND METHODS	23
2.1. Materials and production of materials	23
2.1.1. Chemicals	23
2.1.2. Enzymes	23
2.1.3. Primers and plasmid constructs	23
2.1.3.1. pSDTMetRS expression construct	23
2.1.3.2. Axonal targeting expression constructs	24
2.1.4. Antibodies used for IB and IF	25
2.1.5. Common buffers and cell culture media	26
2.1.6. Prokaryotic and eukaryotic cell lines	26
2.1.7. Animals	26
2.2. Methods	27
2.2.1. Neuronal primary cultures	27
2.2.2. Metabolic labeling of newly synthesized proteins	27

2.2.3. Cell lysis	28
2.2.4. Reduction and alkylation	28
2.2.5. Click Chemistry	28
2.2.5.1. BONCAT–Bio-Orthogonal Non-Canonical Amino acid Tagging	28
2.2.5.2. NeutrAvidin purification	29
2.2.6. Sample preparation for mass spectrometry	29
2.2.7. Mass spectrometry	29
2.2.8. FUNCAT–Fluorescent Non-Canonical Amino acid Tagging	30
2.2.8.1. FUNCAT of cultured hippocampal neurons	30
2.2.9. Transfection	31
2.2.9.1. Calcium phosphate transfection of HEK293T cells	31
2.2.9.2. Transfection of hippocampal neurons and immunocytochemistry	31
2.2.10. Ribosomal Immunolocalization	32
2.2.10.1. Image acquisition, 3D reconstructions, and distance measurement	32
2.2.11. Subcellular fractionation and synaptosomes isolation	33
2.2.12. Immunoblotting	33
2.2.13. Gene Ontology	34
3. RESULTS	35
3.1. Development-dependent expression of translation machinery components in primary hippocampal neurons	35
3.2. Analysis of the newly synthesized proteins in dendrites of primary hippocampal cultures	40
3.2.1. Analysis of newly synthesized proteins in synaptic areas of primary hippocampal neurons	43
3.3. Targeting of MetRS to postsynaptic densities	45
3.3.1. Cell-selective metabolic labeling of newly synthesized postsynaptic proteins	47
3.3.2. Visualization of newly synthesized proteins at postsynaptic terminals	49
3.4. Targeting of MetRS to presynaptic terminals	51
3.4.1. Cell-selective metabolic labeling of newly synthesized proteins	56

3.4.2. Visualization of newly synthesized proteins at presynaptic terminals	57
3.5. Isolation and characterization of synaptic structures from primary cortical cultures	60
3.6. Developmental changes in the synaptic proteome of synaptosomes	63
3.6.1. Metabolic labeling of newly synthesized proteins in neuronal cultures using BONCAT	63
3.6.2. Identification of newly synthesized proteins in synaptosomes	64
3.7. Gene Ontology analysis of the identified newly synthesized proteins in synaptosomes from primary cortical neuron cultures	69
3.8. Fluorescent <i>In Situ</i> Hybridization detection of mRNA transcripts the candidate proteins	76
4. DISCUSSION	82
4.1. Developmental expression and subcellular localization of translation machinery components in neuronal compartments	82
4.2. Visualization and quantification of newly synthesized proteins in dendrites and synaptic areas using FUNCAT technique	84
4.3. Visualization of newly synthesized proteins at pre and postsynaptic sites	86
4.4. Identification of <i>de novo</i> synthesized synaptic proteomes during development	90
4.4.1. Synaptosome fractionation	90
4.4.2. Developmental-dependent changes in the <i>de novo</i> synthesized synaptic proteomes	92
5. OUTLOOK	96
6. LITERATURE	98
7. APPENDIX	136
8. ABBREVIATIONS	162
9. CURRICULUM VITAE	165
10. SCIENTIFIC PUBLICATIONS	166

Figures and Tables

Figure 1. Decentralization of gene expression in neurons.	3
Figure 2. Distribution of the translation machinery along dendritic domains.	4
Figure 3. Local protein synthesis and synaptic function.	6
Figure 4. Local protein synthesis in axonal domains.	8
Figure 5. Visualization of dendritic protein synthesis using a protein synthesis GFP-based reporter.	11
Figure 6. Chemical reagents and overview of BONCAT and FUNCAT technique.	17
Figure 7. Cell-selective protein labeling using mutant MetRS.	21
Figure 8. Development-dependent distribution of ribosomes in dendrites of hippocampal neurons.	36
Figure 9. Distribution of translation machinery components in primary hippocampal neurons (DIV11).	39
Figure 10. BDNF increases protein synthesis, levels of ribosomes and the number of synapsin-positive puncta in dendrites of hippocampal neurons.	42
Figure 11. ProSAP1/Shank2 targeting sequence leads to increased MetRS-GFP–fusion protein localization at postsynaptic areas.	46
Figure 12. Cell-selective incorporation of ANL into newly synthesized proteins.	48
Figure 13. Metabolic labeling of newly synthesized proteins at postsynaptic areas using the FUNCAT method.	51
Figure 14. LtoGMetRS-GFP expression using Cod-H as a targeting sequence cloned in the pEGFP-C1 vector.	52
Figure 15. LtoGMetRS-GFP expression using ORFTau and Cod-H as targeting sequences cloned in the pEGFP-C1 vector.	53

Figure 16. LtoGMetRS expression using ORFTau and Cod-H as targeting sequences cloned in the pCMV vector.	54
Figure 17. Axon-like expression of the fusion protein using ORFTau and Cod-H as targeting sequences cloned in the pcDNA vector.	55
Figure 18. Long-term expression of the fusion protein in a neuron expressing the pORFTau-Cod-H construct.	56
Figure 19. ANL incorporation into newly synthesized proteins using the pLtoGMetRS-ORFTau-Cod-H construct.	57
Figure 20. Axon-like expression of the fusion protein is lost after LtoGMetRS incorporation into the pORFTau-Cod-H construct.	58
Figure 21. Metabolic labeling of newly synthesized proteins at presynaptic terminals using FUNCAT.	60
Figure 22. Subcellular fractionation procedure for the enrichment of synaptic structures.	61
Figure 23. Protein enrichment in neuronal fractions isolated from primary cortical neuron cultures.	62
Figure 24. Metabolic labeling of newly synthesized proteins in primary cortical neurons.	64
Figure 25. Detection, purification, and identification of newly synthesized proteins in synaptosomes.	65
Figure 26. Metabolic labeling of newly synthesized proteins in synaptosomes from primary cortical neuron cultures.	66
Figure 27. Gene Ontology analysis of the identified newly synthesized proteins in synaptosomes from primary cortical neuron cultures.	70
Figure 28. Development-dependent protein enrichment.	72
Figure 29. Enrichment analyses of over-represented annotations (GO terms) from the biological process domain.	74
Figure 30. Biochemical analysis of selected candidate proteins in synaptosomes during development.	75
Figure 31. NR1 mRNA detection by FISH.	77
Figure 32. Erc2 mRNA detection by FISH.	79
Figure 33. Piccolo mRNA detection by FISH.	81

Table 1. Enzymes and buffers.	23
Table 2. List of primary antibodies, including applications and dilutions.	25
Table 3. List of secondary antibodies, including applications and dilutions.	26
Table 4. Summary of the newly synthesized synaptic proteome	68
Table 5. Long-lived protein	68
Table 6. GO term example, including gene names of identified newly synthesized proteins for each developmental stage.	71
Supplementary Scheme 1.	140
Supplementary Figure S1.	136
Supplementary Figure S2.	137
Supplementary Figure S3.	137
Supplementary Figure S4.	138
Supplementary Figure S5.	139
Supplementary Figure S6.	139
Supplementary Table 1.	141
Supplementary Table 2.	141
Supplementary Table 3.	142
Supplementary Table 4.	143
Supplementary Table 5.	143
Supplementary Table 6.	144
Supplementary Table 7.	147
Supplementary Table 8.	150
Supplementary Table 9.	154
Supplementary Table 10.	158
Supplementary Table 11.	159
Supplementary Table 12.	160
Supplementary Table 13.	161

SUMMARY

Synapses are functional contacts between neurons that mediate the integration of neurotransmission in the nervous system. The establishment of synaptic contacts during brain development, a process also known as synaptogenesis, as well as long-lasting forms of synaptic plasticity is characterized by dynamic changes of the neuronal proteome. Apart from post-translational modifications and protein degradation, the synthesis of new proteins plays a vital role in synaptic function. The discovery of translation machinery components and mRNAs in distal neuronal compartments demonstrate that neurons are capable of synthesizing proteins not only in the soma but also locally in distal parts of their dendrites and axons. This feature allows the regulation of protein translation in response to local demand and the conversion of new experience into structural and functional changes. Despite the growing amount of evidence demonstrating that local translation plays an essential role in synaptic function and plasticity, the functional role that local protein synthesis plays during brain development remains unclear.

In this study, we studied the developmental expression and subcellular localization of different components of the translation machinery in dendrites and axons. Biochemical analysis of isolated synaptosomal fractions suggests that the recruitment of the translation machinery and synaptic components to synapses starts early during development. In a related approach, we examined the levels of newly synthesized proteins in dendrites and synaptic areas using fluorescent non-canonical amino acid tagging, also known as FUNCAT. Similarly, we applied this technique also to visualize newly synthesized proteins within the pre and postsynaptic terminals.

To obtain a comprehensive representation of the temporal and spatial characteristics of the synaptic proteome, we examined the *de novo* synthesized proteomes in isolated synaptosomes prepared from primary cortical cultures at different developmental stages. For the detection, enrichment, and identification of the newly synthesized synaptic proteins, we used the recently developed bio-orthogonal non-canonical amino acid tagging technology (BONCAT), followed by affinity purification and two-dimensional

mass spectrometry. A significant number of proteins were associated with synaptic localization as derived from Synprot, a comprehensive synaptic protein database, and validated using a neuropil transcriptome database. The identified newly synthesized proteomes were organized for biological interpretation in the context of the Gene Ontology (GO), revealing significant changes in the protein content encompassing different GO categories throughout development, from where candidate proteins were selected. Taken together, our results indicate that local protein synthesis in neurons is not restricted to late developmental stages but also might play a crucial role on the molecular changes in the synaptic proteome relevant for synapse formation, organization, and function during early stages of neuronal development.

ZUSAMMENFASSUNG

Synapsen sind die Hauptmediatoren der neuronalen Kommunikation in Nervensystemen. Ihre Bildung während der Gehirnentwicklung, ein Prozess, der als Synaptogenese bezeichnet wird, als auch lang anhaltende Formen von synaptischer Plastizität sind durch dynamische Änderungen des neuronalen Proteoms gekennzeichnet. Abgesehen von posttranslationalen Modifikationen und Proteinabbau, spielt die Synthese neuer Proteine eine wichtige Rolle für die synaptische Funktion. Interessanterweise sind Neuronen in der Lage Proteine nicht nur im Soma zu synthetisieren, sondern auch lokal in distalen Teilen ihrer Dendriten. Die Durchführbarkeit der lokalen Proteinsynthese wird durch beides, das Vorhandensein von Bestandteilen der Translationsmaschinerie und mRNA in distalen neuronalen Kompartimenten, realisiert. Dieser Mechanismus erlaubt die Regulation der Proteintranslation als Reaktion auf die lokale Nachfrage und ermöglicht, dass neue Erfahrungen in strukturelle und funktionale Änderungen konvertiert werden.

Trotz der steigenden Anzahl an Beweisen, dass lokale Translation eines der Schlüsselereignisse für diese Prozesse darstellt, ist unklar, ob lokale Proteinsynthese in Neuronen eine funktionale Rolle während der Hirnentwicklung spielt. In dieser Studie untersuchen wir die entwicklungsbedingte Expression und subzelluläre Lokalisation von verschiedenen Komponenten der Translationsmaschinerie in Dendriten und Axonen. Biochemische Analysen von Fraktionen, die für synaptische Strukturen angereichert wurden, weisen darauf hin, dass die Rekrutierung der Translationsmaschinerie und synaptischen Komponenten in die Synapsen frühzeitig in der Entwicklung beginnt. In einer begleitenden Vorgehensweise wurde die translationale Kapazität von Dendriten und Synapsen mittels FUNCAT (**f**luorescent **n**on-**c**anonical **a**mino **a**cid **t**agging) untersucht. Zielsysteme werden mit zellselektiver metabolischer Markierung kombiniert, um frisch synthetisierte Proteine an prä- und postsynaptischen Terminalen kenntlich zu machen.

Um diesen Aspekt genauer zu analysieren, identifizierten wir akut synthetisierte Proteine in isolierten Synaptosomen, die aus primären Hippokampuskulturen unterschiedlicher Entwicklungsstadien angefertigt wurden. Für diese biochemischen Analysen von *de-novo*-synthetisierten Proteomen verwendeten wir die kürzlich entwickelte BONCAT-Technologie (**bioorthogonal non-canonical amino acid tagging**), gefolgt von Affinitätsreinigung und zweidimensionaler Massenspektrometrie. Dabei identifizierte Proteome liefern ein umfassendes Bild über die zeitlichen und räumlichen Eigenschaften der synaptischen Proteome. Die identifizierten Proteome enthalten Gerüstmoleküle, Adhäsionsmoleküle, prä- und postsynaptische Proteine, metabotrope und ionotrope Rezeptoren, synaptische Vesikelproteine, Komponenten der Proteinsynthese und Abbaumaschinerie, Signalmoleküle sowie Zytoskelettproteine. Diese Proteine wurden der synaptischen Lokalisierung zugeordnet, wie aus Synprot, einer umfassenden Datenbank synaptischer Proteine, abgeleitet wurde, und durch Verwendung einer Neuropil-Transkriptom-Datenbank bestätigt. Die identifizierten kürzlich synthetisierten Proteine wurden zur biologischen Interpretation im Kontext von Gene Ontology (GO) organisiert. Vergleichsanalysen zwischen Proteomen zeigten signifikante Veränderungen im Proteingehalt in verschiedenen GO-Kategorien (biologische Prozesse, Zellkompartimente und molekulare Funktion) während der Entwicklung, woraus Kandidatenproteine ausgewählt wurden. Unsere Ergebnisse weisen klar darauf hin, dass lokale Proteinsynthese in Neuronen nicht auf späte Entwicklungsstadien beschränkt ist, sondern auch an komplexen Veränderungen von Proteomen, welche für die Synapsenbildung und -funktion während der frühen Gehirnentwicklung von Bedeutung sind, beteiligt ist.

1. INTRODUCTION

Human brain development is a complex process resulting in an elaborate network of several hundreds of billions of neurons in the mature brain. This extraordinary network of neurons communicates with each other via specialized adhesive junction known as synapses (Whittaker, 1968; Pereda, 2014; Harris and Weinberg, 2012). Each synapse, in particular, the chemical synapse, is a functional contact between neuronal processes, composed of a presynaptic bouton that communicates with a postsynaptic terminal in a highly structured manner (Harris, 2008; Garner and Shen, 2008; Harris and Weinberg, 2012). Synaptic communication between neurons leads to the establishment of functional neural networks that mediate sensory and motor processing, underlying complex behavioral phenomena and cognition (Laughlin and Sejnowski, 2003; Bargmann, 2012; Triller and Sheng, 2012). Dysfunction and inappropriate synapse formation are thought to underlie several developmental neuropathies (Grant, 2012; Malinow, 2012; Triller and Sheng, 2012; Verpelli and Sala, 2012). Even in the mature central nervous system (CNS), changes in synapse structure and function continues to be a dynamic process which is fundamental to learning and memory as well as other adaptive abilities of the brain (Caroni et al., 2012; Mayford et al., 2012; Sala and Segal, 2014; Dieterich and Kreutz, 2016).

Perhaps one of the interesting physical features of the nervous system is the specificity of its connections (Benson et al., 2001). This specificity arises from several developmental processes, including the generation of new synapses (Waites et al., 2005), a process known as synaptogenesis (Steward and Falk, 1985; Fletcher et al., 1994; Waites et al., 2005). The establishment of synapses is a finely regulated process, at which presynaptic and postsynaptic cells synthesize multiple components and regulate numerous signals in a highly regulated spatiotemporal manner (Jin, 2005; Garner et al., 2002; Waites et al., 2005; Garner and Shen, 2008). Regarding this, levels of protein synthesis peak during synaptogenesis (Phillips et al., 1990), suggesting that the new synapses require a high amount of new proteins. In fact, long-term exposure to protein synthesis inhibitors prevents synapse assembly in invertebrate neurons (Schacher and Wu, 2002; Meems

et al., 2003), supporting the essential role of protein synthesis in synapses formation.

1.1. Decentralization of gene expression

The potential ability of a single neuron to build up as many as 10^4 synapses (Garner et al., 2002; Hanus and Schuman, 2013) relies in part on tightly regulated transcription, translation, post-transcriptional and post-translational modifications as well as degradation (Zhang et al., 2011). Studies in diverse cell types have provided evidences suggesting that the localization of messenger RNAs (mRNAs) to subcellular compartments serves as a mechanism for regulating and coordinating gene expression (Gonsalvez et al., 2005; Martin and Zukin, 2006; Sutton and Schuman, 2006; Bramham and Wells, 2007; Lécuyer et al., 2007; Holt and Schuman, 2013). Translation of localized mRNAs decentralizes the control of gene expression from the nucleus (Besse and Ephrussi, 2008; Martin and Ephrussi, 2009; Holt and Schuman, 2013), supplying the macromolecular content needed in response to specific physiological changes. This mode of decentralization enables each synapse to operate as an autonomous entity during synaptic function (Figure 1).

Different forms of synaptic activity require precise mechanisms to deliver a new set of proteins within a spatially limited synaptic domain (Kang and Schuman, 1996; Huber, et al., 2000; Vickers et al., 2005; Govindarajan et al., 2011; Hanus and Schuman, 2013). The synaptic protein content is modulated by local translation of mRNAs in both dendrites and axons as previously described (Chicurel et al., 1993; Schuman, 1999; Steward and Schuman, 2001; Tang and Schuman, 2002; Yoon et al., 2009; Zivraj et al., 2010; Cajigas et al., 2012). Therefore, the mRNA localization and local translation at synaptic compartments provide a fine mechanism for the local control of synaptic protein expression, which is crucial for activity-dependent alterations and synaptic function (Steward, 1997; Steward et al., 1998; Aakalu et al., 2001; Kang and Schuman, 1996; Vickers and Wyllie, 2007; Holt and Schuman, 2013).

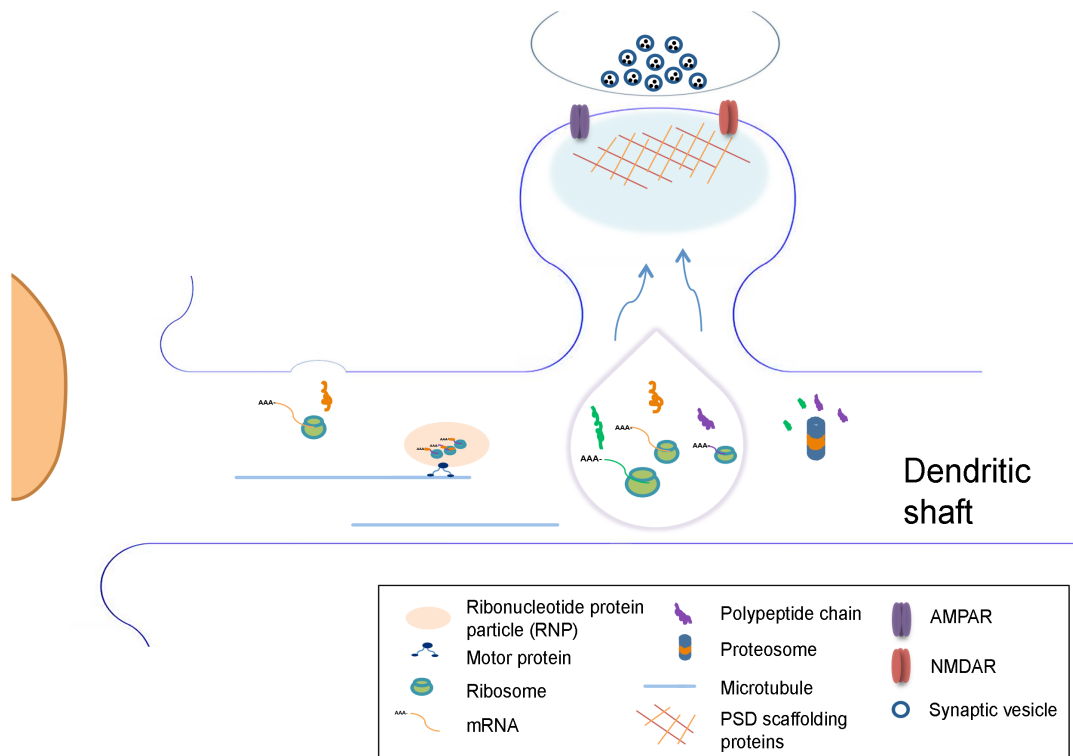


Figure 1. Decentralization of gene expression in neurons. The localization of mRNAs to subcellular domains provides an essential mechanism for the regulation of gene expression at synapses. Local translation of these mRNAs enables each neuron to control synaptic function in a spatial and temporal manner. Ribosomes and proteasome are recruited along dendrites to modulate local translation and degradation of the synaptic proteome in response to synaptic activity and physiological changes.

1.1.1. Control of dendritic protein translation

mRNA localization and recruitment of translation machinery components have emerged as major mechanisms for regulation of protein translation in dendrites (Kuhl and Skehel, 1998; Sutton and Schuman, 2005; Steward, 2007). The first evidence suggesting that protein synthesis could take place outside of the soma came from the observation of ribosome particles in proximal dendritic regions of monkey spinal cord motoneurons (Bodian, 1965). Similarly, polyribosomes were found beneath dendritic spines of dentate granule cell neurons (Steward and Levy, 1982) (Figure 2). In addition, rapid incorporation of radiolabeled amino acids into proteins was detected in synaptic fractions (Droz and Barondes, 1969; Rao and Steward,

1991; Torre and Steward, 1992; Weiler and Greenough, 1993) and dendrites of hippocampal slices (Feig & Lipton, 1993), suggesting that the translation machinery might be localized at subcellular domains.

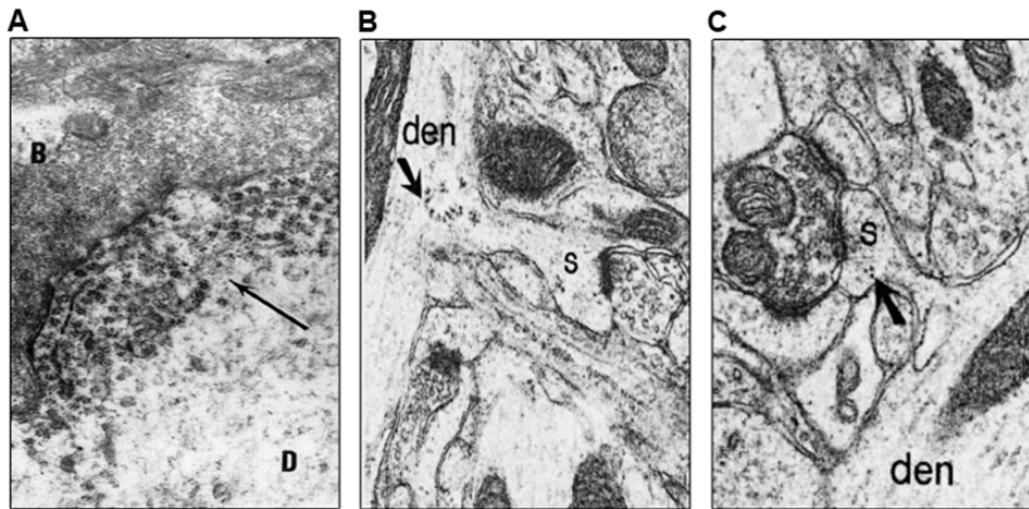


Figure 2. Distribution of the translation machinery along dendritic domains. (A) A dendrite (D) exhibiting a number of ribosomal clusters (arrow) beneath a large synaptic bouton in spinal motoneuron of a chimpanzee (B). Electron micrograph represents a magnification of 25,000X. Image taken from Bodian (1965). (B-C) Ribosomes distributed along dendritic domains of dentate granule cells. (B) Clusters of polyribosome (arrow) localized at the base of a dendritic (den) spine (s). (C) Few ribosomes (arrow) are noticed occasionally in spine heads (s). Image taken from Steward and Levy (1982).

The detection of translation machinery components, including ribosomal proteins, transfer RNAs (tRNAs), initiation and elongation factors, elements of the cotranslational signal recognition mechanism (Tiedge and Brosius, 1996), as well as a population of mRNAs encoding diverse proteins, including cytoskeletal components, activity-regulated cytoskeleton-associated proteins, kinases, and receptors (Garner et al., 1988; Burgin, K.E. et al., 1990; Bruckenstein et al., 1990; Kleiman et al., 1990; Craig et al., 1993; Furuichi et al., 1993; Miyashiro et al., 1994; Link et al., 1995; Lyford et al., 1995; Racca et al., 1996; Tongiorgi et al., 1997; Cajigas et al., 2012), have suggested that dendritic protein synthesis provides a mechanism by which dendrites and synapses tightly regulate their cellular and molecular functions, avoiding the need for protein delivery and transport from the soma (Schuman, 1999). Indeed, dendritic localization of translation machinery

components promotes protein translation during synaptic stimulation (Bagni et al., 2000; Schuman et al., 2006). Previous studies have reported that some of these components display activity-dependent redistribution along dendrites (Ostroff et al., 2002; Smart et al., 2003). Consequently, dendritic localization of mRNAs and translation machinery components is a prerequisite for dendritic protein synthesis, demonstrating the soma-independent potential of dendrites for local protein translation (Sutton and Schuman, 2005).

1.1.2. Dendritic protein synthesis and synaptic function

During the last decade, emerging data have indicated that local translation plays a crucial role in synaptic development and plasticity (Martin, 1997; Martin et al., 2000; Jiang and Schuman, 2002; Ostroff et al., 2002; Sutton et al., 2004; Sutton and Schuman, 2005, 2006; Schuman et al., 2006; Derkach et al., 2007) (Figure 3). Several studies sustain a functional role for local protein synthesis in vertebrates. Functional evidences in isolated hippocampal dendrites and synaptoneuroosomes showed that new protein synthesis occurs after depolarization (Rao and Steward, 1991) and is required for the rapid enhancement of synaptic transmission induced by dendritic application of brain-derived neurotrophic factor (BDNF) (Kang and Schuman, 1996), offering a potential mechanism to modulate selective synaptic changes. Different studies have also demonstrated that isolated hippocampal dendritic areas can support protein synthesis-dependent forms of long-term potentiation (LTP) (Cracco et al., 2005; Vickers et al., 2005; Huang and Kandel, 2005). Moreover, local dendritic exposure to inhibitors of protein synthesis inhibits late LTP in intact slices, showing the important role of dendritic protein synthesis during long-lasting plasticity and synaptic function (Bradshaw et al., 2003).

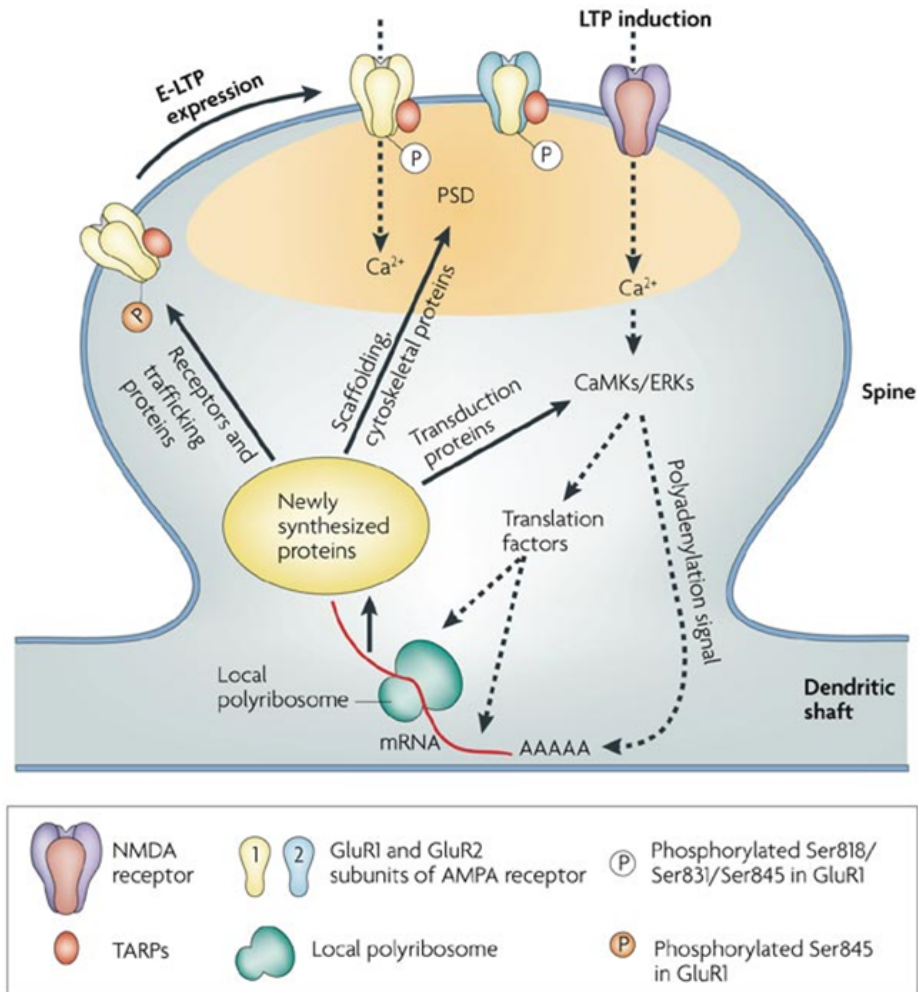


Figure 3. Local protein synthesis and synaptic function. Local translation of mRNAs can take place at the dendritic spine in response to neuronal activity. Synaptic activity (e.g., during LTP induction) activates NMDA receptors, triggering Ca²⁺ influx that activates CaMKs/ERKs pathways, which modulate local protein synthesis through the phosphorylation of translation factors and CPEBs, and subsequent translation of CPE-containing proteins. Postsynaptic local translation contributes to enhancing synaptic strength by delivering new proteins involved in cytoskeletal organization, signal transduction, scaffolding, trafficking and insertion of membrane receptor, among others. AMPARs, AMPA-type glutamate receptors; CaMKs, Calcium/calmodulin-dependent protein kinases; CPE, Cytoplasmic polyadenylation element; CPEB, Cytoplasmic polyadenylation element binding protein; LTP, long-term potentiation; E-LTP, early phase LTP; ERKs, Extracellular signal-related kinases; NMDARs, NMDA (N-methyl-D-aspartate) receptors; PSD, postsynaptic density. Adapted from Derkach and colleagues (2007).

The local translation appears to be associated with different forms of synaptic plasticity. In fact, dendritic protein synthesis is also required for hippocampal long-term depression (LTD) (Huber et al., 2000). Dendritic protein synthesis is also involved in homeostatic synaptic plasticity. Indeed, the spontaneous release of neurotransmitter from presynaptic terminals (miniature excitatory synaptic events or minis) acts as a signal for synaptic integrity of the synapse, however, prevention of neurotransmitter release causes an increase in local protein synthesis levels to enhance the synaptic response at postsynaptic sites (Sutton et al., 2004, 2006). The synaptic response induced by mini blockade increases synaptic expression of surface GluR1 and transient insertion of Ca²⁺-permeable AMPA (alpha-amino-3-hydroxy-5-methyl-4-isoxazole propionic acid) receptors by local protein synthesis (Sutton et al., 2006).

1.1.3. Local protein synthesis in axons

Although the idea of local translation in axons has been controversial over the past decades (Holt and Schuman, 2013), mounting evidence has revealed the localization of translation machinery components in axons, thus supporting the idea of axonal protein synthesis. Early studies confirmed the presence of mRNAs, tRNAs, rRNAs and elongation factors in the squid giant axon (Black and Lasek, 1977; Giuditta et al., 1991; Martin et al., 1998; Giustetto et al., 2003; Lyles et al., 2006). More recently, several ribosomal proteins (P0, L4, L29, L17 and RPP) as well as translation initiation factors (eIF2 α , eIF4e, and eIF5) were observed in regenerating adult rat sensory axons (Campbell and Holt, 2001; Zheng et al., 2001; Verma et al., 2005). Furthermore, the presence of ribosomes was observed in the axoplasmic compartment of invertebrate and mammalian vertebrate axons using high-resolution electron microscopy techniques (Koenig and Martin, 1996; Koenig et al., 2000; Kun et al., 2007; Pannese and Ledda, 1991; Sotelo et al., 1999).

Several studies have demonstrated that axonal protein synthesis plays a key role in diverse axonal functions, including axon growth and pathfinding, synaptic plasticity, signal transduction, long-term viability (Martin et al., 1997; Campbell and Holt, 2001; Zhang and Poo, 2002; Hanz et al.,

2003; Verma et al., 2005; Hillefors et al., 2007), as well as in retrograde trafficking of importins and transcription factors (Hanz et al., 2003; Cox et al., 2008; Ben-Yaakov et al., 2012) (Figure 4). Furthermore, axonal protein translation is engaged in response to injury and is essential for axon regeneration and maintenance (Zheng et al., 2001; Verma et al., 2005; Jung et al., 2012; Yoon et al., 2012).

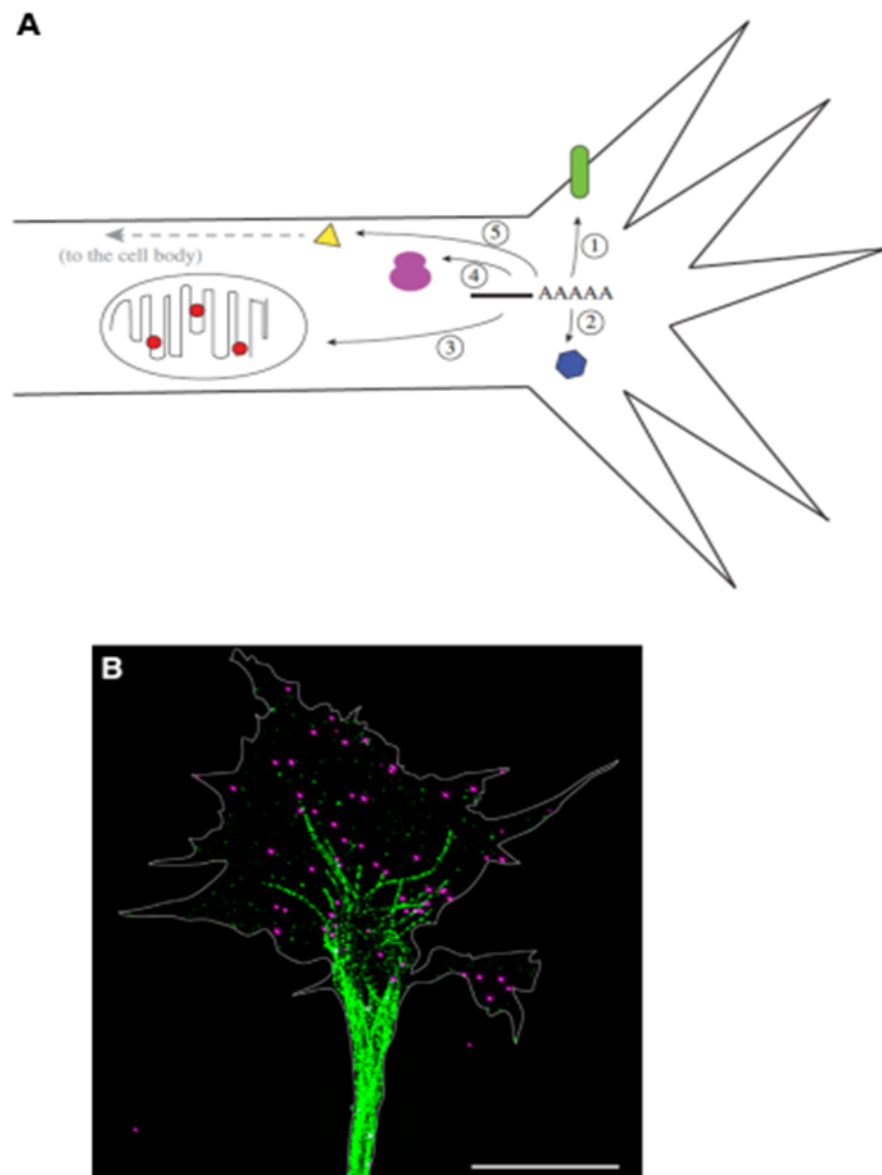


Figure 4. Local protein synthesis in axonal domains. (A) Local translation of axonally localized mRNAs plays an important role in the regulation of different transmembrane proteins, including cell adhesion molecules (integrins, protocadherins) and guidance receptors (EphB4, Nrp2), and secreted proteins such as guidance molecules (semaphorins, ephrins) (1). Intra-axonal translation also regulates the translation of functional proteins

within the axon shaft (e.g. proteins involved in protein degradation, apoptosis, and membrane trafficking) as well as the translation of functional proteins within the growth cone (e.g. proteins involved in axon maintenance and elongation, cytoskeletal and motor proteins) (2). In addition, local translation provides proteins required for mitochondrial (3) or ribosomal (4) function and proteins that are retrogradely transported to the cell body (5), which may influence nuclear functions (e.g. CREB). Adapted from Deglincerti and Jaffrey (2012). (B) Subcellular localization of β -actin mRNAs (magenta, in situ hybridization signal) in the axonal growth cone of a retinal ganglion cell neuron (RGC), which are associated, in part, with components of the cytoskeleton (green, anti-tyrosinated tubulin). RGCs were isolated from cultured *Xenopus laevis* eye primordium. Scale bar: 5 μ m. Adapted from Jung and colleagues (2014).

Local protein synthesis is involved in mediating the responses of growth cones to different guidance cues such as semaphorin 3A (Sema3A) and netrin-1, translation inhibition prevents these responses chemotropic responses (Campbell and Holt, 2001; Wu et al., 2005; Leung et al., 2006; Hengst et al., 2009). In addition, Ming and coworkers (2002) showed that local protein translation is required for the adaptation responses of cultured *Xenopus* spinal neuron growth cones to extracellular guidance cues. In addition, asymmetric gradients of attractive cues trigger an asymmetric recruitment of β -actin mRNA and an increase in β -actin translation on the axon growth cone, indicating that local protein synthesis is an essential mechanism for axon guidance (Leung et al., 2006; Yao et al., 2006; Welshhans and Bassell, 2011).

1.2. Visualization of protein synthesis in neuronal compartments

A number of studies have contributed to the development of procedures to visualize protein synthesis dynamics in neuronal compartments. First demonstrations of dendritic protein synthesis in mammalian neurons came from a protein synthesis green fluorescent protein (GFP)-based reporter in which the GFP coding region is flanked by the 5' and 3' untranslated regions (UTR) from Ca^{2+} /calmodulin-dependent kinase II- α subunit (CAMKII- α) (Aakalu et al. 2001), whose mRNA is known to be dendritically localized. In this work, the authors examined the local

translational regulation of this dendritic protein synthesis reporter by BDNF stimulation in mechanically isolated dendrites from cultured hippocampal neurons (Figure 5). This reporter paved the way for further exploration of the molecular mechanisms by which dopamine induces protein synthesis-dependent forms of synaptic plasticity (Smith et al., 2004) as well as to investigate the activity-dependent regulation of dendritic protein synthesis in cultured hippocampal neurons (Sutton et al., 2004). Furthermore, a comparable protein synthesis reporter was developed to examine activity-dependent dendritic mRNA transport and localization of *Drosophila* CaMKII to postsynaptic sites (Ashraf et al. 2006). Subsequent studies have improved these reporters by using photoconvertible fluorescent proteins to investigate dendritic protein synthesis of Kv1.1 voltage-gated potassium channel protein in hippocampal neurons (Raab-Graham et al., 2006) and visualize local protein translation of sensorin at *Aplysia* sensory-motor synapses during long-term facilitation (Wang et al., 2009). In addition, a different type of protein synthesis reporter, using biarsenical dyes that bind to tetracysteine tags (FIAsH/ReAsH), the system FIAsH-EDT2/ReAsH-EDT2, has been developed to study trafficking and dendritic synthesis of the AMPA receptor subunits GluA1 and GluA2 in rat cultured neurons (Ju et al., 2004).

Time-specific tagging for the age measurement of proteins (TimeSTAMP) method (Lin et al., 2008) is another interesting method for the visualization and quantification of newly synthesized proteins. In TimeSTAMP, newly synthesized proteins of interest are visualized in a drug-dependent manner. The epitope tags are cleaved from the newly synthesized proteins by a sequence-specific protease after translation. Newly synthesized proteins are able to keep their tags by adding a protease inhibitor, which allows the visualization of the newly synthesized proteins. By TimeSTAMP, the authors identified new synapses based on newly synthesized PSD95 protein in hippocampal neurons and visualized the distribution of newly synthesized CaMKII protein in fly brains. More recently, nonradioactive methods such as the surface sensing of translation (SUnSET) have been developed to monitor mRNA translation. SUnSET, a nonradioactive fluorescence-activated cell sorting–based assay, uses puromycin and monoclonal antibodies to puromycin for visualization and quantification of

protein synthesis rate (Schmidt et al., 2009). This method has been successfully applied in mouse dendritic and T cells to monitor translation activity and cellular activation by immunofluorescence microscopy and fluorescence-activated cell sorting (FACS). A different method, named non-canonical amino acid tagging (BONCAT) (Dieterich et al., 2006; 2007), uses non-canonical amino acids bearing functional groups for labeling, enrichment, and identification of newly synthesized proteins. Similarly, Dieterich and colleagues (2010) developed a sister technique named FUNCAT (fluorescent non-canonical amino acid tagging), which utilizes fluorescent probes for the visualization of newly synthesized proteins. Both methods will be described in more detail in the following sections.

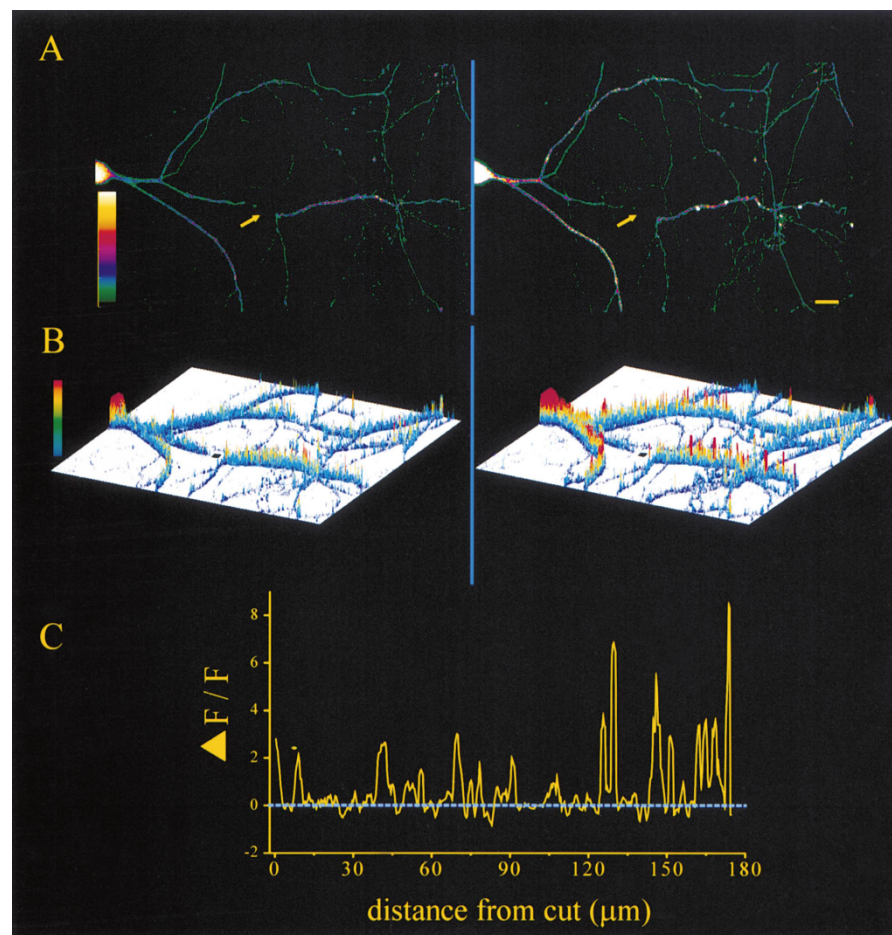


Figure 5. Visualization of dendritic protein synthesis using a protein synthesis GFP-based reporter. (A). Transected neuron (arrow) exhibited increases in fluorescence intensities of a GFP-based reporter after BDNF application. Changes in the fluorescence intensity between pre (0 min, left image) and post (120 min, right image) BDNF application are observed

in both the cell body and dendrites. Scale bar: 15 μm . (B) Representation of the effects of BDNF on the dendritic fluorescence of the neuron shown in (A). BDNF induces increases in GFP synthesis along the transected dendrite, revealing translational hot spots where protein synthesis occurs. (C) Profile of fluorescence changes ($\Delta F/F$) between 0 and 120 min for the transected dendrite shown in (A) and (B). Image taken from Aakalu and colleagues (2001).

1.3. Neuroproteomics of the synapse

Neuroproteomics studies have contributed to unveil the molecular complexity of the synapse. Several proteomic studies have analyzed the synaptic proteome composition of synaptic compartments, including synaptosomes and synaptic vesicles, mainly through well-established subcellular fractionation procedures (Stadler and Tashiro, 1979; Sherman, 1989; Krapfenbauer et al., 2003; Jordan et al., 2004; Li et al., 2004; Peng et al., 2004; Yoshimura et al., 2004; Collins et al., 2005; Cheng et al., 2006; Collins et al., 2006; Dosemeci et al., 2006; Boyken et al., 2013; Weingarten et al., 2014). The isolation of synaptic structures further decreases the complexity of the system, enabling the enrichment and identification of less abundant proteins (Ramos-Ortolaza et al., 2010). Enrichment of synaptosomal fractions has demonstrated to be a suitable initial fraction for the characterization of synaptic vesicles (Whittaker et al., 1964, Blondeau et al., 2004, Coughenour et al. 2004; Morciano et al. 2005; Witzmann et al., 2005; Morciano et al. 2009; Weingarten et al., 2014), synaptic membranes (Stevens et al., 2003; Witzmann et al., 2005), and postsynaptic components (Walikonis et al., 2000; Satoh et al. 2002; Yamauchi et al., 2002; Li et al., 2004; Peng et al., 2004; Yoshimura et al., 2004; Phillips et al. 2005; Witzmann et al., 2005; Cheng et al. 2006; Dosemeci et al. 2007; Jordan et al. 2006). Certainly, synaptosome preparations have facilitated the detailed exploration of the presynaptic active zone proteome, including proteins associated with synaptic vesicle trafficking, receptors, synaptic plasma membrane, cytoskeleton organization, neurotransmission, intracellular signal transduction, adhesion molecules, protein and lipid composition of synaptic vesicles (Witzmann et al., 2005; Morciano et al., 2009; Takamori et al., 2006; Boyken et al., 2013; Weingarten et al., 2014). The isolation of synaptic

structures has enabled the analysis of the synapse phosphoproteome (Collins et al., 2005; Trinidad et al., 2005), as well as the characterization of the postsynaptic density proteome, including essential proteins involved in postsynaptic signaling, ubiquitination, RNA trafficking, protein translation, cell adhesion and cell-cell interaction, endocytosis, motor proteins, and cytoskeletal proteins (Li et al., 2004; Jordan et al., 2004; Yoshimura et al., 2004; Witzmann et al., 2005; Collins et al., 2006; Dosemeci et al. 2007), thus improving our understanding of synaptic function under normal and pathological conditions.

Synapses are dynamic entities with respect to neurotransmission, morphology and protein composition. A substantial body of studies has improved significantly our knowledge of synapse architecture, organization and function by revealing the protein composition of synaptic contacts. Certainly, studies on protein synthesis and degradation, abundance, modifications and molecular characterization of synaptic proteins have shed light on the proteome dynamics of the synapse (Collins et al., 2005; Schrimpf et al. 2005; Witzmann et al. 2005; Grant, 2006; Pocklington et al., 2006; Cohen et al., 2013; Dieterich and Kreutz, 2016). Comprehensive knowledge of the synaptic proteome dynamics is essential for the understanding of the synapse development as well as synaptic function and plasticity. Despite the existing approaches for the analysis of phosphorylated and glycosylated synaptic proteins (Collins et al., 2005; Trinidad et al., 2005; Trinidad et al., 2006; Trinidad et al., 2008; Trinidad et al., 2012), methodologies for studying low abundance and global changes in the synaptic protein content are not yet fully implemented. Therefore, new methods to identify molecular changes occurring at synaptic structures are desired to establish a global assessment of the synaptic proteome dynamics during development as well as for the identification of potential therapeutic targets associated with synaptopathies (Grabrucker et al., 2009; Grant, 2012; Kadakkuzha and Puthanveetil, 2013).

1.3.1. Targeting of proteins to pre and postsynaptic sites

Delivery and local control of protein synthesis at subcellular domains are fundamental mechanisms for sustaining specific cellular functions (Lin et

al., 2008), particularly in pre and postsynaptic specializations. These specializations contain a diverse group of proteins that are transported along axonal or dendritic domains towards the pre or postsynaptic terminals, respectively (Ziv and Garner, 2004; Boeckers, 2006). The targeting of these proteins is regulated by specific targeting signals allocated within defined sequence regions. For example, scaffolding elements of the postsynaptic density (PSD) such as ProSAP1/Shank2 and ProSAP2/Shank3 protein are directed towards the PSD via targeting signals located in the C-terminal end (460aa) (Boeckers et al., 2005). This targeting information includes a bipartite targeting signal comprised of a small region of 135aa and the Sterile Alpha Motif (SAM) domain (Grabrucker et al., 2009). Based on this targeting signal, Grabrucker and coworkers (2009) developed a new vector system called pSDTarget to clone proteins of interest flanked by the bipartite targeting signal, enabling direct delivery of proteins to PSDs. Consequently, existing methods to study protein synthesis in combination with this targeting vector system might contribute to visualize local protein synthesis at PSDs.

The mRNA localization to subcellular compartments relies on specific targeting signals as part of the post-transcriptional regulation of gene expression and neuronal cell polarity (Aronov et al., 2001). Results from earlier studies in neuronal cultures have indicated that tau mRNA is distributed to proximal axonal segments (Aronov et al., 1999; 2001). As a microtubule-associated protein (MAP), tau promotes microtubule assembly and stability, which is essential for both establishing and maintaining neuronal polarity (Goedert et al., 1991; Harada et al., 1994). In an exploratory study in non-differentiated and neuronally differentiated P19 cells, Aronov and coworkers (2001) found that regulation of tau mRNA localization depends on sequence elements located within the 3' UTR, such sequence elements includes a defined fragment containing 240 base pairs (fragment H: 2519-2760), which was required for axonal targeting and tau mRNA stabilization. Consequently, this fragment H has the potential to be used as part of a targeting system to examine protein delivery into axonal domains of neuronal cultures.

1.4. Proteome profiling

One of the challenges in biology is the difficulty to separate, visualize and characterize proteins from complex biological systems with single-cell resolution. Multiple proteomic techniques have been developed to explore the proteome of diverse cellular systems, post-translational modifications, and to compare, per example, the protein profiles of a stimulated versus non-stimulated cell (Sullivan et al., 2000; Irish et al., 2004; Jensen, 2006; Walther and Mann, 2010; Schlatzer et al., 2012; Wei et al., 2013; Niepel et al., 2013). In this context, mass spectrometry (MS) is the method of choice for the identification and characterization of multiple cellular processes, including pathways associated with neurodegenerative diseases (Edgar et al., 1999; Khawaja et al., 2004; Beasley et al., 2006), molecular constituents of the presynaptic active zone (Morciano et al., 2009; Weingarten et al., 2014) and postsynaptic density (Li et al., 2004; Yoshimura et al., 2004; Trinidad et al., 2005), post-translational modifications such as phosphorylation (Ficarro et al., 2002, Collins et al., 2005; Gruhler et al., 2005; Munton et al., 2007) and glycosylation (Elortza et al., 2003; Larsen et al., 2005), as well as cancer research (Rush et al., 2005; Wulfschuhle et al., 2003).

Two-dimensional gel electrophoresis (2D) of proteins, with subsequent MS analysis, is a widely used method that has preceded, and accompanied, the genesis of the proteomics research (Rabilloud and Lelong, 2011). 2D electrophoresis is a traditional technique for purifying individual proteins from complex samples according to their isoelectric point and molecular weight. However, proteins that are too basic or too acidic, too large or too small are not accurately resolved (Issaq and Veenstra, 2008). Furthermore, reduced sensitivity to resolve low abundance proteins adds a limitation in the study of different proteomes.

Different MS methods based on stable isotope quantitation have shown great promise for the identification and quantitation of complex protein mixtures. One of such method involves the use of Isotope-Coded Affinity Tags (ICAT) followed by tandem MS. This approach utilizes chemical reagents consisting of a thio-reactive group, a linker containing stable isotopes (light or heavy form), and a cleavable biotin tag. A different method

based on isobaric labeling used in quantitative proteomics is the Isobaric Tags for Relative and Absolute Quantitation (ITRAQ). It uses stable amine-reactive isobaric tags to label peptides from protein digestions (Zieske, 2006). In addition, methods of growing cells in ^{14}N or ^{15}N media and Stable Isotope Labeling with Amino Acids in Cell Culture (SILAC), which detects differences in protein abundance among samples by incorporating non-radioactive stable isotope-containing amino acids have been implemented for MS-based quantitative proteomics analysis (Washburn et al., 2002; MacCoss et al., 2003; Ong et al., 2002, 2006, 2007). Although these techniques are used to detect differences in the abundance of proteins between biological samples, there persists the limitation for the identification of low-abundance proteins. Approximately 20% of the whole cell proteome can be analyzed in ICAT experiments (Smolka et al., 2001; Shiio and Aebersold, 2006) and a similar amount for ITRAQ (Wu et al., 2006; Dean and Overall, 2007). In addition, there is an important limitation in the analysis of different samples as proteomes might contain proteins with a reduced number or lacking cysteine residues.

1.4.1. Bio-Orthogonal Non-Canonical Amino acid Tagging (BONCAT)

Dieterich et al. (2006 and 2007), taking advantage of bio-orthogonal functional groups (azides and alkynes) and the copper-catalyzed azide-alkyne cycloaddition reaction or so-called 'click chemistry' (Rostovtsev et al., 2002; Tornøe et al., 2002), developed the BONCAT technique for selective enrichment and identification of newly synthesized proteins (Figure 6). These chemical groups are incorporated into proteins by metabolic labeling using reactive non-canonical amino acids, endowing new proteins with a unique chemical functionality, which distinguishes them from the pool of pre-existing proteins. In this technique, newly synthesized proteins are labeled using either the azide-bearing amino acid azidohomoalanine (AHA) or the alkyne-bearing amino acid homopropargylglycine (HPG) as surrogates for methionine. The labeled proteins are affinity tagged, via 'click chemistry' using exogenously delivered probes for detection, affinity purification and subsequent identification by MS. Similarly, newly synthesized proteins can

be visualized through conjugation of these reactive amino acids to fluorescent tags (Figure 6), a technique referred to as fluorescent non-canonical amino acid tagging, or FUNCAT (Dieterich et al., 2010).

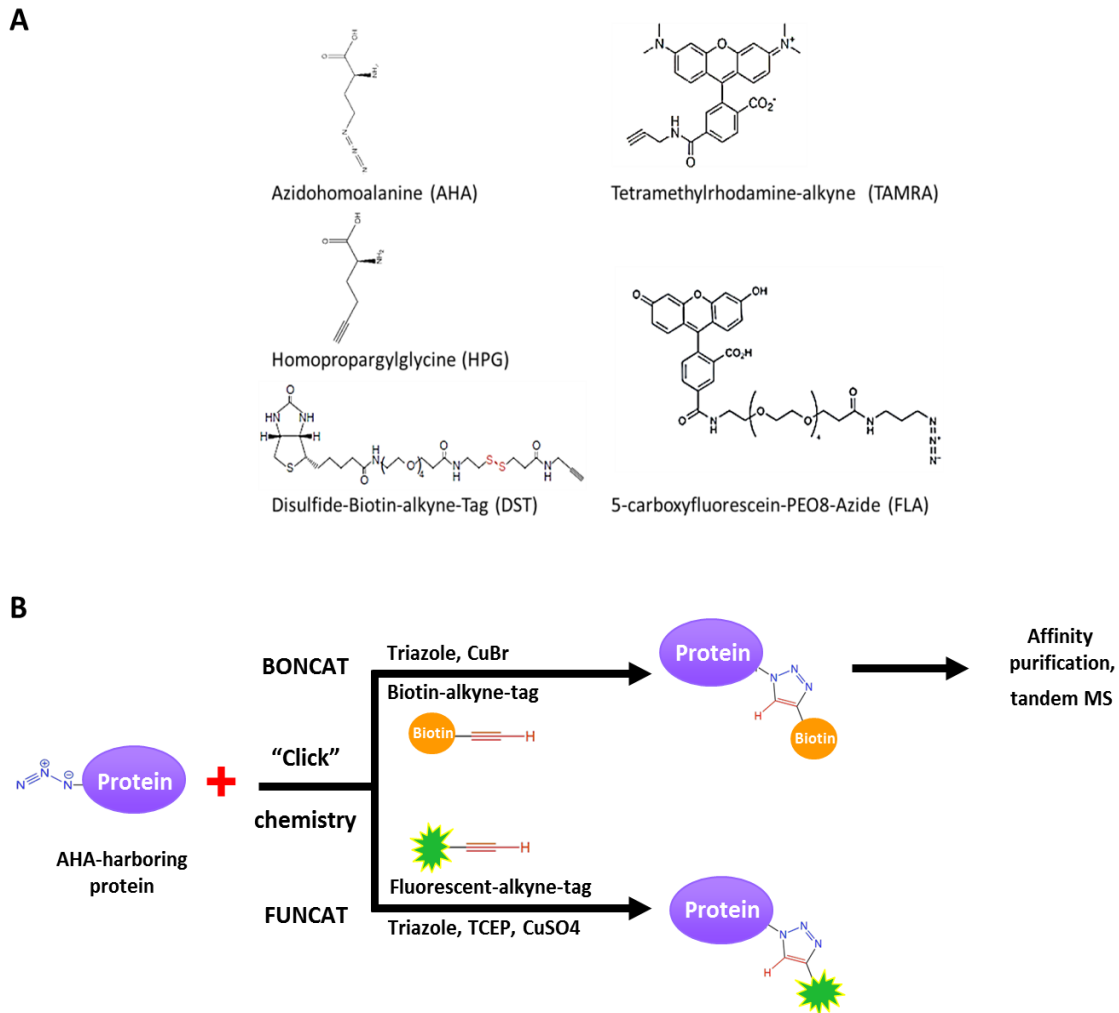


Figure 6. Chemical reagents and overview of BONCAT and FUNCAT technique. (A) Chemical structure of the non-canonical amino acid AHA and HPG, biotin-alkyne-tag, and fluorescent TAMRA-alkyne tag and FLA-azide tag. (B) In BONCAT, cells are metabolically labeled with azide (AHA) - or alkyne (HPG)-bearing non-canonical amino acid. After cell lysis, the AHA- or HPG-harboring proteins are tagged with an alkyne or azide-bearing affinity tag via the copper-catalyzed [3+2] azide-alkyne cycloaddition reaction (referred as “click chemistry”) and subsequently purified by affinity chromatography. Finally, the newly synthesized proteins are identified by tandem MS. In FUNCAT, fluorescent probes are used for the “click chemistry” reaction. These probes allow quantitative analysis of changes in protein synthesis and distribution of newly synthesized protein within cellular systems. TCEP, tris (2-carboxyethyl) phosphine. Adapted from Landgraf, Antileo et al. (2015).

These techniques provide additional tools for the visualization of global protein synthesis dynamics (FUNCAT), as well as enrichment and identification of low abundance proteins (BONCAT) in an unbiased manner.

1.4.2. BONCAT applied to cellular systems

Recently, Hodas and coworkers (2012) have investigated the dopaminergic subproteome in rat hippocampal neuropil using BONCAT. In this study, acute hippocampal slices were incubated with AHA, either with or without a D1/D5 dopamine receptor agonist, SKF81297. Using BONCAT, the authors purified and enriched 891 unique proteins associated with different biological processes and molecular functions. In addition, over 300 newly synthesized proteins were specific to dendrites and axons. Candidate proteins for the samples treated with the D1/D5 dopamine receptor agonist were mostly associated with protein synthesis and synapse function.

In a different system, Yoon and coworkers (2012) combined BONCAT with 2D difference gel electrophoresis (2D-DIGE) to investigate cue-induced changes in subproteomes of cultured *Xenopus* retinal ganglion cell (RGC) axons. This new strategy (DIGE-NCAT) allowed them the identification of the filament protein lamin B2 (LB2), a protein associated with the nuclear membrane, as a major translated protein in axons upon *Engrailed-1* (En-1) stimulation. Furthermore, the axonal LB2 protein was found localized to mitochondria, suggesting that axonally synthesized LB2 protein plays an essential role in axon maintenance and mitochondrial function (Yoon et al., 2012). Undoubtedly, BONCAT is one of the most promising analytical techniques for monitoring changes in proteomes translated under specific physiological and pathophysiological state or in response to stimulation.

1.4.3. FUNCAT applied to visualize *de novo* protein synthesis

FUNCAT has been used to examine the dynamics of newly synthesized proteins in rat hippocampal neurons (Dieterich et al., 2010). The authors were able to visualize newly synthesized proteins in two sequential times through the pulse-chase application of AHA and HPG. In addition, FUNCAT enabled the visualization of BDNF-regulated protein synthesis in dendrites of hippocampal neurons, providing further evidence for local protein synthesis in dendrites.

A number of other studies have recently used FUNCAT to visualize changes in neuronal protein synthesis using diverse stimulation protocols. For instance, employing metabolic labeling and subsequent 'click' reaction to a fluorescent alkyne-tag, Roche and colleagues (2009) confirmed previous findings that axon guidance cues increase protein synthesis in neurons. Furthermore, nerve growth factor (NGF) or semaphorin3A (Sema3A) stimulation increased the amounts of synthesized proteins in both cell bodies and axons. In addition, Tcherkezian and co-workers (2010), using FUNCAT revealed that DCC, a transmembrane receptor, colocalizes with multiple translation components and sites of protein synthesis in cultured commissural and hippocampal neurons. FUNCAT has also been applied to visualize and measure the metabolic turnover rates of synaptic proteins in primary cultures of rat hippocampal neurons (Cohen et al., 2013). Direct measurement of pulse-labeled AHA-bearing proteins in synaptic compartments revealed a reduction to 70% and 55% after 24 and 48 h respectively, as compared to samples control fixed 24 h after pulse labeling.

1.5. Cell-selective metabolic labeling

Protein translation fidelity is ensured by aminoacyl-tRNA synthetases (aaRSs) through the precise ligation of each amino acid to its cognate tRNA (Link et al., 2006). Despite the specificity of aaRSs for their natural amino acids, some studies have exploited their ability to incorporate non-canonical amino acids into newly synthesized proteins. Regarding this, Link and coworkers (2006) have generated a series of mutant *Escherichia coli*

Methionyl-tRNA Synthetases (MetRSs) with a novel aaRS activity that enables site-specific incorporation of the non-canonical amino acid azidonorleucine (ANL) into the nascent polypeptide chain. MetRS mutants containing a single (L13G MetRS) (Link et al., 2006) or triple (NLL-MetRS) (Ngo et al., 2009) amino acid mutations in the methionine-binding pocket are efficient in ANL-incorporation into newly synthesized proteins. Thus, cell-selective labeling of proteins in mixtures of bacterial and mammalian cells was facilitated by the mutant NLL-MetRS activity, as described by Ngo et al. (2009). In this work, cells expressing the mutant MetRS are able to use ANL as a surrogate for methionine (Met) during protein synthesis. Wild-type cells are inert to ANL, proteins made in these cells are unable to incorporate ANL, and thus newly synthesized proteins are not labeled (Figure 7). More recently, transgenic flies expressing both the murine L274G MetRS and the *Drosophila* L262G dMetRS were generated for metabolic incorporation of ANL into newly synthesized proteins in living *Drosophila* (Erdmann et al., 2015). Similarly, Yuet and colleagues (2015) have engineered transgenic *Caenorhabditis elegans* lines expressing a mutant *C. elegans* phenylalanyl-tRNA synthetase capable of incorporating the non-canonical amino acid p-azido-L-phenylalanine into newly synthesized proteins. Therefore, the application of cell-selective metabolic labeling of proteins may contribute to the analysis of proteomes translated into specific subcellular compartments or under different physiological conditions.

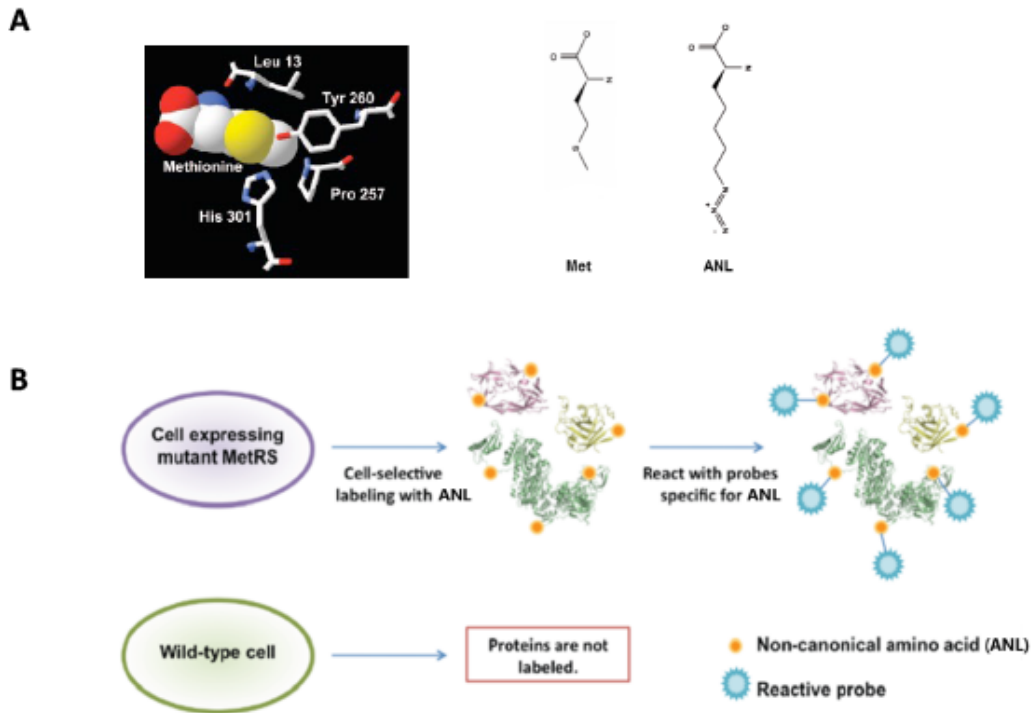


Figure 7. Cell-selective protein labeling using mutant MetRS. (A) Illustration of the cell-specific protein labeling using a mutant form of MetRS (NLL-MetRS), which enables the labeling of proteins by efficient incorporation of the non-canonical amino acid ANL. This unnatural amino acid is not used by the wild-type synthetase during protein synthesis. Therefore, protein labeling is restricted to cells expressing the mutant MetRS. Adapted from Link et al. (2006). (B) Chemical structures: (1) methionine and (2) non-canonical amino acid azidonorleucine (ANL). Adapted from Ngo et al. (2009).

1.6. Objectives

Synapses are complex and highly dynamic structures that are constantly remodeling their molecular content during synaptic function and development. Activity-dependent changes in the synaptic proteome are well described, however, development-dependent changes in the molecular composition of synapses has remained unexplored. Complete understanding of developmental changes in the synaptic proteome will open new perspectives for a better understanding of the organization and function of the synapse as well as processes that underlie diseases and developmental disorders. The aim of this study was, therefore, to investigate the spatial-temporal dynamics of the synaptic proteome during development.

In this study, I describe the development-dependent expression and localization of translation machinery components in primary cultures of rat hippocampal neurons. Subsequently, the translational capacity of dendrites and synapses was examined using FUNCAT technique. Targeting systems are combined with cell-selective metabolic labeling to visualize newly synthesized proteins at pre and postsynaptic terminals. In the following chapters, the development-dependent changes in the synaptic proteome of synaptosomes isolated from primary cortical neurons were investigated using BONCAT technique. An unbiased analysis of the identified newly synthesized proteomes was performed to select potential candidate proteins. Bioinformatics interpretation of the identified proteomes in the context of gene ontology led us to detect significant changes in protein expression during development. Finally, the subcellular mRNA localization was examined for the transcripts of selected candidate proteins by fluorescence *in situ* hybridization (FISH) during representative developmental stages.

Overall, this work takes advantage of the bio-orthogonal chemistry principles from FUNCAT and BONCAT techniques to monitor translational capacities and explore the dynamics of the synaptic proteome, providing further evidence for local protein synthesis as well as relevant information about the molecular constitution of synapses during development, which can promote the discovery of new molecular targets associated with developmental disorders.

2. Materials and Methods

2.1. Materials and production of materials

2.1.1. Chemicals

All chemicals were obtained from Roche, Calbiochem, Clontech, Gibco Life Technologies, Invitrogen, Merck, Roth, Serva, and Sigma-Aldrich.

The non-canonical amino acids azidonorleucine (ANL) and azidohomoalanine (AHA) were synthesized as described by Link et al. (2007) via copper-catalyzed diazo transfer. d_{10} Leu was obtained from Cambridge Isotope Laboratories and the Triazole ligand from Sigma-Aldrich.

2.1.2. Enzymes

Table 1. Enzymes and buffers

Name	Supplier
Restriction enzymes	Fermentas, Thermo Scientific
Phusion DNA polymerase	Fermentas
Antarctic Phosphatase	New England Bio Labs
T4 DNA ligase	Fermentas
dNTPs	Invitrogen
Primers/Oligomers	Invitrogen
5X Phusion Reaction buffer	Fermentas
10X Antarctic Phos Reaction buffer	New England Bio Labs
10X T4 DNA ligase buffer	Fermentas

2.1.3. Primers and plasmid constructs

Primers, cDNA constructs and vector systems used in this study are described in the Supplementary Table 1 and Table 2, respectively.

2.1.3.1. pSDTMetRS expression construct

The pSDTMetRS vector was generated by insertion of the MetRS sequence (wild-type and mutant LtoGMetRS) (7.647 Kbp) into the pSDTarget

vector (Grabrucker et al., 2009), flanked by the bipartite targeting signal Prosap c-term and Prosap Sam-domain from the ProSAP1/Shank2 protein.

The MetRS insert was cloned into pSDT using EcoRI restriction site. pSDT was digested with EcoRI at 37 °C for 1 h and dephosphorylated by Antarctic Phosphatase at 37 °C for 30 min. The MetRS insert was cut out from a pEGFP-C1 vector with EcoRI. The plasmid was ligated with the MetRS insert at 22 °C for 2 h. After bacteria transformation, single colonies were isolated and plasmid DNA was purified by a standard method of plasmid DNA isolation. The orientation of the insert was checked by BamHI control digestion and positive clones were sequenced and amplified by midiprep.

2.1.3.2. Axonal targeting expression constructs

The pCMV-Tag 3B and pcDNA3.1myc (-) A vector were used for the generation of axonal targeting expression construct. Using a PCR-based approach, the ORF Tau sequence (1.125 Kbp) and the 3'UTR Tau mRNA (240 bp) sequence were generated and amplified from a rat brain cDNA (produced by Dr. P. Landgraf) and cloned into each vector. ORF Tau insert was cloned into pCMV-Tag 3B and pcDNA3.1myc (-) A vector using HindIII/Sall and BamHI/KpnI restriction sites, respectively. 3'UTR Tau mRNA insert was cloned into pCMV-Tag 3B and pcDNA3.1myc (-) A vector using Sall/XhoI and AflIII/AflIII restriction sites, respectively. The MetRS insert was cut out from a pEGFP-C1 vector and cloned using EcoRI restriction site in both constructs. Each vector was digested with the proper restriction enzyme at 37 °C for 1 h and dephosphorylated by Antarctic Phosphatase at 37 °C for 30 min. The plasmids were ligated with each insert at 22 °C for 2 h. After competent bacteria transformation, colonies were isolated and plasmid DNA was purified by a standard miniprep method. The orientation of each insert was checked by restriction analysis and DNA sequence from positive clones were sequenced and amplified by midiprep.

2.1.4. Antibodies used for IB and IF

The primary and secondary antibodies used for immunoblot (IB) and immunofluorescence (IF) are presented in Table 2 and Table 3, respectively.

Table 2. List of primary antibodies, including applications and dilutions

Antibody	Supplier	Species	Applications and Dilutions
Actin	Sigma	mouse monoclonal	IB 1:2000
c-Myc	Santa Cruz	mouse monoclonal	IB 1:1000 IF 1:200
eEF2	Cell Signaling	rabbit polyclonal	IF 1:200
GFP	Invitrogen	mouse monoclonal	IB 1:2000
GFP	Abcam	rabbit polyclonal	IB 1:2000
GFAP	Abcam	chicken polyclonal	IB 1:10000
Homer	SYSY	rabbit polyclonal	IF 1:300
MAP2	Sigma	mouse monoclonal	IF 1:500
MAP2	Abcam	rabbit polyclonal	IF 1:500
MAP2	SYSY	guinea pig polyclonal	IF 1:500
MetRS	Abcam	rabbit polyclonal	IB 1:2500 IF 1:300
PSD95	Neuromab	mouse monoclonal	IB 1:1000
Synaptophysin	SYSY	mouse monoclonal	IB 1:5000
Synapsin	Sigma	mouse monoclonal	IF 1:500
S6 ribosomal protein	Cell Signaling	rabbit monoclonal	IB 1:2500 IF 1:200
Tau1	Millipore	mouse monoclonal	IB 1:3000 IF 1:1000
ribosomal RNA 5.8s Y10b	Abcam	mouse monoclonal	IF 1:200
Biotin	Bethyl	rabbit Affinity Purified	IB 1:10000

Table 3. List of secondary antibodies, including applications and dilutions

Antibody	Supplier	Species	Applications and Dilutions
Immunoglobulin-HRP linked secondary antibody	Dianova (Jackson ImmunoResearch)	mouse polyclonal	IB 1:10000
Immunoglobulin-HRP linked secondary antibody	Dianova (Jackson ImmunoResearch)	rabbit polyclonal	IB 1:10000
Immunoglobulin-HRP linked secondary antibody	Dianova (Jackson ImmunoResearch)	chicken polyclonal	IB 1:10000
Immunoglobulin-HRP linked secondary antibody	Dianova (Jackson ImmunoResearch)	guinea pig polyclonal	IB 1:10000
Alexa Fluor 488	Invitrogen	mouse, rabbit polyclonal	IF 1:1000
Alexa Fluor 568	Invitrogen	mouse, rabbit polyclonal	IF 1:1000
Alexa Fluor 647	Invitrogen	mouse, rabbit polyclonal	IF 1:1000

2.1.5. Common buffers and cell culture media

Common buffers and cell culture media used in this study are listed in the Supplementary Table 3 and 4. Some buffers are described directly in the methods.

2.1.6. Prokaryotic and eukaryotic cell lines

Cell line	Supplier	Application
<i>E.coli</i> XL10-Gold	Stratagene	Electrocompetent bacteria; DNA amplification, cloning
HEK 293T cells	ATCC	Protein labeling, transfections, expression analysis

2.1.7. Animals

All animal experiments were performed in compliance with the guidelines for the welfare of experimental animals issued by the Federal Government of Germany, the National Institutes of Health and the Max Planck Society.

2.2. Methods

2.2.1. Neuronal primary cultures

Primary cultures of rat hippocampal or cortical neurons were prepared as described previously by Goslin et al. (1998). Briefly, cells from embryonic day 18 rat brains were dissociated with trypsin and plated onto poly-D-lysine coated glass coverslips in Dulbecco's modified eagle medium (DMEM) (Gibco) containing 10% fetal calf serum (FCS), antibiotics (100 U/ml penicillin, 100 mg/ml streptomycin) and 0.8 mM glutamine. The culture media was exchanged against Neurobasal medium (Gibco) complemented with B27 supplement (Gibco), 0,5mM-Glutamine (Invitrogen) and 100 U/ml penicillin/streptomycin (Invitrogen) 24 h after plating, and maintained at 37 °C in 5% CO₂.

2.2.2. Metabolic labeling of newly synthesized proteins

Cortical primary cultures (5 Million per flask, 75cm²) or HEK293T cells (80% confluent per flak, 75cm²) were used for metabolic labeling of newly synthesized proteins. The culture media was removed and cells were washed and pre-incubated with a HEPES-buffered solution (HBS) (Malgaroli and Tsien, 1992) for 30 min at 37°C, 5% CO₂ and 95% humidity to deplete endogenous methionine. For metabolic labeling, cells were supplemented with 4 mM AHA, 4 mM d₁₀Leu, 4 mM ANL or 4 mM methionine for 2 h at 37°C, 5% CO₂ and 95% humidity. The labeling media was removed, and subsequently, cells were gently washed and scraped with phosphate buffered saline (PBS) pH 7.4 + PI w/o EDTA. The samples were spun down at 3,000 rpm at 4 °C for 5 min. For subcellular fractionation, the neuronal pellet was washed and collected in 5 mM Hepes pH 7.4 and 0.32 M sucrose (buffer A) with complete protein inhibitors and immediately used them for subcellular fractionation and synaptosomes isolation.

2.2.3. Cell lysis

The cell pellet was mixed with PBS pH 7.8 + PI w/o EDTA, 20% (v/v) SDS and Benzonase. After boiling (95 °C), the lysate was cooled down on ice and the volume was adjusted to 1 ml with PBS pH 7.8 PI w/o EDTA and 20% (v/v) Triton X-100. Samples were spun down at 3,000 rpm at 4 °C for 5 min. The supernatant was saved and used for BONCAT.

2.2.4. Reduction and alkylation

Samples were incubated with immobilized TCEP disulfide reducing resin at room temperature (RT) for 2 h. Upon resuspension, proteins were alkylated using 92.5 mg/ml iodoacetamide at RT for 1 hour in the dark. After a first desalting step, the click chemistry reaction was assembled as described by Dieterich et al. (2007).

2.2.5. Click Chemistry

2.2.5.1. BONCAT–Bio–Orthogonal Non–Canonical Amino Acid Tagging

BONCAT reaction mix containing 200 mM triazole ligand, 25 mM biotin alkyne-affinity or disulfide biotin alkyne (DST) tag (Szychowski et al., 2010) and 7.5 mg/ml copper-(I)-bromide suspension was prepared in either a 1ml or 5ml total volume. The samples were thoroughly mixed and incubated under constant agitation overnight at 4°C and spun down at 3,000 rpm at 4°C for 5 min. The resulting supernatant was desalted using ZEBA desalt spin columns according to the manufacturer's protocol. The columns were equilibrated with 0.05% SDS in PBS pH 7.8 before use. The samples were analyzed by Dot Blot after desalting step. Before NeutrAvidin purification, 1% (v/v) Igepal and 20% SDS were added to the samples and incubated under constant agitation.

2.2.5.2. NeutrAvidin purification

The NeutrAvidin agarose was equilibrated by two brief washes with PBS pH 7.8 at RT; samples were added and incubated for 2 h under permanent agitation at RT. The samples were spun down at 3,000 rpm for 5 min and the supernatant was saved. Subsequently, the NeutrAvidin agarose was washed three times for 5 min with 1% v/v Igepal in PBS pH 7.8, three times with PBS pH 7.8 and once with 50 mM ammonium bicarbonate. Aliquots of biotinylated proteins were solubilized in sample buffer at 95°C for Western Blot analysis.

2.2.6. Sample preparation for mass spectrometry

To elute newly synthesized proteins from the NeutrAvidin resin, the protein-bound slurry was incubated with 2% β -Mercaptoethanol for 1 h in the dark with agitation. The supernatant was eluted and lyophilized for mass spectrometry analysis.

2.2.7. Mass spectrometry

The mass spectrometry analysis was done in the lab of Dr. Thilo Kähne at the Institute for Experimental Internal Medicine, Magdeburg (IEIM, Otto von Guericke University). The measurements were done with a Nano-LC-ESI-Iontrap-tandem-mass spectrometer. MS/MS data sets were processed with DataAnalysis (Bruker Daltonics, Germany), searched with the Mascot algorithm against the UniProt database considering the modifications and subsequently compiled in a ProteinScape SQL-dataset (Bruker Daltonics, Germany). Typical false discovery rates (FDR) were below 0.3%. The analysis of the absence or presence of AHA/d₁₀Leu modifications was done manually for each MS/MS data set after MS analysis.

2.2.8. FUNCAT–Fluorescent Non-Canonical Amino Acid Tagging

2.2.8.1. FUNCAT in cultured hippocampal neurons

Dissociated hippocampal cultures (11-21 DIV) were incubated in methionine-free Hib medium (Hib-Met) (Brewer and Price, 1996) for 30 min to deplete endogenous methionine, followed by incubation with Hib-Met with 4 mM AHA, 4 mM AHA plus BDNF (50 ng/ml), 4 mM ANL or 4 mM Met for 2h. The cultures were incubated for 15 min with Hib-Met to remove excess of AHA or ANL. They were immediately fixed with 4% paraformaldehyde in PBS for 20 min. For FUNCAT, in order to avoid copper bromide–derived precipitates we used tris (2-carboxyethyl) phosphine (TCEP) in combination with copper sulfate to generate the Cu (i) catalyst during the reaction. Briefly, reaction mix composed of 200 mM triazole ligand, red-fluorescent tetramethylrhodamine (TAMRA) azide tag (1:8,000), 500 mM TCEP and 49.94 mg/ml CuSO₄ was mixed in a 5ml total volume (PBS, pH 7.6), with vigorous vortexing after addition of each reagent. We incubated hippocampal primary cultures overnight at RT with the reaction mix in a humid box under gentle agitation. After incubation, cells are washed three times for 10 min each with 1% Tween-20, 0.5 mM EDTA in PBS, pH 7.4, followed by three times washing steps with PBS, pH 7.6, before immunostaining using standard conditions.

For immunolabeling, we treated primary cells sequentially with PBS, blocking solution (0.1% Triton X-100, 2 mg/ml BSA, 5% sucrose, 10% normal horse serum in PBS), primary antibody in blocking solution at 4 °C overnight or RT for 1.5 h, three times PBS pH7.4 for 10 min, Alexa488- or Alexa647-conjugated secondary antibody (Invitrogen) in blocking solution, three times PBS pH7.4 for 10 min, and finally mounted in Mowiol before imaging. For cell imaging, Axioplan 2 microscope (Zeiss) was used, pictures were taken with a 63x objective using the AxioVision software. Image processing and analysis were done with ImageJ software.

2.2.9. Transfection

2.2.9.1. Calcium phosphate transfection of HEK293T cells

Human embryonic kidney (HEK293T, ATTC, Manassas, VA) cells were grown in DMEM supplemented with 10% FCS and transfected with corresponding constructs using the calcium phosphate method. DNA was added to transfection solution A (500 mM CaCl₂ in ultrapure water, sterile filtered and stored at 4 °C), mixed with transfection solution B (140 mM NaCl, 50 mM HEPES, 1.5 mM Na₂PO₄ in ultrapure water, sterile filtered and stored at 4°C) and finally added to the cells. The cells were incubated for 4 h before media was exchanged against fresh DMEM media. Cells were lysed with 1 ml of ice-cold lysis buffer (50 mM Tris HCl pH 7.4, 0.5% Triton X-100, 10% (v/v) glycerol, 100 mM NaCl, 1.5 mM MgCl₂) containing protease inhibitors, 24 h after transfection. The cell lysate was centrifuged for 10 min at maximum speed and cleared supernatant was subjected to Western blot analysis. All cells were maintained at 37 °C in a humidified incubator with 5% CO₂.

2.2.9.2. Transfection of hippocampal neurons and immunocytochemistry

The original medium from a 24-well plate is removed and stored. Fresh Neurobasal complete medium (B27 supplement, Glutamine, penicillin/streptomycin) was added to the cells. For 6-wells, transfection mix was prepared as follows: 6 µl Lipofectamine 2000 with 150 µl Opti-MEM were incubated for 5 min at RT before mixing with 150 µl Opti-MEM and 6 µg DNA. 50 µl of the transfection mix was added to each well plate after 20 min of incubation at RT. Cells were incubated 4 h before two washing steps with a fresh Neurobasal complete medium, put back original media, and incubated until experimentation. Hippocampal neurons were fixed at the proper stage depending on the experiment.

For immunofluorescence, the primary cultures were fixed with 4% paraformaldehyde (PFA) at 4°C for 20 min and processed for immunohistochemistry. After washing three times for 10 min with PBS pH 7.4 at RT, the blocking was performed using blocking solution (0.1% Triton X-100,

2mg/ml BSA, 5% sucrose, 10% normal horse serum in PBS) for 1.5 h, and cells were washed again 3 times for 5 min with PBS pH 7.4 at RT, followed by the primary antibody at 4°C overnight or RT for 1.5 h. After three times 10 min washing steps with PBS pH 7.4, cells were incubated with a second antibody coupled either to Alexa568 or Alexa647 for 1,5 h. Cells were washed again three times in PBS pH 7.4 for 10 min and mounted in Mowiol for fluorescence microscopy.

2.2.10. Ribosomal Immunolocalization

2.2.10.1. Image acquisition, 3D reconstructions, and distance measurement

Images were acquired on a Leica TCS SP5 scanning system using 63X oil immersion objective with or without a 2-fold zoom scanner head and LCS software (Leica, Wetzlar, Germany). Fluorescence intensities were measured on maximum projections from confocal stacks taken with the same settings for all samples. Scanning was done at 400 Hz with format 1024 X 1024 pixels to minimized bleaching levels. The brightness and contrast levels of the presented images were minimally adjusted using Image J software. No additional digital image processing was performed.

Stacks were subjected to a 3D-blind deconvolution algorithm implemented in AutoDeblur X2 (Media Cybernetics) software. Twenty iterations were applied. Resulting image stacks were normalized by a linear histogram stretch and 3D-rendered in Imaris 6 (Bitplane AG, Zurich, Switzerland). We performed all post-acquisition processing and analysis with ImageJ (NIH) and Imaris (Bitplane Scientific Software). To facilitate the analysis of fluorescence signal as a function of distance from the soma, we linearized dendrites and extracted their unprocessed full-frame images using the Straighten plug-in from ImageJ. The distance measurement was done using Openview software (Noam E. Ziv, Israel). Synaptic areas were selected automatically with Auto Box Dimensions setting function (Width: 10 pixels; Height: 10 pixels). Box_puncta_msk was selected from Image Processing to locate puncta and box them. The distances, in pixels, were collected in the

measurement window and transformed into metric units (μm) using the Unit of Length (Pixel Width and Height) information from the original picture. Statistical analyses were done with GraphPad Prism.

2.2.11. Subcellular fractionation and synaptosomes isolation

Subcellular fractions and synaptosomes were isolated as described previously (Gundelfinger and Tom Dieck, 2000), with minor modifications. The detail of this preparation, including buffers, is described in Supplementary Scheme 1 and Supplementary Table 5.

Cortical primary cultures were homogenized (12 strokes at 900 rpm) in 5 mM HEPES pH 7.4 and 0.32 M sucrose (buffer A) including protein inhibitors (PI). The homogenate was centrifuged at 1.000xg for 10 min; the supernatant was collected (S1). The pellet (P1; nuclei and cell debris) was re-suspended, homogenized and centrifuged at 1.000xg for 10 min; the supernatant was collected (S1'). Both supernatants (S/S1') were mixed and centrifuged at 12.000xg for 15 min (see Suppl. Scheme 1). The supernatant was removed, and the pellet washed with buffer A. The crude membrane fraction (P2) was re-homogenized and centrifuged at 12.000xg for another 20 min. The pellet was re-suspended in 5 mM Tris pH 8.1 and 0.32 M sucrose (buffer B) and loaded on a discontinuous sucrose gradient (0.8, 1.0, and 1.2 M sucrose). The sucrose gradient was centrifuged for 1.1 h at 16.000xg. Synaptosome fractions were taken from the top to the bottom of the gradient then re-suspended in 5 volumes of incubation buffer and centrifuged for 15 min at 25.800xg. For immunoblot analysis of subcellular fractions, 10 μg proteins were loaded per lane; protein concentration was measured by Amido black method to ensure equal protein loading.

2.2.12. Immunoblotting

Standard western blot protocols (Seidenbecher et al., 2004) were applied for protein detection. Briefly, protein samples were solubilized in SDS-loading buffer, denatured at 95 °C for 5 min, and loaded on SDS-PAGE. Gels were blotted on a nitrocellulose membrane, stained with Ponceau-red for

10 min wash, and then blocked at RT for 1.5 h with 5% low-fat milk in TBS-T buffer. After blocking, primary antibody (diluted in TBS and 0.025% sodium azide) was applied to the membrane and incubated at 4°C overnight or RT for 1.5 h. Subsequently, membranes were extensively washed with TBS-T and TBS buffers before incubated with peroxidase-coupled secondary antibodies at RT for 1.5 h. Chemiluminescence detection was done using Immobilon Western Chemiluminescent HRP Substrate (Millipore), OdysseyFc Infrared Imaging system (Li-Cor™ Biosciences).

2.2.13. Gene Ontology

An in-house script, provided by Dr. Rainer Pielot, was used to convert a set of protein names to gene names. Gene ontology (GO) terms for the identified newly synthesized proteins were determined and extracted by GOMiner (Zeeberg et al., 2003). One file was generated per ontology (biological process, molecular function, and cellular component). We used an additional custom script to combine the results from the three ontologies in one file. Once we have a collection of ontology terms and their frequencies in the input dataset, we next determined the statistical significance of the results by R software. A *P*-value for each annotation was calculated via the one-sided Fisher's exact test. A *P* < 0.05 was used to select representative terms within the dataset.

The web-accessible programs, Database for Annotation, Visualization and Integrated Discovery (DAVID) (Huang et al., 2009) and GeneCodis (Carmona-Saez et al., 2007; Nogales-Cadenas et al., 2009; Tabas-Madrid et al., 2012) were used to determine biological annotations that are significantly associated with our list of genes/proteins. In both analyses, the default settings included *P*-value (*P* < 0.05) calculated using a modified Fisher Exact *P*-value (EASE Score) (DAVID) and the Hypergeometric distribution (GeneCodis) for gene-enrichment analysis. In addition, Benjamini-Hochberg FDR correction was used for multiple testing and whole *Rattus norvegicus* genome as a genome background.

3. RESULTS

3.1. Development-dependent expression of translation machinery components in primary hippocampal neurons

The synaptic localization of the translation machinery facilitates the translation of a wide range of proteins involved in synaptic plasticity (Weiler and Greenough, 1993; Bagni C et al., 2000; Schuman et al., 2006). While components of the translation machinery have been analyzed to some extent (Tiedge H and Brosius J, 1996; Kim HK et al., 2005), our knowledge about the dendritic and axonal distribution of these components during the immature stages of neuronal development is rather limited. Therefore, the following experiments were focused on the development-dependent distribution of essential components of the translation machinery as well as putative recruitments of these components to synapses and how the levels of these components are adjusted during early neuronal development. This work analyzes different time frames as representative stages of neuronal development in order to study the subcellular localization of the translation machinery during immature, intermediate and mature developmental stage.

As a first step towards the characterization of translation machinery components in neuronal processes, we analyzed the development-dependent subcellular distribution of ribosomes using the Y10b antibody raised against the 5.8S ribosomal RNA (Kim HK et al., 2005). In addition, neurons were immunostained for synapsin, a marker for presynaptic specializations (Fletcher et al., 1994), in order to analyze the potential spatial association between ribosomes and synaptic contacts. Immunostaining of young neurons (DIV5) showed ribosome clusters preferentially near the soma but also to some extent in distal dendrites, revealing that constituents of the translation machinery are present in dendritic domains of neurons at immature developmental stages (Figure 8A). Some ribosomal clusters are noticeable in the more distal part of dendrites (proximity 70 μm), as it is illustrated in Figure 8B by the reconstruction of a dendritic segment from hippocampal neuron at DIV7. In addition, ribosomal clusters surrounded by synapsin-labeled presynaptic specializations were often noticeable along the somatodendritic

domain of cultured hippocampal neurons at an intermediate stage of maturation (DIV11) as well as in mature stages (DIV17) (Figure 8A). This finding is in line with previous studies on the dendritic distribution of ribosomal P protein (DIV14) (Tiedge H and Brosius J, 1996) and dendritic transport of RNA granules (Kim HK et al., 2005).

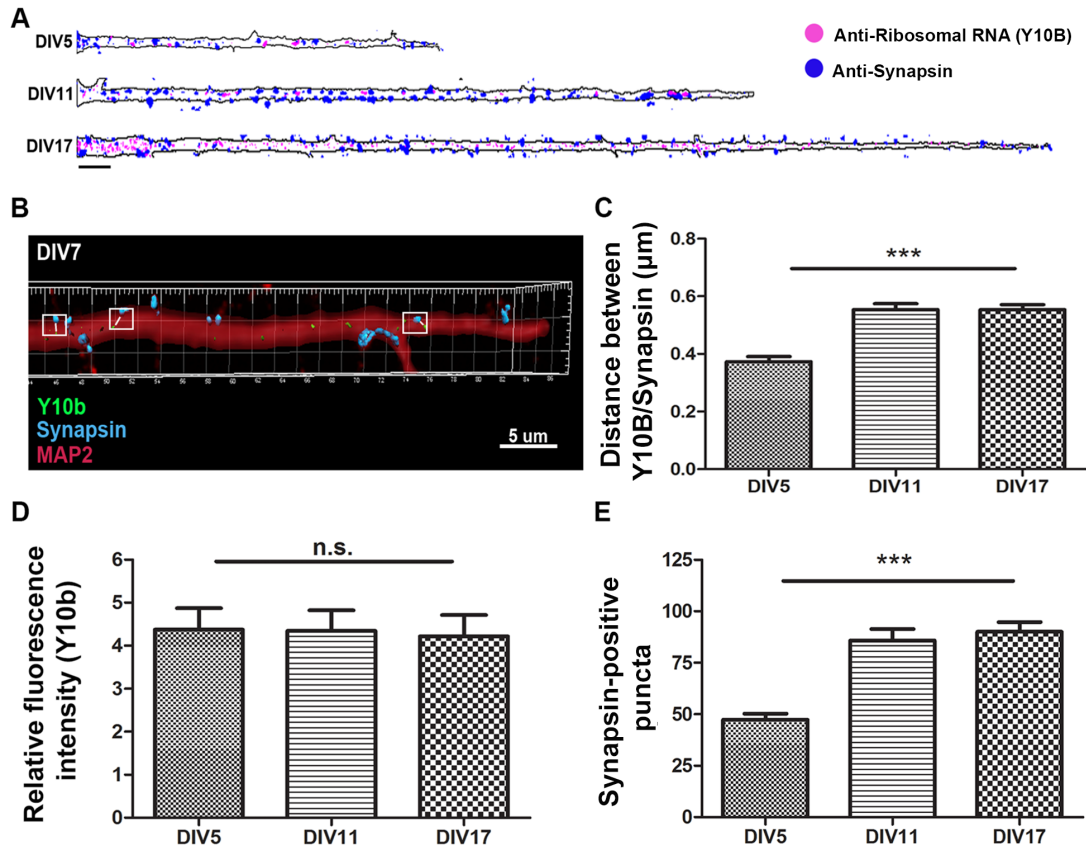


Figure 8. Development-dependent distribution of ribosomes in dendrites of hippocampal neurons. Cultured hippocampal neurons at different developmental stages (DIV: days in vitro) were fixed and immunostained to analyze the dendritic distribution of ribosomes. (A) Main dendrites were straightened to visualize the distribution of Y10b, as a ribosomal marker (magenta), and synapsin (blue) as a marker for pre- synapses. MAP2 immunostaining was used as a specific dendritic marker to generate a mask that outlines the dendritic structure. Shown are entire dendrites for each developmental time point. Scale bar = 10 μm . (B) Exemplary reconstruction of a distal dendritic segment from a neuron at DIV7 illustrates the distribution of ribosomes (Y10b) and synapsin. Analysis of the distance between ribosomes and synapsin (C), relative fluorescence intensity measurement of Y10b (D) and the mean number of synapsin positive puncta (E) per dendrite was analyzed for cultured hippocampal neurons at different developmental stages. The white boxes in B indicate measurement areas. The relative fluorescence intensity is a measure of the amount of the marker per dendrite. *** $P < 0.05$; one-way ANOVA with Tukey multiple-comparison

testing. All data represent means \pm SEM obtained from three independent experiments, and a total number of 26–30 cells per time point. (DIV5: 15, 8 and 7 cells, respectively; DIV11: 10, 11 and 7 cells, respectively; DIV17: 7, 11 and 8 cells, respectively).

In mature neurons, the signal for the presynaptic marker synapsin exhibits a dispersed distribution pattern, which is associated with increases in the density of presynaptic specializations (Figure 8A). During the second week in culture, the complexity of the ribosome localization pattern is increased; abundant levels of ribosomes are distributed along dendritic domains and frequently observed allocated near synaptic sites.

In order to evaluate if there is a putative development-dependent recruitment of ribosome clusters specifically to synaptic contacts, we measured the distance between the ribosomal marker Y10b and synaptic marker synapsin in dendrites of cultured hippocampal neurons at different maturation stages (DIV5, DIV11 and DIV17) using OpenView software (Cohen et al., 2013). Figure 8B illustrates a representative reconstruction of a distal dendrite segment highlighting a synaptic area (white boxes) analyzed by OpenView software. At DIV5, the average distance between ribosomes and the presynaptic marker was $0.37 \pm 0.2 \mu\text{m}$ (Figure 8C). The distance between markers at this immature stage differs from DIV11 ($0.55 \pm 0.17 \mu\text{m}$) and DIV17 ($0.55 \pm 0.11 \mu\text{m}$). The increase in distance between markers observed at intermediate (DIV11) and mature (DIV17) cultures might be the result of the development-dependent changes in the dendritic spine morphology.

The Y10b fluorescence intensity levels were quantified at synaptic sites in order to examine development-dependent changes in the number of ribosomes in dendritic spines. Interestingly, similar levels of Y10b intensities were found regardless of the developmental stage, indicating that neurons might be able to maintain a constant dendritic population of ribosomes allocated at synaptic sites to support local protein synthesis during development (Figure 8D). Additionally, dendrites analyzed from neurons at an intermediate stage of maturation (DIV11; N puncta: 85) as well as mature neurons (DIV17; N puncta: 90) revealed a significant increase in the average number of synapsin-positive puncta compared to immature cultures (DIV5; N puncta: 47) (Figure 8E).

The results showed that ribosomal clusters are present in immature dendrites (Figure 8), suggesting that local protein synthesis might take place in dendritic domains of immature neurons. In addition to the ribosomal distribution analysis, the endogenous distribution of different translation machinery components in primary hippocampal cultures was performed at an intermediate stage of neuronal development (DIV11) as the second and third weeks of culturing are associated with dendritic growth and synapse formation (Kaeck and Banker, 2006; Cohen et al., 2013).

One key factor for protein synthesis is the eukaryotic initiation factor (eIF4), which is involved in the recognition and recruitment of mRNAs to the ribosome to initiate protein translation. A further important factor in protein translation is the eukaryotic elongation factor (eEF2), a protein that binds ribosomes and promotes the translocation of the nascent protein chain within the active site of the ribosome. Similarly, proteins such as aminoacyl tRNA synthetases are important to charge amino acids onto their respective tRNA molecules. As these enzymes are cellular components of the translation machinery required for protein synthesis, they are expected to be present not only at the somatic areas but rather to be found in any distal domain where local synthesis is required. Therefore, we examined the subcellular distribution of eIF4 and eEF2 as well as the distribution of Methionyl-tRNA synthetase (MetRS).

eIF4 and eEF2 proteins are distributed both in dendrites and axons as revealed by immunofluorescence in hippocampal neurons (DIV11). The abundant signal of eIF4 and eEF2 far from the soma (Figure 9A) provides additional evidence for the idea that protein translation can be triggered in distal axonal and dendritic domains. Furthermore, extensive levels of MetRS were also detected in distal neuronal compartments (Figure 9B). Indeed,

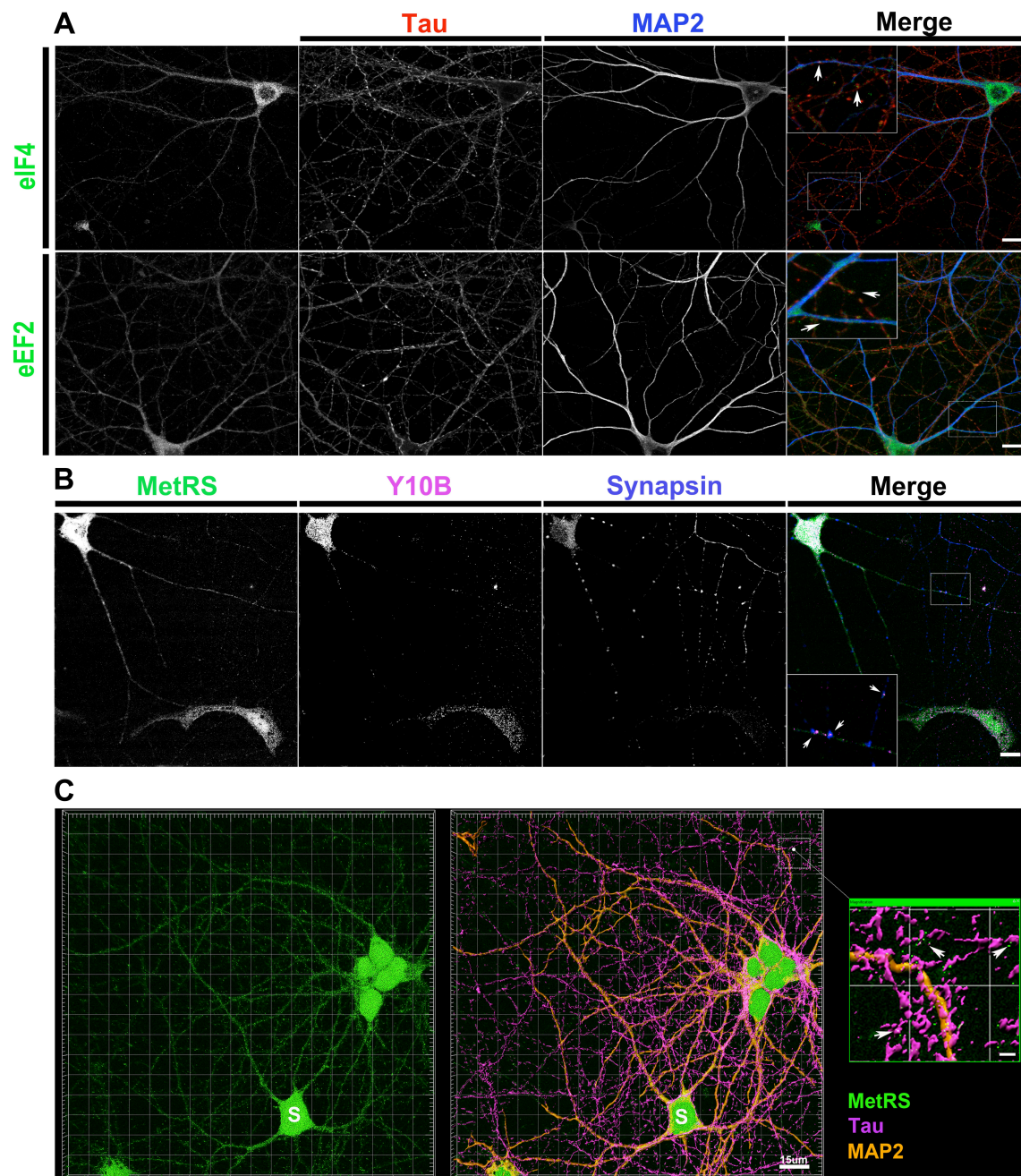


Figure 9. Distribution of translation machinery components in primary hippocampal neurons (DIV11) (A) Immunostaining for eIF4 and eEF2 (green) in axons (Tau, red) and dendrites (MAP2, blue). Neurons showed substantial levels of eIF4 and eEF2 in dendritic and axonal processes. Scale bar= 10 μm . (B) Representative examples of immunostaining for MetRS (green), Y10b (magenta) and synapsin (blue). Note the distal distribution of MetRS and ribosomes in dendritic processes. (C) Immunostaining for MetRS (green), Tau (magenta) and MAP2 (light orange) markers. Three-dimensional image reconstruction shows highly expressed MetRS in neuronal somata (S) as well as distribution along dendrites and axons (white arrowheads). The right image provides higher magnification of the selected area, scale bar = 5 μm .

MetRS immunostainings showed a subcellular distribution along dendrites as well as in axonal processes (Figure 9B, high magnification), further supporting previous reports referring to translation machinery in axons (Michaevlevski I et al., 2010, Malmqvist T et al., 2014) (Figure 9C).

Taken together, these results show the subcellular distribution of ribosomes along dendritic domains of hippocampal neuron cultures during development and suggest that this subcellular localization might be crucial for local translation already at immature developmental stages. In addition, the dendritic and axonal distribution of translation machinery components in immature neurons suggests a soma-independent potential of dendrites and axons to regulate local protein synthesis at early stages of neuronal development.

3.2. Analysis of the newly synthesized proteins in dendrites of primary hippocampal cultures

The levels of newly synthesized protein were analyzed in dendrites from neurons at an intermediate developmental stage (DIV13) using the so-called FUNCAT technique (Dieterich et al., 2010), which allows the *in situ* visualization of newly synthesized proteins. To this end, BDNF was utilized in order to determine changes in the levels of newly synthesized proteins in response to synaptic stimulation. A previous study has demonstrated that BDNF is able to induce local translation of a GFP-based protein synthesis reporter in mechanically isolated dendrites (Aakulu et al., 2001). In addition, Dieterich and colleagues (2010) observed increases in newly synthesized protein levels in both somata and dendrites after BDNF application using the FUNCAT technique. However, the effects of BDNF on the dendritic distribution of ribosomes and newly synthesized proteins in synaptic sites of developing neurons require further investigation. To address this question, a set of three-dimensional image analysis was carried out in dendrites from neurons treated with AHA alone or in presence of BDNF. We analyzed the signal intensities of newly synthesized proteins from straightened dendrites using the TAMRA-defined area as a mask. As a result, neurons incubated for 2 h with AHA produced robust labeling of newly synthesized proteins in

dendritic projections (Figure 10A) and somata (data not shown). Furthermore, AHA treatment enabled to label fractions of newly synthesized proteins in synaptic areas as shown by three-dimensional image reconstruction of dendrites from these neurons (Figure 10B).

Quantitative analysis in dendritic processes of BDNF-treated neurons revealed a substantial increase (ranging from 2 to 3.3-fold) of the Tamra signal along the entire dendritic processes compared to untreated neurons, showing extended protein labeling in distal dendritic domains (Figure 10C). The major magnitude of detected newly synthesized proteins might reflect an increase in soma and dendritic protein synthesis after BDNF application. In addition, a prominent increase in the total number of ribosome clusters was perceived along dendritic segments of neurons treated with BDNF as illustrated in a representative distribution (Figure 10D) and quantification of ribosome clusters (Figure 10E). These findings demonstrate that BDNF-induced increases in protein synthesis result in not only a global increase of new proteins in the cell body and dendrites but also increases in the total number and distribution of ribosome clusters along dendrites.

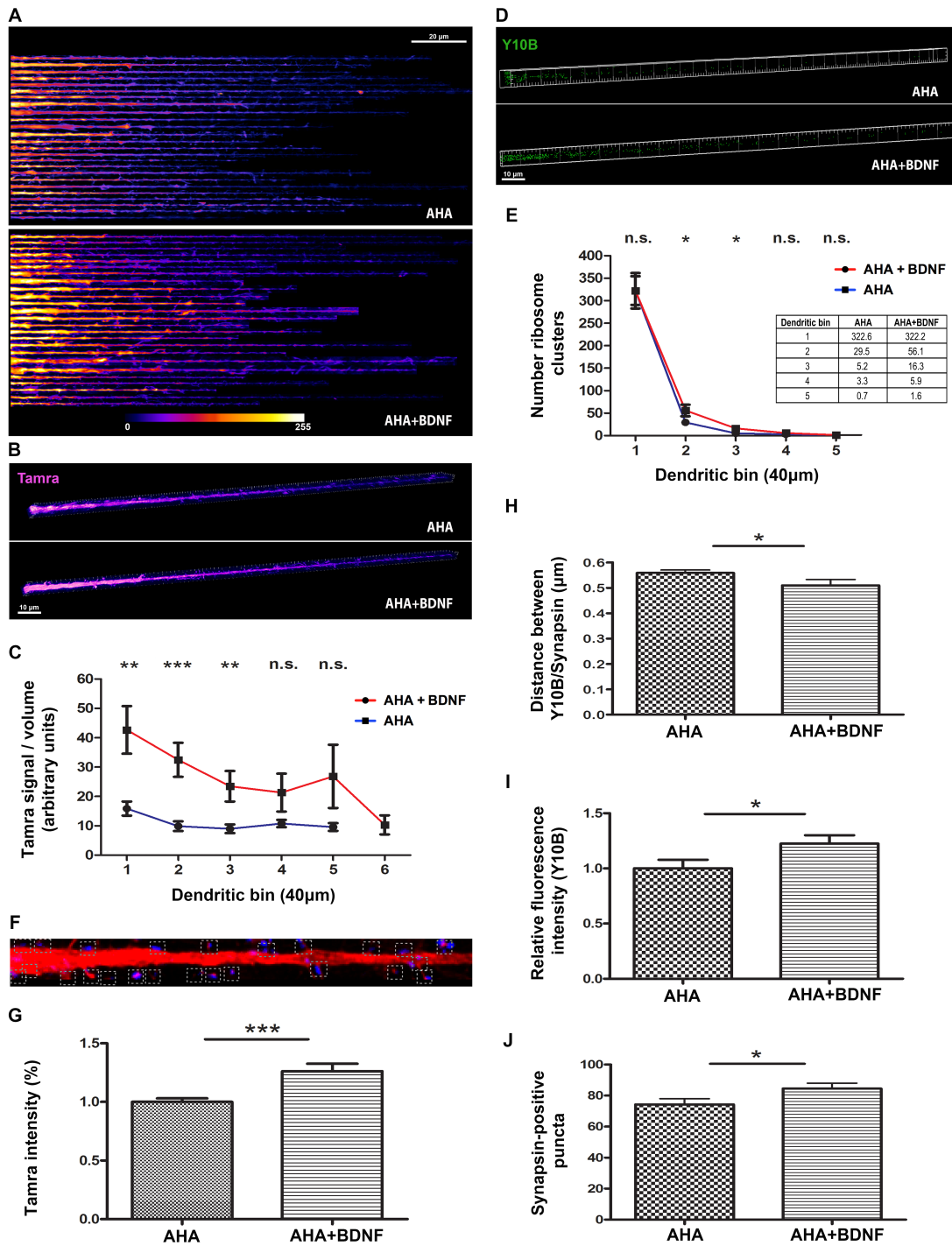


Figure 10. BDNF increases protein synthesis, levels of ribosomes and the number of synapsin-positive puncta in dendrites of hippocampal neurons. Cultured hippocampal neurons (DIV13) were incubated with 4 mM AHA, 4 mM AHA in the presence of BDNF (50 ng/ml) or 4 mM Met (data not shown) for 2 h. Neurons were fixed, tagged with Tamra alkyne tag (Magenta) and immunostained for the ribosomal marker Y10b (green) and synapsin (not shown). (A) Tamra signal intensities (“Fire”) in straightened main dendrites for AHA and AHA plus BDNF groups are shown. Left, proximal dendrite; right, distal dendrite. Color lookup table indicates fluorescence intensity (pixel intensities 0–255). (B–C) Newly synthesized proteins

(Magenta) detected in dendrites of hippocampal neurons incubated with AHA plus BDNF. Main dendrites were straightened and segmented (bin 40 μm) to facilitate the fluorescent intensity measurements. Representative images are shown. Left, proximal dendrite; right, distal dendrite. The graph shows Tamra signal-to-volume ratios. $***P < 0.05$; $**P < 0.05$; Student's t-test. (D-E) Ribosomal distribution in dendrites after BDNF application. The graph shows the number of ribosome clusters along dendrites. $*P < 0.05$; Student's t-test. (F) Dendritic segment illustrates representative measurements at synaptic sites (white boxes) using OpenView software. Tamra signal (red) and synaptic marker synapsin (blue) are shown. (G) Quantitative analysis of Tamra intensities at synaptic sites. $***P < 0.05$; Student's t-test. (H) The average distance between ribosomes and synapsin-positive puncta. The distance was measured using Openview software. Significant differences in the distance (μm) between markers were found after BDNF application. $*P < 0.05$; Student's t-test. (I) Quantitative analysis of fluorescence intensities for the ribosomal marker Y10b at synaptic sites revealed changes in the Y10b levels after BDNF application. $*P < 0.05$; Student's t-test. (J) Mean synapsin-positive puncta. The overall number of synapsin-positive puncta increased after BDNF stimulation. $*P < 0.05$; Student's t-test. All data are represented as mean \pm SEM obtained from three independent experiments (AHA+BDNF condition: 12, 7 and 6 cells, respectively; AHA condition: 7, 7 and 8 cells, respectively), a total number of 22–25 cells per condition.

3.2.1. Analysis of newly synthesized proteins in synaptic areas of primary hippocampal neurons

Next, the levels of newly synthesized proteins at postsynaptic sites were also measured after BDNF application in neurons from an intermediate stage of maturation (DIV13). We used the OpenView software to measure levels of newly synthesized proteins (Tamra intensity) in synapsin-positive areas (Figure 10F, white box).

Neurons incubated (2 h) with AHA showed considerable levels of new proteins in areas associated with synapsin-positive puncta (Figure 10G). Meanwhile, neurons incubated with BDNF (50 ng/ml) exhibited a 26% increase ($***P < 0.05$) in the signal of newly synthesized proteins at synapsin-positive areas as compared with neurons incubated with AHA alone (Figure 10G). These findings suggest that developing neurons respond to acute BDNF application, in part, by altering the levels of dendritic newly synthesized proteins, whose effects are extended into postsynaptic sites as we detected substantial increases of newly synthesized proteins in synaptic areas.

Similarly, the effect of BDNF application on the ribosome distribution was examined at postsynaptic areas. For this purpose, the distance between ribosomes (Y10b) and the synaptic marker synapsin was measured in dendrites from BDNF-treated and untreated neurons. After BDNF application, a significant change ($*P < 0.05$) was observed in the distance between markers ($0.51 \pm 0.19 \mu\text{m}$) as compared to cells incubated with AHA alone ($0.56 \pm 0.07 \mu\text{m}$), suggesting a potential recruitment of ribosomes toward synapses after BDNF stimulation (Figure 10H).

Subsequent Y10b intensity quantification was performed to evaluate whether the reduction in distance between markers was associated with increases in ribosomal levels at postsynaptic sites after BDNF application. The quantification of Y10b intensity revealed a significant difference ($*P < 0.05$) in the ribosomal levels at postsynaptic sites between BDNF-treated and untreated neurons (Figure 10I), which might reflect a potential recruitment of ribosomes into dendritic spines modulated by BDNF. In addition, quantitative analysis indicated that BDNF induced a significant increase ($*P < 0.05$) in the number of synapsin-positive puncta (Figure 10J), consistent with previous studies on synaptogenesis (Alsina et al., 2001; Aguado et al., 2003; Sanchez et al., 2006; Cheng et al., 2012). These findings suggest that increases in protein synthesis triggered by BDNF might alter the number of ribosome clusters, induce the recruitment of ribosomes into postsynaptic sites and modify synapse density.

Based on these results, the increases in newly synthesized proteins and ribosome levels observed in dendritic domains and synaptic sites, suggest potential changes in the translation capacity of dendrites in response to synaptic stimulation, which might have additional effects on the amount and distribution of ribosomes at synaptic compartments as well as synapse density.

3.3. Targeting of MetRS to postsynaptic densities

The targeting of pre and postsynaptic proteins are regulated by specific targeting signals encoded within defined sequence regions. For example, the targeting information for the post-synaptic scaffolding protein ProSAP1/Shank2 is located in the C-terminus of the protein (Boeckers et al., 2006). Accordingly, Grabrucker and colleagues (2009) used these targeting signals to develop a new vector system called pSDTarget to clone proteins of interest flanked by a bipartite targeting signal, which enables the direct delivery of proteins to postsynaptic densities. Therefore, we considered the pSDTarget vector system as a suitable tool to study and visualize local protein synthesis at postsynaptic densities in combination with FUNCAT.

Based on the pSDTarget vector system, we cloned the Methionyl-tRNA synthetase (MetRS) sequence (GenBank: BC079643.1), flanked by the bipartite targeting signals, into the pSDTarget vector to generate the pSDT-MetRS-GFP construct (Supplementary Figure S1). Primary hippocampal neurons (DIV7) were transfected with the pSDT-MetRS-GFP construct to examine the targeting of MetRS to postsynaptic sites. Neurons were allowed to overexpress the fusion proteins before proceeding with immunostaining (DIV15).

pSDT-MetRS-GFP exhibited an expression pattern dispersed along somatodendritic processes with noticeable levels of the fusion protein in postsynaptic densities as confirmed using an antibody directed against the postsynaptic density scaffolding protein Homer1 (Figure 11A). This expression pattern is not detected in neurons transfected with pMetRS-GFP lacking the bipartite targeting signal, which expression pattern was distributed only through the soma and somatodendritic extensions (Figure 11A and 11B). High-resolution imaging and subsequent image processing (deconvolution and three-dimensional image reconstruction) showed a preferential, but not exclusive, accumulation at postsynaptic areas (Figure 11B). The evidence from high-resolution imaging demonstrated that pSDT-MetRS-GFP construct might be used as a potential targeting system to evaluate protein synthesis at postsynaptic sites. Since this system has limitations for local visualization of newly synthesized proteins, a cell-selective metabolic labeling method was

further used along with a non-canonical amino acid (azidonorleucine, ANL), which can exclusively be utilized by a mutant form of MetRS (LtoGMetRS) (mouse L274GMetRS, clone designed by Dr. Daniela Dieterich).

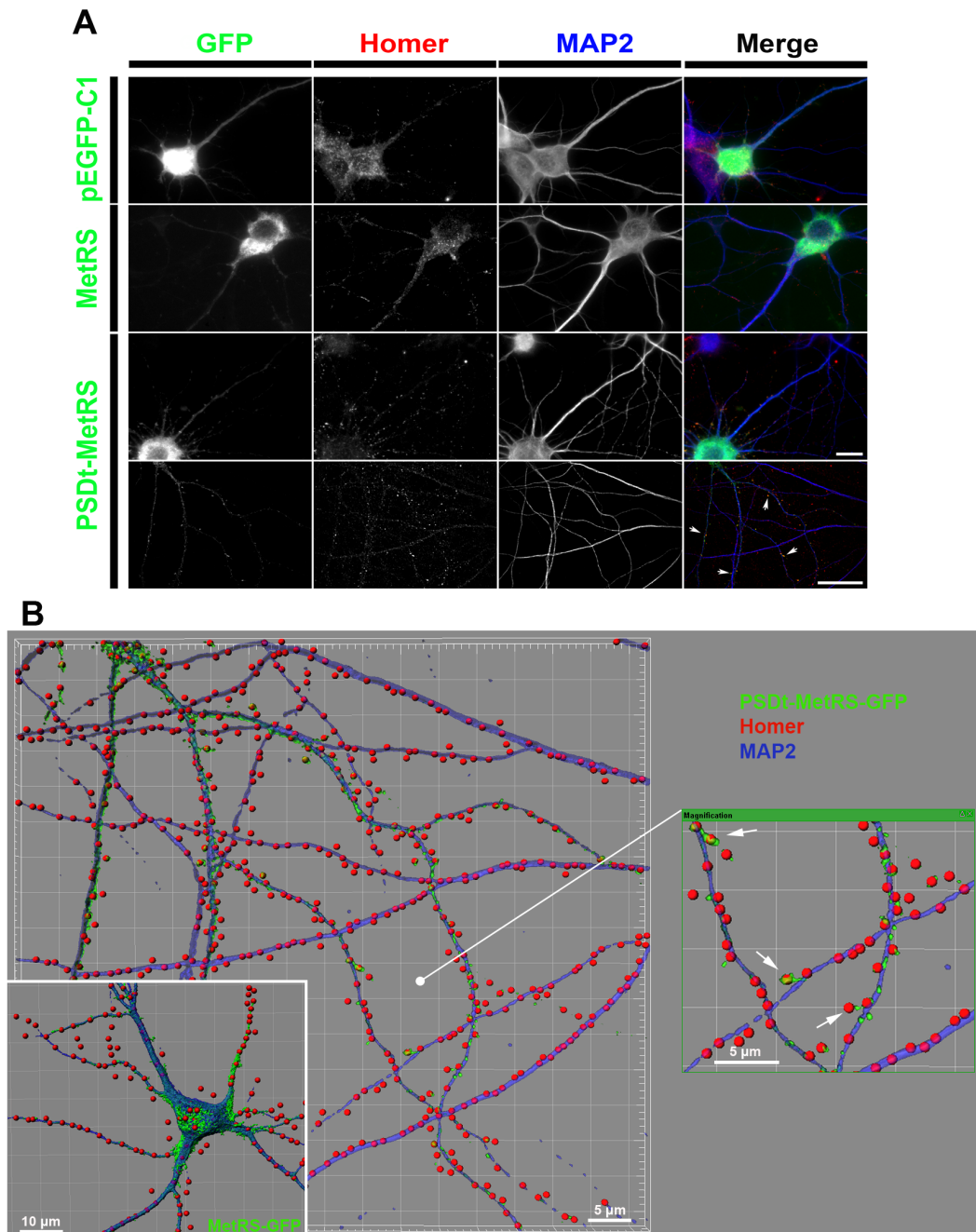


Figure 11. ProSAP1/Shank2 targeting sequence leads to increased MetRS-GFP–fusion protein localization at postsynaptic areas. Hippocampal neurons (DIV7) were transfected with pEGFP-C1, pMetRS-GFP and pSDT-MetRS-GFP construct. Subsequently, 192 h (DIV15) after transfection, neurons were immunostained against the dendritic marker protein MAP2 (blue) and postsynaptic marker protein Homer1 (red) to analyze targeting of MetRS to postsynaptic densities. (A) Neurons (DIV15) expressing the pSDT-MetRS-GFP construct

show enriched GFP signal at synaptic sites. In contrast, immunostaining of neurons transfected with pMetRS-GFP showed no obvious localization at postsynaptic areas. High-resolution imaging (lower panel) shows an enrichment of MetRS at postsynaptic sites (white arrows) in neurons transfected with pSDT-MetRS-GFP. Scale bar = 10 μm . Scale bar (High-resolution image, lower panel) = 40 μm . (B) High-resolution three-dimensional image reconstruction shows an abundant MetRS-GFP signal at postsynaptic sites in neurons transfected with pSDT-MetRS-GFP (see magnification right image, white arrows), and homogenous dendritic distribution of MetRS-GFP in neurons transfected with MetRS-GFP (left, inset image). Images display MetRS-GFP and pSDT-MetRS-GFP (green), dendritic marker MAP2 (blue) and postsynaptic marker Homer (red). Scale bar = 10 μm . The right image provides higher magnification of the selected area. Scale bar = 5 μm .

3.3.1. Cell-selective metabolic labeling of newly postsynaptic proteins

Cell-selective metabolic labeling was applied in cultured hippocampal neurons as an attempt to selective visualization of newly synthesized proteins at postsynaptic densities. Non-canonical amino acids were used to achieve the selective protein labeling, which is omitted by the endogenous translation machinery and are not used in protein synthesis (Ngo et al., 2009). In this thesis, the mutant LtoGMetRS, capable of charging the non-canonical amino acid azidonorleucine (ANL) into recombinant proteins (Dr. A. Müller, doctoral thesis, 2012; Müller et al., 2015), was utilized to perform cell-selective metabolic labeling. The incorporation of ANL into new proteins facilitates the selective visualization of newly synthesized proteins in a specific manner. This approach provides us with the ability to differentiate and detect new proteins made in neurons expressing LtoGMetRS from those made in neurons expressing wild-type MetRS (WTMetRS).

Cell-selective incorporation (GINCAT; Dr. A. Müller, doctoral thesis, 2012) of ANL into newly synthesized proteins was verified in HEK293 cells transfected with pSDT-GFP construct bearing the WTMetRS or mutant LtoGMetRS. Transfected cells were incubated with ANL or Met for 2 h, subsequently, the cell lysates were subjected to tagging reaction by Cu(I)-catalyzed conjugation to DST-tag (BONCAT) (Materials and Methods). Western blot analysis showed that ANL-harboring proteins (biotin signal) were restricted to samples from cells expressing LtoGMetRS, covering the entire

molecular weight range (Figure 12). Control samples from cells expressing WTMetRS were inactive to ANL as suggested by the absence of biotin signal. Similarly, biotin signal was not observed in cells incubated with Met (Figure 12), demonstrating the specificity of cells expressing LtoGMetRS for ANL incorporation.

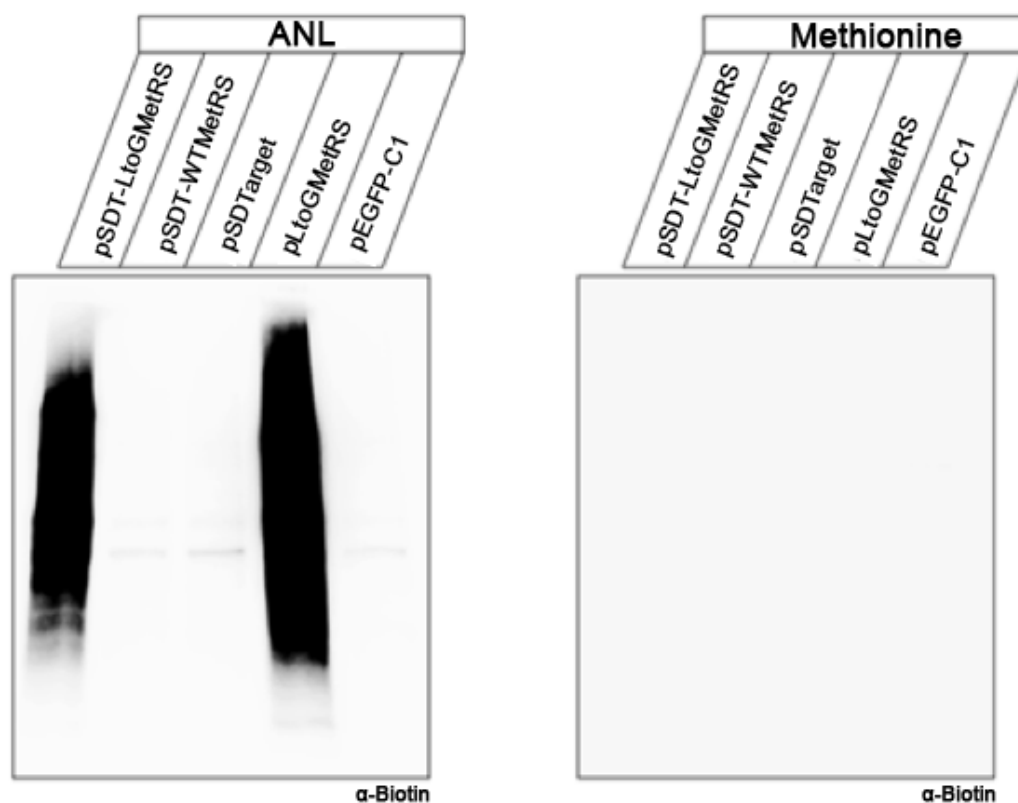


Figure 12. Cell-selective incorporation of ANL into newly synthesized proteins. ANL-bearing proteins from HEK293 cells transfected with pSDT-LtoGMetRS-GFP or pLtoGMetRS were detected by Western blot analysis. Newly synthesized proteins only from cells expressing LtoGMetRS are able to incorporate ANL. pEGFP-C1, pWTMetRS-GFP, and pSDTarget-GFP vector were used as a control. ANL-bearing proteins were detected with a α -biotin antibody. Biotin signal was not detected in cells treated with Methionine. 20 μ l of sample was loaded per lane.

3.3.2. Visualization of newly synthesized proteins at postsynaptic terminals

Next, hippocampal neurons (DIV7) were transfected with pSDT-LtoGMetRS-GFP, pSDT-WTMetRS-GFP, pSDT-GFP or pLtoGMetRS-GFP constructs. Labeling of neuronal cultures was performed as described above (Material and Methods). After 2 h of incubation with either ANL or Met, neurons were fixed, permeabilized, and subsequently subjected to “click chemistry” reaction by Cu (II)-catalyzed conjugation to Tamra-alkyne tag (FUNCAT). Qualitative analysis showed that newly synthesized proteins were detected in neurons expressing both pSDT-LtoGMetRS-GFP and pLtoGMetRS-GFP constructs (Figure 13A).

The results were consistent with GINCAT experiments from transfected Hek293T cells analyzed by Western blot (Figure 12), thus ANL incorporation is ensured only when LtoGMetRS is expressed (Figure 12 and Figure 13). Tamra signal was restricted to neurons expressing LtoGMetRS (Figure 13A). Control neurons expressing pWTMetRS-GFP, pSDT-GFP or pGFP-C1 were inert for ANL labeling, as indicated by the absence of Tamra signal (Figure 13A). Increased levels of newly synthesized proteins (Tamra intensity) were detected at postsynaptic areas; however, newly synthesized proteins were also detected along somatodendritic processes (Figure 13A). As expected, either Tamra (Figure 13B) or biotin signal (Figure 12) was not observed in cells treated with Met.

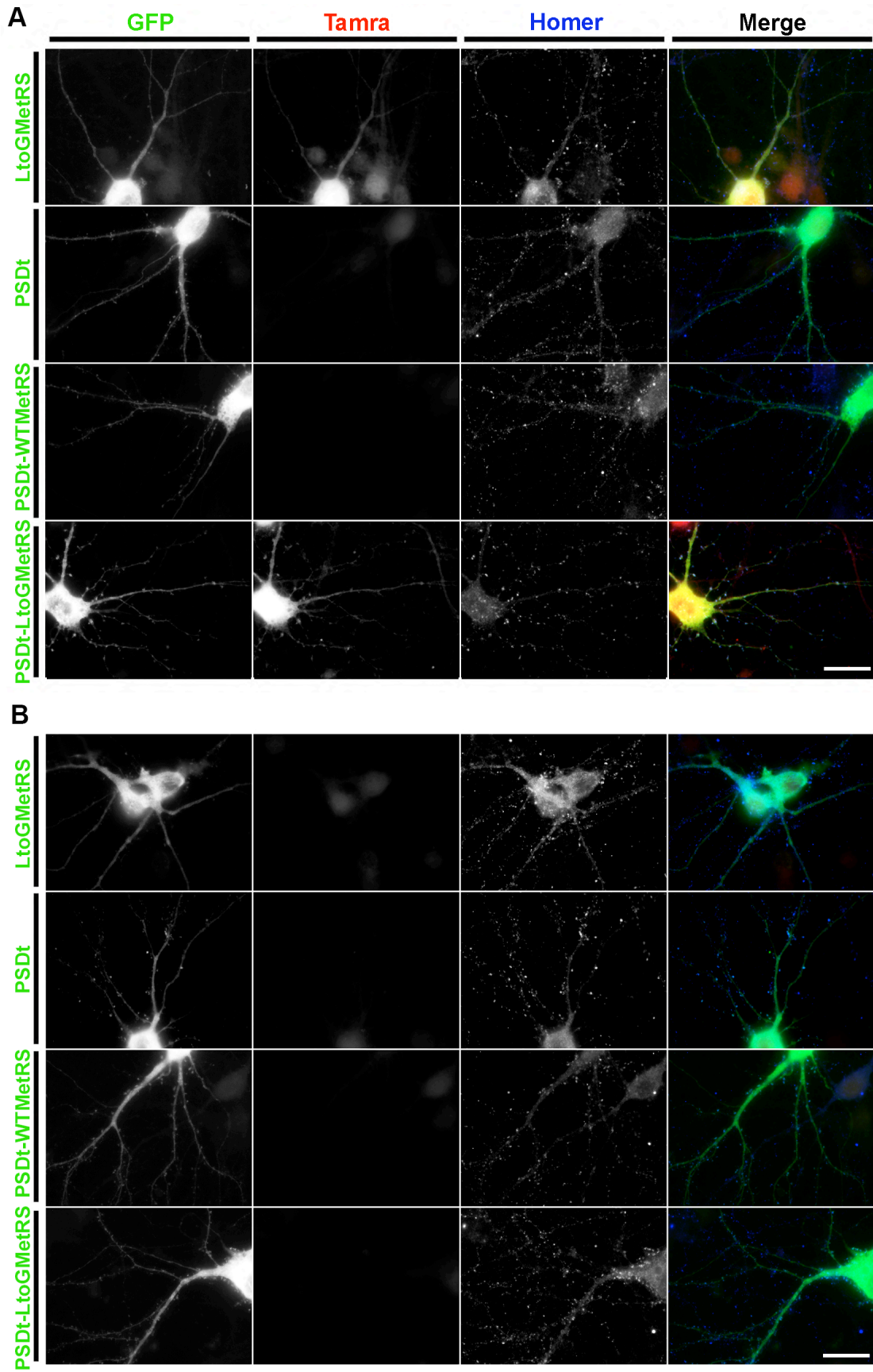


Figure 13. Metabolic labeling of newly synthesized proteins at postsynaptic areas using the FUNCAT method. Transfected hippocampal neurons (DIV15) were incubated for 2 h with 4 mM ANL (A) and 4 mM methionine (B), clicked to Tamra-alkyne tag and subsequently stained for the postsynaptic marker (Homer1, blue). Tamra signal is detectable only in neurons expressing LtoGMetRS. Specific protein synthesis at postsynaptic sites was noticed as an accumulation of Tamra signal at synaptic sites in neurons transfected with the pSDT-LtoGMetRS-GFP construct. Tamra signal is not detected in neurons treated with Met (B). Representative images from three independent experiments are shown. Scale bar = 10 μ m.

3.4. Targeting of LtoGMetRS to presynaptic terminals

Tau is a neuron-specific protein, found mainly in axons, relevant for microtubule stabilization (Aronov et al., 1999). The regulation of tau mRNA localization includes specific sequence elements located within its 3'UTR, one of such elements comprises a fragment containing 240 base pairs (fragment H: 2519-2760; Gen Bank: X79321.1), which has been shown to be required for axonal targeting and tau mRNA stabilization (Aronov et al., 2001). Therefore, the fragment H might be a useful tool to study targeting and subcellular localization of fusion proteins in neuronal cells.

To enable the investigation of protein synthesis at presynaptic processes during development, we designed a series of constructs containing both the fragment H and LtoGMetRS sequence. The fragment H (Cod-H) was cloned into a pEGFP-C1 vector (Supplementary Figure S2) in order to prove axonal targeting. Similarly, both Cod-H and LtoGMetRS sequences were introduced into pEGFP -GFP vector to examine the axonal expression of MetRS (Figure 14). Hippocampal neurons (DIV3) were transfected with either pCod-H-GFP or pCod-H-LtoGMetRS-GFP construct and pEGFP-C1 vector as a control. After 24h (DIV4), the GFP expression pattern showed no specific targeting into axonal processes (Figure 14). In addition, we did not observe axonal GFP expression after overexpressing the fusion proteins for additional days before proceeding with immunofluorescence staining (DIV 8)

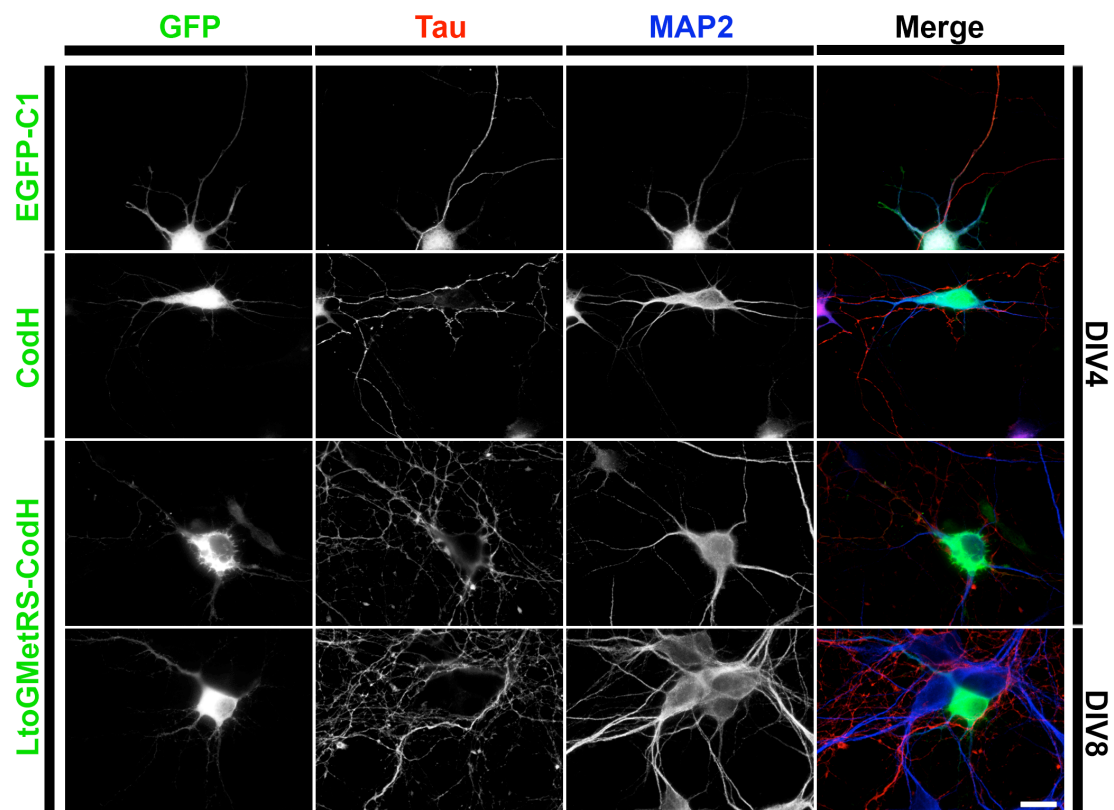


Figure 14. LtoGMetRS-GFP expression using Cod-H as a targeting sequence cloned in the pEGFP-C1 vector. Hippocampal neurons (DIV3) were transfected with pCod-H-GFP or pLtoGMetRS-Cod-H-GFP construct to investigate protein translation in axons. Cells were fixed and immunostained for axonal (Tau, red) and dendritic (MAP2, blue) markers 24 h (DIV4) or 120 h (DIV8) after transfection. Not apparent axonal expression of the pLtoGMetRS-Cod-H-GFP construct was observed in both time points. Shown are representative images from three independent experiments. Scale bar = 10 μ m.

(Figure 14, lower panel). Furthermore, cloning the open reading frame from the tau sequence (ORFTau, *Mus musculus*; Gen Bank: 17762) (Supplementary Figure 2) into these constructs did not change the GFP expression pattern (Figure 15).

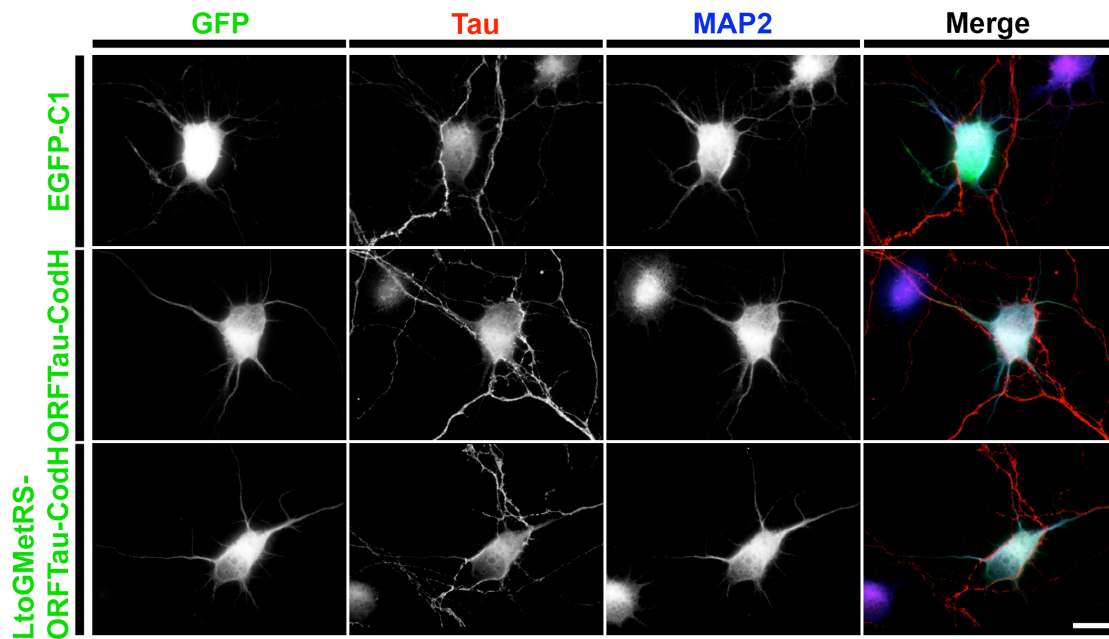


Figure 15. LtoGMetRS-GFP expression using ORFTau and Cod-H as targeting sequences cloned in the pEGFP-C1 vector. Hippocampal neurons (DIV3) were transfected with both pORFTau-Cod-H-GFP and pLtoGMetRS-ORFTau-Cod-H-GFP constructs to investigate protein translation in axons. Neurons were fixed and immunostained for axonal (Tau, red) and dendritic (MAP2, blue) markers 24 h after transfection. Axonal expression of fusion proteins was not observed using both constructs. Images are representative of three independent experiments. Scale bar = 10 μ m.

In order to avoid potential negative effect due to the additional size conferred by the GFP sequence, we changed our GFP expression system to one containing the c-myc tag such as pCMV-Tag3B and pCDNA 3.1myc vector. Therefore, in a separate set of experiments, two different constructs containing either the ORFTau and Cod-H or both and the LtoGMetRS sequence was designed using pCMV and pcDNA vector (Supplementary Figure S3).

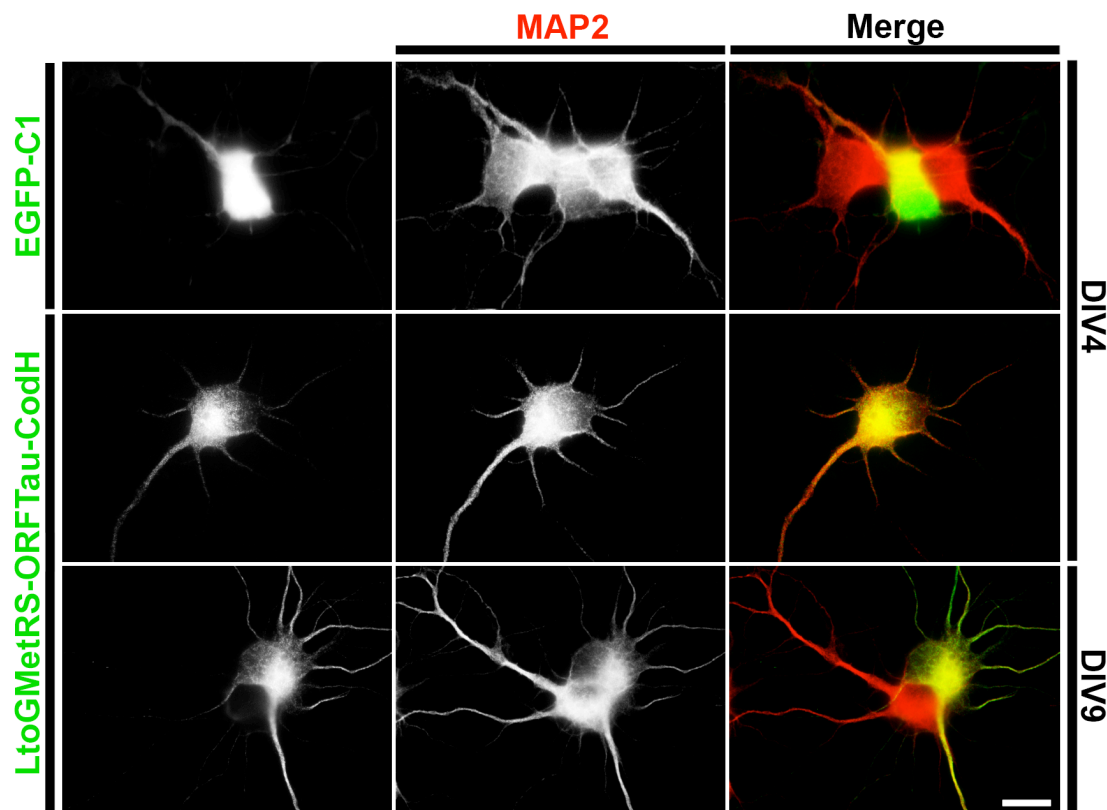


Figure 16. LtoGMetRS expression using ORFTau and Cod-H as targeting sequences cloned in the pCMV vector. Hippocampal neurons (DIV3) were transfected with the pLtoGMetRS-ORFTau-Cod-H construct to study protein translation in axons. Neurons were fixed and immunostained for the c-myc tag (green) and dendritic marker (MAP2, red) 24 h (DIV4) or 144 h (DIV9; lower panel) after transfection. Antibody against c-myc epitope was used to detect fusion protein expression. Axonal expression was not observed; note the similar MAP2 expression pattern of the fusion protein. Representative images from three independent experiments are shown. Scale bar = 10 μ m.

Neurons expressing the pLtoGMetRS-ORFTau-Cod-H-c-myc construct, cloned in pCMV vector, did not exhibit a targeting of the fusion protein into axonal processes 24 h (DIV4) after transfection or after long-term expression (DIV9) (Figure 16).

In contrast, neuronal cultures (DIV3) transfected with the pORFTau-Cod-H construct, cloned in pcDNA vector, revealed a subcellular axon-like expression of the fusion protein 24 h (DIV4) after transfection. A substantial expression in axons of the fusion protein was observed after long-term expression (DIV9) (Figure 17).

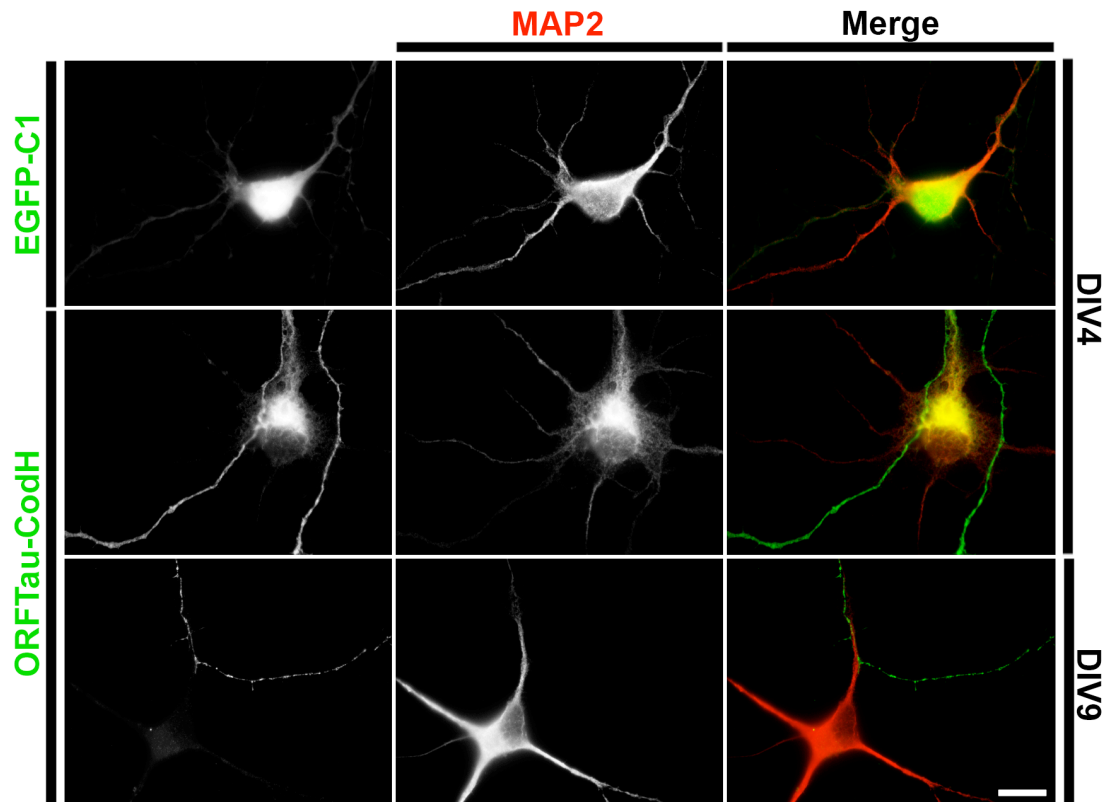


Figure 17. Axon-like expression of the fusion protein using ORFTau and Cod-H as targeting sequences cloned in the pcDNA vector. Hippocampal neurons (DIV3) were transfected with the pORFTau-Cod-H construct. Cells were fixed and immunostained for the c-myc tag (green) and dendritic marker (MAP2, red) 24 h (DIV4) or 144 h (DIV9; lower panel) after transfection. Fusion protein expression was detected using an antibody against c-myc epitope. Axon-like expression was observed in cells transfected with the pORFTau-Cod-H construct in both time points. Note the specific axonal targeting after long-term expression (DIV9; lower panel). Shown are representative images from three independent experiments. Scale bar = 10 μ m.

The fusion protein exhibited a widespread expression along axon-like processes after long-term expression, extending its expression pattern into noticeable presynaptic terminals (See bouton magnification, Figure 18).

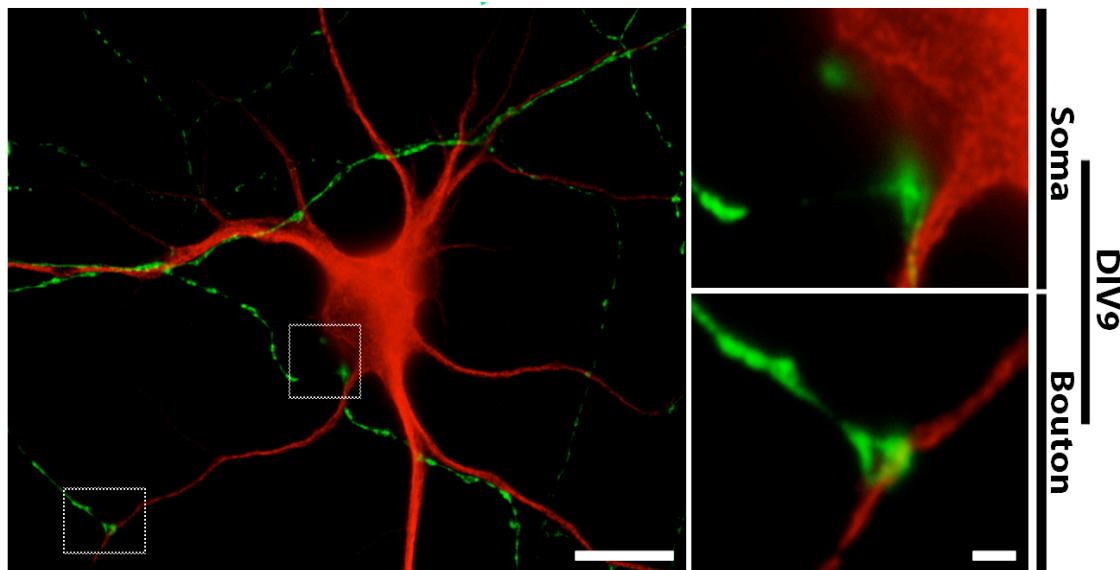


Figure 18. Long-term expression of the fusion protein in a neuron expressing the pORFTau-Cod-H construct. Hippocampal neuron (DIV9) transfected with the pORFTau-Cod-H construct, highlighting axon-like expression of the fusion protein from the soma (right, upper box), and receiving a synaptic contact from a different cell (right, lower box). Antibody against c-myc epitope (green) was used to detect fusion protein expression. Representative image from three independent experiments is shown. Scale bar left = 10 μm . Scale bar right, lower box = 3 μm .

3.4.1. Cell-selective metabolic labeling of newly synthesized proteins

Once established a suitable targeting system, the mutant LtoGMetRS was cloned into our targeting system as an attempt to study local protein synthesis at presynaptic compartments. Expression of the fusion protein was confirmed by western blot using samples from Hek293T cells transfected with pLtoGMetRS-ORFTau-Cod-H, and antibodies against c-myc epitope, Tau, and MetRS (Supplementary Figure S4). ANL-harboring proteins were detected in samples from transfected cells expressing LtoGMetRS after GINCAT procedure (Figure 19).

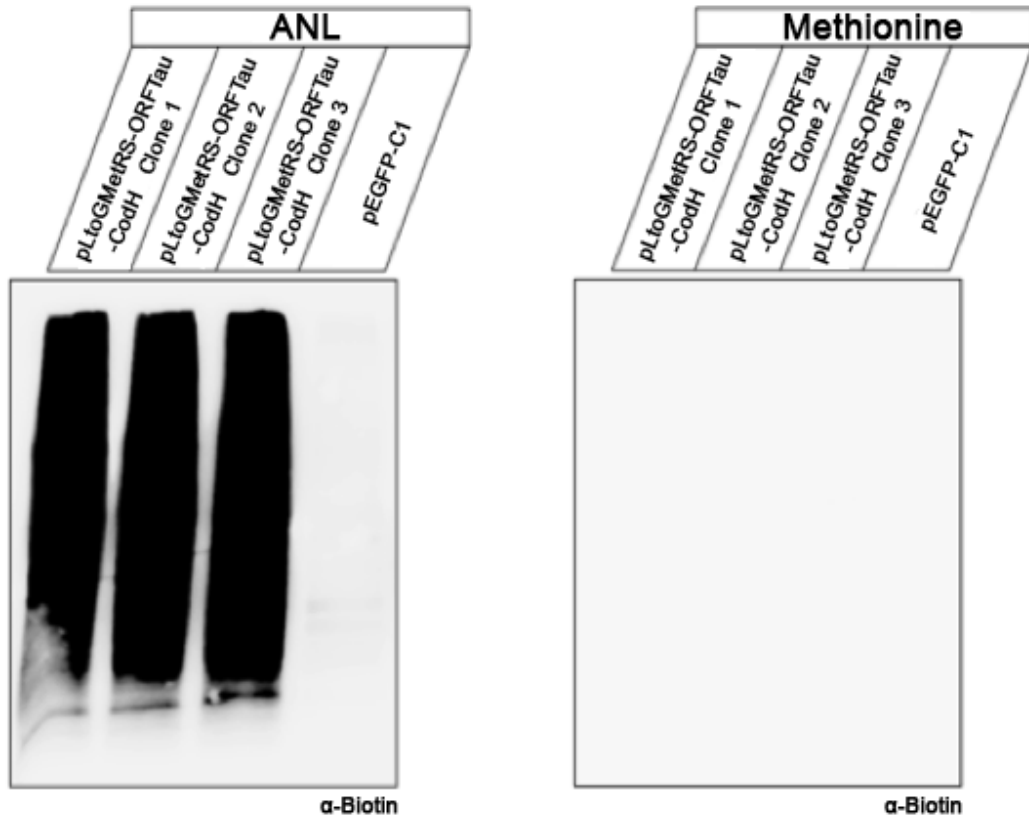


Figure 19. ANL incorporation into newly synthesized proteins using the pLtoGMetRS-ORFTau-Cod-H construct. Western blot analysis for ANL-bearing proteins from transfected HEK293 cells with different pLtoGMetRS-ORFTau-Cod-H clones. Cells expressing LtoGMetRS are able to incorporate ANL for protein synthesis. The pEGFP-C1 vector was used as a control. ANL-bearing proteins were detected with a α -biotin antibody. Biotin signal was not detected in cells treated with Methionine. 20 μ l of sample was loaded per lane.

However, axon-like expression of the fusion protein previously detected for the pORFTau-Cod-H construct was not observed after cloning the mutant LtoGMetRS (Figure 20).

3.4.2. Visualization of newly synthesized proteins at presynaptic terminals

In contrast to the ability of HEK293 cells transfected with the pLtoGMetRS-ORFTau-Cod-H construct to incorporate ANL (Figure 19), neurons expressing this construct fails to express the fusion protein in axon-like processes, therefore the labeling of newly synthesized proteins was

indistinguishable in axons (Figure 21A and 21B). The misplaced protein sorting to axonal processes suggests that the incorporation of the mutant LtoGMetRS into the targeting system might interfere with the tau axonal localization signals recognized by the cytoskeleton, preventing the proper mRNA transport into axons.

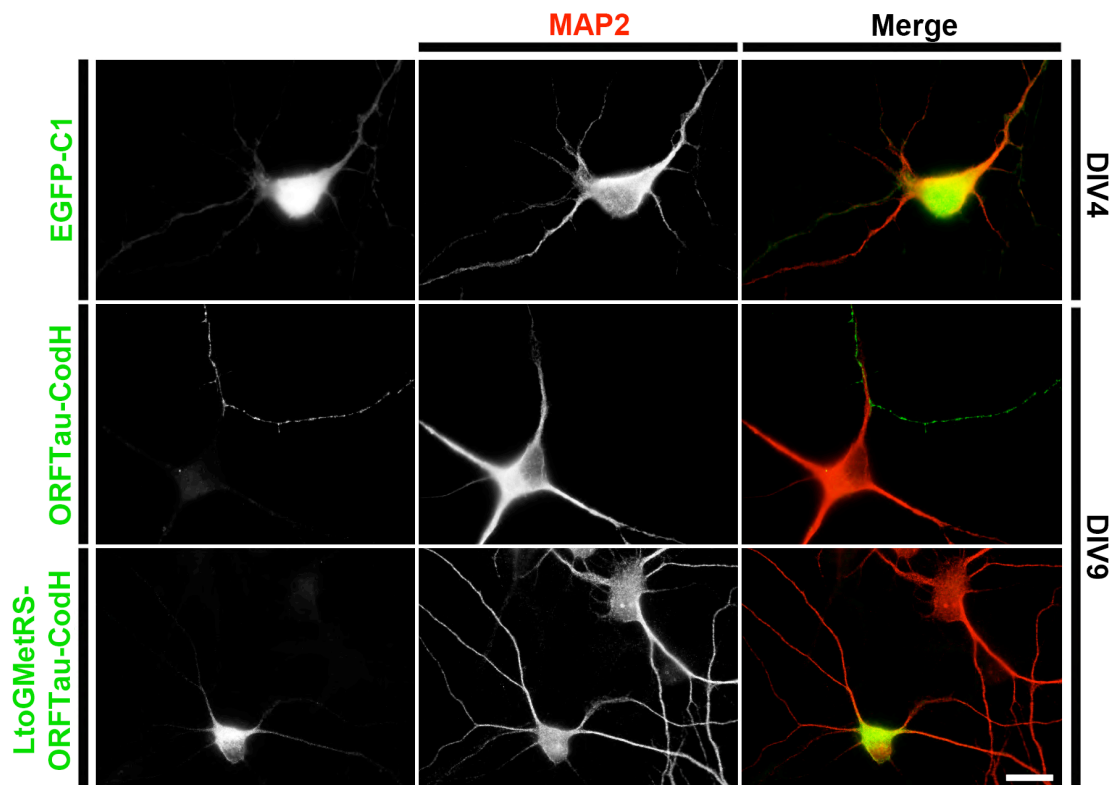


Figure 20. Axon-like expression of the fusion protein is lost after LtoGMetRS incorporation into the pORFTau-Cod-H construct. Hippocampal neurons (DIV3) were transfected with both pORFTau-Cod-H and pLtoGMetRS-ORFTau-Cod-H constructs to investigate axonal protein synthesis. Cells were fixed and immunostained for the c-myc tag (green) and dendritic marker (MAP2, red) 144 h (DIV9) after transfection. Note that axon-like expression was prevented after LtoGMetRS incorporation (DIV9; lower panels). Images are representative of three independent experiments. Scale bar = 10 μ m.

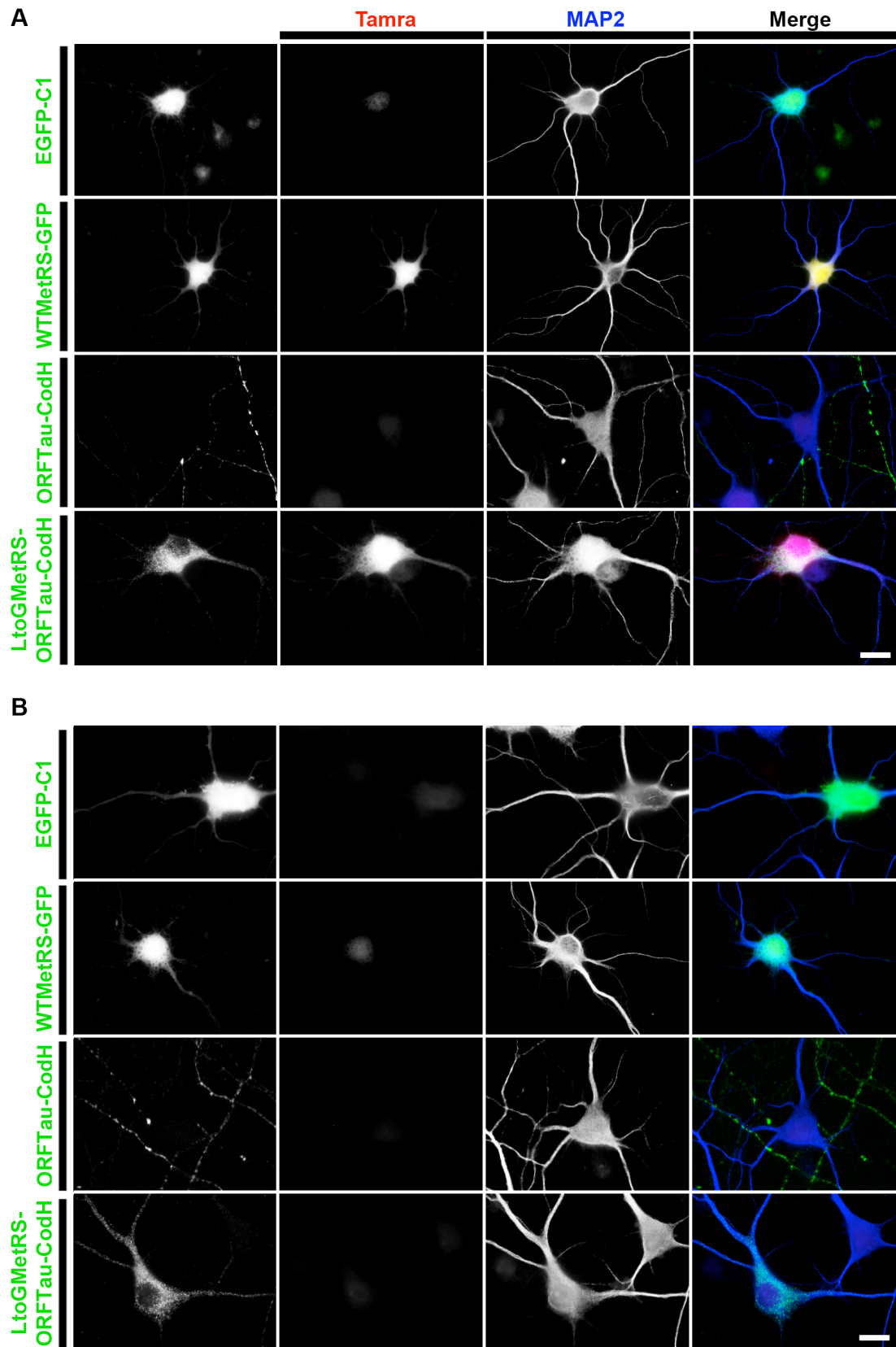
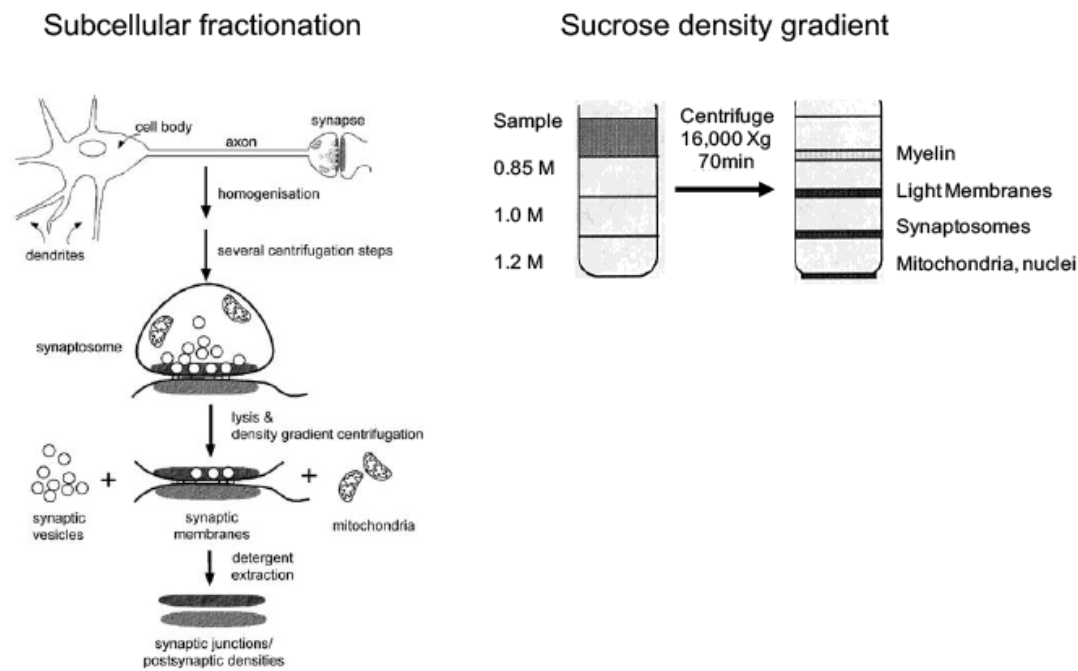


Figure 21. Metabolic labeling of newly synthesized proteins at presynaptic terminals using FUNCAT. Hippocampal neurons (DIV10) transfected with the pORFTau-Cod-H construct containing or not LtoGMetRS were incubated for 2 h with 4 mM ANL (A) or 4 mM methionine (B), clicked to Tamra-alkyne tag and immunostained for the dendritic marker MAP2 and c-myc tag. Tamra signal is detected in soma and dendrites only in neurons expressing LtoGMetRS, however, axonal newly synthesized proteins are not detected in neurons transfected with the pLtoGMetRS-ORFTau-Cod-H construct. Tamra signal is not detected in neurons treated with Met (B). Shown are representative images from three independent experiments. Scale bar = 10 μ m.

3.5. Isolation and characterization of synaptic structures from primary cortical cultures

Several proteomic studies have analyzed the subcellular proteome of synapses by isolating subcellular structures such as synaptosomes, synaptic vesicles, and membranes, using well-established fractionation procedures (Stadler and Tashiro, 1979; Sherman, 1989; Krapfenbauer et al., 2003). In this thesis, a subcellular fractionation procedure was utilized for the enrichment of synaptic proteome from neuronal cultures, as described previously by Gundelfinger and Tom Dieck (2000) (Figure 22). The enrichment of isolated synaptosomes can be examined by biochemical analysis using pre and postsynaptic markers, or electron microscopy to inspect the synaptosomal integrity. The following section describes the results obtained from a modified protocol of a traditional fractionation procedure to isolate synaptosomes from primary cortical neuron cultures.



Gundelfinger E. and tom Dieck S. *Naturwissenschaften*. 2000

Figure 22. Subcellular fractionation procedure for the enrichment of synaptic structures. Taken from Gundelfinger and tom Dieck, 2000.

In this study, the relative enrichment of synaptic proteins and translation machinery components was examined by Western blotting using neuronal fractions obtained from subcellular fractionation of primary cortical cultures (DIV8 and DIV18) (Figure 23). Pre and postsynaptic proteins (synaptophysin and PSD-95, respectively) were substantially enriched in synaptosome fractions at early time points (DIV8) and highly enriched in fractions from mature cultures (DIV18) (Figure 23). On the other hand, no significant levels of GFAP protein, an astrocyte marker, were detected in synaptosome fractions, confirming that our procedure favorably excludes glial components (data not shown). As a result, a consistent procedure was established to isolate and enrich the synaptic proteome from primary cortical neuron cultures. In addition, different translation machinery components such as MetRS, eEF2, eIF4E factor and S6 ribosomal protein were enriched in synaptosome fractions at early and mature developmental stages. As expected, the glutamate receptor subunit GluR2 was more abundant in mature neuronal cultures (Figure 23). Taking together, substantial enrichment of pre and postsynaptic proteins, as well as translation machinery

components found in immature cultures, suggests an active demand for protein synthesis at synaptic structures already from early developmental stages.

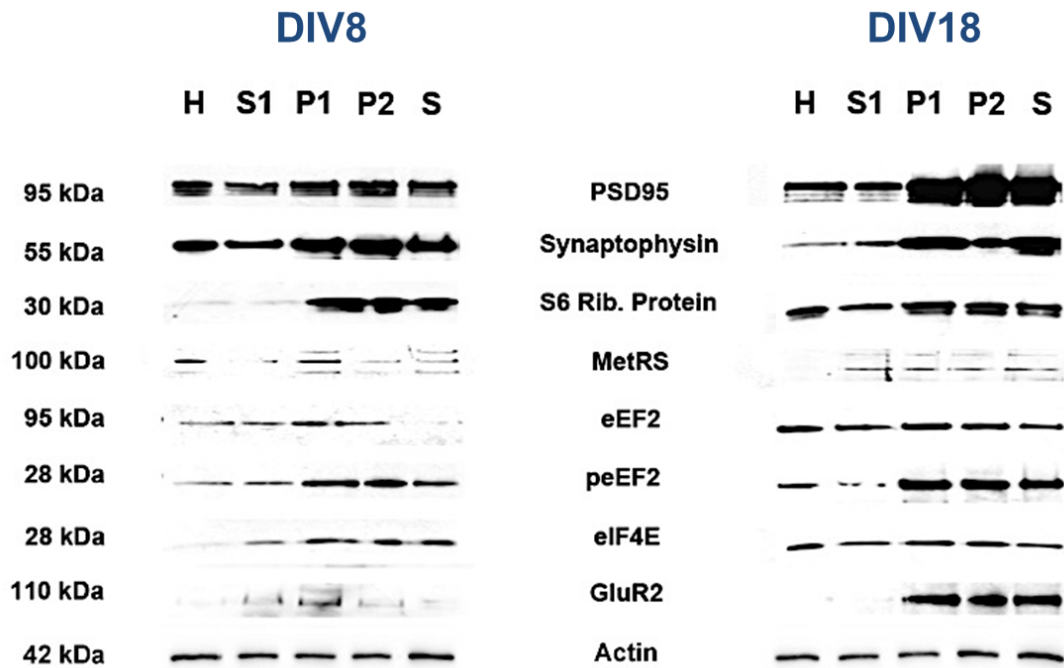


Figure 23. Protein enrichment in neuronal fractions isolated from primary cortical neuron cultures. Identification of synaptic and translation machinery components in neuronal fractions isolated from- immature and mature primary cortical neuron cultures. (H) Homogenate: disruption of the cellular organization; (S1) S1 fraction: soluble proteins, cytoplasmic fraction; (P1) P1 fraction: nuclei, cell debris; (P2) P2 fraction: nuclear fraction, mitochondria, synaptic structures; (S) Synaptosome fraction. Ten μg of total protein was loaded per fraction.

3.6. Developmental changes in the synaptic proteome of synaptosomes

Neuronal processes respond to diverse environmental changes by synthesizing new proteins. Consequently, methods to enrich and identify the newly synthesized synaptic proteome are desired to establish a global assessment of developmental changes in the synaptic proteome. The goal of the following experiments was to examine the spatial-temporal characteristics of the synaptic proteome by determining the molecular changes occurring at synaptic structures during development using the BONCAT technique, which enables detection and purification of newly synthesized proteins (Dieterich et al., 2006).

3.6.1. Metabolic labeling of newly synthesized proteins in neuronal cultures using BONCAT

Analysis of AHA incorporation into the total cellular proteome was performed in primary cortical cultures. For this purpose, primary cortical neurons (DIV17) were incubated for 2 h with AHA or methionine as a control. Methionine and AHA-treated neurons were homogenized and their lysates were tagged with the biotin-alkyne tag as described previously (Materials and Methods). After the “click” reaction, samples analyzed by Dot blot revealed effective AHA incorporation into the neuronal proteome, asserting the ability to detect newly synthesized proteins in neuronal lysates from primary cortical cultures. The high specificity of protein labeling was endorsed by the intense signal detected in AHA-treated neurons, as no signal was detected in neurons treated with methionine (Figure 24A).

Quantitative analysis of global newly synthesized proteins levels revealed that AHA incorporation into the cellular proteome was enriched in circa 42 ng/ μ l (Figure 24B) within an interval of 2 h. Quantitative ratio between newly synthesized proteins and the total protein content showed that a small fraction (3.6%) of the cellular proteome was newly synthesized during an interval of 2 h (Figure 24C).

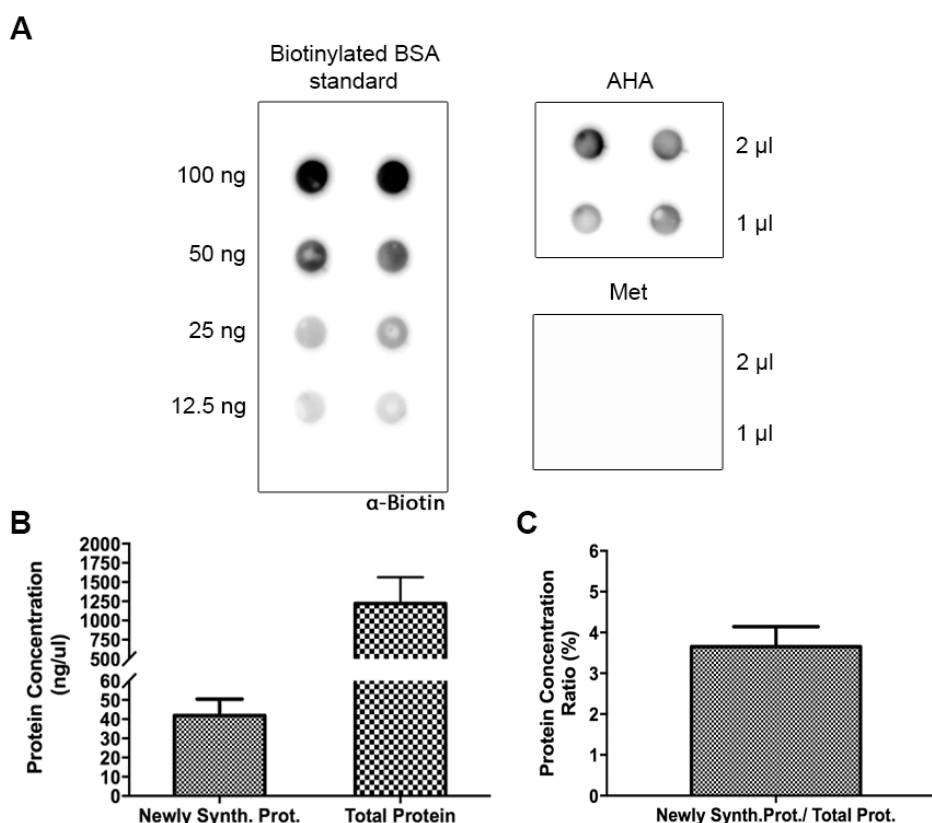


Figure 24. Metabolic labeling of newly synthesized proteins in primary cortical neurons. (A) Neural homogenates (DIV17) were prepared after 2 h of metabolic labeling using AHA or methionine as a control. ‘Click’ chemistry reaction (Vol. reaction mix: 1 ml) was applied and the AHA-bearing proteins were detected by Dot blot using α -biotin antibody. Approximately 30 million primary cortical neurons were used per condition. Duplicates of each condition are shown. Representative blots from three independent experiments. (B) Protein concentration (ng/ μ l) of newly synthesized proteins estimated semi-quantitatively from integrated densities of each dot. (C) Ratio (%) between newly synthesized proteins and total protein concentration.

3.6.2. Identification of newly synthesized proteins in synaptosomes

BONCAT method was performed in synaptosomes in order to describe the molecular profiles characteristic for the synaptic proteome synthesized during development (Figure 25). Primary cortical neuron cultures were incubated for 2 h with both AHA and d_{10} Leu (4mM) and, thereafter, synaptosome fractions were isolated by subcellular fractionation. The total protein content was solubilized and the “click” reaction was applied afterward. In the course of the “Click chemistry” reaction, newly synthesized proteins

were tagged with a DST-alkyne tag (Szychowski et al., 2010), incubated with NeutrAvidin beads, and subsequently released from the beads using β -Mercaptoethanol. Proteomic analysis was conducted by mass spectrometry (MS/MS) in collaboration with Dr. Thilo Kähne (Institute of Experimental Internal Medicine, Otto von Guericke University).

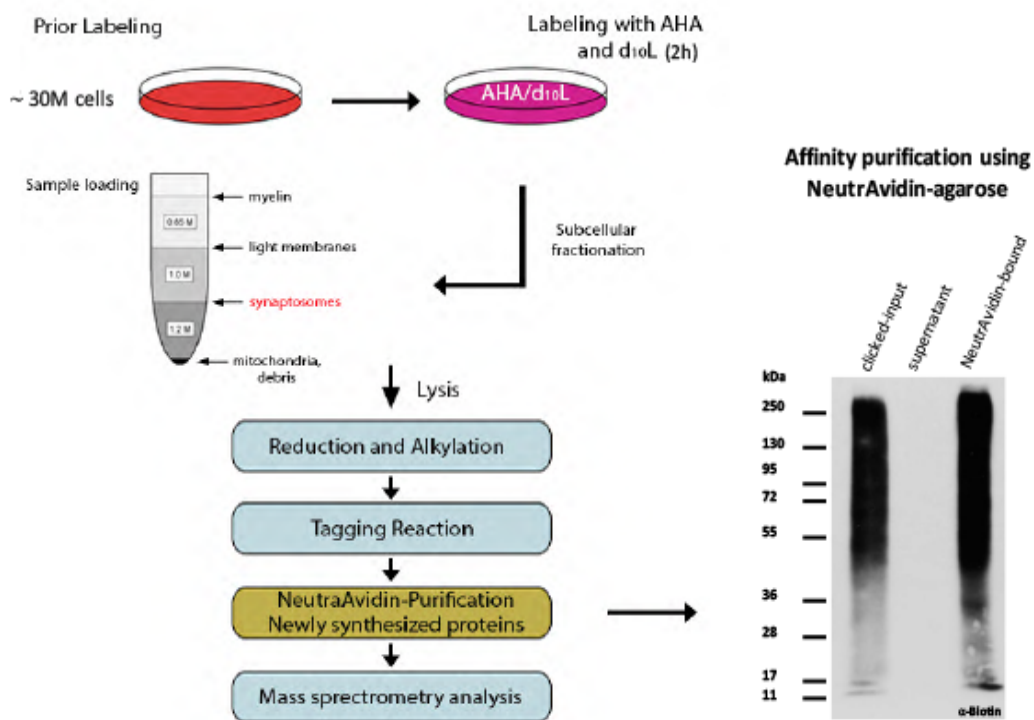


Figure 25. Detection, purification, and identification of newly synthesized proteins in synaptosomes. Primary cortical cultures were incubated for 2 h with AHA and d10 Leu (4mM), which is used as an additional validation component. Labeled proteins derived from isolated synaptosomes were detected via click reaction with DST-biotin-alkyne probe, purified by affinity purification and analyzed by mass spectrometry.

Figure 26A shows the levels of AHA-bearing proteins in the tested developmental stages. Quantitative analysis revealed no statistically significant difference in the levels of newly synthesized proteins during the analyzed developmental stages (Figure 26B).

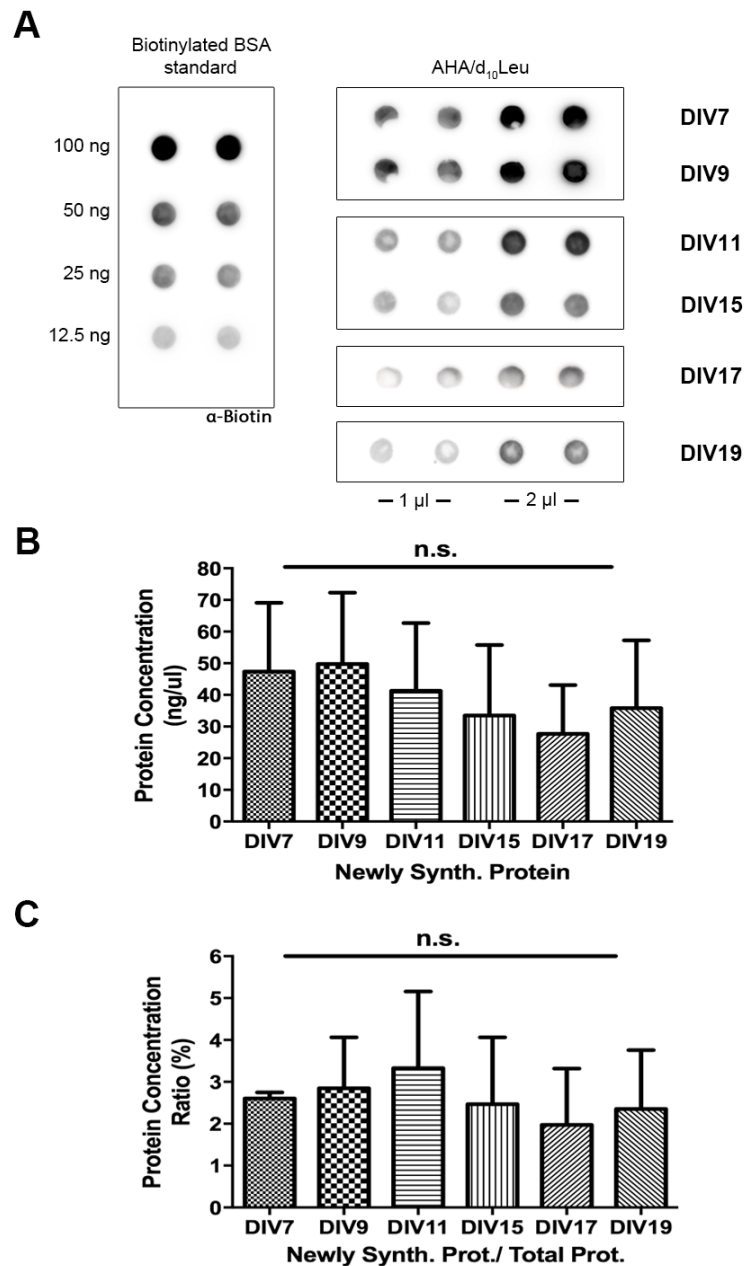


Figure 26. Metabolic labeling of newly synthesized proteins in synaptosomes from primary cortical neuron cultures. (A) Synaptosomes were isolated from primary cortical neuron cultures after 2 h of metabolic labeling using AHA and d₁₀Leu. The ‘Click’ reaction (Vol. reaction mix: 1 ml) was applied to samples of synaptosomes isolated from primary cortical neuron cultures at different developmental stages. Subsequently, AHA-bearing proteins were detected on Dot blots using α-biotin antibody. Newly synthesized proteins were analyzed in synaptosomal fractions isolated from primary cortical neuron cultures seeded with approximately 30 million neurons. Duplicates of each sample are shown. Representative blots from three to four independent experiments per time point. (B) Protein concentration (ng/µl) of newly synthesized proteins estimated from the integrated densities. (C) Ratio (%) between

newly synthesized proteins and total protein concentration. $P < 0.05$; one-way ANOVA with Tukey multiple-comparison testing.

The fraction of newly synthesized proteins was bigger during early and intermediate developmental stages (DIV7-11), reaching lower levels at mature stages, suggesting that a higher demand for protein synthesis might be required for the establishment of new synaptic contacts observed, for example, at intermediate developmental stages (DIV11) (see section 3.1, Figure 8E).

Quantitative representation by acquiring the ration between newly synthesized proteins and total protein concentration revealed low levels of newly synthesized proteins (ranging from 2 to 3.3%) related to the total protein content; no statistically significant difference ($P < 0.05$) was detected between all developmental stages (Figure 26C). Despite this, the highest level of newly synthesized proteins (3.3%) relative to the total proteome was noticed at intermediate developmental stage (DIV11).

Next, the synaptosomal samples were analyzed by tandem MS/MS. The identified proteome is composed of heterogeneous synaptic proteins, including scaffolding proteins, adhesion molecules, pre and postsynaptic proteins, metabotropic and ionotropic receptors, synaptic vesicles proteins, components of protein translation and degradation machinery, signaling molecules as well as cytoskeletal proteins (Supplementary Table 6, 7, 8 and 9). The proteome is connected with relevant network functions related to nervous system development, cell morphology, post-translational modification, cellular assembly, and organization, among others (data not shown). A high percentage of identified newly synthesized proteins were associated with synaptic compartments as derived from SynProt, a comprehensive detergent-resistant synaptic junction protein database (Pielot et al., 2012) (Table 4). Similarly, our proteomic data was validated using a neuropil transcriptome database (Cajigas et al., 2012) to distinguish proteins specifically synthesized in dendrites and axons (Table 4).

Table 4. Summary of the newly synthesized synaptic proteome

Proteins	Total	SynProt	Local Transcriptome	MS/MS	Samples
DIV7	201	48 (24%)	40 (20%)	2	3
DIV9	192	42 (22%)	47 (25%)	2	3
DIV17	249	53 (21%)	46 (19%)	2	4
DIV19	257	62 (24%)	49 (19%)	2	3

A summary table including the number and percentage (%) of proteins found in both Synprot (Pilot et al., 2012) and neuropil transcriptome database (Cajigas et al., 2012), in addition to the number of MS analysis and samples for each time point.

In addition, some proteins with exceptional long lifespans were noticed as we confirmed in a long-lived proteins list from Toyama et al. (2013) (Table 5), which might provide valuable information about long-term protein complex (e.g. CSPG2) as well as development-dependent damage accumulation (Toyama et al., 2013).

For systematic comparative analysis, we used Ingenuity IPA software to identify common molecules across protein lists. As a result, we identified Apolipoprotein B (APOB; Entrez ID: 54225) as the sole common protein among the protein lists from the analyzed developmental stages. Although APOB was associated with synaptic compartments (Synprot), its mRNA is not identified in the local transcriptome database (Cajigas et al., 2012).

The fact that a fraction of identified proteins is associated with synaptic structures as well as mRNA transcripts of these identified proteins are found in dendrites and axons, suggests that these identified proteins might be locally synthesized during neuronal development.

Table 5. Long-lived proteins

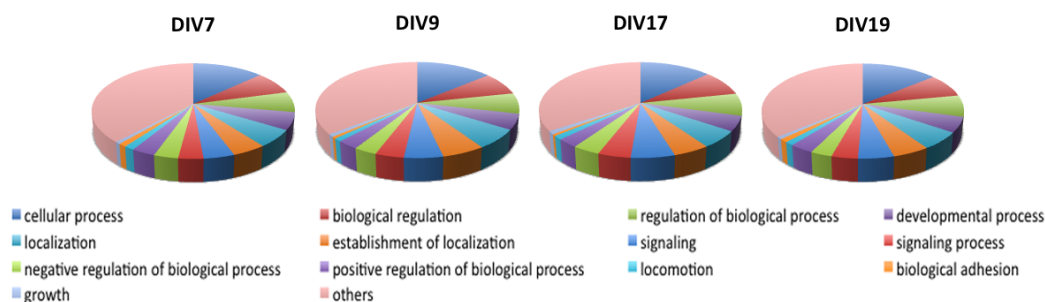
DIV7	DIV9	DIV11	DIV15	DIV17	DIV19
ENPP6		CSPG2	CSPG2	H4	CSPG2
		NUP155			MBP
					PLP1
					NUP85

The table shows proteins that were found in a long-lived protein list from Toyama et al. (2013) for each time point.

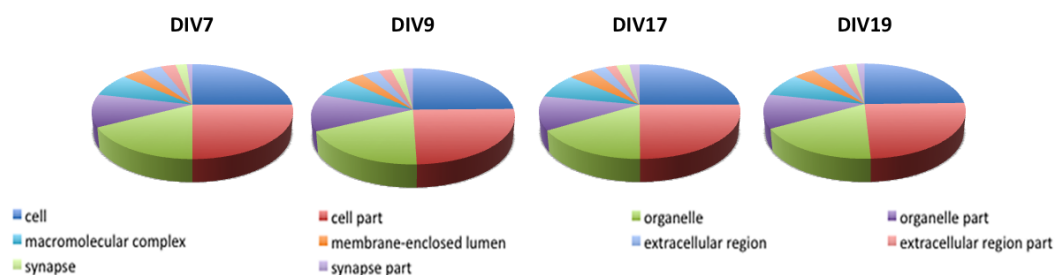
3.7. Gene Ontology analysis of the identified newly synthesized proteins in synaptosomes from primary cortical neuron cultures

The identified newly synthesized protein data set was organized for biological interpretation in the context of Gene Ontology (GO). GO analysis was used to identify the gene and protein functions represented by each identified protein. For this purpose, classification of genes into biologically coherent categories (also called 'terms') was performed using GoMiner software (Zeeberg et al., 2003). The identified newly synthesized proteins represent diverse GO terms related to biological processes, cellular components and molecular functions (Supplementary Table 10). In order to find relevant changes in the synaptic proteome, we compared all data sets between each other by pie charts, displaying the more representative terms from the GO analysis (Figure 27). Accordingly, no significant differences were observed between percentages of proteins associated with prominent GO terms among all-time points and GO domains (Figure 27), however, we noticed changes in the protein composition along the analyzed developmental stages (Table 6).

GO: Biological Process



GO: Cellular Component



GO: Molecular Function

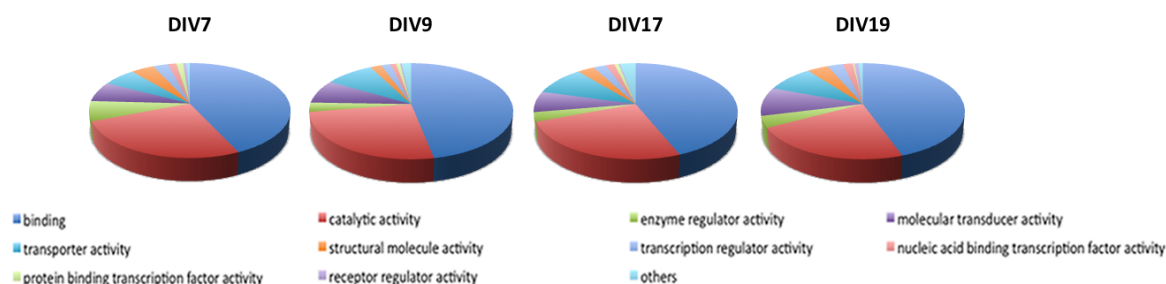


Figure 27. Gene Ontology analysis of the identified newly synthesized proteins in synaptosomes from primary cortical neuron cultures. Pie chart representation of the more prominent GO terms for each GO domain (Biological Process, Cellular Component, Molecular Function). No significant differences were observed between percentages of proteins associated to GO terms in all developmental stages. Samples of identified newly synthesized proteins were analyzed in synaptosome fractions isolated from primary cortical neuron cultures with approximately 30 million neurons. Data represent two sets of MS/MS measurements, using three to four samples of synaptosome fraction per measurement (Table 4). GO analysis was performed using GoMiner software (Zeeberg et al., 2003).

Table 6. GO term example, including gene names of identified newly synthesized proteins for each developmental stage.

GO Term	DIV7	DIV9	DIV11	DIV15	DIV17	DIV19
Axon (GO:0030424)	NRCAM	ACTB	KCNMA1	ERC2	HTT	ACTB
	OPHN1	NTM	HTT	PAFAH1B1	GAD2	GRM3
	ATP1A3	RHOA	GRM7	NRP2	CCK	APP
	GRIK3	ERC2	MYH10	SCN11A	PVALB	NTRK2
	APC	GABBR1	HAP1	DISC1	KLC1	PRX
	GHRL		SCN3A	SCN3A	PRX	BIN1
	MYH10		ERC2	NCDN	CACNA1B	MBP
	TUBB3		PTK2B	ITPR2	ADCY10	
	ANXA3		ITPR2	ILK	DFNB31	
	ITPR2			ADRBK2	DISC1	
	KLHL24			ROBO1	MBP	
				ACTB	IMPA1	
				PTK2B	GRIN2B	
				PTPRN2	NF1	
				MYH10	HTR3A	
				DSCAM	HCN4	
				PYGB	ACTB	
				GRM3	NCAM1	
				CHRM1	ESR1	
				PRX	PRPH	
				GRIN1	ATP1A3	
				ADCY10		
				ALS2		
			LRFN3			
			CHRM4			

Note the change in the protein composition of the Axon GO (GO: 0030424) along the analyzed developmental stages. Despite changes in protein composition, we noticed a set of proteins present in at least three different developmental stages (MYH10, ITPR2, ACTB, PRX, and ERC2).

Next, the development-dependent changes in the synaptic proteome were analyzed using statistical methods to exclude any association resulting from chance. Applying bioinformatics approaches developed by Dr. Rainer Pielot (Leibniz Institute for Neurobiology, Magdeburg, Germany), we observed statistically significant changes ($P < 0.05$; Fisher's exact test) in the number of proteins associated with GO terms which represent proteins involved in transmission, transport, endocytosis, protein trafficking, neurological process, growth, and signaling among others (Figure 28, Supplementary Figure S5 and S6).

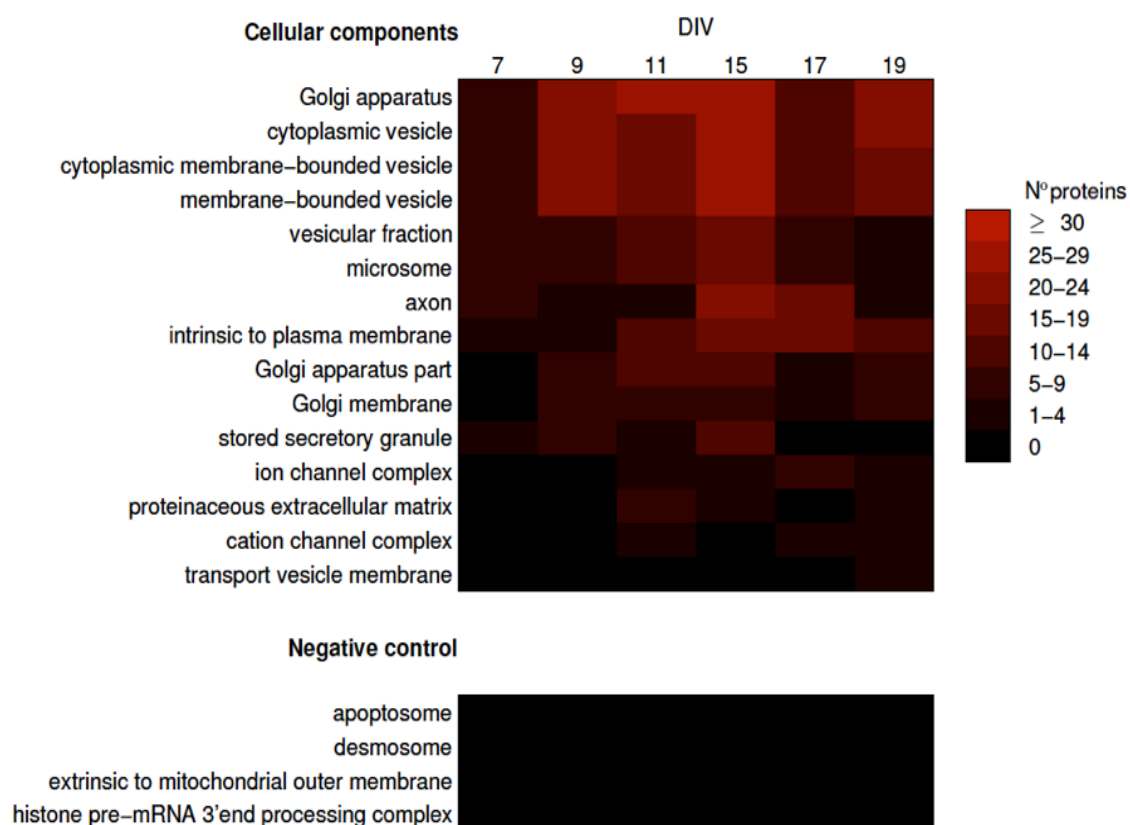


Figure 28. Development-dependent protein enrichment. Heat map illustrates the number of proteins associated with prominent GO terms from the cellular component domain. Significant changes ($P < 0.05$; Fisher's exact test) in the number of proteins associated with cellular components were observed mainly at intermediate developmental stages. Protein enrichment is represented in red. Negative control represents GO terms lacking protein association. All data were obtained from two sets of MS/MS measurements, using three to four samples of synaptosome fraction per time point (Table 4). GO analysis was performed using GoMiner software (Zeeberg et al., 2003).

The **Database for Annotation, Visualization and Integrated Discovery (DAVID)** (Dennis et al., 2003; Huang et al., 2009) and **GeneCodis** (Carmona-Saez et al., 2007; Nogales-Cadenas et al., 2009; Tabas-Madrid et al., 2012) were used as additional web-based software for the functional analysis of gene lists. For gene-enrichment analysis, P -values ($P < 0.05$) were calculated using either the Hypergeometric distribution (GeneCodis) or a modified Fisher Exact P -value (EASE Score) (DAVID). Both softwares provide a comprehensive tool to determine the biological annotations that frequently appear together and are significantly associated with a given set of genes or proteins. Figure 29 shows an enrichment analysis using DAVID software,

highlighting significant P-values associated with each GO term from the biological process domain. Enrichment analyses for the biological process, cellular components and molecular functions domains using both softwares are presented in Supplementary Table 11, 12 and 13, respectively.

Although important differences were detected between DAVID and GeneCodis analysis, mainly on the number of genes and P-values associated with GO terms as well as the frequency of GO terms in all time points, both analyses exhibited major over-representation of GO terms at developmental stages DIV15-17. Amid these annotations, we found a number of important processes associated with neuronal development such as axogenesis, vesicle-mediated transport, microtubule-based movement, synapse assembly, synapse organization, cell adhesion, nervous system development, and learning, among others (Figure 29).

Graphical representation of the data set by heat maps (Figure 28 and 29) revealed that a large group of GO terms exhibited up and down regulation throughout the analyzed developmental stages. Different candidate proteins were selected based on P-values and enriched GO terms associated with fundamental synaptic functions: ERC2 (GO term: synapse assembly, synapse organization), NCAM (GO term: cell adhesion), NR2B (GO term: nervous system development, learning) and NR1 (GO term: synapse assembly, synapse organization).

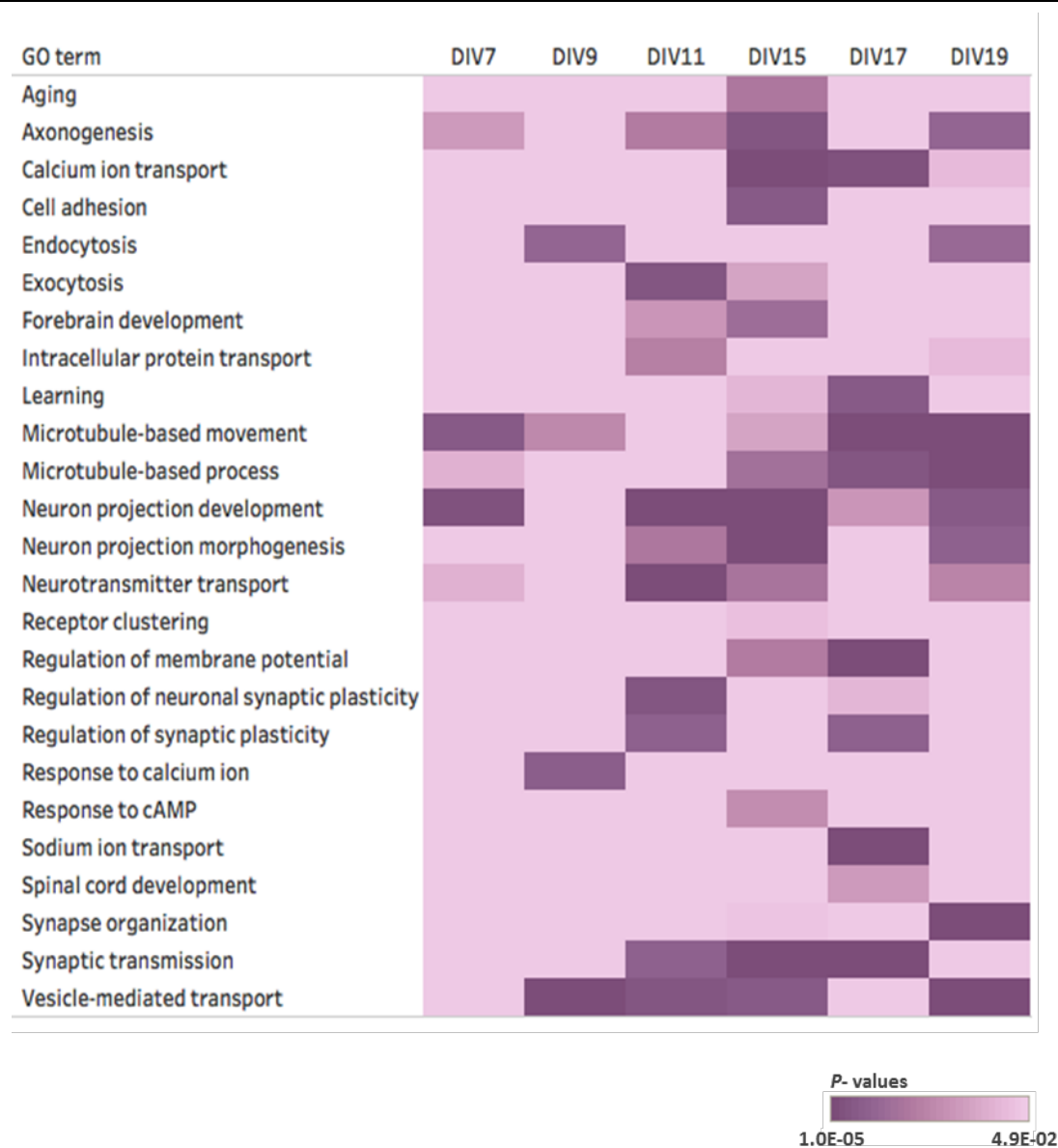


Figure 29. Enrichment analyses of over-represented annotations (GO terms) from the biological process domain. Heat map highlights prominent GO terms with corresponding *P*-values along the analyzed developmental stages. Note major over-representation of GO terms at developmental stages DIV15-17. GO analysis was performed using DAVID software.

The endogenous expression of selected candidate proteins was analyzed by Western blotting, which demonstrates persistent expression of NCAM and NR2B proteins during development, preferentially expressed at DIV8, DIV20 and DIV21. The endogenous expression of NCAM protein was notably higher compared to the others candidates (Figure 30). Meanwhile, endogenous ERC2 and NR1 protein reached the highest levels at mature developmental stages (DIV20 and DIV21) (Figure 30).

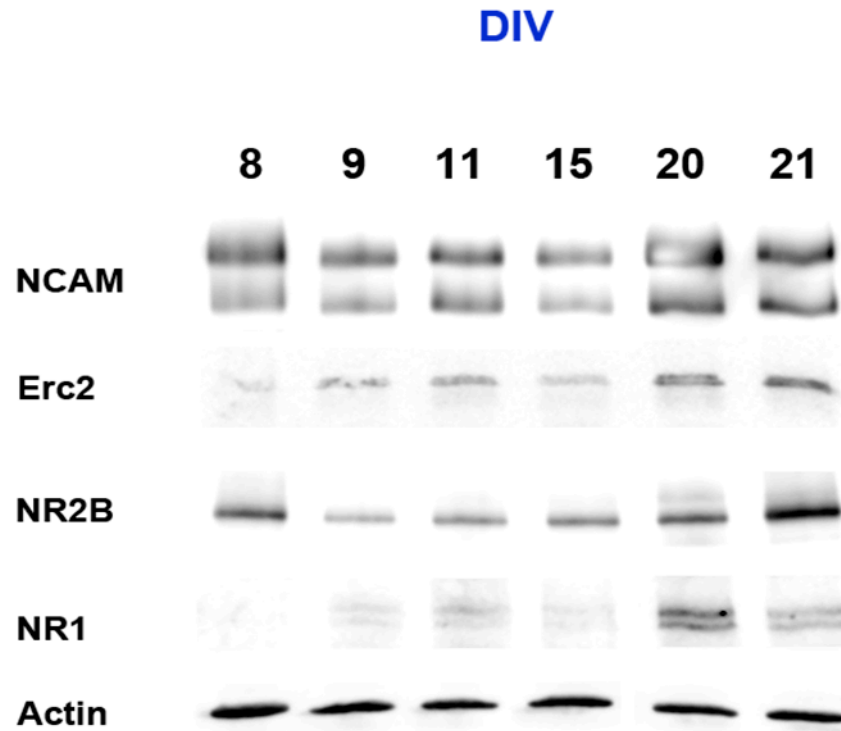


Figure 30. Biochemical analysis of selected candidate proteins in synaptosomes during development. Endogenous levels of selected candidate proteins were analyzed in synaptosomes by Western blot. Synaptosome fractions were isolated from primary cortical neuron cultures with approximately 30 million neurons per time point. Note substantial expression levels for all candidate proteins at mature developmental stages (DIV20-21). Ten μg of total protein was loaded per each time point. DIV: days *in vitro*. Representative blots from two independent experiments.

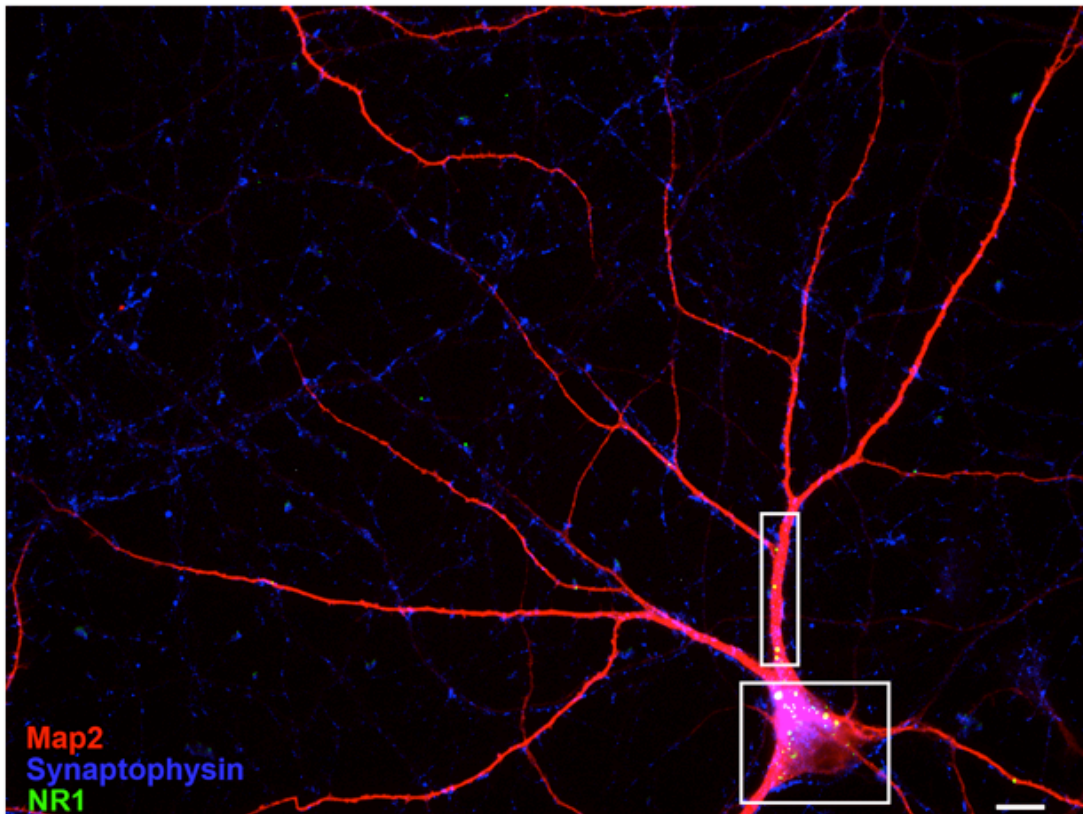
Interestingly, the highest levels of protein expression were observed at DIV20 in the majority of candidate proteins, suggesting that different cellular and molecular functions associated with the expression of these proteins might be activated at mature developmental stages.

3.8. Fluorescent *in situ* hybridization detection of mRNA transcripts encoding candidate proteins

In the next set of experiments, we examined the subcellular mRNAs localization of the transcripts encoding candidate proteins previously identified. Fluorescent *in situ* hybridization (FISH) (Cajigas et al., 2012) was used to visualize mRNA localization in neuronal domains of primary cortical neuron cultures, using specific probes for individual mRNAs. We selected pre (Erc2 and Piccolo) and postsynaptic (NR1) proteins as candidate proteins to investigate the amount and distribution of their transcripts during representative developmental stages (DIV7, DIV11, and DIV19).

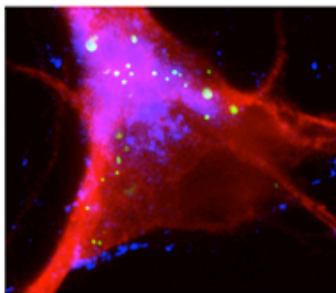
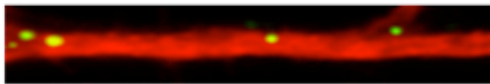
The quantitative analysis for NR1 mRNAs (Figure 31) revealed an increase in the copy number during development in both cell body (average counts: 14.9, 26.6, 61.3, respectively) and dendrites (average counts: 1.6, 2.7, 4.5, respectively) (Figure 31B and 31C). In addition, no significant changes were observed in the cell body: dendrite ratio (%) for the transcripts in each neuronal compartment (ratio: 85.6:14.4, 89.7:10.3, 92.6:7.4, respectively) (Figure 31C). These findings show a proportional increase in the number of NR1 mRNAs in both cell body and dendrites during development. A comparable observation was reported in a quantitative analysis of NR1 mRNA levels using RNA extracts from the frontal cortex at postnatal and adult ages (Franklin et al., 1993). This evidence suggests that a continuous synthesis and delivery of mRNAs from the cell body into dendritic domains is necessary to maintain the functional role of the NR1 receptor in synaptic function during brain development (Cui et al., 2004; Adesnik et al., 2008).

A



B

Raw



MAP2 Mask



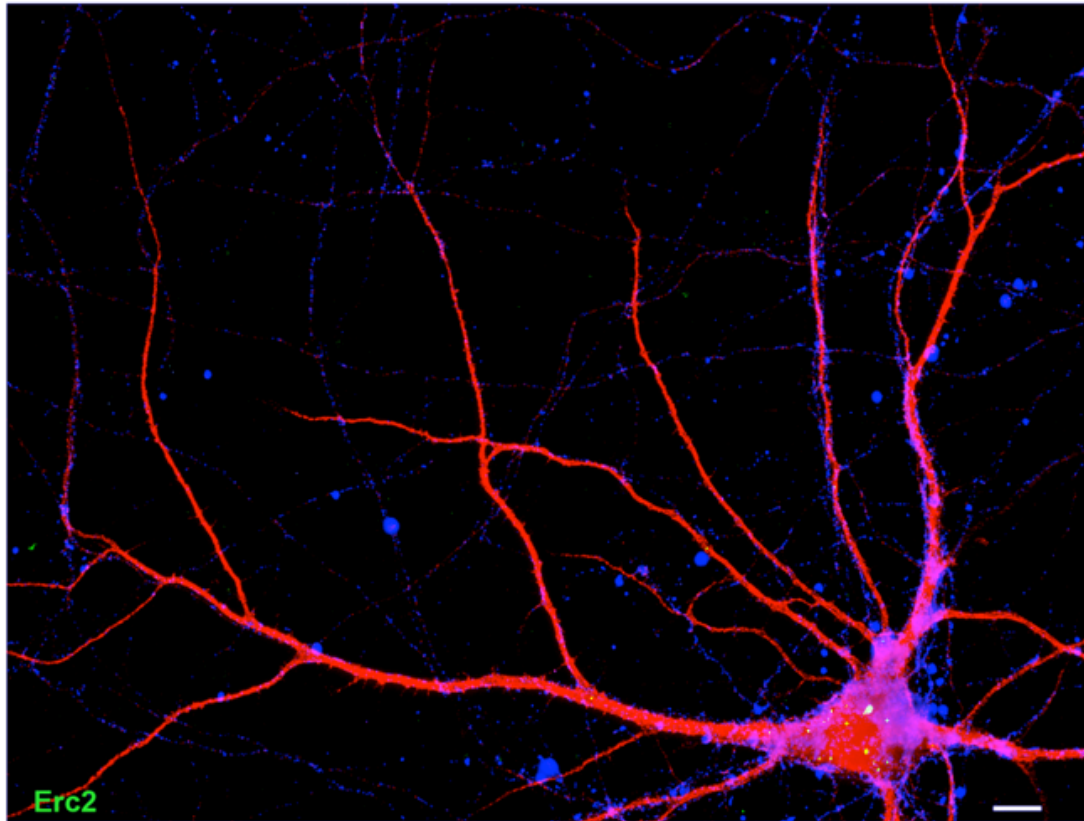
C

	Counts		Ratio (%)					TOTAL
	Cell Body	Dendrites	Cell Body	Dendrites	Cell Exp1	Cell Exp2	Cell Exp3	
NR1								
DIV7	14.96	1.56	85.56	14.44	7	8	10	25
DIV11	26.56	2.68	89.71	10.29	8	8	9	25
DIV19	61.31	4.46	92.65	7.35	10	9	7	26

Figure 31. NR1 mRNA detection by FISH. (A) The fish signal for NR1 (green) in primary cortical neurons (DIV11). (B) MAP2 immunostaining (red) was used to generate a mask that outlines the dendritic structure. Main dendrites were straightened for the analysis. Synaptophysin (blue) was used as a presynaptic marker. (C) Quantitative analysis for the

average number of NR1 mRNAs counted in the cell body and proximal dendritic segments (100 μm). Control experiments showed very low background levels (data not shown). Scale bar = 10 μm .

In a similar analysis performed for the presynaptic Erc2 transcripts (Figure 32A), an increase in copy number was observed in cell body (average counts: 7.5, 16.9, 18.8, respectively), meanwhile a constant number of mRNA particles was detected contacting dendritic domains (average counts: 2.1, 2, 2, respectively) during the analyzed developmental stages (Figure 32B). Since Erc2 is a key player in the organization of the cytomatrix at the active zone (CAZ), an increasing number of mRNAs in the cell body might provide a cellular mechanism to control the mRNA levels in neuronal compartments, and, therefore, regulate levels of Erc2 protein at CAZ during development.

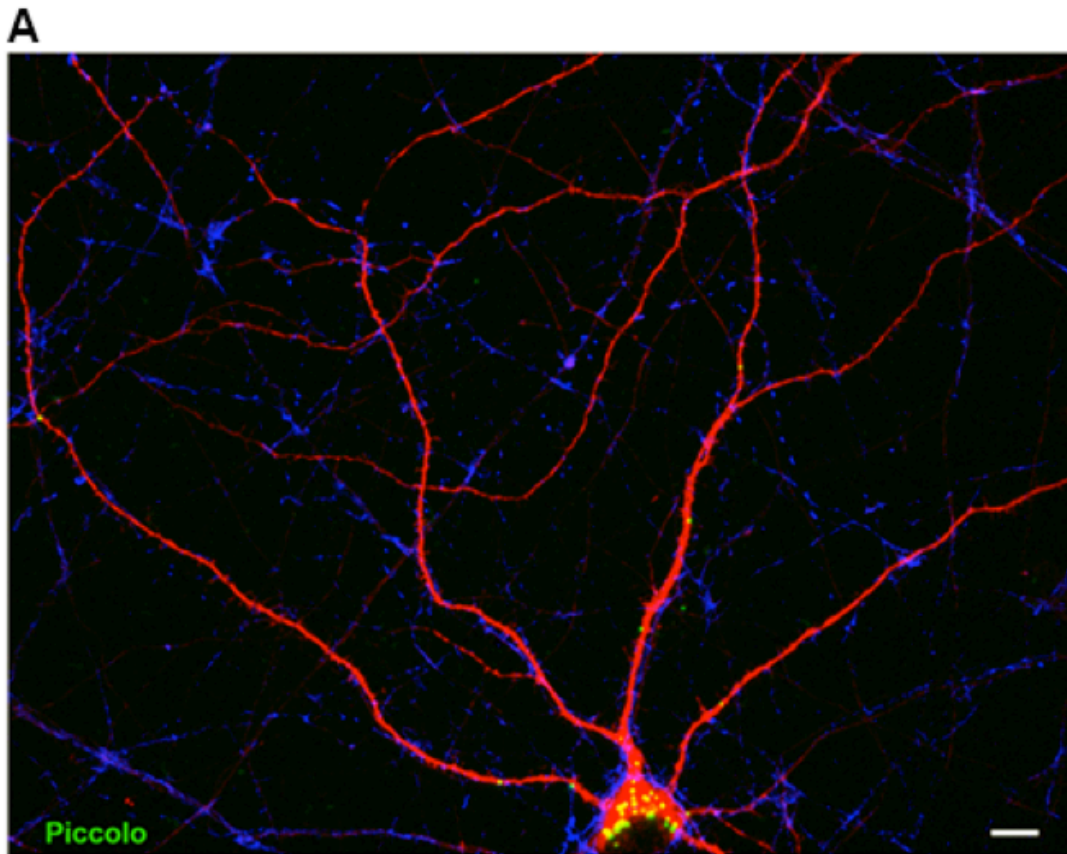
A**B**

Erc2	Counts		Ratio (%)		Cell Exp1	Cell Exp2	Cell Exp3	TOTAL
	Cell Body	(*)Dendrites	Cell Body	(*)Dendrites				
DIV7	7.52	2.12	78.51	21.49	10	5	10	25
DIV11	16.92	2	88.37	11.63	5	9	10	24
DIV19	18.77	2.04	88.83	11.17	11	5	10	26

Figure 32. Erc2 mRNA detection by FISH. (A) The fish signal for Erc2 (green) in primary cortical neurons (DIV11). MAP2 immunostaining (red) was used as a dendritic marker; meanwhile, Tau (blue) was used as an axonal marker. (B) Quantitative analysis for the number of Erc2 mRNA particles counted in the cell body and detected (*) contacting proximal dendritic segments (100 μ m). Control experiments showed very low background levels (data not shown). Scale bar = 10 μ m.

Turning now to the experimental evidence on Piccolo mRNAs, we noticed an increase in the copy number of transcripts in the cell body (average counts: 15.8, 16.8, 22.1, respectively) and mRNA particles contacting dendritic domains (average counts: 2.2, 3.2, 2.9, respectively) (Figure 33B).

The higher copy number of Piccolo mRNAs (Figure 33A) contacting dendritic domains compare to Erc2 might indicate that Piccolo is recruited more actively into axons during mature developmental stages to support the organization of CAZ and synaptic vesicle trafficking. Both mRNA transcripts were occasionally allocated near synaptic sites, however, a few numbers of mRNAs was found localized at distal domains from where they could modulate local translation and support the function of Erc2 and Piccolo protein in the organization of the cytomatrix at the CAZ as well as neurotransmitter release (Wang et al., 1999; Ohtsuka et al., 2002). As has been noted, the abundance of mRNAs particles varied for each mRNA type. In fact, the increasing number of Erc2 mRNAs in the cell body during development might be part of a cellular mechanism that controls the number of mRNAs in neuronal compartments. Altogether, these results suggest a potential recruitment of mRNA particles into distal neuronal domains to modulate local translation of essential proteins associated with the synaptic function, starting already from immature developmental stages.



B

	Counts		Ratio (%)		Cell Exp1	Cell Exp2	Cell Exp3	TOTAL
	Cell Body	(*)Dendrites	Cell Body	(*)Dendrites				
Piccolo								
DIV7	15.85	2.18	85.08	14.92	13	10	10	33
DIV11	16.8	3.24	83.10	16.90	10	5	10	25
DIV19	22.08	2.92	86.35	13.65	10	5	10	25

Figure 33. Piccolo mRNA detection by FISH. (A) The fish signal for Piccolo (green) in primary cortical neurons (DIV11). MAP2 (red) and Tau (blue) immunostaining was used as a dendritic and axonal marker, respectively. (B) An average number of Piccolo mRNA particles counted in the cell body and detected (*) contacting proximal dendritic segments (100 μ m). Experiments using the sense or lacking the secondary probe as a control showed very low background levels (data not shown). Scale bar = 10 μ m.

4 DISCUSSION

4.1 Developmental expression and subcellular localization of translation machinery components in neuronal compartments

The classic view that protein translation is spatially restricted to the cell body of neurons, following the central dogma of biology, prevailed until almost the end of the twentieth century (Holt and Schuman, 2013). Remarkably, neurons are also capable of synthesizing proteins locally in distal parts of their dendrites. In this respect, the capacity of dendrites for protein synthesis relies on the discovery of translation machinery components and diverse mRNAs (Bodian, 1965; Steward and Levy, 1982; Tiedge and Brosius, 1996; Gardiol et al., 1999; Pierce et al., 2000; Tang and Schuman, 2002). A substantial body of studies demonstrates the crucial role of local translation in synaptic function; however, very little attention has been paid to the functional role of local translation during brain development. In the present study, the intention was to investigate the developmental expression and subcellular localization of essential constituents of the translation machinery, including ribosomes, eIF4, eEF2, and methionyl-tRNA synthetase (MetRS) in dendrites and axons of hippocampal neurons. The experiments addressed in this thesis cover different time windows as representative stages of a neuron's maturation during neuronal development in culture, revealing cellular characteristics associated with immature, intermediate and mature developmental stage of neuronal cultures.

Early evidence suggesting that local protein synthesis might take place in dendrites come from anatomical observation of polyribosomes localized at the base of dendritic spines (Bodian, 1965; Steward and Levy, 1982). In this context, I noticed substantial levels of ribosome clusters in dendrites already at early stages of neuronal development (Figure 8, see DIV5 and 7), ribosomes were found dispersed along dendritic domains and often detected nearby synaptic specializations. In mature neurons, the abundant levels of ribosomes were distributed throughout dendrites and frequently associated with synapsin-positive specializations (Figure 8A). Interestingly, quantitative analysis revealed comparable levels of ribosomes allocated at synaptic sites

regardless of the developmental stage, suggesting that a subpopulation of ribosomes remains as a reserve pool of ribosomes at postsynaptic sites to support local protein synthesis during development (Figure 8D).

A further intriguing aspect of this analysis is the reduced distance ($0.37 \pm 0.2 \mu\text{m}$) between ribosomes and presynaptic specializations in hippocampal neurons at immature developmental stages compare to mature neurons. Regarding this, Fletcher et al. (1994) have shown that immature somata and dendrites of hippocampal neurons are capable of inducing the formation of presynaptic specializations by competent axons that contact them only after they reach a critical stage of maturation, which are 3 or 4 days in culture. As synaptogenesis normally occurs at a relatively early stage of dendritic growth (Fletcher et al., 1994), the reduced distance observed between ribosomes and presynaptic specializations might reflect an initial recruitment of ribosomes to support subsequent dendritic protein synthesis, which could determine the timing of synapse formation. It remains to be investigated the inhibitory effects of protein synthesis inhibitors on the ribosome localization and timing of synaptogenesis at earlier developmental stages (e.g. interval DIV3-5).

On the other hand, essential cellular components of the translation apparatus such as MetRS, eIF4, and eEF2 protein are present not only in somatic areas but also in distal domains (Figure 9). Here, extensive and heterogeneous levels of these components were detected in distal dendrites and axons of hippocampal neurons (DIV11) (Figure 9), thus supporting evidence from previous studies showing translation machinery components available for local translation in axon of cultured rat cortical neurons (Malmqvist T et al., 2014) and rat sciatic nerve (Michaevlevski I et al., 2010). In addition, the prominent presence of ribosomes and MetRS (data not shown) in dendritic domains from very early time points (DIV3-5) as well as eIF4 and eEF2 protein along dendritic and axonal domains in intermediate developmental stages (DIV11) demonstrate the soma-independent potential of both dendrites and axons to modulate protein synthesis already at early developmental stages. Therefore, these results suggest that the relative levels of translation machinery components in the neuronal compartments might be modulated in a development-dependent manner.

4.2 Visualization and quantification of newly synthesized proteins in dendrites and synaptic areas using FUNCAT technique

Although different methods have been utilized to visualize and monitor local protein translation during the past decades, these methods are focused mainly on genetic manipulation of single candidate proteins (Aakalu et al., 2001; Ju et al., 2004; Smith et al., 2004; Sutton et al., 2004; Raab-Graham et al., 2006; Wang et al., 2009). The development of non-radioactive methods (Ong et al., 2002, 2006; Schmidt et al., 2009) and the incorporation of the 'click chemistry' concept have facilitated the visualization and quantitative analysis of cellular proteomes under different states or conditions (Dieterich et al., 2006, 2007, 2010; Hodas et al., 2012; Yoon et al., 2012; Baleriola et al., 2014). Based on this concept, Dieterich et al. (2010) introduced the FUNCAT technique, which allows selective labeling of newly synthesized proteins in a spatial and temporal manner. Interestingly, the authors noticed newly synthesized proteins in proximal dendrites after 20 min exposure to the non-canonical amino acids AHA or HPG. In our FUNCAT experiments, we used longer incubations (2 h) of AHA not only to resolve newly synthesized proteins in distal dendrites but also in postsynaptic areas.

Labeling of newly synthesized proteins in dendrites (Figure 10A,B) and postsynaptic areas (Figure 10F) were explored in response to synaptic stimulation using BDNF, a neurotrophic factor that has been demonstrated to promote synaptogenesis (Alsina et al., 2001; Sanchez et al., 2006) and local protein translation in mechanically isolated dendrites (Aakalu et al., 2001). The result revealed a spatial distribution of new proteins throughout dendrites in response to BDNF. Bath application of BDNF (50 ng/ml) was sufficient to induce a substantial increase (ranging from 2 to 3.3-fold) in the levels of newly synthesized proteins along dendrites, showing higher levels in proximal dendritic segments and extended protein labeling in distal dendritic domains (Figure 10C), these results are in line with Dieterich et al. (2010) observations. The increased levels of newly synthesized proteins detected in dendrites might be explained by an overall increase in the cell body and dendritic protein translation in response to BDNF, which could also alter the levels of protein synthesis in dendritic spines. Regarding this, I observed a significant

increase (26%) in the levels of newly synthesized proteins at postsynaptic sites in hippocampal neurons treated with BDNF (Figure 10G). Notably, tom Dieck et al. (2015) developed a new technology that couples FUNCAT or puromycylation with proximity ligation assay (PLA), which allows the direct visualization of specific newly synthesized proteins. The implementation of this new strategy to our analysis could facilitate the visualization of specific proteins of interest, for example, in dendritic spines.

Interestingly, I noticed a prominent increase in the number of ribosome clusters along dendrites of BDNF-treated neurons (Figure 10D, E). In addition, a significant increase in the levels of ribosomes was perceived at postsynaptic sites of these neurons. Moreover, we observed a significant reduction in the distance between ribosomes and synapsin-positive specializations, suggesting a potential recruitment of ribosomes into dendritic spines induced by BDNF (Figure 10H). These findings are consistent with previous observations on redistribution of polyribosomes from the dendritic shaft into spines during LTP in developing rat hippocampal slices (Ostroff et al., 2002). At the same time, it is tantalizing to speculate that these increases in the ribosome levels observed along dendritic domains and postsynaptic sites might reflect the local assembly of ribosomes or ribosomal subunits. In fact, the proteomic analysis performed in this thesis identified components of the 40S ribosomal subunit (Rps27a; DIV9) and 60S ribosomal subunit (Rpl7a; DIV17) as newly synthesized proteins (Supplementary table 7 and 8) as well as component required for the assembly of the 40S ribosomal subunit (RSSA; DIV17) locally synthesized (data not shown) in synaptosomal fractions. Certainly, it is an important challenge to demonstrate in the future. In this concern, mRNAs encoding translation machinery components are upregulated in the cell body and neurites of hippocampal neurons in response to BDNF (Manadas et al., 2009), and also identified in the synaptic neuropil (Cajigas et al., 2012) and axonal transcriptome analyses (Taylor et al., 2009; Zivraj et al., 2010; Gumy et al., 2011; Estrada-Bernal et al., 2012). This evidence supports the idea that translation machinery assembly is taking place locally to modulate protein synthesis on site (Holt and Schuman, 2013).

It is important to note that BDNF induced the formation of a significant number of presynaptic specializations during the incubation period (2 h)

(Figure 10J), exhibiting similar modulatory effects on the synapse density as described previously (Alsina et al., 2001; Aguado et al., 2003; Sanchez et al., 2006; Cheng et al., 2012). These findings suggest that synaptic stimulation induces not only increases in dendritic protein translation results and newly synthesized proteins at postsynaptic sites, but also in the number of presynaptic specializations and clusters of ribosomes along dendrites. Finally, this study provides additional evidence for the translational responses involved in synaptic plasticity.

4.3 Visualization of newly synthesized proteins at pre and postsynaptic sites

Transport of mRNAs and protein delivery into subcellular domains are essential mechanisms for the establishment and maintenance of cell polarity (Hirokawa et al., 2006; Holt & Bullock, 2009; Medioni et al., 2012; Xing and Bassell, 2013). In neurons, transport and localization of mRNAs provide a means of protein delivery to their functional sites, thus controlling local protein synthesis at synapses (Sutton & Schuman, 2006; Bramham & Wells, 2007; Costa-Mattioli et al., 2009). The mechanisms of mRNA transport, as well as sorting, trafficking, and targeting of proteins, are regulated by specific sequence elements that specify their localization. In this sense, Grabrucker and coworkers (2009) developed a new targeting vector (pSDTarget), based on a bipartite targeting signal from the ProSAP1/Shank2 protein, which enables protein delivery to PSDs. Taking this targeting vector into consideration, I cloned the MetRS sequence into the pSDTarget vector (Supplementary Figure 1) to explore and visualize local protein synthesis at postsynaptic sites.

In my experiments, primary hippocampal neurons expressing the pSDT-MetRS-GFP construct showed a clear accumulation of the fusion protein in postsynaptic densities. In contrast, control neurons transfected with the pMetRS-GFP exhibited a homogenous distribution of MetRS-GFP along somatodendritic domains (Figure 11A). High-resolution imaging confirmed the subcellular enrichment of MetRS-GFP at postsynaptic densities in neurons transfected with pSDT-MetRS-GFP (Figure 11A and 4B). This evidence

demonstrated that ProSAP1/Shank2 targeting sequence leads to the localization of MetRS-GFP–fusion protein at postsynaptic densities. Certainly, the long-term expression (192 h) of the pSDT-MetRS-GFP construct caused cumulative levels of MetRS-GFP along dendritic domains, attributable, in part, to the ongoing synthesis of the fusion protein during the mRNA transport.

Cellular protein translation fidelity relies, in part, on the aminoacyl-tRNA synthetase (aaRS) activity by charging each tRNA with the appropriate amino acid (Link et al., 2006; Yadavalli and Ibba, 2012). Within the aaRSs family, methionyl-tRNA synthetase (MetRS) plays an essential role in protein translation, acting as a key regulator during the initiation phase of protein synthesis. Therefore, MetRS has become a natural target to be explored by protein engineers (Link et al., 2006). In this context, effective methods for cell-selective protein labeling have been described in bacterial cells (Link et al., 2006) and mixed cellular system of bacterial and mammalian cells (Ngo et al., 2009) expressing a mutant MetRS from *E. coli* carrying a mutation in the methionine-binding pocket, which enables the incorporation of the non-canonical amino acid azidonorleucine (ANL) into nascent proteins. In view of this information, I cloned the murine MetRS, carrying the single mutation leucine to glycine at position 274 (designed by Dr. Daniela Dieterich) in the methionine-binding pocket of MetRS (LtoGMetRS) (Dr. A. Müller, doctoral thesis, 2012; Erdmann et al., 2015; Müller et al., 2015), into the pSDT vector to generate the pSDT-LtoGMetRS-GFP construct.

In the present study, the intention was to visualize newly synthesized proteins at postsynaptic areas using the pSDT-LtoGMetRS-GFP construct in combination with cell-selective metabolic labeling in hippocampal neurons. The labeling of newly synthesized proteins at postsynaptic densities was achieved using ANL and FUNCAT technique (Dieterich et al., 2010). Cell-selective ANL incorporation into proteins was confirmed in HEK293 cells expressing pSDT-LtoGMetRS construct (Figure 12). The expression of the mutant LtoGMetRS enabled ANL incorporation and detection of newly synthesized proteins as previously described by Dr. A. Müller (GINCAT procedure, doctoral thesis 2012; Müller et al., 2015). ANL-harboring proteins were restricted to cells expressing LtoGMetRS, covering a broad range of molecular weights (Figure 12). Similarly, FUNCAT experiments showed that

only neurons expressing the mutant LtoGMetRS are able to incorporate ANL during protein translation (Figure 13). We also noticed a subcellular enrichment of Tamra signal at postsynaptic densities in neurons transfected with pSDT-LtoGMetRS-GFP. The cumulative level of the fusion protein and Tamra signal observed along dendritic domains might be attributable to the ongoing translation of the fusion protein during the transport of its mRNA as mentioned above. Here, we described the generation of a targeting system (pSDT-LtoGMetRS-GFP), which allows expression of LtoGMetRS and subsequent detection of newly synthesized proteins at postsynaptic sites in hippocampal neurons. This approach provides us with the ability to detect and differentiate new proteins made in neurons expressing the mutant LtoGMetRS from those made in neurons expressing the wild-type MetRS. Similar cell-specific protein labeling approach has been successfully implemented for proteome labeling in living *Drosophila* larvae and adult flies (Erdmann et al., 2015). The use of pSDT-LtoGMetRS targeting system in combination with metabolic labeling could be considered in future experiments to determine changes in the postsynaptic subproteome involved in synaptic function. Certainly, application of the described approaches might facilitate the enrichment, detection, and visualization of low abundance proteins at postsynaptic sites under, per example, local synaptic stimulation (e.g. BDNF).

The transport and localization of tau mRNA is another example of mRNA transport regulation, which involves specific sequence elements located within the 3' UTR tau mRNA. This sequence contains a defined fragment of 240 base pairs (fragment H) required for axonal targeting and tau mRNA stabilization as previously described (Aronov et al., 2001). Considering this study, I designed different constructs containing both the fragment H (Cod-H) and mutant LtoGMetRS sequence to investigate protein synthesis in presynaptic compartments. In the first set of experiments, unspecific axonal targeting of the fusion protein was observed when Cod-H was cloned with or without the mutant LtoGMetRS into a pEGFP-C1 vector (Figure 14). In this context, GFP variants represent a significant increase in the size of fusion proteins (about 25 kDa in size) and thus may have consequences in the folding or targeting of the fusion protein that we are trying to express (Snapp, 2005; Chudakov et al., 2010), particularly after LtoGMetRS (Figure 14) and

ORFTau incorporation (Figure 15). To overcome this problem, I utilized different expression systems containing the small c-myc tag such as pCMV-Tag3B (Figure 16) and pcDNA 3.1myc (Figure 17) vector.

Effective axonal targeting was observed only when Cod-H and ORFTau were cloned into pcDNA vector (Figure 17 and 18). Despite the clear staining of axonal-like compartments, the subsequent LtoGMetRS incorporation suppressed the axonal targeting of the fusion protein (Figure 20). Certainly, I cannot ignore possible undetectable levels of the fusion protein in axonal compartments. The functional activity of LtoGMetRS was unaffected as I detected substantial levels of newly synthesized proteins in HEK293 cells (Figure 19) and hippocampal neurons (FUNCAT experiments) (Figure 21) transfected with the pLtoGMetRS-ORFTau-Cod-H construct.

Aronov and colleagues (2001) demonstrated in differentiated P19 cells that axonal tau mRNA localization depends on the fragment H. In our experiments, the axonal targeting was not observed when the fragment H (Cod-H) was first cloned into EGFP (Figure 14), pCMV or pcDNA vector (data not shown). However, I observed effective axonal targeting only after insertion of ORFTau (Figure 17 and 18), suggesting that hippocampal neurons require additional elements to achieve effective axonal targeting, revealing a major complexity of neuronal cultures as compared to differentiated P19 cells, which require retinoic acid treatment for differentiation into neuronal cells (Jones-Villeneuve et al., 1982; McBurney et al., 1988; McBurney, 1993).

On another hand, it has been shown that the amino N-terminus of human MetRS is required for cytoplasmic localization of this enzyme (Kaminska et al., 2009), therefore the fusion of GFP to the N-terminus of murine MetRS might affect its localization. It could be argued that due to the close vicinity between GFP (pEGFP vector) or ORFTau-Cod-H (pCMV or pcDNA vector) and LtoGMetRS could alter the folding pattern of the N-terminus LtoGMetRS and, consequently, the targeting of the fusion protein. In addition, the ability of the fusion protein to interact with microtubules, which facilitates its anterograde axonal transport, might be reduced or lost after LtoGMetRS incorporation. Adding a longer spacer (e.g. extra Gs) in between the LtoGMetRS cDNA and the GFP coding region or ORFTau-Cod-H might help to stabilize the fusion protein mRNA as well as proper targeting into

axonal compartments. Also, changes in the orientation of the LtoGMetRS sequence (C-terminal–N-terminal) could be considered to evaluate effective axonal targeting.

It is important to mention that the staining of axonal compartments using anti-tau antibody was not included as the host species of the anti-tau antibody is not compatible with the host species of the anti-c-myc antibody, both antibodies raised against mouse were independently effective to stain axonal compartments. Although antibodies raised against different species (anti-tau sheep or anti-c-myc rabbit) were tested, they failed to stain axonal compartments. Therefore, additional experiments using anti-tau and an anti-c-myc antibody raised in different species is required to confirm axonal targeting of the fusion protein.

4.4 Identification of *de novo* synthesized synaptic proteomes during development

4.4.1 Synaptosome isolation

Synaptosomes are resealed membranous structures containing the presynaptic terminal and fractions of postsynaptic components obtained during brain tissue homogenization (Whittaker et al., 1964). The morphological features of the nerve terminals are preserved in synaptosomes, which are usually isolated from nerve tissue homogenates via density gradient centrifugation (Whittaker et al., 1964; Hajos, 1975; Whittaker, 1993; Bai and Witzmann, 2007; Ramos-Ortolaza et al., 2010). In this thesis, I introduce a satisfactory procedure, adapted from a well-established subcellular fractionation (Gundelfinger and Tom Dieck, 2000), for the enrichment of synaptic structures from primary cortical cultures (Materials and Methods) (Figure 22). Our initial challenge was the isolation of synaptic structures from hippocampal cultures at early developmental stages; however, the large amount of material required for subsequent MS analysis became an important limitation. Instead, primary cortical cultures provided us a suitable platform for the isolation of synaptic structures, despite the significant amount of neuronal culture (~ 30 million cells) needed for each subcellular fractionation. We

established an effective procedure for the isolation and enrichment of synaptosomes containing pre (synaptophysin) and postsynaptic (PSD-95) proteins as well as elements of the synaptic cleft (NCAM, data not shown). Components of the translation machinery and excitatory neurotransmitter receptor (GluR2) were also present in both immature (DIV8) and mature neuronal cultures (DIV18) (Figure 23), suggesting that the integrity of the nerve terminals is not altered in the isolated synaptosome fractions.

Subcellular fractionation never generates synaptosomes fractions pure, fractions contain up to 50% of synaptosomes (Morgan, 1976) and diverse subcellular and non-neuronal contaminations (Cotman & Matthews, 1971; Henn et al., 1976; Dodd et al., 1981). In this context, the synaptosome fractions obtained with our fractionation procedure are almost devoid of glial components (data not shown).

Recently, a novel approach, named Fluorescence Activated Synaptosome Sorting (FASS), has been established to isolate intact glutamatergic synaptosomes (Biesemann et al., 2014). This method employs a knock-in mouse line that expresses a fully functional VGLUT1^{VENUS} protein (Herzog et al., 2011), which labels all synapses containing VGLUT1. Certainly, future experiments using the pSDT-LtoGMetRS-GFP or pCDNA-LtoGMetRS-ORFTau-Cod-H constructs in combination with FASS (Biesemann et al., 2014) and FUNCAT/BONCAT technique might facilitate the exploration of local protein synthesis at synapses.

Taken together, biochemical analysis of synaptosome fractions supports our previous evidence on the recruitment of translation machinery components to synaptic compartments (see section 3.1, 3.2 and 3.2.1), suggesting an active demand for protein synthesis at synapses during early stages of neuronal development.

4.4.2 Developmental-dependent changes in the *de novo* synthesized synaptic proteome

Synapse formation is an essential process that requires fine regulation of protein synthesis during nervous system development (Schacher and Wu, 2002; Liu et al., 2003; Wiersma-Meems et al., 2005). Each synapse responds quickly to diverse intrinsic and extrinsic factors by synthesizing new proteins (Twiss and van Minnen, 2006; Fallon and Taylor, 2013; Jung et al., 2012; Batista and Hengst, 2016). In this context, molecular changes in the synaptic proteome modulated by protein synthesis, degradation and post-translational modification play vital roles in synapse assembly, synaptic function and plasticity during development (Costa-Mattioli et al., 2009; Cajigas et al., 2010; Loya et al., 2010; Alvarez-Castelao and Schuman, 2015). For a better understanding of the spatial-temporal characteristics of the synaptic proteome, we explored the molecular changes occurring at synaptosomes during development using BONCAT technique (Dieterich et al., 2006).

Quantitative analysis demonstrated effective AHA incorporation into proteins and revealed that primary cortical neurons are capable of synthesizing in average 3.6% of their total protein content during a period of 2 h (Figure 24C). Similarly, I examined the changes in the synaptic proteome by quantifying the amount of newly synthesized proteins in synaptosomes in order to gain knowledge on how neurons regulate their synaptic content during development. In this context, low levels (ranging from 2 to 3.3%) of newly synthesized proteins related to the total protein content were observed throughout time windows. On the other hand, despite the major abundance of newly synthesized proteins noticed during early developmental stages (DIV7-11), no statistically significant difference was detected between all-time points (Figure 26B and C), suggesting that there is a small, but constant, supply of new protein at each developmental stage.

The great complexity of chemical synapses is characterized by a dynamic replacement of proteins (Cajigas et al., 2010; Cohen et al., 2013; Fallon and Taylor, 2013; Alvarez-Castelao and Schuman, 2015). A recent analysis of synaptic protein turnover in primary cultures of rat neurons demonstrated that the majority of the identified synaptic proteins exhibited

relatively slow turnover rates; about 0.7% of the synaptic protein content was turned over every hour (Cohen et al., 2013). Concerning this point, the low level of newly synthesized proteins detected along the tested developmental stages is in line with lower turnover rates of synaptic proteins identified by Cohen et al. (2013), suggesting that neurons adjust their synaptic proteomes at slow rates under physiological conditions. Taking into account results from Cohen et al. (2013), a significant number of proteins (~ 26,5% per time point) was identified as synaptic proteins with half-lifetimes ranging from 0.21 to 59.7 days (data not shown) (half-life range taken from Supplementary Table S1, Cohen et al., 2013). A minor number of these synaptic proteins (~ 6,7%) were detected in sequential developmental stages (data not shown). In addition, we found few long-lived proteins along the tested developmental stages as confirmed in a long-lived proteins list from Toyama et al. (2013) (Table 5).

Altogether, these results suggest that a dynamic protein renewal is taking place at each developmental stage and, thus, revealing that the composition of the synaptic proteome might change in a development-dependent manner. In general terms, a substantial number of identified newly synthesized proteins are associated with synaptic compartments, as derived from SynProt database (Pielot et al., 2012), meanwhile their mRNAs were validated in a neuropil transcriptome database (Cajigas et al., 2012) (Table 4), implying that these proteins might, indeed, be synthesized locally at synaptic terminals.

Although initial GO analysis revealed no significant differences between percentages of identified newly synthesized proteins associated with prominent GO terms (Figure 27), I observed changes in the protein composition (Table 6) and number associated with these GO terms (Figure 28) across all developmental stages. Additional web-based tools (DAVID and GeneCodis software) were used in order to incorporate statistical significance into our gene-enrichment analysis and therefore exclude any association resulting from chance (Figure 29). Here, I describe the enrichment of over-represented annotations that frequently appear associated with the biological process (Supplementary Table 11), cellular component (Supplementary Table 12) and molecular function (Supplementary Table 13) using both DAVID and GeneCodis software. Besides the clear difference in the *P*-values, we

observed a larger number of genes associated with each GO term using DAVID analysis. The main reason that might explain such difference is the fact that DAVID integrates species-specific gene/protein identifiers and annotations from a variety of well-known bio-databases (e.g. NCBI, PIR, SWISS-PROT, GO, OMIM, PubMed, KEGG, BIOCARTA, AffyMetrix, TIGR, Pfam, BIND, MINT, DIP, etc.), which is keeping updated, giving access to the current state of functional annotation (Dennis et al., 2003). In contrast, GeneCodis uses as a reference set all genes from the corresponding genome at the NCBI Entrez Gene database (Carmona-Saez et al., 2007).

Despite the differences detected between GO analyses, both DAVID and Gencodis exhibited over-represented annotations mainly at DIV15-17 (Figure 29, Supplementary Table 11, 12 and 13), thus validating effective changes in the majority of over-represented annotations at these developmental stages. From these annotations, I further analyzed a number of candidate proteins associated with important neuronal development: Erc2 (GO term: synapse assembly, synapse organization), NCAM (GO term: cell adhesion), NR2B (GO term: nervous system development, learning) and NR1 (GO term: synapse assembly, synapse organization). The endogenous expression was relatively constant during development for the majority of these candidate proteins. Notably, protein expression for NCAM was higher compared to the other candidates. Despite of detectable levels of protein expression at early stages, in particular for NCAM and NR2B, the highest expression levels of all candidate proteins were observed in mature developmental stages (DIV20 and DIV21) (Figure 30), suggesting that different cellular mechanisms and molecular functions associated with these proteins might preferentially be activated at these developmental stages.

Subcellular localization of mRNAs encoding selected candidate proteins (NR1, Erc2, and Piccolo) revealed a persistent increase in the number of mRNAs in cell body during development (Figure 31, 32 and 33), suggesting that a continuous synthesis and delivery of mRNAs particles takes place in the cell body, which might control the abundance of mRNAs in neuronal compartments during development. Certainly, the low copy number of transcripts detected in the different neuronal compartments (Figure 31B, 32B, and 33B) might represent technical limitations that can be optimized in future

analyses. Nevertheless, the initial localization of mRNA particles at distal domains of young neurons suggests the cell body-independent capacity of dendrites and axons to modulate local translation of essential proteins required for synaptic function, starting from early developmental stages.

It is my belief that this study provides new insights into understanding the development-dependent molecular changes at chemical synapses. In particular, it adds evidence to the existing knowledge on the molecular constitution, remodeling, and functional organization of chemical synapses during development. The molecular changes detected in the synaptic proteome might reflect the neuronal network dynamics at each developmental stage as well as represent a valuable source for the identification of molecular targets associated with developmental disorders.

5. Outlook

The work described in this thesis has drawn different aspects of the role of protein translation in the synaptic proteome during neuronal development. Certainly, there remain unsolved questions and future challenges.

As synapse formation in hippocampal neurons is not initiated until postsynaptic elements reach a critical maturation stage (3 or 4 days in culture) (Fletcher et al., 1994), the following question arises: Is the recruitment of ribosomes the responsible to induce the maturation of dendrites, thus facilitating the initiation of synaptogenesis? Blocking the transport of ribosomes at earlier developmental stages (>DIV5) by lowering the temperature or depleting nuclei of ATP (Bataillé et al., 1990) or cytoskeleton disruption (e.g. Cytochalasin D) (Ligon and Steward, 2000) as well as protein translation inhibition (e.g. Anisomycin) might provide new insights about the role of dendritic distribution of ribosomes in dendrite maturation.

Another intriguing question raised in this thesis and others (Holt and Schuman, 2013) is the potential assembly of ribosomes or ribosomal subunits in dendrites and axons. This possibility is suggested by the identification of components of the 40S and 60S ribosomal subunits as newly synthesized proteins in synaptosomes, and a component required for the assembly of the 40S ribosomal subunit as local newly synthesized protein (data not shown). In addition, several mRNAs for components of the translation machinery have been identified in neurites of hippocampal neurons (Manadas et al., 2009), synaptic neuropil (Cajigas et al., 2012) and axonal transcriptome (Taylor et al., 2009; Zivraj et al., 2010; Gummy et al., 2011; Estrada-Bernal et al., 2012). Ribosome biogenesis could be examined by genetic incorporation of non-canonical amino acids into candidate ribosomal proteins, which are identified as newly synthesized proteins in synaptosomes. To this end, the pulse-chase epitope labeling strategy (Stelter and Hurt, 2014) could be applied in neuronal cultures to monitor the assembly of ribosomes in axonal growth cones and dendrites in response to extrinsic cues (e.g. BDNF).

The incorporation of the mutant LtoGMetRS sequence in the targeting system (pORFTau-Cod-H construct) prevented the proper targeting of the

fusion protein into presynaptic terminals. Therefore, the mRNA stabilization of the fusion protein by either adding a longer spacer (e.g. extra Gs) between the LtoGMetRS and ORFTau-Cod-H sequence or changing the orientation of the LtoGMetRS sequence might result in a correct axonal targeting. Certainly, targeting systems such as pLtoGMetRS-ORFTau-Cod-H and pSDT-LtoGMetRS constructs as well as Fluorescence Activated Synaptosome Sorting (Biesemann et al., 2014) in combination with metabolic labeling could provide an additional tool to investigate the changes in the local synaptic proteome at pre or postsynaptic terminals.

Finally, a potential examination of local translation and the spatial fate of the identified newly synthesized proteins within dendrites or axons could be addressed with the proximity ligation assay (PLA)-based strategy developed by tom Dieck et al. (2015). This method has allowed the direct detection of nascent endogenous proteins in pre and postsynaptic terminals by coupling FUNCAT or puromycylation with PLA (tom Dieck et al., 2015). Therefore, local translation, turnover or distribution of candidate proteins such as NR1, Erc2, and Piccolo could be analyzed in more detail using this method in the future.

6. LITERATURE

Aakalu G., Smith W. B., Nguyen N., Jiang C., Schuman E. M. (2001). Dynamic visualization of local protein synthesis in hippocampal neurons. *Neuron*. 30(2):489-502.

Adesnik H., Li G., During, M. J., Pleasure S. J., Nicoll R. A. (2008). NMDA receptors inhibit synapse unsilencing during brain development. *Proc Natl Acad Sci*. 105(14):5597-5602.

Aguado F., Carmona M. A., Pozas E., Aguilo A., Martinez-Guijarro F. J., Alcantara S., Soriano E. (2003). BDNF regulates spontaneous correlated activity at early developmental stages by increasing synaptogenesis and expression of the K⁺/Cl⁻ co-transporter KCC2. *Development*. 130(7):1267-1280.

Alsina B., Vu T., Cohen-Cory S. (2001). Visualizing synapse formation in arborizing optic axons in vivo: dynamics and modulation by BDNF. *Nat. Neurosci*. 4:1093-1101.

Alvarez-Castelao B., Schuman EM. (2015). The Regulation of Synaptic Protein Turnover. *J Biol Chem*. 290(48):28623-30.

Andersen J. S., Lam Y. W., Leung A. K., Ong S. E., Lyon C. E., Lamond A. I., Mann M. (2005). Nucleolar proteome dynamics. *Nature*. 433(7021):77-83.

Angenstein F., Greenough W., Weiler I.J. (1998). Metabotropic glutamate receptor-initiated translocation of protein kinase p90rsk to polyribosomes: A possible factor regulating synaptic protein synthesis. *Proc Natl Acad Sci*. 95:15078–15083.

Ariel P., Ryan T. A. (2010). Neuronal protein economics: keeping tabs on synthesis. *Nat Neurosci*. 13(7):781-782.

Aronov S., Aranda G., Behar L., Ginzburg I. (2001). Axonal tau mRNA localization coincides with tau protein in living neuronal cells and depends on axonal targeting signal. *J Neurosci.* 21(17):6577-6587.

Aronov S., Marx R., Ginzburg I. (1999). Identification of 3'UTR region implicated in tau mRNA stabilization in neuronal cells. *J Mol Neurosci.* 12(2): 131-145.

Ashraf S. I., McLoon A. L., Sclarsic S. M., Kunes S. (2006). Synaptic protein synthesis associated with memory is regulated by the RISC pathway in *Drosophila*. *Cell.* 124(1):191-205.

Ashton A. C., Ushkaryov Y. A. (2005). Properties of synaptic vesicle pools in mature central nerve terminals. *J Biol Chem.* 280(44):37278-37288.

Bagni C., Mannucci L., Dotti C. G., Amaldi F. (2000). Chemical stimulation of synaptosomes modulates alpha -Ca²⁺/calmodulin-dependent protein kinase II mRNA association to polysomes. *J Neurosci.* 20(10):RC76.

Bai F., Witzmann F. A. (2007). Synaptosome proteomics. *Subcell Biochem.* 43:77-98.

Bailey CH., Kandel ER. (1993). Structural changes accompanying memory storage. *Annu Rev Physiol.* 55:397–426.

Bailey C.H., Bartsch D., Kandel ER. (1996). Toward a molecular definition of long-term memory storage. *Proc. Natl. Acad. Sci.* 93:13445–13452.

Baleriola J., Walker CA., Jean YY., Crary JF., Troy CM., Nagy PL., Hengst U. (2014) Axonally synthesized ATF4 transmits a neurodegenerative signal across brain regions. *Cell.* 158(5):1159-72.

Barco A., Alarcon J. M., Kandel E. R. (2002). Expression of constitutively active CREB protein facilitates the late phase of long-term potentiation by enhancing synaptic capture. *Cell*. 108:689–703.

Bargmann CI. (2012). Beyond the connectome: how neuromodulators shape neural circuits. *Bioessays*. 34(6):458-65.

Bataillé N., Helser T., Fried HM. (1990). Cytoplasmic transport of ribosomal subunits microinjected into the *Xenopus laevis* oocyte nucleus: a generalized, facilitated process. *J Cell Biol*. 111(4):1571-82.

Batista AF., Hengst U. (2016). Intra-axonal protein synthesis in development and beyond. *Int J Dev Neurosci*. 55:140-149.

Beasley CL., Pennington K., Behan A., Wait R., Dunn MJ., Cotter D. (2006). Proteomic analysis of the anterior cingulate cortex in the major psychiatric disorders: Evidence for disease-associated changes. *Proteomics*. 6(11): 3414-25.

Benson DL., Colman DR., Huntley GW. (2001) Molecules, maps, and synapse specificity. *Nat Rev Neurosci*. 2(12):899-909.

Ben-Yaakov K., Dagan SY., Segal-Ruder Y., Shalem O., Vuppalanchi D., Willis DE., Yudin D., Rishal I., Rother F., Bader M., Blesch A., Pilpel Y., Twiss JL., Fainzilber M. (2012). Axonal transcription factors signal retrogradely in lesioned peripheral nerve. *EMBO J*. 31(6):1350-63.

Besse F., Ephrussi A. (2008). Translational control of localized mRNAs: restricting protein synthesis in space and time. *Nat Rev Mol Cell Biol*. 9(12): 971-80.

Biesemann C., Gronborg M., Luquet E., Wichert S. P., Bernard V., Bungers S. R., Herzog E. (2014). Proteomic screening of glutamatergic mouse brain synaptosomes isolated by fluorescence activated sorting. *EMBO J.* 33(2): 157-170.

Bodian D. (1965). A suggestive relationship of nerve cell RNA with specific synaptic sites. *Proc. Natl Acad. Sci.* 53:418–425.

Boeckers T. M., Liedtke T., Spilker C., Dresbach T., Bockmann J., Kreutz M. R., Gundelfinger E. D. (2005). C-terminal synaptic targeting elements for postsynaptic density proteins ProSAP1/Shank2 and ProSAP2/Shank3. *J Neurochem.* 92(3):519-524.

Boeckers T. M. (2006). The postsynaptic density. *Cell Tissue Res.* 326(2): 409-422.

Boeckers TM., Grabrucker AM., Vaida B., Bockmann J. (2009). Efficient targeting of proteins to post-synaptic densities of excitatory synapses using a novel pSDTarget vector system. *J Neurosci Meth.* 181(2):227–234.

Bourne J. N., Harris K. M. (2008). Balancing structure and function at hippocampal dendritic spines. *Annu. Rev. Neurosci.* 31:47–67.

Boyken J., Grønberg M., Riedel D., Urlaub H., Jahn R., Chua JJ. (2013). Molecular profiling of synaptic vesicle docking sites reveals novel proteins but few differences between glutamatergic and GABAergic synapses. *Neuron.* 78(2):285-97.

Black MM., Lasek RJ. (1977). The presence of transfer RNA in the axoplasm of the squid giant axon. *J Neurobiol.* 8(3):229-37.

Blondeau F., Ritter B., Allaire P. D., Wasiak S., Girard M., Hussain N. K., McPherson P. S. (2004). Tandem MS analysis of brain clathrin-coated vesicles reveals their critical involvement in synaptic vesicle recycling. *Proc Natl Acad Sci.* 101(11):3833-3838.

Bradshaw K.D., Emptage N.J., Bliss T.V.P. (2003). A role for dendritic protein synthesis in hippocampal late LTP. *Eur. J. Neurosci.* 18:3150-3152.

Bramham C. R., Wells D.G. (2007). Dendritic mRNA: transport, translation, and function. *Nat. Rev. Neurosci.* 8:776–789.

Bramham C. R., (2008). Local protein synthesis, actin dynamics, and LTP consolidation. *Curr. Opin. Neurobiol.* 18:524–531.

Bresler T., Shapira M., Boeckers T., Dresbach T., Futter M., Garner CC., Rosenblum K., Gundelfinger ED., Ziv NE. (2004). Postsynaptic density assembly is fundamentally different from presynaptic active zone assembly. *J. Neurosci.* 24:1507-1520.

Brewer GJ., Price PJ. (1996). Viable cultured neurons in ambient carbon dioxide and hibernation storage for a month. *Neuroreport.* 7(9):1509-12.

Bruckenstein D. A., Lein P. J., Higgins D., Fremeau R. T., Jr. (1990). Distinct spatial localization of specific mRNAs in cultured sympathetic neurons. *Neuron.* 5(6):809-819.

Burgin A.B., Pace N.R., (1990). Mapping the active site of ribonuclease P RNA using a substrate containing a photoaffinity agent. *EMBO J.* 9(12):4111-8.

Burgin K. E., Waxham M. N., Rickling S., Westgate S. A., Mobley W. C., Kelly P. T. (1990). In situ hybridization histochemistry of Ca²⁺/calmodulin-dependent protein kinase in developing rat brain. *J. Neurosci.* 10:1788–1798.

Cajigas I.J., Will T., Schuman E.M. (2010). Protein homeostasis and synaptic plasticity. *EMBO J.* 29(16):2746-52.

Cajigas I. J., Tushev G., Will T. J., tom Dieck S., Fuerst N., Schuman E. M. (2012). The local transcriptome in the synaptic neuropil revealed by deep sequencing and high-resolution imaging. *Neuron.* 74(3):453-466.

Campbell D. S., Holt C. E. (2001). Chemotropic responses of retinal growth cones mediated by rapid local protein synthesis and degradation. *Neuron.* 32(6):1013-1026.

Carmona-Saez P., Chagoyen M., Tirado F., Carazo JM., Pascual-Montano A. (2007). GENECODIS: A web-based tool for finding significant concurrent annotations in gene lists. *Genome Biology.* 8(1): R3.

Caroni P., Donato F., Muller D. (2012). Structural plasticity upon learning: regulation and functions. *Nat Rev Neurosci.* 13(7):478-90.

Casadio A., Martin K. C., Giustetto M., Zhu H., Chen M., Bartsch D., Kandel E. R. (1999). A transient, neuron-wide form of CREB-mediated long-term facilitation can be stabilized at specific synapses by local protein synthesis. *Cell.* 99(2):221-237.

Chang E. J., Archambault V., McLachlin D. T., Krutchinsky A. N., Chait B. T. (2004). Analysis of protein phosphorylation by hypothesis-driven multiple-stage mass spectrometry. *Anal Chem.* 76(15):4472-4483.

Cheng D., Hoogenraad C. C., Rush J., Ramm E., Schlager M. A., Duong D. M., Peng J. (2006). Relative and absolute quantification of postsynaptic density proteome isolated from rat forebrain and cerebellum. *Mol Cell Proteomics.* 5(6):1158-1170.

Cheng A., Wan R., Yang J.L., Kamimura N., Son T.G., Ouyang X., Luo Y., Okun E., Mattson M.P. (2012). Involvement of PGC-1 α in the formation and maintenance of neuronal dendritic spines. *Nat Commun.* 3:1250.

Chicurel M.E., Terrian D.M., Potter H. (1993). mRNA at the synapse: analysis of a synaptosomal preparation enriched in hippocampal dendritic spines. *J Neurosci.* 13:4054-4063.

Chudakov D. M., Matz M. V., Lukyanov S., Lukyanov K. A. (2010). Fluorescent proteins and their applications in imaging living cells and tissues. *Physiol Rev.* 90(3):1103-1163.

Cohen L. D., Zuchman R., Sorokina O., Muller A., Dieterich D. C., Armstrong J. D., Ziv N. E. (2013). Metabolic turnover of synaptic proteins: kinetics, interdependencies, and implications for synaptic maintenance. *PLoS One.* 8(5): e63191.

Collins M.O., Husi H., Yu L., Brandon J.M., Anderson C.N., Blackstock W.P., Choudhary J.S., Grant S.G. (2006). Molecular characterization and comparison of the components and multiprotein complexes in the postsynaptic proteome. *J Neurochem.* 97 Suppl 1:16-23.

Collins M. O., Yu L., Coba M. P., Husi H., Campuzano I., Blackstock W. P., Grant S. G. (2005). Proteomic analysis of in vivo phosphorylated synaptic proteins. *J Biol Chem.* 280(7):5972-5982.

Costa-Mattioli M., Sossin W. S., Klann E., Sonenberg N. (2009). Translational control of long-lasting synaptic plasticity and memory. *Neuron.* 61(1):10-26.

Cotman C. W., Matthews D. A. (1971). Synaptic plasma membranes from rat brain synaptosomes: isolation and partial characterization. *Biochim Biophys Acta.* 249(2):380-394.

Coughenour H. D., Spaulding R. S., Thompson C. M. (2004). The synaptic vesicle proteome: a comparative study in membrane protein identification. *Proteomics*. 4(10):3141-3155.

Cox L. J., Hengst U., Gurskaya N. G., Lukyanov K. A., Jaffrey S. R. (2008). Intra-axonal translation and retrograde trafficking of CREB promotes neuronal survival. *Nat Cell Biol*. 10(2):149-159.

Cracco J.B., Serrano P., Moskowitz S.I., Bergold P.J., Sacktor T.C. (2005). Protein synthesis-dependent LTP in isolated dendrites of CA1 pyramidal cells. *Hippocampus*. 15:551–556.

Craig A. M., Olds J. L., Schreurs B. G., Scharenberg A. M., Alkon D. L. (1993). Quantitative distribution of protein kinase C alpha, beta, gamma, and epsilon mRNAs in the hippocampus of control and nictitating membrane conditioned rabbits. *Brain Res Mol Brain Res*. 19(4):269-276.

Craig A.M., Graf E.R., Linhoff M.W. (2006). How to build a central synapse: clues from cell culture. *Trends Neurosci*. 29:8-20.

Cui Z., Wang H., Tan Y., Zaia K. A., Zhang S., Tsien J. Z. (2004). Inducible and reversible NR1 knockout reveals crucial role of the NMDA receptor in preserving remote memories in the brain. *Neuron*. 41(5):781-793.

Davis H.P., Squire L.R. (1984). Protein synthesis and memory: a review. *Psychol. Bull*. 96:518–559.

Dean R. A., Overall C. M. (2007). Proteomics discovery of metalloproteinase substrates in the cellular context by iTRAQ labeling reveals a diverse MMP-2 substrate degradome. *Mol Cell Proteomics*. 6(4):611-623.

Deglincerti A., Jaffrey S. R. (2012). Insights into the roles of local translation from the axonal transcriptome. *Open Biol*. 2(6):120079.

Dennis G. Jr., Sherman B. T., Hosack D. A., Yang J., Gao W., Lane H. C., Lempicki R. A. (2003). DAVID: Database for Annotation, Visualization, and Integrated Discovery. *Genome Biol.* 4(5): P3.

Derkach V. A., Oh M. C., Guire E. S., Soderling T. R. (2007). Regulatory mechanisms of AMPA receptors in synaptic plasticity. *Nat Rev Neurosci.* 8(2): 101-113.

Dieterich DC., Kreutz MR. (2016). Proteomics of the Synapse - A Quantitative Approach to Neuronal Plasticity. *Mol Cell Proteomics.* 15(2):368-81.

Dieterich DC., Link AJ., Graumann J., Tirrell DA., Schuman EM. (2006). Selective identification of newly synthesized proteins in mammalian cells using bioorthogonal noncanonical amino acid tagging (BONCAT). *PNAS.* 103: 9482-9487.

Dieterich DC., Lee JJ., Link AJ., Graumann J., Tirrell DA., Schuman EM. (2007). Labeling, detection, and identification of newly synthesized proteomes with bioorthogonal non-canonical amino-acid tagging. *Nat Proto.* 2:532-540.

Dieterich D. C., Hodas J. J., Gouzer G., Shadrin I. Y., Ngo J. T., Triller A., Schuman E. M. (2010). In situ visualization and dynamics of newly synthesized proteins in rat hippocampal neurons. *Nat Neurosci.* 13(7):897-905.

Dodd P. R., Hardy J. A., Oakley A. E., Edwardson J. A., Perry E. K., Delaunoy J. P. (1981). A rapid method for preparing synaptosomes: comparison, with alternative procedures. *Brain Res.* 226(1-2):107-118.

Dosemeci A., Makusky AJ., Jankowska-Stephens E., Yang X., Slotta DJ., Markey SP. (2007). Composition of the synaptic PSD-95 complex. *Mol Cell Proteomics.* 6(10):1749-60.

Dosemeci A., Tao-Cheng J. H., Vinade L., Jaffe H. (2006). Preparation of postsynaptic density fraction from hippocampal slices and proteomic analysis. *Biochem Biophys Res Commun.* 339(2):687-694.

Droz B., Barondes S. M. (1969). Nerve endings: rapid appearance of labeled protein shown by electron microscope radioautography. *Science.* 165:1131–1133.

Dunkley P. R., Jarvie P. E., Robinson P. J. (2008). A rapid Percoll gradient procedure for preparation of synaptosomes. *Nat Protoc.* 3(11):1718-1728.

Edgar PF., Schonberger SJ., Dean B., Faull RL., Kydd R., Cooper GJ. (1999). A comparative proteome analysis of hippocampal tissue from schizophrenic and Alzheimer's disease individuals. *Mol Psychiatry.* 4(2):173-8.

Elortza F., Nühse TS., Foster LJ., Stensballe A., Peck SC., Jensen ON. (2003). Proteomic analysis of glycosylphosphatidylinositol-anchored membrane proteins. *Mol Cell Proteomics.* 2(12):1261-70.

Engert F., Bonhoeffer T. (1999). Dendritic spine changes associated with hippocampal long-term synaptic plasticity. *Nature.* 399:66-70.

Erdmann I., Marter K., Kobler O., Niehues S., Abele J., Muller A., Dieterich D. C. (2015). Cell-selective labelling of proteomes in *Drosophila melanogaster*. *Nat Commun.* 6:7521.

Estrada-Bernal A., Sanford S. D., Sosa L. J., Simon G. C., Hansen K. C., Pfenninger K. H. (2012). Functional complexity of the axonal growth cone: a proteomic analysis. *PLoS One.* 7(2):e31858.

Fallon JR., Taylor AB. (2013). Protein Synthesis in Neurons. In: eLS. John Wiley & Sons, Ltd: Chichester.

Feig S., Lipton P. (1993). Pairing the cholinergic agonist carbachol with patterned Schaffer collateral stimulation initiates protein synthesis in hippocampal CA1 pyramidal cell dendrites via a muscarinic, NMDA-dependent mechanism. *J Neurosci.* 13(3):1010-21.

Ficarro SB., McClelland ML., Stukenberg PT., Burke DJ., Ross MM., Shabanowitz J., Hunt DF., White FM. (2002). Phosphoproteome analysis by mass spectrometry and its application to *Saccharomyces cerevisiae*. *Nat Biotechnol.* 20(3):301-5.

Fletcher T. L., De Camilli P., Banker G. (1994). Synaptogenesis in hippocampal cultures: evidence indicating that axons and dendrites become competent to form synapses at different stages of neuronal development. *J Neurosci.* 14(11 Pt 1):6695-6706.

Franklin SO., Elliott K., Zhu YS., Wahlestedt C., Inturrisi CE. (1993). Quantitation of NMDA receptor (NMDAR1) mRNA levels in the adult and developing rat CNS. *Brain Res Mol Brain Res.* 19(1-2):93-100.

Frey U., Morris R. G. (1997). Synaptic tagging and long-term potentiation. *Nature.* 385:533–536.

Friedman HV., Bresler T., Garner CC., Ziv NE. (2000). Assembly of new individual excitatory synapses: time course and temporal order of synaptic molecule recruitment. *Neuron.* 27:57-69.

Furuichi T., Simon-Chazottes D., Fujino I., Yamada N., Hasegawa M., Miyawaki A., Mikoshiba K. (1993). Widespread expression of inositol 1,4,5-trisphosphate receptor type 1 gene (*Insp3r1*) in the mouse central nervous system. *Receptors Channels.* 1(1):11-24.

Garcia B. A., Shabanowitz J., Hunt D. F. (2005). Analysis of protein phosphorylation by mass spectrometry. *Methods.* 35(3):256-264.

Gardiol A., Racca C., Triller A. (1999). Dendritic and postsynaptic protein synthetic machinery. *J Neurosci.* 19(1):168-179.

Garner C. C., Shen K. (2008). Structure and Function of Vertebrate and Invertebrate Active Zones. In J.W. Hell, M.D. Ehlers (eds.), *Structural and Functional Organization of the Synapse*, pp 63-89.

Garner C. C., Tucker R. P. Matus A. (1988). Selective localization of messenger RNA for cytoskeletal protein MAP2 in dendrites. *Nature.* 336:674–677.

Garner CC., Zhai RG., Gundelfinger ED., Ziv NE. (2002). Molecular mechanisms of CNS synaptogenesis. *Trends Neurosci.* 25(5):243-51.

Giuditta A., Menichini E., Perrone Capano C., Langella M., Martin R., Castigli E., Kaplan B.B., (1991). Active polysomes in the axoplasm of the squid giant axon. *J. Neurosci. Res.* 28:18–28.

Giustetto M., Hegde A.N., Si K., Casadio A., Inokuchi K., Pei W., Kandel E.R., Schwartz J.H. (2003). Axonal transport of eukaryotic translation elongation factor 1alpha mRNA couples transcription in the nucleus to long-term facilitation at the synapse. *Proc. Natl. Acad. Sci.* 100:13680–13685.

Goedert M., Crowther R. A., Garner C. C. (1991). Molecular characterization of microtubule-associated proteins tau and MAP2. *Trends Neurosci.* 14(5): 193-199.

Gonsalvez G.B., Urbinati C.R., Long R.M., (2005). RNA localization in yeast: moving towards a mechanism. *Biol Cell.* 97(1):75-86.

Goslin K., Asmussen H., Banker G. (1998). Rat hippocampal neurons in low-density culture. In: Banker G., Goslin K., editors. *Culturing nerve cells*. Cambridge, MA: MIT Press. pp. 339–370.

Govindarajan A., Israely I., Huang S. Y., Tonegawa S. (2011). The dendritic branch is the preferred integrative unit for protein synthesis-dependent LTP. *Neuron*. 69:132–146.

Grabrucker A. M., Vaida B., Bockmann J., Boeckers T. M. (2009). Efficient targeting of proteins to post-synaptic densities of excitatory synapses using a novel pSDTarget vector system. *J Neurosci Methods*. 181(2):227-234.

Grant S. G. (2006). The synapse proteome and phosphoproteome: a new paradigm for synapse biology. *Biochem Soc Trans*. 34(Pt 1):59-63.

Grant S. G. (2012). Synaptopathies: diseases of the synaptome. *Curr Opin Neurobiol*. 22(3):522-529.

Gronborg M., Kristiansen T. Z., Iwahori A., Chang R., Reddy R., Sato N., Pandey A. (2006). Biomarker discovery from pancreatic cancer secretome using a differential proteomic approach. *Mol Cell Proteomics*. 5(1):157-171.

Gruhler A., Olsen JV., Mohammed S., Mortensen P., Faergeman NJ., Mann M., Jensen ON. (2005). Quantitative phosphoproteomics applied to the yeast pheromone signaling pathway. *Mol Cell Proteomics*. 4(3):310-27.

Gumy L. F., Yeo G. S., Tung Y. C., Zivraj K. H., Willis D., Coppola G., Fawcett J. W. (2011). Transcriptome analysis of embryonic and adult sensory axons reveals changes in mRNA repertoire localization. *RNA*. 17(1):85-98.

Gundelfinger E D., tom Dieck S. (2000). Molecular organization of excitatory chemical synapses in the mammalian brain. *Die Naturwissenschaften* (12):513-23.

Hajos F. (1975). An improved method for the preparation of synaptosomal fractions in high purity. *Brain Res*. 93(3):485-489.

Hang H. C., Yu C., Kato D. L., Bertozzi C. R. (2003). A metabolic labeling approach toward proteomic analysis of mucin-type O-linked glycosylation. *Proc Natl Acad Sci.* 100(25):14846-14851.

Hanus C., Schuman EM. (2013). Proteostasis in complex dendrites. *Nat Rev Neurosci.* 14(9):638-48.

Hanz S., Perlson E., Willis D., Zheng J. Q., Massarwa R., Huerta J. J., Fainzilber M. (2003). Axoplasmic importins enable retrograde injury signaling in lesioned nerve. *Neuron.* 40(6):1095-1104.

Harada A., Oguchi K., Okabe S., Kuno J., Terada S., Ohshima T., Hirokawa N. (1994). Altered microtubule organization in small-calibre axons of mice lacking tau protein. *Nature.* 369(6480):488-491.

Harris KM. (2008). Diversity in Synapse Structure and Composition. In J.W. Hell, M.D. Ehlers (eds.), *Structural and Functional Organization of the Synapse.*

Harris KM., Stevens JK. (1989). Dendritic spines of CA 1 pyramidal cells in the rat hippocampus: serial electron microscopy with reference to their biophysical characteristics. *J Neurosci.* 9:2982–2997.

Harris KM., Weinberg RJ. (2012). Ultrastructure of synapses in the mammalian brain. *Cold Spring Harb Perspect Biol.* 4(5). pii: a005587.

Hengst U., Deglincerti A., Kim HJ., Jeon NL., Jaffrey SR. (2009) Axonal elongation triggered by stimulus-induced local translation of a polarity complex protein. *Nat Cell Biol.* 11(8):1024-30.

Henn FA., Anderson DJ., Rustad DG. (1976). Glial contamination of synaptosomal fractions. *Brain Res.* 101:341–344.

Herzog E., Nadrigny F., Silm K., Biesemann C., Helling I., Bersot T., Steffens H., Schwartzmann R., Nägerl UV., El Mestikawy S., Rhee J., Kirchhoff F., Brose N. (2011). In vivo imaging of intersynaptic vesicle exchange using VGLUT1Venus knock-in mice. *J Neurosci.* 31:15544–15559.

Hillefors M., Gioio A. E., Mameza M. G., Kaplan B. B. (2007). Axon viability and mitochondrial function are dependent on local protein synthesis in sympathetic neurons. *Cell Mol Neurobiol.* 27(6):701-716.

Hirokawa N. (2006). mRNA transport in dendrites: RNA granules, motors, and tracks. *J Neurosci.* 26:7139–7142.

Hodas J. J., Nehring A., Hoche N., Sweredoski M. J., Pielot R., Hess S., Schuman E. M. (2012). Dopaminergic modulation of the hippocampal neuropil proteome identified by bioorthogonal noncanonical amino acid tagging (BONCAT). *Proteomics.* 12(15-16):2464-2476.

Holt C. E., Bullock S. L. (2009). Subcellular mRNA localization in animal cells and why it matters. *Science.* 326(5957):1212-1216.

Holt C.E., Schuman E.M. (2013). The central dogma decentralized: new perspectives on RNA function and local translation in neurons. *Neuron.* 80(3): 648-57.

Huang DW., Sherman BT., Lempicki RA. (2009). Bioinformatics enrichment tools: paths toward the comprehensive functional analysis of large gene lists. *Nucleic Acids Res.* 37(1):1-13.

Huang DW., Sherman BT., Lempicki RA. (2009). Systematic and integrative analysis of large gene lists using DAVID Bioinformatics Resources. *Nature Protoc.* 4(1):44-57.

Huang Y.Y., Kandel E.R. (2005). Theta frequency stimulation induces a local form of late phase LTP in the CA1 region of the hippocampus. *Lear. Mem.* 12:587-593.

Huber K.M., Kayser M.S., Bear M.F. (2000). Role for rapid dendritic protein synthesis in hippocampal mGluR-dependent long-term depression. *Science.* 288:1254–1257.

Hwang S. I., Lundgren D. H., Mayya V., Rezaul K., Cowan A. E., Eng J. K., Han D. K. (2006). Systematic characterization of nuclear proteome during apoptosis: a quantitative proteomic study by differential extraction and stable isotope labeling. *Mol Cell Proteomics.* 5(6):1131-1145.

Irish JM., Hovland R., Krutzik PO., Perez OD., Bruserud Ø., Gjertsen BT., Nolan GP. (2004). Single cell profiling of potentiated phospho-protein networks in cancer cells. *Cell.* 118(2):217-28.

Issaq H., Veenstra T. (2008). Two-dimensional polyacrylamide gel electrophoresis (2D-PAGE): advances and perspectives. *Biotechniques.* 44(5):697-698, 700.

Jensen ON. (2006). Interpreting the protein language using proteomics. *Nat Rev Mol Cell Biol.* 7(6):391-403.

Jiang C., Schuman E. M. (2002). Regulation and function of local protein synthesis in neuronal dendrites. *Trends Biochem Sci.* 27(10):506-513.

Jones-Villeneuve E. M. V., McBumey M. W., Rogers K. A., Kalnins V. I. (1982). Retinoic acid induces embryonal carcinoma cells to differentiate into neurons and glial cells. *J. Cell Biol.* 94:253-262.

Jordan B. A., Fernholz B. D., Boussac M., Xu C., Grigorean G., Ziff E. B., Neubert T. A. (2004). Identification and verification of novel rodent postsynaptic density proteins. *Mol Cell Proteomics.* 3(9):857-871.

Jordan B. A., Fernholz B. D., Neubert T. A., Ziff E. B. (2006). New Tricks for an Old Dog: Proteomics of the PSD. In J. T. Kittler & S. J. Moss (Eds.), *The Dynamic Synapse: Molecular Methods in Ionotropic Receptor Biology*. Boca Raton (FL).

Ju W., Morishita W., Tsui J., Gaietta G., Deerinck TJ., Adams SR., Garner CC., Tsien RY., Ellisman MH., Malenka RC. (2004). Activity-dependent regulation of dendritic synthesis and trafficking of AMPA receptors. *Nat Neurosci.* 7:244-253.

Jung H., Yoon B. C., Holt C. E. (2012). Axonal mRNA localization and local protein synthesis in nervous system assembly, maintenance and repair. *Nat Rev Neurosci.* 13(5):308-324.

Jung H., Gkogkas C. G., Sonenberg N., Holt C. E. (2014). Remote control of gene function by local translation. *Cell.* 157(1):26-40.

Kadakkuzha B. M., Puthanveetil S. V. (2013). Genomics and proteomics in solving brain complexity. *Mol Biosyst.* 9(7):1807-1821.

Kaech S., Banker G. (2006). Culturing hippocampal neurons. *Nat Protoc.* 1(5): 2406-2415.

Kaji H., Saito H., Yamauchi Y., Shinkawa T., Taoka M., Hirabayashi J., Isobe T. (2003). Lectin affinity capture, isotope-coded tagging and mass spectrometry to identify N-linked glycoproteins. *Nat Biotechnol.* 21(6):667-672.

Kaminska M., Havrylenko S., Decottignies P., Le Marechal P., Negrutskii B., Mirande M. (2009). Dynamic Organization of Aminoacyl-tRNA Synthetase Complexes in the Cytoplasm of Human Cells. *J Biol Chem.* 284(20):13746-13754.

Kandel ER. (2001). The molecular biology of memory storage: a dialogue between genes and synapses. *Science*. 294:1030–1038

Kang H., Schuman EM. (1996). A requirement for local protein synthesis in neurotrophin-induced hippocampal synaptic plasticity. *Science*. 273(5280):1402-6.

Kelleher R. J., Bear M. F. (2008). The autistic neuron: troubled translation? *Cell*. 135:401-406.

Khawaja X., Xu J., Liang JJ., Barrett JE. (2004). Proteomic analysis of protein changes developing in rat hippocampus after chronic antidepressant treatment: Implications for depressive disorders and future therapies. *J Neurosci Res*. 75(4):451-60.

Khidekel N., Ficarro S. B., Peters E. C., Hsieh-Wilson L. C. (2004). Exploring the O-GlcNAc proteome: direct identification of O-GlcNAc-modified proteins from the brain. *Proc Natl Acad Sci*. 101(36):13132-13137.

Kim H. K., Kim Y. B., Kim E. G., Schuman E. (2005). Measurement of dendritic mRNA transport using ribosomal markers. *Biochem Biophys Res Commun*. 328(4):895-900.

Kleiman R., Banker G., Steward O. (1990). Differential subcellular localization of particular mRNAs in hippocampal neurons in culture. *Neuron*. 5(6):821-830.

Koenig E., Martin R. (1996). Cortical plaque-like structures identify ribosome-containing domains in the Mauthner cell axon. *J Neurosci*. 16(4):1400-1411.

Koenig E., Martin R., Titmus M., Sotelo-Silveira J. R. (2000). Cryptic peripheral ribosomal domains distributed intermittently along mammalian myelinated axons. *J Neurosci*. 20(22):8390-8400.

Krapfenbauer K., Fountoulakis M., Lubec G. (2003). A rat brain protein expression map including cytosolic and enriched mitochondrial and microsomal fractions. *Electrophoresis*. 24(11):1847-1870.

Kuhl D., Skehel P. (1998). Dendritic localization of mRNAs. *Curr Opin Neurobiol*. 8(5):600-6.

Kun A., Otero L., Sotelo-Silveira J. R., Sotelo J. R. (2007). Ribosomal distributions in axons of mammalian myelinated fibers. *J Neurosci Res*. 85(10): 2087-2098.

Larsen MR., Højrup P., Roepstorff P. (2005). Characterization of gel-separated glycoproteins using two-step proteolytic digestion combined with sequential microcolumns and mass spectrometry. *Mol Cell Proteomics*. 4(2): 107-19.

Laughlin SB., Sejnowski TJ. (2003). Communication in neuronal networks. *Science*. 301(5641):1870-4.

Lécuyer E., Yoshida H., Parthasarathy N., Alm C., Babak T., Cerovina T., Krause H. M. (2007). Global analysis of mRNA localization reveals a prominent role in organizing cellular architecture and function. *Cell*. 131(1): 174-187.

Leung K. M., van Horck F. P., Lin A. C., Allison R., Standart N., Holt C. E. (2006). Asymmetrical beta-actin mRNA translation in growth cones mediates attractive turning to netrin-1. *Nat Neurosci*. 9(10):1247-1256.

Li K. W., Hornshaw M. P., Van Der Schors R. C., Watson R., Tate S., Casetta B., Smit A. B. (2004). Proteomics analysis of rat brain postsynaptic density. Implications of the diverse protein functional groups for the integration of synaptic physiology. *J Biol Chem*. 279(2):987-1002.

Ligon LA., Steward O. (2000). Role of microtubules and actin filaments in the movement of mitochondria in the axons and dendrites of cultured hippocampal neurons. *J Comp Neurol.* 427(3): 351-61.

Lin A. C., Holt C. E. (2008). Function and regulation of local axonal translation. *Curr. Opin. Neurobiol.* 18, 60–68.

Lin M. Z., Glenn J. S., Tsien R. Y. (2008). A drug-controllable tag for visualizing newly synthesized proteins in cells and whole animals. *Proc Natl Acad Sci.* 105(22):7744-7749.

Link A. J., Vink M. K., Agard N. J., Prescher J. A., Bertozzi C. R., Tirrell D. A. (2006). Discovery of aminoacyl-tRNA synthetase activity through cell-surface display of noncanonical amino acids. *Proc Natl Acad Sci.* 103(27):10180-10185.

Link A. J., Vink M. K., Tirrell D. A. (2007). Preparation of the functionalizable methionine surrogate azidohomoalanine via copper-catalyzed diazo transfer. *Nat Protoc.* 2(8):1879-1883.

Link W., Konietzko U., Kauselmann G., Krug M., Schwanke B., Frey U., Kuhl D. (1995). Somatodendritic expression of an immediate early gene is regulated by synaptic activity. *Proc Natl Acad Sci.* 92(12):5734-5738.

Liu K., Hu JY., Wang D., Schacher S. (2003). Protein synthesis at synapse versus cell body: enhanced but transient expression of long-term facilitation at isolated synapses. *J Neurobiol.* 56(3):275-86.

Loya CM., Van Vactor D., Fulga TA. (2010). Understanding neuronal connectivity through the post-transcriptional toolkit. *Genes Dev.* 24(7): 625-35.

Lu B., Nagappan G., Guan X., Nathan P. J., Wren P. (2013). BDNF-based synaptic repair as a disease-modifying strategy for neurodegenerative diseases. *Nat Rev Neurosci.* 14(6):401-416.

Lyford G. L., Yamagata K., Kaufmann W. E., Barnes C. A., Sanders L. K., Copeland N. G., Worley P. F. (1995). Arc, a growth factor and activity-regulated gene, encodes a novel cytoskeleton-associated protein that is enriched in neuronal dendrites. *Neuron*. 14(2):433-445.

Lyles V., Zhao Y., Martin KC. (2006). Synapse formation and mRNA localization in cultured *Aplysia* neurons. *Neuron*. 49(3): 349-56.

Macchi P., Hemraj I., Goetze B., Grunewald B., Mallardo M., Kiebler M. A. (2003). A GFP-based system to uncouple mRNA transport from translation in a single living neuron. *Mol Biol Cell*. 14(4): 1570-1582.

MacCoss M. J., Wu C. C., Liu H., Sadygov R., Yates J. R., 3rd. (2003). A correlation algorithm for the automated quantitative analysis of shotgun proteomics data. *Anal Chem*. 75(24):6912-6921.

Maletic-Savatic M., Malinow R., Svoboda K. (1999). Rapid dendritic morphogenesis in CA1 hippocampal dendrites induced by synaptic activity. *Science*. 283:1923-1927.

Malgaroli A., Tsien R. W. (1992). Glutamate-induced long-term potentiation of the frequency of miniature synaptic currents in cultured hippocampal neurons. *Nature*. 357(6374):134-139.

Malinow R. (2012). New developments on the role of NMDA receptors in Alzheimer's disease. *Curr Opin Neurobiol*. 22(3): 559-63.

Malmqvist T., Anthony K., Gallo J. M. (2014). Tau mRNA is present in axonal RNA granules and is associated with elongation factor 1A. *Brain Res*. 1584, 22-27.

Manadas B., Santos A. R., Szabadfi K., Gomes J. R., Garbis S. D., Fountoulakis M., Duarte C. B. (2009). BDNF-induced changes in the expression of the translation machinery in hippocampal neurons: protein levels and dendritic mRNA. *J Proteome Res.* 8(10):4536-4552.

Martin K. C., Barad M., Kandel E. R. (2000). Local protein synthesis and its role in synapse-specific plasticity. *Curr Opin Neurobiol.* 10(5):587-592.

Martin K. C., Casadio A., Zhu H., Yaping E., Rose J. C., Chen M., Kandel E. R. (1997). Synapse-specific, long-term facilitation of aplysia sensory to motor synapses: a function for local protein synthesis in memory storage. *Cell.* 91(7):927-938.

Martin KC., Ephrussi A. (2009). mRNA localization: gene expression in the spatial dimension. *Cell.* 136 (4):719-30.

Martin R., Vaida B., Bleher R., Crispino M., Giuditta A. (1998). Protein synthesizing units in presynaptic and postsynaptic domains of squid neurons. *J Cell Sci.* 111 (Pt 21):3157-66.

Martin K. C., Zukin R. S. (2006). RNA trafficking and local protein synthesis in dendrites: an overview. *J. Neurosci.* 26, 7131-7134.

Martin S. J., Grimwood P. D., Morris R. G. (2000). Synaptic plasticity and memory: an evaluation of the hypothesis. *Annu Rev Neurosci.* 23, 649-711.

Mayford M., Siegelbaum SA., Kandel ER. (2012) Synapses and memory storage. *Cold Spring Harb Perspect Biol.* 4(6). pii: a005751.

McBurney M. W., Reuhl K. R., Ally A. I., Nasipuri S., Bell J. C., Craig J. (1988). Differentiation and maturation of embryonal carcinoma-derived neurons in cell culture. *J Neurosci.* 8(3):1063-1073.

McBurney M. W. (1993). P19 embryonal carcinoma cells. *Int J Dev Biol.* 37(1):135-140.

Medioni C., Mowry K., Besse F. (2012). Principles and roles of mRNA localization in animal development. *Development.* 139(18):3263-76.

Meems R., Munno D., van Minnen J., Syed NI. (2003). Synapse formation between isolated axons requires presynaptic soma and redistribution of postsynaptic AChRs. *J Neurophysiol.* 89:2611–2619.

Michaevlevski I., Medzihradzsky K. F., Lynn A., Burlingame A. L., Fainzilber M. (2010). Axonal transport proteomics reveals mobilization of translation machinery to the lesion site in injured sciatic nerve. *Mol Cell Proteomics.* 9(5): 976-987.

Miller S., Yasuda M., Coats J. K., Jones Y., Martone M. E., Mayford M. (2002). Disruption of dendritic translation of CaMKIIalpha impairs stabilization of synaptic plasticity and memory consolidation. *Neuron.* 36(3):507-519.

Ming G. L., Wong S. T., Henley J., Yuan X. B., Song H. J., Spitzer N. C., Poo M. M. (2002). Adaptation in the chemotactic guidance of nerve growth cones. *Nature.* 417(6887):411-418.

Miyashiro K., Dichter M., Eberwine J. (1994). On the nature and differential distribution of mRNAs in hippocampal neurites: implications for neuronal functioning. *Proc Natl Acad Sci.* 91(23):10800-10804.

Morciano M., Burre J., Corvey C., Karas M., Zimmermann H., Volkandt W. (2005). Immunolocalization of two synaptic vesicle pools from synaptosomes: a proteomics analysis. *J Neurochem.* 95(6):1732-1745.

Morciano M., Beckhaus T., Karas M., Zimmermann H., Volkandt W. (2009). The proteome of the presynaptic active zone: from docked synaptic vesicles to adhesion molecules and maxi-channels. *J Neurochem.* 108(3):662-675.

Morgan I. G. (1976). Synaptosomes and cell separation. *Neuroscience*. 1(3):159-165.

Munton RP., Tweedie-Cullen R., Livingstone-Zatchej M., Weinandy F., Waidelich M., Longo D., Gehrig P., Potthast F., Rutishauser D., Gerrits B., Panse C., Schlapbach R., Mansuy IM. (2007). Qualitative and quantitative analyses of protein phosphorylation in naive and stimulated mouse synaptosomal preparations. *Mol Cell Proteomics*. 6(2): 283-93.

Müller A. (2012). Zell-spezifische, metabolische Markierung von neu synthetisierten Proteinen in einem Neuron-Glia-Netzwerk. Dissertation. Magdeburg, Univ., Fak. für Naturwiss.

Nagai T., Ibata K., Park ES., Kubota M., Mikoshiba K., Miyawaki A. (2002). A variant of yellow fluorescent protein with fast and efficient maturation for cell-biological applications. *Nat. Biotechnol*. 20(1):87–90.

Nehls S., Snapp E. L., Cole N. B., Zaal K. J., Kenworthy A. K., Roberts T. H., Lippincott-Schwartz J. (2000). Dynamics and retention of misfolded proteins in native ER membranes. *Nat Cell Biol*. 2(5):288-295.

Newpher T. M., Ehlers M. D. (2009). Spine microdomains for postsynaptic signaling and plasticity. *Trends Cell Biol*. 19(5):218–227.

Ngo J. T., Champion J. A., Mahdavi A., Tanrikulu I. C., Beatty K. E., Connor R. E., Tirrell D. A. (2009). Cell-selective metabolic labeling of proteins. *Nat Chem Biol*. 5(10):715-717.

Niepel M., Hafner M., Pace EA., Chung M., Chai DH., Zhou L., Schoeberl B., Sorger PK. (2013). Profiles of Basal and stimulated receptor signaling networks predict drug response in breast cancer lines. *Sci Signal*. 6(294):ra84.

Nogales-Cadenas R., Carmona-Saez P., Vazquez M., Vicente C., Yang X., Tirado F., Carazo JM., Pascual-Montano A. (2009). GeneCodis: interpreting gene lists through enrichment analysis and integration of diverse biological information. *Nucleic Acids Res.* 37 (Web Server issue): W317-22.

Ohtsuka T., Takao-Rikitsu E., Inoue E., Inoue M., Takeuchi M., Matsubara K., Takai Y. (2002). Cast: a novel protein of the cytomatrix at the active zone of synapses that forms a ternary complex with RIM1 and munc13-1. *J Cell Biol.* 158(3):577-590.

Ong S. E., Blagoev B., Kratchmarova I., Kristensen D. B., Steen H., Pandey A., Mann M. (2002). Stable isotope labeling by amino acids in cell culture, SILAC, as a simple and accurate approach to expression proteomics. *Mol Cell Proteomics.* 1(5):376-386.

Ong S.E., Mann M. (2006). A practical recipe for stable isotope labeling by amino acids in cell culture (SILAC). *Nature Protocols.* 1 (6):2650–60.

Ong S.E., Mann M. (2007). Stable isotope labeling by amino acids in cell culture for quantitative proteomics. *Methods in Molecular Biology.* 359:37–52.

Ostroff LE., Fiala JC., Allwardt B., Harris KM. (2002). Polyribosomes redistribute from dendritic shafts into spines with enlarged synapses during LTP in developing rat hippocampal slices. *Neuron.* 35:535-545.

Pannese E., Ledda M. (1991). Ribosomes in myelinated axons of the rabbit spinal ganglion neurons. *J Submicrosc Cytol Pathol.* 23(1):33-38.

Pawlik T. M., Hawke D. H., Liu Y., Krishnamurthy S., Fritsche H., Hunt K. K., Kuerer H. M. (2006). Proteomic analysis of nipple aspirate fluid from women with early-stage breast cancer using isotope-coded affinity tags and tandem mass spectrometry reveals differential expression of vitamin D binding protein. *BMC Cancer.* 6:68.

Peng J., Kim M. J., Cheng D., Duong D. M., Gygi S. P., Sheng M. (2004). Semiquantitative proteomic analysis of rat forebrain postsynaptic density fractions by mass spectrometry. *J Biol Chem.* 279(20):21003-21011.

Pereda AE. (2014). Electrical synapses and their functional interactions with chemical synapses. *Nat Rev Neurosci.* 15(4):250-63.

Peters E. C., Brock A., Ficarro S. B. (2004). Exploring the phosphoproteome with mass spectrometry. *Mini Rev Med Chem.* 4(3):313-324.

Phillips G. R., Florens L., Tanaka H., Khaing Z. Z., Fidler L., Yates J. R., 3rd, Colman D. R. (2005). Proteomic comparison of two fractions derived from the transsynaptic scaffold. *J Neurosci Res.* 81(6):762-775.

Phillips LL., Pollack AE., Steward O. (1990). Protein synthesis in the neuropil of the rat dentate gyrus during synapse development. *J Neurosci Res.* 26:474-482.

Pielot R., Smalla K. H., Muller A., Landgraf P., Lehmann A. C., Eisenschmidt E., Dieterich D. C. (2012). SynProt: A Database for Proteins of Detergent-Resistant Synaptic Protein Preparations. *Front Synaptic Neurosci.* 4:1.

Pierce J. P., van Leyen K., McCarthy J. B. (2000). Translocation machinery for synthesis of integral membrane and secretory proteins in dendritic spines. *Nat Neurosci.* 3(4):311-313.

Piper M., Holt C. (2004). RNA translation in axons. *Annu Rev Cell Dev Biol.* 20:505-523.

Pocklington A. J., Armstrong J. D., Grant S. G. (2006). Organization of brain complexity--synapse proteome form and function. *Brief Funct Genomic Proteomic.* 5(1):66-73.

Raab-Graham KF., Haddick PC., Jan YN., Jan LY. (2006). Activity- and mTOR-dependent suppression of Kv1.1 channel mRNA translation in dendrites. *Science*. 314:144-148.

Rabilloud T., Lelong C. (2011). Two-dimensional gel electrophoresis in proteomics: a tutorial. *J Proteomics*. 74(10):1829-1841.

Racca C., Catania M. V., Monyer H., Sakmann B. (1996). Expression of AMPA-glutamate receptor B subunit in rat hippocampal GABAergic neurons. *Eur J Neurosci*. 8(8):1580-1590.

Ramos-Ortolaza D. L., Bushlin I., Abul-Husn N., Annangudi S. P., Sweedler J., Devi L. A. (2010). Quantitative neuroproteomics of the synapse. *Methods Mol Biol*. 615:227-246.

Rao A. Steward O. (1991). Evidence that protein constituents of postsynaptic membrane specializations are locally synthesized: analysis of proteins synthesized within synaptosomes. *J Neurosci*. 11(9):2881-95.

Richter J. D., Klann E. (2009). Making synaptic plasticity and memory last: mechanisms of translational regulation. *Genes Dev*. 23:1–11

Roche F. K., Marsick B. M., Letourneau P. C. (2009). Protein synthesis in distal axons is not required for growth cone responses to guidance cues. *J Neurosci*. 29(3):638-652.

Rostovtsev V. V., Green L. G., Fokin V. V., Sharpless K. B. (2002). A stepwise Huisgen cycloaddition process: copper(I)-catalyzed regioselective "ligation" of azides and terminal alkynes. *Angew Chem Int Ed Engl*. 41(14): 2596-2599.

Rush J., Moritz A., Lee KA., Guo A., Goss VL., Spek EJ., Zhang H., Zha XM., Polakiewicz RD., Comb MJ. (2005). Immunoaffinity profiling of tyrosine phosphorylation in cancer cells. *Nat Biotechnol*. 23(1):94-101.

Sala C., Segal M. (2014). Dendritic spines: the locus of structural and functional plasticity. *Physiol Rev.* 94(1):141-88.

Sanchez A. L., Matthews B. J., Meynard M. M., Hu B., Javed S., Cohen Cory S. (2006). BDNF increases synapse density in dendrites of developing tectal neurons in vivo. *Development.* 133(13):2477-2486.

Satoh K., Takeuchi M., Oda Y., Deguchi-Tawarada M., Sakamoto Y., Matsubara K., Takai Y. (2002). Identification of activity-regulated proteins in the postsynaptic density fraction. *Genes Cells.* 7(2):187-197.

Schacher S., Wu F. (2002). Synapse formation in the absence of cell bodies requires protein synthesis. *J Neurosci.* 22:1831–1839.

Schlatzer DM., Sugalski J., Dazard JE., Chance MR., Anthony DD. (2012). A quantitative proteomic approach for detecting protein profiles of activated human myeloid dendritic cells. *J Immunol Methods.* 375(1-2):39-45.

Schmidt EK., Clavarino G., Ceppi M., Pierre P. (2009). SUnSET, a nonradioactive method to monitor protein synthesis. *Nat Methods.* 6(4):275-7.

Schrimpf S. P., Meskenaite V., Brunner E., Rutishauser D., Walther P., Eng J., Sonderegger P. (2005). Proteomic analysis of synaptosomes using isotope-coded affinity tags and mass spectrometry. *Proteomics.* 5(10):2531-2541.

Schuman E.M. (1999). Minireview. mRNA Trafficking and Local Protein Synthesis at the Synapse. *Neuron.* 23:645–648.

Schuman E. M., Dynes J. L., Steward O. (2006). Synaptic regulation of translation of dendritic mRNAs. *J Neurosci.* 26(27):7143-7146.

Schuman EM., Taylor AM., Dieterich DC., Ito HT., Kim SA. (2010). Microfluidic Local Perfusion Chambers for the Visualization and Manipulation of Synapses. *Neuron*. 66(1):57-68.

Sebeo J., Hsiao K., Bozdagi O., Dumitriu D., Ge Y., Zhou Q., Benson D. L. (2009). Requirement for protein synthesis at developing synapses. *J. Neurosci*. 29:9778–9793.

Sherman A. D. (1989). Isolation of metabolically distinct synaptosomes on Percoll gradients. *Neurochem Res*. 14(1):97-101.

Shiio Y., Aebersold R. (2006). Quantitative proteome analysis using isotope-coded affinity tags and mass spectrometry. *Nat Protoc*. 1(1):139-145.

Smart F. M., Edelman G. M., Vanderklish P. W. (2003). BDNF induces translocation of initiation factor 4E to mRNA granules: evidence for a role of synaptic microfilaments and integrins. *Proc Natl Acad Sci*. 100(24):14403-14408.

Smith WB., Starck SR., Roberts R., Schuman EM. (2004). Dopaminergic stimulation of local protein synthesis enhances surface expression of GluR1 and synaptic transmission in hippocampal neurons. *Neuron*. 45:765-779.

Smolka M. B., Zhou H., Purkayastha S., Aebersold R. (2001). Optimization of the isotope-coded affinity tag-labeling procedure for quantitative proteome analysis. *Anal Biochem*. 297(1):25-31.

Snapp E. (2005). Design and use of fluorescent fusion proteins in cell biology. *Curr Protoc Cell Biol*. Chapter 21, Unit 21.4.

Sotelo J. R., Kun A., Benech J. C., Giuditta A., Morillas J., Benech C. R. (1999). Ribosomes and polyribosomes are present in the squid giant axon: an immunocytochemical study. *Neuroscience*. 90(2):705-715.

Spacek J., Hartmann M. (1983). Three-dimensional analysis of dendritic spines. I. Quantitative observations related to dendritic spines and synaptic morphology in cerebral and cerebellar cortices. *Anat. Embryol. (Berl)*. 167(2):289-310.

Stadler H., Tashiro T. (1979). Isolation of synaptosomal plasma membranes from cholinergic nerve terminals and a comparison of their proteins with those of synaptic vesicles. *Eur J Biochem*. 101(1):171-178.

Stelter P., Hurt E. (2014). A pulse-chase epitope labeling to study cellular dynamics of newly synthesized proteins: a novel strategy to characterize NPC biogenesis and ribosome maturation/export. *Methods Cell Biol*. 122:147-63.

Stepanyants A., Hof PR., Chklovskii DB. (2002). Geometry and structural plasticity of synaptic connectivity. *Neuron*. 34:275–288.

Stevens S. M. Jr., Zharikova A. D., Prokai L. (2003). Proteomic analysis of the synaptic plasma membrane fraction isolated from rat forebrain. *Brain Res Mol Brain Res*. 117(2):116-128.

Steward O. (1997). mRNA localization in neurons: a multipurpose mechanism? *Neuron*. 18:9–12.

Steward O., Falk PM. (1985). Polyribosomes under developing spine synapses: growth specializations of dendrites at sites of synaptogenesis. *J Neurosci Res*. 13:75-88.

Steward O., Levy WB. (1982). Preferential localization of polyribosomes under the base of dendritic spines in granule cells of the dentate gyrus. *J. Neurosci*. 2:284–91.

Steward O., Schuman E.M. (2001). Protein synthesis at synaptic sites on dendrites. *Annu Rev Neurosci*. 24:299-325.

- Steward O., Schuman E. M. (2003). Compartmentalized synthesis and degradation of proteins in neurons. *Neuron*. 40:347–359.
- Steward O., Wallace CS., Lyford GL., Worley PF. (1998). Synaptic activation causes the mRNA for the IEG Arc to localize selectively near activated postsynaptic sites on dendrites. *Neuron*. 21(4):741-51.
- Sullivan KE., Cutilli J., Piliero LM., Ghavimi-Alagha D., Starr SE., Campbell DE., Douglas SD. (2000). Measurement of cytokine secretion, intracellular protein expression, and mRNA in resting and stimulated peripheral blood mononuclear cells. *Clin Diagn Lab Immunol*. 7(6):920-4.
- Sutton MA., Ito HT., Cressy P., Kempf C., Woo JC., Schuman EM. (2006). Miniature neurotransmission stabilizes synaptic function via tonic suppression of local dendritic protein synthesis. *Cell*. 125(4):785-99.
- Sutton M. A., Schuman E. M. (2005). Local translational control in dendrites and its role in long-term synaptic plasticity. *J Neurobiol*. 64(1):116-131.
- Sutton M.A. Schuman E.M. (2006). Dendritic protein synthesis, synaptic plasticity, and memory. *Cell*. 127(1):49-58.
- Sutton M. A., Wall N. R., Aakalu G. N., Schuman E. M. (2004). Regulation of dendritic protein synthesis by miniature synaptic events. *Science*. 304(5679): 1979-1983.
- Szychowski J., Mahdavi A., Hodas J. J., Bagert J. D., Ngo J. T., Landgraf P., Tirrell D. A. (2010). Cleavable biotin probes for labeling of biomolecules via azide-alkyne cycloaddition. *J Am Chem Soc*. 132(51):18351-18360.
- Tabas-Madrid D., Nogales-Cadenas R., Pascual-Montano A. (2012). GeneCodis3: a non-redundant and modular enrichment analysis tool for functional genomics. *Nucleic Acids Res*. 40 (Web Server issue): W478-83.

Takamori S., Holt M., Stenius K., Lemke EA., Grønborg M., Riedel D., Urlaub H., Schenck S., Brügger B., Ringler P., Müller SA., Rammner B., Gräter F., Hub JS., De Groot BL., Mieskes G., Moriyama Y., Klingauf J., Grubmüller H., Heuser J., Wieland F., Jahn R. (2006). Molecular anatomy of a trafficking organelle. *Cell*. 127(4):831-46.

Tang S. J., Schuman E. M. (2002). Protein synthesis in the dendrite. *Philos. Trans. R. Soc. Lond. B. Biol. Sci.* 357(1420) 521-529.

Taylor A. M., Berchtold N. C., Perreau V. M., Tu C. H., Li Jeon N., Cotman C. W. (2009). Axonal mRNA in uninjured and regenerating cortical mammalian axons. *J Neurosci.* 29(15):4697-4707.

Tcherkezian J., Brittis P. A., Thomas F., Roux P. P., Flanagan J. G. (2010). Transmembrane receptor DCC associates with protein synthesis machinery and regulates translation. *Cell*. 141(4):632-644.

Tiedge H., Brosius J. (1996). Translational machinery in dendrites of hippocampal neurons in culture. *J Neurosci.* 16(22):7171-7181.

tom Dieck S., Kochen L., Hanus C., Heumüller M., Bartnik I., Nassim-Assir B., Merk K., Mosler T., Garg S., Bunse S., Tirrell DA., Schuman EM. (2015). Direct visualization of newly synthesized target proteins in situ. *Nat Methods.* 12(5):411-4.

Tongiorgi E., Righi M., Cattaneo A. (1997). Activity-dependent dendritic targeting of BDNF and TrkB mRNAs in hippocampal neurons. *J Neurosci.* 17(24):9492-9505.

Toni N., Teng E. M., Bushong E. A., Aimone J. B., Zhao C., Consiglio A., Gage F. H. (2007). Synapse formation on neurons born in the adult hippocampus. *Nat Neurosci.* 10(6):727-734.

Tornøe C. W., Christensen C., Meldal M. (2002). Peptidotriazoles on solid phase: [1,2,3]-triazoles by regioselective copper(I)-catalyzed 1,3-dipolar cycloadditions of terminal alkynes to azides. *J Org Chem.* 67(9):3057-3064.

Torre E.R., Steward O. (1992). Demonstration of local protein synthesis within dendrites using a new cell culture system that permits the isolation of living axons and dendrites from their cell bodies. *J Neurosci.* 12(3):762-72.

Toyama B. H., Savas J. N., Park S. K., Harris M. S., Ingolia N. T., Yates J. R., Hetzer, M. W. (2013). Identification of long-lived proteins reveals exceptional stability of essential cellular structures. *Cell.* 154(5):971-982.

Trachtenberg JT., Chen BE., Knott GW., Feng G., Sanes JR., Welker E., Svoboda K. (2002). Long-term in vivo imaging of experience-dependent synaptic plasticity in adult cortex. *Nature.* 420:788-794.

Triller A., Sheng M. (2012). Synaptic structure and function. *Curr Opin Neurobiol.* 22(3):363-5.

Trinidad JC., Barkan DT., Gullledge BF., Thalhammer A., Sali A., Schoepfer R., Burlingame AL. (2012). Global identification and characterization of both O-GlcNAcylation and phosphorylation at the murine synapse. *Mol Cell Proteomics.* 11(8):215-29.

Trinidad JC., Specht CG., Thalhammer A., Schoepfer R., Burlingame AL. (2006). Comprehensive identification of phosphorylation sites in postsynaptic density preparations. *Mol Cell Proteomics.* 5(5):914-22.

Trinidad JC., Thalhammer A., Specht CG., Schoepfer R., Burlingame AL. (2005). Phosphorylation state of postsynaptic density proteins. *J Neurochem.* 92(6):1306-16.

Trinidad JC., Thalhammer A., Specht CG., Lynn AJ., Baker PR., Schoepfer R., Burlingame AL. (2008). Quantitative analysis of synaptic phosphorylation and protein expression. *Mol Cell Proteomics*. 7(4):684-96.

Twiss JL., van Minnen J. (2006). New insights into neuronal regeneration: the role of axonal protein synthesis in pathfinding and axonal extension. *J Neurotrauma*. 23(3-4):295-308.

Vaughn C. P., Crockett D. K., Lin Z., Lim M. S., Elenitoba-Johnson K. S. (2006). Identification of proteins released by follicular lymphoma-derived cells using a mass spectrometry-based approach. *Proteomics*. 6(10):3223-3230.

Verma P., Chierzi S., Codd A. M., Campbell D. S., Meyer R. L., Holt C. E., Fawcett J. W. (2005). Axonal protein synthesis and degradation are necessary for efficient growth cone regeneration. *J Neurosci*. 25(2):331-342.

Verpelli C., Sala C. (2012). Molecular and synaptic defects in intellectual disability syndromes. *Curr Opin Neurobiol*. 22(3):530-6.

Vickers C.A., Dickson K., Wyllie D.J. (2005). Induction and maintenance of late-phase long-term potentiation in isolated dendrites of rat hippocampal CA1 pyramidal neurones. *J. Physiol*. 568:803–813.

Vickers CA., Wyllie DJ. (2007). Late-phase, protein synthesis-dependent long-term potentiation in hippocampal CA1 pyramidal neurones with destabilized microtubule networks. *Br J Pharmacol*. 151(7):1071-7.

Vitale M., Renzone G., Matsuda S., Scaloni A., D'Adamio L., Zambrano N. (2012). Proteomic characterization of a mouse model of familial Danish dementia. *J Biomed Biotechnol*. 2012:728178.

Waites CL., Craig AM., Garner CC. (2005). Mechanisms of vertebrate synaptogenesis. *Annu Rev Neurosci*. 28:251-74.

Walikonis R. S., Jensen O. N., Mann M., Provance D. W. Jr., Mercer J. A., Kennedy M. B. (2000). Identification of proteins in the postsynaptic density fraction by mass spectrometry. *J Neurosci.* 20(11):4069-4080.

Walther TC., Mann M. (2010). Mass spectrometry-based proteomics in cell biology. *J Cell Biol.* 190(4):491-500.

Wang D. O., Kim S. M., Zhao Y., Hwang H., Miura S. K., Sossin W. S., Martin K. C. (2009). Synapse- and stimulus-specific local translation during long-term neuronal plasticity. *Science.* 324(5934):1536-1540.

Wang X., Kibschull M., Laue M. M., Lichte B., Petrasch-Parwez E., Kilimann M. W. (1999). Aczonin, a 550-kD putative scaffolding protein of presynaptic active zones, shares homology regions with Rim and Bassoon and binds profilin. *J Cell Biol.* 147(1):151-162.

Washburn M. P., Ulaszek R., Deciu C., Schieltz D. M., Yates J. R., 3rd. (2002). Analysis of quantitative proteomic data generated via multidimensional protein identification technology. *Anal Chem.* 74(7):1650-1657.

Wei W., Shin YS., Ma C., Wang J., Elitas M., Fan R., Heath JR. (2013). Microchip platforms for multiplex single-cell functional proteomics with applications to immunology and cancer research. *Genome Med.* 5(8):75.

Weiler I.J., Greenough W.T. (1993). Metabotropic glutamate receptors trigger postsynaptic protein synthesis. *Proc Natl Acad Sci.* 90(15):7168-71.

Weingarten J., Lassek M., Mueller BF., Rohmer M., Lunger I., Baeumlisberger D., Dudek S., Gogesch P., Karas M., Volkmandt W. (2014). The proteome of the presynaptic active zone from mouse brain. *Mol Cell Neurosci.* 59:106-18.

Welshhans K., Bassell G. J. (2011). Netrin-1-induced local beta-actin synthesis and growth cone guidance requires zipcode binding protein 1. *J Neurosci.* 31(27):9800-9813.

Whittaker VP. (1968). Synaptic transmission. *Proc Natl Acad Sci.* 60(4):1081-91.

Whittaker V. P., Michaelson I. A., Kirkland R. J. (1964). The separation of synaptic vesicles from nerve-ending particles ('synaptosomes'). *Biochem J.* 90(2):293-303.

Whittaker V. P. (1993). Thirty years of synaptosome research. *J Neurocytol.* 22(9):735-742.

Wiersma-Meems R., Van Minnen J., Syed NI. (2005). Synapse formation and plasticity: the roles of local protein synthesis. *Neuroscientist.* 11(3):228-37.

Witzmann F. A., Arnold R. J., Bai F., Hrcirova P., Kimpel M. W., Mechref Y. S., Simon J. R. (2005). A proteomic survey of rat cerebral cortical synaptosomes. *Proteomics.* 5(8):2177-2201.

Wu KY., Hengst U., Cox LJ., Macosko EZ., Jeromin A., Urquhart ER., Jaffrey SR. (2005). Local translation of RhoA regulates growth cone collapse. *Nature.* 436(7053):1020-4.

Wu W. W., Wang G., Baek S. J., Shen R. F. (2006). Comparative study of three proteomic quantitative methods, DIGE, cI-CAT, and iTRAQ, using 2D gel- or LC-MALDI TOF/TOF. *J Proteome Res.* 5(3):651-658.

Wulfschuhle JD., Liotta LA., Petricoin EF. (2003). Proteomic applications for the early detection of cancer. *Nat Rev Cancer.* 3(4):267-75.

Xing L., Bassell GJ. (2013) mRNA localization: an orchestration of assembly, traffic and synthesis. *Traffic.* 14(1):2-14.

Yadavalli SS., Ibbra M. (2012). Quality control in aminoacyl-tRNA synthesis its role in translational fidelity. *Adv Protein Chem Struct Biol.* 86:1-43.

Yamauchi Y., Abe-Dohmae S., Yokoyama S. (2002). Differential regulation of apolipoprotein A-I/ATP binding cassette transporter A1-mediated cholesterol and phospholipid release. *Biochim Biophys Acta.* 1585(1):1-10.

Yan W., Lee H., Yi E. C., Reiss D., Shannon P., Kwieciszewski B. K., Katze M. G. (2004). System-based proteomic analysis of the interferon response in human liver cells. *Genome Biol.* 5(8): R54.

Yao J., Sasaki Y., Wen Z., Bassell G. J., Zheng J. Q. (2006). An essential role for beta-actin mRNA localization and translation in Ca²⁺-dependent growth cone guidance. *Nat Neurosci.* 9(10):1265-1273.

Yoon B. C., Zivraj K. H., Holt C. E. (2009). Local translation and mRNA trafficking in axon pathfinding. *Results Probl Cell Differ.* 48:269-288.

Yoon B. C., Jung H., Dwivedy A., O'Hare C. M., Zivraj K. H., Holt C. E. (2012). Local translation of extranuclear lamin B promotes axon maintenance. *Cell.* 148(4):752-764.

Yoshimura Y., Yamauchi Y., Shinkawa T., Taoka M., Donai H., Takahashi N., Yamauchi T. (2004). Molecular constituents of the postsynaptic density fraction revealed by proteomic analysis using multidimensional liquid chromatography-tandem mass spectrometry. *J Neurochem.* 88(3):759-768.

Yuet KP., Doma MK., Ngo JT., Sweredoski MJ., Graham RL., Moradian A., Hess S., Schuman EM., Sternberg PW., Tirrell DA. (2015). Cell-specific proteomic analysis in *Caenorhabditis elegans*. *Proc Natl Acad Sci.* 112(9): 2705-10.

Zeeberg B. R., Feng W., Wang G., Wang M. D., Fojo A. T., Sunshine M., Weinstein J. N. (2003). GoMiner: a resource for biological interpretation of genomic and proteomic data. *Genome Biol.* 4(4): R28.

Zhang H., Li X. J., Martin D. B., Aebersold R. (2003). Identification and quantification of N-linked glycoproteins using hydrazide chemistry, stable isotope labeling and mass spectrometry. *Nat Biotechnol.* 21(6):660-666.

Zhang J., Goodlett D. R., Montine T. J. (2005). Proteomic biomarker discovery in cerebrospinal fluid for neurodegenerative diseases. *J Alzheimers Dis.* 8(4): 377-386.

Zhang J., Goodlett D. R., Quinn J. F., Peskind E., Kaye J. A., Zhou Y., Montine T. J. (2005). Quantitative proteomics of cerebrospinal fluid from patients with Alzheimer disease. *J Alzheimers Dis.* 7(2):125-133; discussion 173-180.

Zhang L., Weng W., Guo J. (2011). Posttranscriptional mechanisms in controlling eukaryotic circadian rhythms. *FEBS Lett.* 585(10):1400-1405.

Zhang X., Poo M. M. (2002). Localized synaptic potentiation by BDNF requires local protein synthesis in the developing axon. *Neuron.* 36:675-688.

Zheng J. Q., Kelly T. K., Chang B., Ryazantsev S., Rajasekaran A. K., Martin K. C., Twiss J. L. (2001). A functional role for intra-axonal protein synthesis during axonal regeneration from adult sensory neurons. *J Neurosci.* 21(23): 9291-9303.

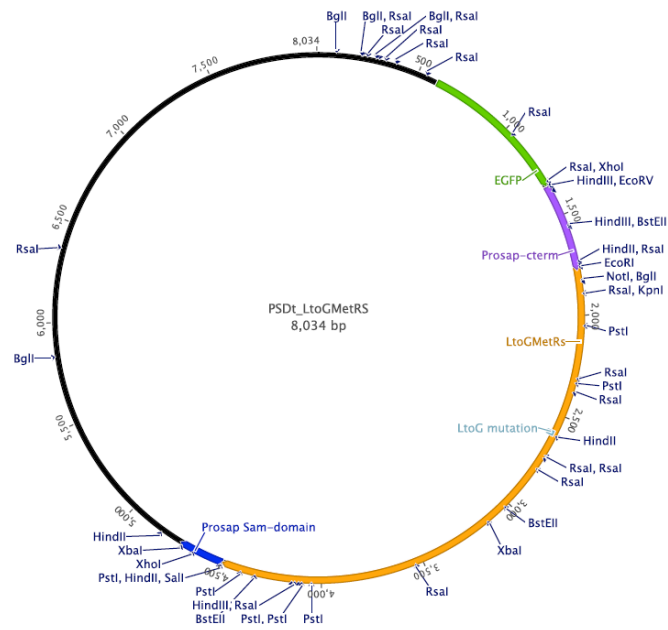
Zhou Y., Wang Y., Kovacs M., Jin J., Zhang J. (2005). Microglial activation induced by neurodegeneration: a proteomic analysis. *Mol Cell Proteomics.* 4(10):1471-1479.

Zieske L. R. (2006). A perspective on the use of iTRAQ reagent technology for protein complex and profiling studies. *J Exp Bot.* 57(7):1501-1508.

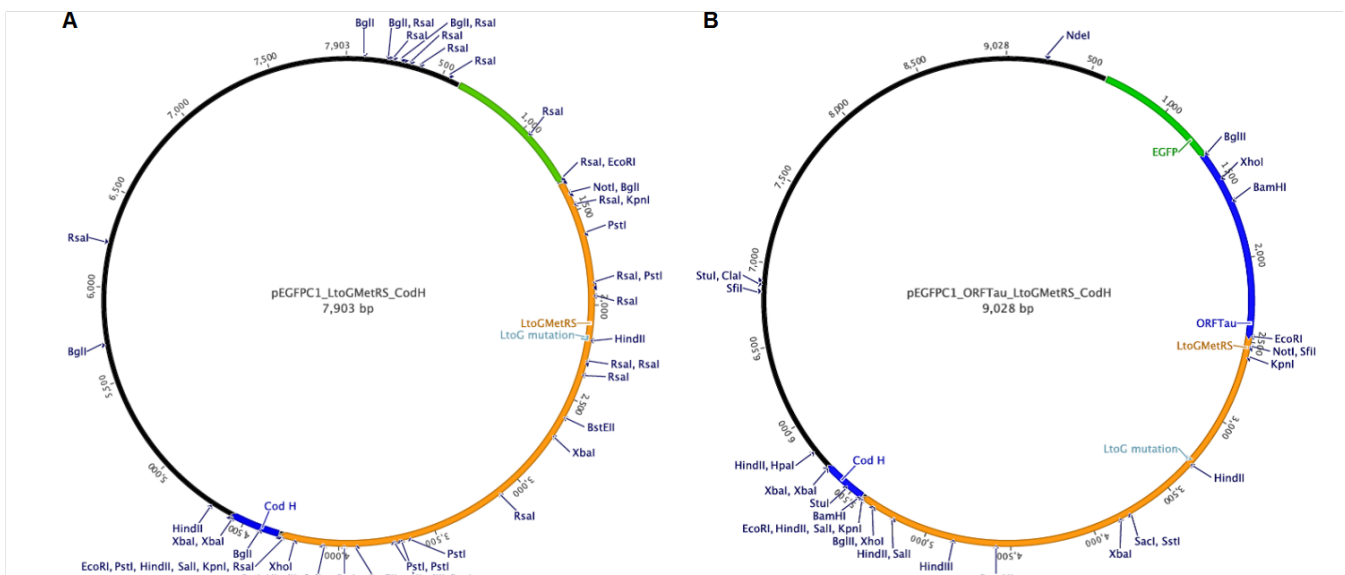
Ziv N. E., Garner C. C. (2004). Cellular and molecular mechanisms of presynaptic assembly. *Nat Rev Neurosci.* 5(5):385-399.

Zivraj K. H., Tung Y. C., Piper M., Gumy L., Fawcett J. W., Yeo G. S., Holt C. E. (2010). Subcellular profiling reveals distinct and developmentally regulated repertoire of growth cone mRNAs. *J Neurosci.* 30(46):15464-15478.

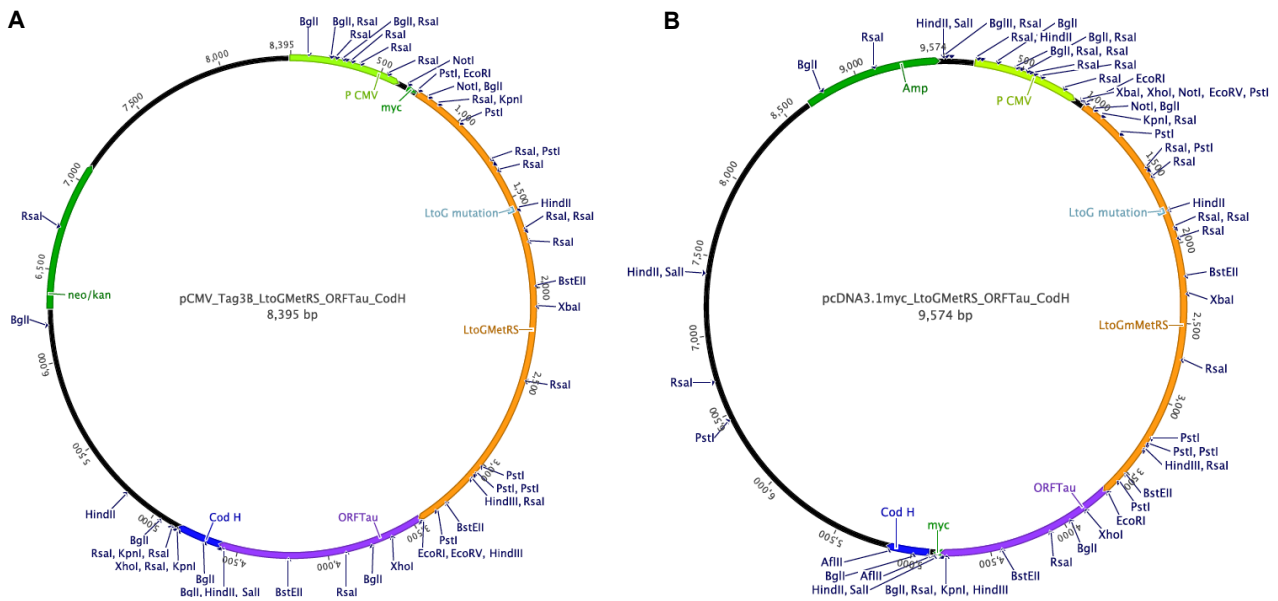
7. APPENDIX



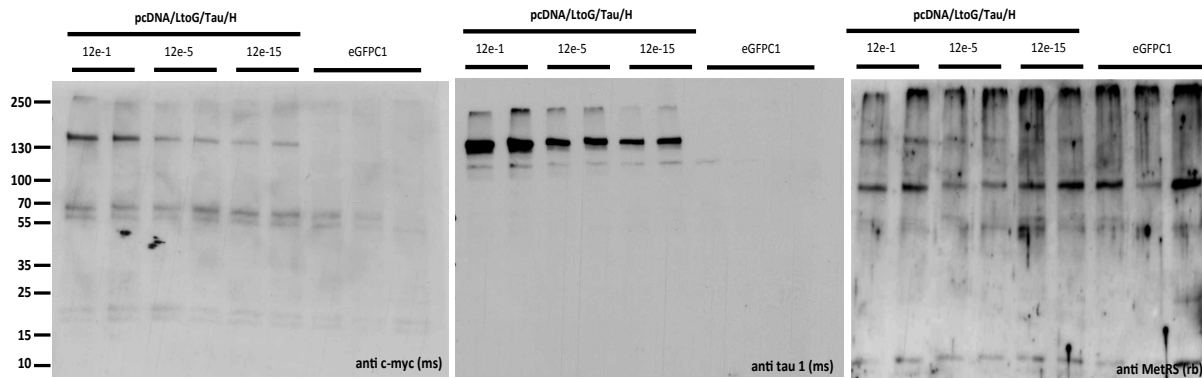
Supplementary Figure S1. Representation of the pSDTarget-LtoGMetRS construct designed for the targeting of MetRS to postsynaptic densities. The LtoGMetRS sequence was cloned into pSDTargeting vector, flanked by the bipartite targeting signals Prosap c-term and Prosap Sam-domain, using the restriction sites EcoRI-BamHI (Supplementary Table 2). The full-length sequence of the pSDTargeting vector is accessible as Supplementary Table 1 online (Grabrucker et al., 2009).



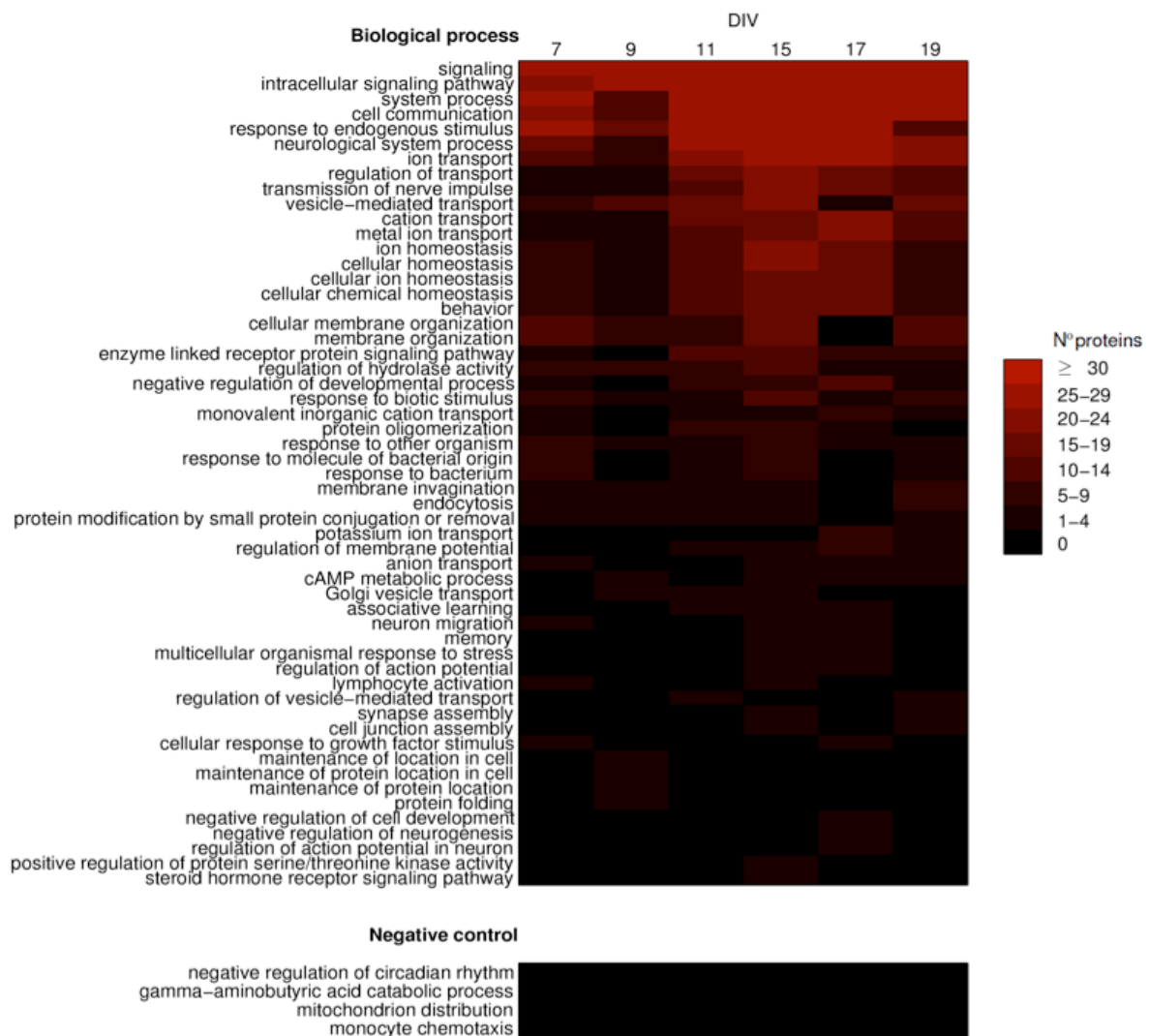
Supplementary Figure S2. Representation of pEGFPC1-LtoGMetRS-Cod-H and pEGFPC1-ORFTau-LtoGMetRS-Cod-H construct designed for the targeting of MetRS to presynaptic specializations. LtoGMetRS and the fragment H (Cod-H) (A), as well as ORFTau sequence (B), were cloned into the EGFP-C1 vector using restriction sites described in Supplementary Table 2. The appropriate DNA template was amplified by specific primers (Supplementary Table 1) for subcloning of cDNA into expression vectors. The following sequences were used as a template: *Mus musculus* MetRS (NM_001171582.1) and *Rattus norvegicus* tau microtubule-associated protein (Gen Bank: X79321.1).



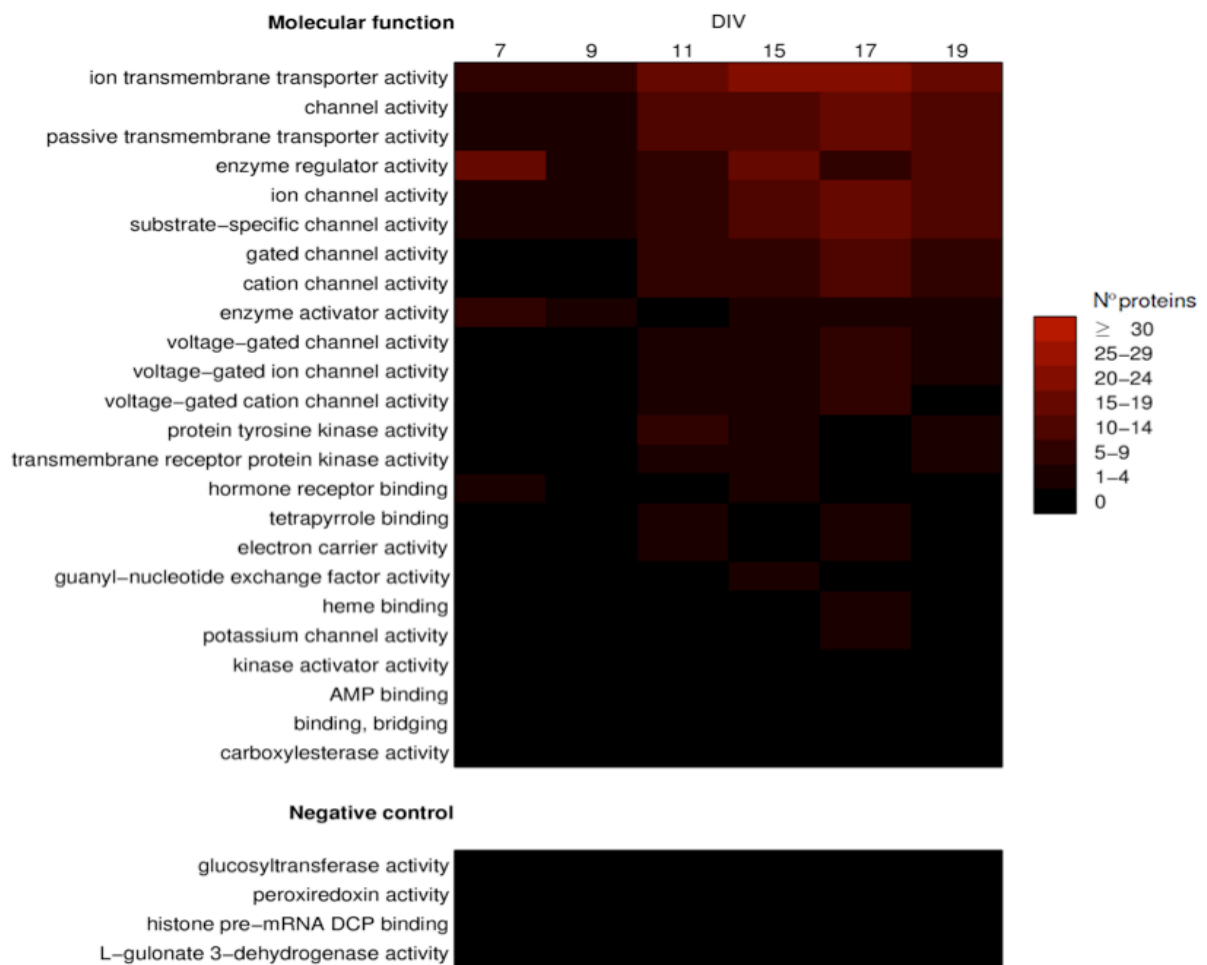
Supplementary Figure S3. Representation of pCMVTag3B-LtoGMetRS-ORFTau-Cod-H and pcDNA-LtoGMetRS-ORFTau-Cod-H constructs designed for the targeting of MetRS to presynaptic specializations. LtoGMetRS, Cod-H and ORFTau sequence was cloned into pCMVTag3B (left) and pcDNA (right) vector using restriction sites described in Supplementary Table 2. The appropriate DNA template was amplified by specific primers (Supplementary Table 1) for subcloning of cDNA into expression vectors. *Mus musculus* MetRS (NM_001171582.1) and *Rattus norvegicus* tau microtubule-associated protein (Gen Bank: X79321.1) sequence were used as a template. Expression of the fusion protein was detected using an antibody against the c-myc tag peptide.



Supplementary Figure S4. Western blot analysis demonstrated the expression of the fusion protein in samples from Hek293T cells transfected with different clones of the pcDNA-LtoGMetRS-ORFTau-Cod-H construct. The fusion protein was detected using antibodies against c-myc epitope, Tau, and MetRS protein.



Supplementary Figure S5. Heat map illustrates the development-dependent protein enrichment associated with prominent GO terms from the biological process domain. Protein enrichment is represented by significant changes in the number of proteins associated with biological processes in all developmental stages. Negative control represents GO terms lacking protein association. All data were obtained from two sets of MS/MS measurements, using between three to four samples of synaptosome fractions per time point (Table 4). GO analysis was performed by GoMiner software (Zeeberg et al., 2003).



Supplementary Figure S6. Heat map illustrates development-dependent protein enrichment associated with prominent GO terms from the molecular function domain. Significant changes in the number of proteins associated with molecular functions were observed at mature developmental stages. Negative control represents GO terms lacking protein association. Data were obtained from two sets of MS/MS measurements and between three to four samples of synaptosome fractions per time point (Table 4). GO analysis was performed using GoMiner software (Zeeberg et al., 2003).

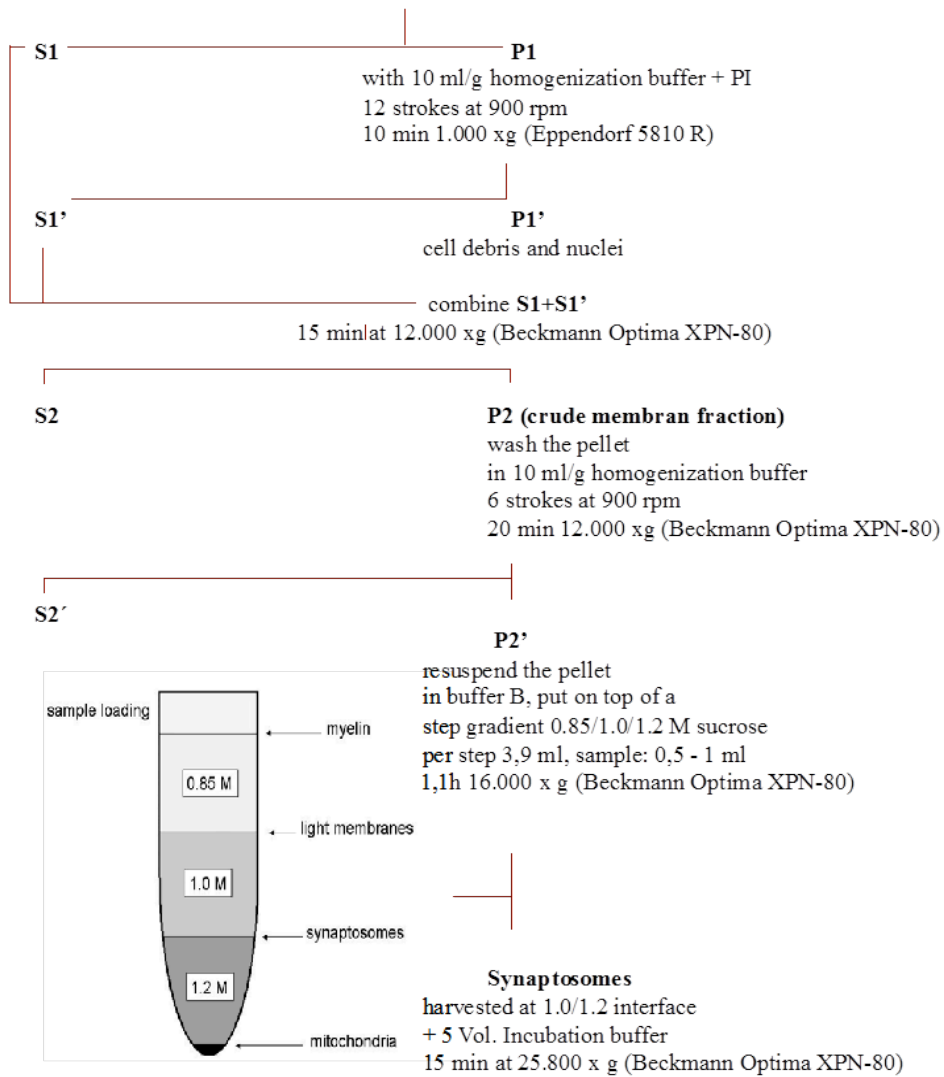
Supplementary Scheme 1. Subcellular fractionation

Cortical primary cultures in homogenization buffer + protease inhibitors (10 ml/g)

12 strokes at 900 rpm using Teflon pistil (Potter S)

H (Homogenate)

10 min 1.000 x g (Eppendorf 5810 R)



Supplementary Tables

Supplementary Table 1. Primer used for cloning. The table shows the primer binding sequences that bind to the corresponding cDNA sequence

Nr.	Primer	Primer-sequence (5'→3')	DNA template/ position	Application/ vector
1	TAUratBgllIffw	GAAGATCTATGGCTGAACCCCGCCA	mTau (cDNA) bp: 232-248	Subcloning pEGFP-C1
2	TAUratEcoRIrev	GGAATTCGACAAACCCTGCTTGCC	mTau (cDNA) bp: 1354-1338	Subcloning pEGFP-C1
3	Tau3'UTRfwBam	CGGGATCCGGCGCCATCGTGGATGGA	mTau (cDNA) bp: 2751-2768	Subcloning pEGFP-C1
4	Tau3'UTRrevXba	GCTCTAGAAGCTCTGGGAGGCTAGCA	mTau (cDNA) bp: 2991-2974	Subcloning pEGFP-C1
5	LtofWEcoRI	GGAATTCATGAGACTGTTCGTGAGC	mMetRS (cDNA) bp: 158-175	Subcloning pcDNA 3.1(-)A
6	LtoGrev1EcoRI	GGAATTCCTTTTCTTCTTGCCTTT	mMetRS (cDNA) bp: 2887-2870	Subcloning pcDNA 3.1(-)A
7	TauEcoRIffw	GGAATTCATGGCTGAACCCCGCCAGG	mTau (cDNA) bp: 230-250	Subcloning pcDNA 3.1(-)A
8	TauKpnIrev(-)	GGGGTACCCAAACCCTGCTTGCCAA	mTau (cDNA) bp: 1353-1336	Subcloning pcDNA 3.1(-)A
9	CodHfwAflII	AGCTTAAGGGCGCCATCGTGGATGGA	mTau (cDNA) bp: 2751-2768	Subcloning pcDNA 3.1(-)A
10	CodHrevAflII	AGCTTAAGAGCTCTGGGAGGCTAGCA	mTau (cDNA) bp: 2992-2974	Subcloning pcDNA 3.1(-)A
11	LtofWEcoRI	GGAATTCATGAGACTGTTCGTGAGC	mMetRS (cDNA) bp: 158-175	Subcloning pCMV-Tag3B
12	LtoGrev1EcoRI	GGAATTCCTTTTCTTCTTGCCTTT	mMetRS (cDNA) bp: 2887-2870	Subcloning pCMV-Tag3B
13	TauHindIIIffw	CCCAAGCTTATGGCTGAACCCCGCCA	mTau (cDNA) bp: 232-248	Subcloning pCMV-Tag3B
14	TauSallrevStop	GCGTCGACTCACAACCCTGCTTGCC	mTau (cDNA) bp: 1356-1339	Subcloning pCMV-Tag3B
15	CodHfwSall	GCGTCGACGGCGCCATCGTGGATGGA	mTau (cDNA) bp: 2751-2768	Subcloning pCMV-Tag3B
16	CodHrevXhoI	CCGCTCGAGAGCTCTGGGAGGCTAGCA	mTau (cDNA) bp: 2991-2974	Subcloning pCMV-Tag3B

Supplementary Table 2. List of constructs. The table shows cDNA expression constructs used in this thesis

Nr.	Name	Insert	Restriction site	Vector	Application
1	pSDt-LtoGMetRS	LtoGMetRS, bp: 1-2706 (from 007 construct; Anke Müller)	EcoRI-BamHI	pEGFP-C1	Heterologous Expression
2	EGFP-LtoGMetRS-codH	LtoGMetRS, bp: 1-2933 (from DCD 67/7 construct) 3'UTR Tau (CodH), bp: 2751-2991	EcoRI-EcoRI BamHI-XbaI	pEGFP-C1	Heterologous Expression
3	EGFP-Tau-LtoGMetRS-codH	LtoGMetRS, bp: 1-2933 (from DCD 67/7 construct) Tau (ORF), bp: 232-1354 3'UTR Tau (CodH), bp: 2751-2991	EcoRI-EcoRI BglII-EcoRI BamHI-XbaI	pEGFP-C1	Heterologous Expression
4	LtoGMetRS-Tau-Myc-codH	LtoGMetRS, bp: 158-2887 Tau (ORF), bp: 230-1353 3'UTR Tau (CodH), bp: 2751-2992	EcoRI-EcoRI EcoRI-KpnI AflII-AflII	pcDNA 3.1(-)A	Heterologous Expression
5	Myc-LtoGMetRS-Tau-codH	LtoGMetRS, bp: 158-2887 Tau (ORF), bp: 232-1356 3'UTR Tau (CodH), bp: 2751-2991	EcoRI-EcoRI HindIII-Sall Sall-XhoI	pCMV-Tag3B	Heterologous Expression

Supplementary Table 3. Common buffers

Name	Composition	pH	Applications
Electrophoresis buffer	192 mM glycine, 0.1 % (w/v) SDS, 25 mM Tris-base,	8.3	SDS-PAGE gel electrophoresis
Blotting buffer	192 mM Glycine, 0.2 % (w/v) SDS, 20% (v/v) Methanol, 25 mM Tris-base	8.3	SDS-PAGE gel transfer
4x SDS-sample buffer	250 mM Tris-HCl, pH 6.8, 1% (w/v) SDS, 40% (v/v) Glycerol 20% (v/v) b-mercaptoethanol, 0,004 % Bromophenol Blue	6.8	Denaturing sample buffer for SDS-PAGE
TBS	25 mM Tris-HCl, 150 mM NaCl	7.4	Wash buffers, PD, IP, Lysis buffers,
TBS-T	TBS+ 0,1% (v/v) Twien-20	7.4	Wash buffers
TBS-A	TBS+0.02% NaN ₃	7.4	Antibody dilution, sepharoses and membranes storage
Blocking solution (for IB)	5% (w/v) non-fatty milk powder (or BSA) in TBS-T		Blocking of nitrocellulose membranes
Ponceau solution	0.5 % (w/v) Ponceau S in 3% (v/v) acetic acid solution		Staining of the proteins on the nitrocellulose membrane
Coomassie Brilliant Blue staining	0.125 % (w/v) Coomassie Brilliant Blue R250, 50% (v/v)		Staining of proteins on SDS-PAGE gel
Coomassie destaining	7% (v/v) acetic acid		Removal of unspecific staining of SDS-PAGE gels
Drying buffer	50% (v/v) methanol, 5% (v/v) glycerol		Drying of coomassie stained SDS-PAGE gels
Permeabilization buffer	PBS, 0.2% Triton-X-100	7.4	Permeabilization of cells for immunocytochemistry
Quenching solution	25mM Glycin in PBS	7.4	Quenching of cells for immunocytochemistry
Blocking solution (B-Block)	0.1% Triton X-100, 2 mg/ml BSA, 5% sucrose, 10% normal horse serum in PBS	7.4	Blocking of cells for immunocytochemistry, dilution of antibody
10x PBS	1.4 M NaCl, 83 mM Na ₂ HPO ₄ ,	7.4	IF, wash buffers
50xTAE buffer	2 M Tris-acetate, 0.05 M EDTA		Agarose gel electrophoresis
6x DNA loading dye	30% glycerol, 0.25 % bromophenol blue, 0.25 % xylene		Loading dye for agarose gel electrophoresis

Supplementary Table 4. Common media

Name	Composition	Applications
SOC-medium	20 g/l Bacto- trypton, 5 g/l Yeast-extract, 10 mM NaCl, 2,5 mM KCl, 10 mM Mg ₂ SO ₄ , 10 mM MgCl ₂ , 20 mM Glucose	Bacterial medium
LB-medium	5 g/l Yeast-extract, 10 g/l Bacto- trypton, 5 g/l NaCl	Bacterial medium
DMEM “-”	DMEM (Gibco)	Cell culture of COS-7 cells, transfections
DMEM “+”	DMEM (-), 10% fetal calf serum (FCS), 2 mM L-Glutamine, 100 U/mL Penicillin, 100 g/mL Streptomycin (Gibco)	Cell culture of COS-7 cells
DMEM for neuronal culture	DMEM (-), 10% FCS, 100 U/ mL Penicillin, 100 g/mL Streptomycin, 2 mM L-Glutamine	Primary neuronal cell culture
Neurobasal medium “+”	Neurobasal TM , 1x B27 (Gibco), 100 U/ mL Penicillin, 100 g/mL Streptomycin, 0.5 mM L-Glutamine	Primary neuronal cell culture, transfections
Opti-MEM	Opti-MEM (Gibco)	Transfections

Supplementary Table 5. Solutions for subcellular fractionation and synaptosome isolation

500 mM HEPES pH 7.4 (5,958 g plus ca. 40 ml bidest, add 50 ml)	50 ml
500 mM Tris/HCl pH 8.1 (6,057g plus ca. 90 ml bidest, add 100 ml)	100 ml
2 M Sucrose (410,76g add 600 ml)	600 ml
Protease-Inhibitor Cocktail tablets (PI)	(1 per 50 ml)

Buffers

buffer A: 0.32 M sucrose, 5 mM HEPES, pH 7.4 80 ml (2M), 5 ml (0,5M)	500 ml
buffer A + PI prepare freshly	150 ml
buffer B: 0.32 M sucrose, 5 mM Tris, pH 8.1 32 ml (2M), 2 ml (0,5M)	200 ml
0.85 M Sucrose/5 mM Tris/HCl pH 8.1 85 ml (2M), 2ml (0,5M)	200 ml
1.0 M Sucrose/5 mM Tris/HCl pH 8.1 100 ml (2M), 2ml (0,5M)	200 ml
1.2 M Sucrose/5 mM Tris/HCl pH 8.1 120 ml (2M), 2ml (0,5M)	200 ml
Incubation buffer: 25 mM HEPES pH 7.4, 20 mM glucose, 3.5 mM KCl, 1.8 mM CaCl ₂ , 1.2 mM Na ₂ HPO ₄ , 1 mM MgCl ₂ , 129 mM NaCl	200 ml

Supplementary Table 6. Newly synthesized proteins identified in synaptosomes isolated from cortical primary cultures at DIV7

Nr.	Accession	Protein	MW [kDa]	Scores	#Peptides	SC [%]	Synprot	Transcriptome
1	HMDH_RAT	3-hydroxy-3-methylglutaryl-coenzyme A reductase	96.6	441.8	29	13.4	-	yes
2	3HIDH_RAT	3-hydroxyisobutyrate dehydrogenase, mitochondrial	35.3	584.9	38	33.4	-	-
3	5NTD_RAT	5'-nucleotidase	63.9	153.4	7	11.5	-	-
4	THIC_RAT	Acetyl-CoA acetyltransferase, cytosolic	41.1	402.8	23	26.2	-	-
5	ACTG_RAT	Actin, cytoplasmic 2	41.8	421.2	14	51.2	-	yes
6	APC_RAT	Adenomatous polyposis coli protein1	310.3	583.7	34	9.5	yes	yes
7	ADCY4_RAT	Adenylate cyclase type 4	118.7	122.4	5	7.1	-	-
8	AKAP6_RAT	A-kinase anchor protein 6	254.2	374.2	18	8.3	yes	yes
9	AL1L1_RAT	Aldehyde dehydrogenase family 1 member L1	99.1	359.7	17	26.6	yes	-
10	ANXA3_RAT	Annexin A3	36.3	200.3	11	23.1	yes	-
11	ABEC1_RAT	C->U-editing enzyme APOBEC-1	27.3	100.4	3	21.0	-	-
12	APOB_RAT	Apolipoprotein B-100	535.7	1633.7	94	17.6	-	-
13	APAF_RAT	Apoptotic protease-activating factor 1	141.1	241.1	8	8.1	-	yes
14	ARLY_RAT	Argininosuccinate lyase	51.5	122.8	7	11.3	-	-
15	ARMX3_RAT	Armadillo repeat-containing X-linked protein 3	42.5	184.3	8	23.0	-	yes
16	BCL10_RAT	B-cell lymphoma/leukemia 10	26.0	131.8	4	30.9	-	-
17	BMP2_RAT	Bone morphogenetic protein 2	44.4	284.9	13	17.6	-	-
18	BIN3_RAT	Bridging integrator 3	29.7	206.1	7	22.9	-	-
19	CELR3_RAT	Cadherin EGF LAG seven-pass G-type receptor 3	359.1	381.5	17	6.5	-	-
20	CPSM_RAT	Carbamoyl-phosphate synthase [ammonia], mitochondrial	164.5	242.9	12	9.8	-	-
21	CACP_RAT	Carnitine O-acetyltransferase	70.8	404.5	22	20.4	-	-
22	CLD7_RAT	Claudin-7	22.4	1508.2	158	27.5	-	-
23	CORA1_RAT	Collagen alpha-1(XVII) chain	187.7	1102.7	64	23.6	-	-
24	COG6_RAT	Conserved oligomeric Golgi complex subunit 6	72.9	435.9	26	39.1	-	yes
25	CUL5_RAT	Cullin-5	90.8	242.8	11	11.5	yes	yes
26	CDK17_RAT	Cyclin-dependent kinase 17	59.4	331.2	13	26.4	-	yes
27	DALD3_RAT	DALR anticodon-binding domain-containing protein 3	59.0	114.1	3	11.2	-	yes
28	DPEP3_RAT	Dipeptidase 3	53.3	129.4	10	23.2	-	-
29	DYH12_RAT	Dynein heavy chain 12, axonemal	357.0	469.8	28	9.2	-	-
30	ENPP1_RAT	Ectonucleotide pyrophosphatase/phosphodiesterase family member 1	102.9	350.4	22	13.7	-	-
31	ENPP6_RAT	Ectonucleotide pyrophosphatase/phosphodiesterase family member 6	50.7	223.8	16	30.5	yes	-
32	ERLN2_RAT	Erlin-2	37.7	214.1	10	33.0	-	yes
33	ESYT1_RAT	Extended synaptotagmin-1	121.1	291.2	14	17.3	-	-
34	FGF23_RAT	Fibroblast growth factor 23	27.9	234.3	10	37.5	-	-
35	FINC_RAT	Fibronectin	272.3	335.6	19	9.0	-	-
36	FOXQ1_RAT	Forkhead box protein Q1	41.1	117.1	5	20.8	-	-
37	FHL5_RAT	Four and a half LIM domains protein 5	32.9	196.5	12	27.1	-	-
38	GEPH_RAT	Gephyrin	83.2	1383.4	127	27.7	yes	-
39	GRIK3_RAT	Glutamate receptor, ionotropic kainate 3	104.0	255.4	11	22.2	-	-
40	GPC2_RAT	Glypican-2	63.3	340.5	14	27.1	-	-
41	HEAT6_RAT	HEAT repeat-containing protein 6	136.4	574.7	28	25.2	-	-
42	HSP74_RAT	Heat shock 70 kDa protein 4	94.0	226.7	17	15.5	-	-
43	HS90A_RAT	Heat shock protein HSP 90-alpha	84.8	346	12	13.9	yes	yes
44	HNRPM_RAT	Heterogeneous nuclear ribonucleoprotein M	73.7	2948.7	234	45.1	yes	-
45	IKKB_RAT	Inhibitor of nuclear factor kappa-B kinase subunit beta	86.8	297.4	23	25.4	-	-
46	ITPR2_RAT	Inositol 1,4,5-trisphosphate receptor type 2	306.9	407.8	21	10.6	-	-
47	ALS_RAT	Insulin-like growth factor-binding protein complex acid labile subunit	66.8	160.4	11	17.6	-	-
48	IRPL1_RAT	Interleukin-1 receptor accessory protein-like 1	79.7	434.7	18	37.2	yes	-
49	ITSN1_RAT	Intersectin-1	137.1	126.1	3	4.2	yes	-
50	KALRN_RAT	Kalirin	336.4	390.4	20	7.6	yes	yes
51	KLH24_RAT	Kelch-like protein 24	68.3	225.5	6	13.8	-	-
52	K1C19_RAT	Keratin, type I cytoskeletal 19	44.6	233.2	9	28.3	-	-
53	KIF2A_RAT	Kinesin-like protein KIF2A	79.7	384	20	28.9	yes	yes
54	LRFN1_RAT	Leucine-rich repeat and fibronectin type III domain-containing protein 1	81.9	360.1	21	28.3	-	-
55	LCAP_RAT	Leucyl-cystinyl aminopeptidase	117.1	290.8	11	14.4	-	-
56	LT4R2_RAT	Leukotriene B4 receptor 2	37.9	107.2	5	12.6	-	-
57	LPPR4_RAT	Lipid phosphate phosphatase-related protein type 4	83.3	264.2	10	14.1	yes	yes
58	ARMC9_RAT	LisH domain-containing protein ARMC9	82.3	374.1	20	20.3	-	-
59	ADDG_RAT	Gamma-adducin	78.8	339.1	11	19.7	-	-
60	ABHD5_RAT	1-acylglycerol-3-phosphate O-acyltransferase ABHD5	39.1	150.2	8	14.2	-	-
61	ACSL3_RAT	Long-chain-fatty-acid--CoA ligase 3	80.4	114.8	5	7.8	yes	-
62	ACSL4_RAT	Long-chain-fatty-acid--CoA ligase 4	74.3	288.6	16	13.7	-	-
63	AT2C2_RAT	Calcium-transporting ATPase type 2C member 2	103.0	326.7	15	19.1	-	-
64	ATP7B_RAT	Copper-transporting ATPase 2	155.9	641.8	35	18.0	-	-
65	CCND3_RAT	G1/S-specific cyclin-D3	32.4	216.9	15	37.5	-	-
66	CRF_RAT	Corticotiberin	20.7	377.5	24	44.9	-	yes
67	FMO1_RAT	Dimethylaniline monooxygenase [N-oxide-forming] 1	59.8	154.6	6	16.7	-	-

68	GHRL_RAT	Appetite-regulating hormone	13.2	214.4	37	32.5	-	-
69	CH60_RAT	60 kDa heat shock protein, mitochondrial	60.9	2724.8	226	29.3	yes	-
70	MA2C1_RAT	Alpha-mannosidase 2C1	115.9	91.5	4	3.2	yes	-
71	DAB2P_RAT	Disabled homolog 2-interacting protein	109.9	532	27	29.3	yes	-
72	LIPS_RAT	Hormone-sensitive lipase	116.7	813.4	51	35.6	-	-
73	MAP1A_RAT	Microtubule-associated protein 1A	299.3	272.1	13	5.2	yes	yes
74	ML12B_RAT	Myosin regulatory light chain 12B	19.8	164.6	7	27.9	yes	-
75	MYH10_RAT	Myosin-10	228.8	889.3	48	18.7	yes	-
76	MYH3_RAT	Myosin-3	223.7	406.4	20	12.6	-	-
77	MYH4_RAT	Myosin-4	222.7	779.9	46	19.9	-	-
78	MYO5B_RAT	Myosin-Vb	213.6	245.3	11	7.9	yes	yes
79	NEST_RAT	Nestin	208.7	232.6	10	6.7	-	-
80	NRCAM_RAT	Neuronal cell adhesion molecule	133.8	158.2	7	9.9	yes	-
81	NOSTN_RAT	Nostrin	57.3	188.9	9	13.3	-	-
82	NCOA2_RAT	Nuclear receptor coactivator 2	159.3	379.2	27	13.2	-	-
83	NACC1_RAT	Nucleus accumbens-associated protein 1	56.4	247.3	17	35.2	-	-
84	OPHN1_RAT	Oligophrenin-1	91.8	459	36	24.2	-	-
85	PEX5_RAT	Peroxisomal targeting signal 1 receptor	71.0	409.5	20	16.7	-	-
86	PEX6_RAT	Peroxisome assembly factor 2	104.4	587.8	36	27.4	-	-
87	PLAP_RAT	Phospholipase A-2-activating protein	87.0	553.6	35	24.0	-	yes
88	PHLB1_RAT	Pleckstrin homology-like domain family B member 1	93.5	202.8	10	10.2	yes	-
89	PARP1_RAT	Poly [ADP-ribose] polymerase 1	112.6	225.1	11	10.6	yes	-
90	PLOD1_RAT	Procollagen-lysine,2-oxoglutarate 5-dioxygenase 1	83.6	198.6	7	13.0	-	-
91	RGPA2_RAT	Ral GTPase-activating protein subunit alpha-2	210.2	533.3	29	12.6	-	-
92	RIMS3_RAT	Regulating synaptic membrane exocytosis protein 3	32.6	357.1	32	44.6	yes	-
93	ROBO4_RAT	Roundabout homolog 4	102.5	584.5	37	19.4	-	-
94	SARDH_RAT	Sarcosine dehydrogenase, mitochondrial	101.4	387.9	17	21.8	-	-
95	SSPO_RAT	SCO-spondin	550.3	820	47	11.5	-	-
96	SVS2_RAT	Seminal vesicle secretory protein 2	45.5	132.4	5	11.6	-	-
97	SERC1_RAT	Serine incorporator 1	50.5	744.5	36	24.9	-	yes
98	STK3_RAT	Serine/threonine-protein kinase 3	56.1	118.3	4	14.3	-	yes
99	SPA12_RAT	Serp A12	47.5	1140.6	93	43.1	-	-
100	SRP54_RAT	Signal recognition particle 54 kDa protein	55.7	2466.5	224	33.9	yes	yes
101	SI1L2_RAT	Signal-induced proliferation-associated 1-like protein 2	189.5	379.2	24	8.7	yes	-
102	SLIT2_RAT	Slit homolog 2 protein (Fragment)	86.0	140	6	11.0	-	yes
103	NALCN_RAT	Sodium leak channel non-selective protein	200.4	327.5	21	13.2	-	yes
104	GTR2_RAT	Solute carrier family 2, facilitated glucose transporter member 2	57.0	1378.4	110	14.6	-	-
105	NCKX2_RAT	Sodium/potassium/calcium exchanger 2	74.6	118.9	4	10.9	yes	-
106	NAC3_RAT	Sodium/calcium exchanger 3	103.1	327.7	15	21.8	-	-
107	SO1A1_RAT	Solute carrier organic anion transporter family member 1A1	74.1	407.2	28	27.2	-	-
108	SRBS2_RAT	Sorbin and SH3 domain-containing protein 2	134.0	109.3	8	5.1	yes	-
109	SPT20_RAT	Spermatogenesis-associated protein 20	88.1	679	31	19.1	-	-
110	SKA1_RAT	Spindle and kinetochore-associated protein 1	29.4	114	4	17.7	-	-
111	ERG1_RAT	Squalene monooxygenase	64.0	232.5	9	20.1	-	-
112	STRN3_RAT	Striatin-3	87.1	80.7	2	3.8	yes	-
113	ST1C2_RAT	Sulfotransferase 1C2	34.7	83.8	4	14.5	-	-
114	SV2B_RAT	Synaptic vesicle glycoprotein 2B	77.5	917.5	63	37.0	yes	yes
115	THOC5_RAT	THO complex subunit 5 homolog	78.6	186	10	18.6	-	yes
116	PERT_RAT	Thyroid peroxidase	101.4	373.9	24	14.4	-	-
117	TLR4_RAT	Toll-like receptor 4	96.0	208.7	10	12.2	-	-
118	TRAK2_RAT	Trafficking kinesin-binding protein 2	101.6	557	36	35.3	-	-
119	TFR1_RAT	Transferrin receptor protein 1 (Fragment)	70.1	178.8	9	19.1	-	-
120	TRPM1_RAT	Transient receptor potential cation channel subfamily M member 1	184.2	980.1	89	22.2	-	-
121	TRIM3_RAT	Tripartite motif-containing protein 3	80.7	216.4	15	18.0	yes	-
122	SEN2_RAT	tRNA-splicing endonuclease subunit Sen2	52.9	299.3	23	14.3	-	-
123	TSC2_RAT	Tuberin	201.2	741.1	46	21.6	yes	-
124	TBA1B_RAT	Tubulin alpha-1B chain	50.1	343.8	7	30.6	yes	yes
125	TBB2B_RAT	Tubulin beta-2B chain	49.9	444.6	19	43.6	-	-
126	TBB3_RAT	Tubulin beta-3 chain	50.4	435.4	11	41.8	-	yes
127	TBCEL_RAT	Tubulin-specific chaperone cofactor E-like protein	48.0	164.2	6	27.1	-	-
128	UBN2_RAT	Ubiquitin-2	143.6	252.4	11	11.5	-	-
129	UGGG1_RAT	UDP-glucose:glycoprotein glucosyltransferase 1	176.3	557.7	38	14.5	-	yes
130	SYVC_RAT	Valyl-tRNA synthetase	140.3	289.6	18	15.0	yes	-
131	SYVM_RAT	Valyl-tRNA synthetase, mitochondrial	118.8	263.9	13	11.6	yes	-
132	WISP2_RAT	WNT1-inducible-signaling pathway protein 2	27.0	239.8	22	17.2	-	-
133	ZBT8A_RAT	Zinc finger and BTB domain-containing protein 8A	49.9	211.3	12	17.7	-	-
134	ZCCHV_RAT	Zinc finger CCCH-type antiviral protein 1	86.7	411.1	23	31.2	-	-
135	MYCS_RAT	Protein S-Myc	47.0	298.7	14	15.4	-	-
136	TIM_RAT	Protein timeless homolog	138.5	578.9	52	20.2	-	-
137	ZDHC7_RAT	Palmitoyltransferase ZDHC7	35.2	148	17	29.9	-	-
138	PSMD1_RAT	26S proteasome non-ATPase regulatory subunit 1	105.7	359	15	22.7	yes	yes
139	MRP3_RAT	Canalicular multispecific organic anion transporter 2	168.9	402.2	22	15.7	-	-
140	FYN_RAT	Tyrosine-protein kinase Fyn	60.7	456.2	20	25.0	-	-
141	P85A_RAT	Phosphatidylinositol 3-kinase regulatory subunit alpha	83.5	194.6	6	14.5	yes	yes
142	DPOD1_RAT	DNA polymerase delta catalytic subunit	123.5	528.6	24	23.2	-	-

143	TTLL9_RAT	Probable tubulin polyglutamylase TTLL9	53.9	204.1	8	25.2	-	yes
144	ATG7_RAT	Ubiquitin-like modifier-activating enzyme ATG7	77.4	513.2	28	29.9	-	yes
145	AT1A3_RAT	Sodium/potassium-transporting ATPase subunit alpha-3	111.6	181	8	11.6	-	yes
146	TCPG_RAT	T-complex protein 1 subunit gamma	60.6	366.1	24	19.3	yes	yes
147	YIPF3_RAT	Protein YIPF3	37.9	380.7	24	44.1	-	-
148	CO044_RAT	UPF0464 protein C15orf44 homolog	57.1	367.6	19	36.9	-	-
149	OPA1_RAT	Dynamin-like 120 kDa protein, mitochondrial	111.2	151.8	6	7.9	yes	-
150	MEP50_RAT	Methylosome protein 50	37.1	128.4	5	25.1	-	-
151	MRP5_RAT	Multidrug resistance-associated protein 5	160.8	519.4	24	19.8	-	-
152	UN13A_RAT	Protein unc-13 homolog A	196.2	660.5	34	11.2	yes	yes
153	SERA_RAT	D-3-phosphoglycerate dehydrogenase	56.5	952.4	77	30.2	-	-
154	PA24A_RAT	Cytosolic phospholipase A2	85.7	368.8	20	18.6	yes	-
155	MPPB_RAT	Mitochondrial-processing peptidase subunit beta	54.2	286	16	31.5	-	-
156	PLCB2_RAT	1-phosphatidylinositol-4,5-bisphosphate phosphodiesterase beta-2	134.8	221.4	8	6.1	-	-
157	PLCE1_RAT	1-phosphatidylinositol-4,5-bisphosphate phosphodiesterase epsilon-1	255.2	786.5	49	19.0	-	-
158	EAA1_RAT	Excitatory amino acid transporter 1	59.7	650.5	55	28.4	yes	-
159	EAA4_RAT	Excitatory amino acid transporter 4	60.7	498.7	31	37.4	yes	-
160	NR1H2_RAT	Oxysterols receptor LXR-beta	49.7	106.2	4	8.1	-	-
161	RPA2_RAT	DNA-directed RNA polymerase I subunit RPA2	127.6	552.8	31	20.9	-	-
162	F110B_RAT	Protein FAM110B	40.3	222.9	8	36.6	-	-
163	F122A_RAT	Protein FAM122A	30.5	95.6	9	11.5	-	-
164	NPY4R_RAT	Neuropeptide Y receptor type 4	42.5	150.8	6	10.1	-	-
165	PDE7A_RAT	High affinity cAMP-specific 3',5'-cyclic phosphodiesterase 7A	49.2	97	4	10.6	-	-
166	MAK_RAT	Serine/threonine-protein kinase MAK	69.9	249.5	14	19.0	-	-
167	SC11A_RAT	Signal peptidase complex catalytic subunit SEC11A	20.6	144.4	6	41.9	-	yes
168	MERTK_RAT	Tyrosine-protein kinase Mer	109.4	404.8	20	17.5	-	-
169	RETST_RAT	All-trans-retinol 13,14-reductase	67.5	623.9	30	40.4	-	-
170	MYOME_RAT	Myomegalin	261.9	1214	69	18.9	-	-
171	OX1R_RAT	Orexin receptor type 1	46.8	265.1	25	12.7	-	-
172	DDAH2_RAT	N(G),N(G)-dimethylarginine dimethylaminohydrolase 2	29.7	162.1	10	48.8	-	-
173	GLYR1_RAT	Putative oxidoreductase GLYR1	60.4	214	14	14.5	yes	-
174	UD12_RAT	UDP-glucuronosyltransferase 1-2	60.0	224.6	7	20.8	-	-
175	CCNF_RAT	Cyclin-F	86.7	358.4	14	26.2	yes	-
176	DDX4_RAT	Probable ATP-dependent RNA helicase DDX4	77.9	574.8	36	17.4	-	-
177	DUT_RAT	Deoxyuridine 5'-triphosphate nucleotidohydrolase	22.0	149.1	5	21.5	-	-
178	DYHC2_RAT	Cytoplasmic dynein 2 heavy chain 1	491.9	1598.8	104	17.8	-	yes
179	FOXA1_RAT	Hepatocyte nuclear factor 3-alpha	48.7	141.7	4	16.5	-	-
180	NOP58_RAT	Nucleolar protein 58	60.0	612.7	41	35.4	-	yes
181	NOE1_RAT	Noelin	55.4	273.9	14	25.4	yes	yes
182	OSPT_RAT	Protein osteopotential homolog	139.2	1742.6	140	16.3	-	-
183	REG3B_RAT	Regenerating islet-derived protein 3-beta	19.6	418.6	42	37.1	-	-
184	CEAM3_RAT	Carcinoembryonic antigen-related cell adhesion molecule 3	78.3	120.2	6	11.3	-	-
185	SHLB2_RAT	Endophilin-B2	44.8	128.5	7	20.0	yes	yes
186	IGS10_RAT	Immunoglobulin superfamily member 10	284.6	875.1	52	18.5	-	-
187	IQEC3_RAT	IQ motif and SEC7 domain-containing protein 3	128.9	403	18	16.0	yes	yes
188	K2C6A_RAT	Keratin, type II cytoskeletal 6A	59.2	281.8	6	10.0	yes	-
189	LKAP_RAT	Limkain-b1	192.6	252.3	12	10.4	-	-
190	EST2_RAT	Liver carboxylesterase 1	60.1	116.9	3	15.3	-	-
191	LPLC1_RAT	Long palate, lung and nasal epithelium carcinoma-associated protein 1	52.2	386.5	13	33.5	-	-
192	NU5M_RAT	NADH-ubiquinone oxidoreductase chain 5	68.9	1214.1	132	27.7	yes	-
193	OLF19_RAT	Olfactory receptor-like protein 19	35.4	383.5	23	23.2	-	-
194	CT007_RAT	Probable methyltransferase C20orf7 homolog, mitochondrial	38.2	160.8	8	24.8	-	-
195	ARMX6_RAT	Protein ARMCX6	33.4	2502.4	263	32.6	-	yes
196	LMA1L_RAT	Protein ERGIC-53-like	56.3	246.6	15	25.2	-	-
197	SCRG1_RAT	Scrapie-responsive protein 1	11.2	186.1	15	25.5	-	-
198	SIDT1_RAT	SID1 transmembrane family member 1	94.1	132.3	5	7.6	-	yes
199	NTCP5_RAT	Sodium/bile acid cotransporter 5	48.0	303	32	24.4	-	-
200	T2R38_RAT	Taste receptor type 2 member 38	37.2	426.7	28	54.4	-	-
201	T10IP_RAT	Testis-specific protein 10-interacting protein	59.8	89.2	3	7.6	-	-

Listed are all proteins with identified AHA, d10Leu or both modifications. The number and specific modification identified in each protein could not be determined since ProteinScape software was not available any longer at the end of my thesis.

Accession—Database accession number

Protein—Common name of the protein

MW—Molecular weight in Daltons

Scores—Protein score (Mascot score)

#Peptides—Number of peptides identified

SC%—Sequence coverage

Synprot—Synaptic protein database (Pielot et al., 2012)

Transcriptome—Neuropil transcriptome database (Cajigas et al., 2012)

Supplementary Table 7. Newly synthesized proteins identified in synaptosomes isolated from cortical primary cultures at DIV9

Nr.	Accession	Protein	MW [kDa]	Scores	#Peptides	SC [%]	Synprot	Transcriptome
1	ABCA7_RAT	ATP-binding cassette sub-family A member 7	237.6	783.4	40	20.1	-	-
2	ABCB8_RAT	ATP-binding cassette sub-family B member 8, mitochondrial	77.7	1796.2	125	21.0	yes	-
3	ABCB8_RAT	Bile salt export pump	146.2	446.3	24	15.8	-	-
4	ABCD3_RAT	ATP-binding cassette sub-family D member 3	75.3	154.6	7	8.0	yes	-
5	ABTB2_RAT	Ankyrin repeat and BTB/POZ domain-containing protein 2	111.5	349.4	20	20.2	-	-
6	ACACA_RAT	Acetyl-CoA carboxylase 1	265.0	830.8	42	19.0	yes	-
7	ACSM5_RAT	Acyl-coenzyme A synthetase ACSM5, mitochondrial	64.6	175.3	9	14.5	-	-
8	ACTB_RAT	Actin, cytoplasmic 1	41.7	486.1	13	30.4	yes	yes
9	ADAM7_RAT	Disintegrin and metalloproteinase domain-containing protein 7	89.3	409.5	23	18.6	-	-
10	AGAP2_RAT	Arf-GAP with GTPase, ANK repeat and PH domain-containing protein 2	124.4	231.9	13	11.6	yes	-
11	ANKL2_RAT	Ankyrin repeat and LEM domain-containing protein 2	103.3	813.9	47	31.4	-	-
12	ANXA4_RAT	Annexin A4	35.8	226.1	10	25.7	-	-
13	APOB_RAT	Apolipoprotein B-100	535.7	1511.7	77	16.3	-	-
14	ARC_RAT	Activity-regulated cytoskeleton-associated protein	45.3	87.1	3	12.6	yes	yes
15	ARHG6_RAT	Rho guanine nucleotide exchange factor 6	87.0	244.3	14	16.6	-	-
16	ARL1_RAT	ADP-ribosylation factor-like protein 1	20.4	115.6	8	29.3	-	yes
17	ARL2_RAT	ADP-ribosylation factor-like protein 2	20.8	152	10	19.0	-	-
18	ARSK_RAT	Arylsulfatase K	64.2	218.4	8	14.7	-	-
19	ARLY_RAT	Argininosuccinate lyase	51.5	101.5	5	11.3	-	-
20	AT1A1_RAT	Sodium/potassium-transporting ATPase subunit alpha-1	113.0	491.9	26	24.4	yes	yes
21	AT2C2_RAT	Calcium-transporting ATPase type 2C member 2	103.0	794.6	36	28.3	-	-
22	BACE2_RAT	Beta-secretase 2	55.8	123.4	5	7.0	-	-
23	BEGIN_RAT	Brain-enriched guanylate kinase-associated protein	67.0	102.5	4	11.9	yes	-
24	BRCA2_RAT	Breast cancer type 2 susceptibility protein homolog	372.0	740.2	35	13.3	-	-
25	BTBD9_RAT	BTB/POZ domain-containing protein 9	69.1	107.6	7	5.1	-	yes
26	CABIN_RAT	Calcineurin-binding protein cabin-1	242.7	539	39	9.4	-	yes
27	CCND3_RAT	G1/S-specific cyclin-D3	32.4	282.5	16	27.3	-	-
28	CD302_RAT	CD302 antigen	25.4	152.5	5	18.0	-	yes
29	CDC47_RAT	Cell division cycle-associated protein 7	43.0	97.8	4	11.4	-	-
30	CDA7L_RAT	Cell division cycle-associated 7-like protein	49.9	122.2	7	12.6	-	-
31	CLAP2_RAT	CLIP-associating protein 2	140.6	517.3	23	21.5	yes	-
32	CLD16_RAT	Claudin-16	26.1	171.1	4	39.6	-	-
33	COG6_RAT	Conserved oligomeric Golgi complex subunit 6	72.9	235.2	12	22.5	-	yes
34	COG7_RAT	Conserved oligomeric Golgi complex subunit 7	86.2	202.3	7	16.9	-	yes
35	CSPG4_RAT	Chondroitin sulfate proteoglycan 4	251.8	304.4	12	7.4	-	-
36	CTU1_RAT	Cytoplasmic tRNA 2-thiolation protein 1	40.2	146.6	8	20.7	-	-
37	CUL3_RAT	Cullin-3	88.9	282.6	13	13.7	-	-
38	CP24A_RAT	1,25-dihydroxyvitamin D(3) 24-hydroxylase, mitochondrial	59.4	159.6	6	13.4	-	-
39	DEK_RAT	Protein DEK	42.9	216.2	9	28.0	yes	-
40	DGLA_RAT	Sn1-specific diacylglycerol lipase alpha	115.2	340.5	17	16.4	yes	-
41	DHYS_RAT	Deoxyhypusine synthase	40.7	212.7	9	28.5	-	yes
42	DLGP4_RAT	Disks large-associated protein 4	108.0	124.1	6	5.8	-	yes
43	DNJA1_RAT	DnaJ homolog subfamily A member 1	44.8	200.5	10	18.1	yes	-
44	DUOX2_RAT	Dual oxidase 2	171.4	243.4	17	11.5	-	-
45	DYHC2_RAT	Cytoplasmic dynein 2 heavy chain 1	491.9	1637.5	90	17.0	-	yes
46	ECEL1_RAT	Endothelin-converting enzyme-like 1	87.9	423.6	30	17.0	-	-
47	EID3_RAT	EP300-interacting inhibitor of differentiation 3	44.8	94.3	4	11.6	-	-
48	EIF2D_RAT	Eukaryotic translation initiation factor 2D	62.6	284.8	20	25.1	-	-
49	ENPP2_RAT	Ectonucleotide pyrophosphatase/phosphodiesterase family member 2	101.5	238.1	9	16.2	-	-
50	EPN3_RAT	Epsin-3	65.0	179.9	11	5.3	-	-
51	EPOR_RAT	Erythropoietin receptor	55.5	120.2	5	12.2	-	-
52	ERC2_RAT	ERC protein 2	110.5	420.2	25	16.9	-	yes
53	ERR1_RAT	Steroid hormone receptor ERR1	45.4	453.7	26	34.1	-	-
54	EXOC8_RAT	Exocyst complex component 8	81.0	383	21	25.6	yes	-
55	FAHD1_RAT	Fumarylacetoacetate hydrolase domain-containing protein 1	24.5	111.4	5	35.3	-	-
56	F203A_RAT	Protein FAM203A	43.1	197	9	12.0	-	-
57	FAS_RAT	Fatty acid synthase	272.5	651.9	32	15.8	yes	-
58	FAKD2_RAT	FAST kinase domain-containing protein 2	77.7	160.6	12	9.4	-	-
59	FHL2_RAT	Four and a half LIM domains protein 2	32.1	177.4	8	33.7	-	-
60	FIS1_RAT	Mitochondrial fission 1 protein	17.0	174	13	21.1	-	-
61	FNBP1_RAT	Formin-binding protein 1	71.2	85.2	3	5.2	yes	-
62	FSHR_RAT	Follicle-stimulating hormone receptor	77.6	276.6	14	28.6	-	-
63	FUT4_RAT	Alpha-(1,3)-fucosyltransferase	48.7	100.9	4	9.0	-	-
64	GABR1_RAT	Gamma-aminobutyric acid type B receptor subunit 1	111.5	134.9	6	8.9	yes	-

65	GBRG3_RAT	Gamma-aminobutyric acid receptor subunit gamma-3	54.3	199.9	8	19.3	-	-
66	GCC2_RAT	GRIP and coiled-coil domain-containing protein 2	195.0	361.3	18	11.9	-	yes
67	GDF11_RAT	Growth/differentiation factor 11 (Fragment)	39.1	97.4	3	12.5	-	yes
68	GDIB_RAT	Rab GDP dissociation inhibitor beta	50.5	263	14	27.4	-	yes
69	GRM5_RAT	Metabotropic glutamate receptor 5	131.8	198.5	19	6.5	yes	yes
70	HAS2_RAT	Hyaluronan synthase 2	63.5	261.2	12	30.8	-	-
71	HIF1A_RAT	Hypoxia-inducible factor 1-alpha	92.3	212.9	7	12.7	-	-
72	HNRPM_RAT	Heterogeneous nuclear ribonucleoprotein M	73.7	2616.1	186	49.1	yes	-
73	ABEC1_RAT	C->U-editing enzyme APOBEC-1	27.3	99.4	4	22.3	-	-
74	ARHGP_RAT	Rho guanine nucleotide exchange factor 25	64.1	222	14	16.9	-	yes
75	ADO_RAT	Aldehyde oxidase	146.8	248.6	14	12.8	-	-
76	FIBA_RAT	Fibrinogen alpha chain	86.6	182.4	7	18.3	yes	-
77	DYN1_RAT	Dynamin-1	97.2	236.6	9	12.8	-	yes
78	DH11_RAT	Corticosteroid 11-beta-dehydrogenase isozyme 1	31.9	297.9	14	37.5	-	-
79	HEM6_RAT	Coproporphyrinogen-III oxidase, mitochondrial	49.2	204.7	13	24.6	-	-
80	CH60_RAT	60 kDa heat shock protein, mitochondrial	60.9	2544	197	18.8	-	-
81	HS90A_RAT	Heat shock protein HSP 90-alpha	84.8	254	11	19.8	-	yes
82	HSP7C_RAT	Heat shock cognate 71 kDa protein	70.8	88.5	2	6.7	-	yes
83	MRP9_RAT	Multidrug resistance-associated protein 9	152.9	552.5	29	20.2	-	-
84	NB5R3_RAT	NADH-cytochrome b5 reductase 3	34.2	115.7	5	15.6	-	-
85	1433B_RAT	14-3-3 protein beta/alpha	28.0	134.9	4	12.2	-	-
86	TNR6_RAT	Tumor necrosis factor receptor superfamily member 6	36.8	154	12	16.7	-	-
87	RHG29_RAT	Rho GTPase-activating protein 29	141.9	369.4	18	15.6	-	-
88	SCG1_RAT	Secretogranin-1	77.5	281.4	20	11.9	-	yes
89	AFAD_RAT	Afadin	207.5	564	33	15.4	-	-
90	ADT2_RAT	ADP/ATP translocase 2	32.9	153.7	5	14.1	yes	-
91	ANPRC_RAT	Atrial natriuretic peptide receptor 3	59.7	395.8	18	29.3	-	-
92	UBP2_RAT	Ubiquitin carboxyl-terminal hydrolase 2	69.3	247.1	12	22.2	-	yes
93	KCC1G_RAT	Calcium/calmodulin-dependent protein kinase type 1G	53.1	155.8	6	12.0	-	yes
94	GHC2_RAT	Mitochondrial glutamate carrier 2	34.1	1756.1	164	35.6	-	-
95	GTR1_RAT	Solute carrier family 2, facilitated glucose transporter member 1	53.9	423.8	48	9.3	-	yes
96	G6B_RAT	Protein G6b	25.1	132	6	29.7	-	-
97	TBB5_RAT	Tubulin beta-5 chain	49.6	371	11	35.8	-	-
98	CP4F5_RAT	Cytochrome P450 4F5	60.6	150.8	6	16.2	-	-
99	RDH2_RAT	Retinol dehydrogenase 2	35.6	164	6	15.5	-	-
100	TRY1_RAT	Anionic trypsin-1	25.9	281.9	2	28.5	yes	-
101	UD12_RAT	UDP-glucuronosyltransferase 1-2	60.0	256.9	11	22.0	-	-
102	CATL1_RAT	Cathepsin L1	37.6	132.8	5	17.7	-	-
103	HA12_RAT	RT1 class I histocompatibility antigen, AA alpha chain	41.8	296.6	16	8.9	-	-
104	ASB14_RAT	Ankyrin repeat and SOCS box protein 14	66.1	268.7	15	23.5	-	-
105	CCD39_RAT	Coiled-coil domain-containing protein 39	109.5	246.9	11	19.1	-	yes
106	CL060_RAT	Uncharacterized protein C12orf60 homolog	27.4	269.4	9	55.1	-	-
107	EAPA2_RAT	Experimental autoimmune prostatitis antigen 2 homolog	102.0	198.2	5	16.5	-	-
108	K1C10_RAT	Keratin, type I cytoskeletal 10	56.5	208.4	6	12.5	yes	-
109	K2C6A_RAT	Keratin, type II cytoskeletal 6A	59.2	269.3	5	12.1	yes	-
110	LIX1L_RAT	LIX1-like protein	36.6	114.2	7	19.5	-	-
111	MDR2_RAT	Multidrug resistance protein 2	140.6	745.8	46	20.7	-	-
112	METR_N_RAT	Meteorin	31.3	686.9	47	18.2	-	-
113	S2534_RAT	Solute carrier family 25 member 34	33.6	289.2	17	27.4	-	-
114	TBB2C_RAT	Tubulin beta-2C chain	49.8	349.7	6	40.0	yes	yes
115	IL6RA_RAT	Interleukin-6 receptor subunit alpha	50.4	336.9	15	13.2	-	-
116	IPO13_RAT	Importin-13	108.1	588.8	41	17.5	-	-
117	ITPR3_RAT	Inositol 1,4,5-trisphosphate receptor type 3	304.1	1292.8	87	25.9	-	-
118	IZUM1_RAT	Izumo sperm-egg fusion protein 1	43.6	277.3	14	26.1	-	-
119	KAZRN_RAT	Kazrin	86.9	300	14	21.8	-	-
120	KCAB3_RAT	Voltage-gated potassium channel subunit beta-3	43.7	132	6	19.3	-	-
121	KDIS_RAT	Kinase D-interacting substrate of 220 kDa	195.6	239.5	14	5.6	yes	-
122	KIF1B_RAT	Kinesin-like protein KIF1B	204.0	574.5	27	16.2	-	-
123	KLHL7_RAT	Kelch-like protein 7	65.9	259	13	13.1	-	yes
124	LDLR_RAT	Low-density lipoprotein receptor	96.6	457	31	16.5	-	-
125	LGR4_RAT	Leucine-rich repeat-containing G-protein coupled receptor 4	104.1	190	9	9.1	-	-
126	LCAP_RAT	Leucyl-cystinyl aminopeptidase	117.1	527	25	22.8	-	-
127	LRFN2_RAT	Leucine-rich repeat and fibronectin type-III domain-containing protein 2	84.9	532.1	27	26.6	-	yes
128	LRP2_RAT	Low-density lipoprotein receptor-related protein 2	518.9	1093.6	59	14.3	-	-
129	LPPRC_RAT	Leucine-rich PPR motif-containing protein, mitochondrial	156.6	731.1	31	24.6	yes	-
130	LRRN1_RAT	Leucine-rich repeat neuronal protein 1	80.6	225.4	11	9.6	-	yes
131	MAP4_RAT	Microtubule-associated protein 4	110.2	358.5	15	17.3	yes	-
132	MET18_RAT	Histidine protein methyltransferase 1 homolog	40.0	237.9	10	19.9	-	-
133	MTOR_RAT	Serine/threonine-protein kinase mTOR	288.6	1972.9	118	32.8	-	yes
134	MYO9A_RAT	Myosin IXa	301.2	764.3	35	14.1	yes	-
135	NALCN_RAT	Sodium leak channel non-selective protein	200.4	469.3	23	13.5	-	yes
136	NCOA2_RAT	Nuclear receptor coactivator 2	159.3	821.3	60	24.0	-	-

137	NEST_RAT	Nestin	208.7	526.3	25	17.9	-	-
138	NOTC2_RAT	Neurogenic locus notch homolog protein 2	265.2	396.7	21	7.3	-	-
139	NTRI_RAT	Neurotrimin	38.0	160.4	6	19.8	yes	-
140	NUPF1_RAT	Nuclear fragile X mental retardation-interacting protein 1	55.1	227.1	10	15.8	-	-
141	NU153_RAT	Nuclear pore complex protein Nup153	152.7	434.5	15	16.1	-	-
142	NUP50_RAT	Nuclear pore complex protein Nup50	49.8	189	4	24.8	-	-
143	NEC2_RAT	Neuroendocrine convertase 2	70.7	209.1	11	22.1	-	yes
144	PCSK5_RAT	Proprotein convertase subtilisin/kexin type 5	210.2	1056.9	71	17.5	-	-
145	PDE2A_RAT	cGMP-dependent 3',5'-cyclic phosphodiesterase	104.6	842.5	51	28.8	yes	-
146	PDE3B_RAT	cGMP-inhibited 3',5'-cyclic phosphodiesterase B	123.0	357.8	18	19.0	-	-
147	PDE4D_RAT	cAMP-specific 3',5'-cyclic phosphodiesterase 4D	90.5	425.1	20	22.5	yes	yes
148	PDS5A_RAT	Sister chromatid cohesion protein PDS5 homolog A	150.2	528.8	22	19.7	-	yes
149	PHF10_RAT	PHD finger protein 10	55.8	156.2	11	11.3	-	-
150	PLCB2_RAT	1-phosphatidylinositol-4,5-bisphosphate phosphodiesterase beta-2	134.8	277.4	14	12.8	-	-
151	KPCD1_RAT	Serine/threonine-protein kinase D1	102.0	184.8	6	9.3	-	-
152	PSD10_RAT	26S proteasome non-ATPase regulatory subunit 10	25.0	234.8	9	24.7	yes	-
153	PYC_RAT	Pyruvate carboxylase, mitochondrial	129.7	866.8	43	25.2	yes	-
154	RBP1_RAT	RalA-binding protein 1	75.2	201.1	11	16.5	-	yes
155	RHOA_RAT	Transforming protein RhoA	21.8	80.9	3	15.0	-	-
156	RP3A_RAT	Rabphilin-3A	75.8	462.9	20	23.8	-	yes
157	RS27A_RAT	Ubiquitin-40S ribosomal protein S27a	17.9	92	2	24.4	yes	-
158	SCN2A_RAT	Sodium channel protein type 2 subunit alpha	227.7	362.2	13	10.2	yes	yes
159	S61A1_RAT	Protein transport protein Sec61 subunit alpha isoform 1	52.2	113.8	6	9.0	-	-
160	SFXN3_RAT	Sideroflexin-3	35.4	398.1	22	33.6	yes	-
161	SH3G2_RAT	Endophilin-A1	39.9	157.1	7	22.2	yes	yes
162	SHAN2_RAT	SH3 and multiple ankyrin repeat domains protein 2	158.6	250.7	8	10.9	yes	-
163	S22AH_RAT	Solute carrier family 22 member 17	55.8	561.9	42	29.0	-	yes
164	SLC31_RAT	Neutral and basic amino acid transport protein rBAT	78.5	161.7	7	12.9	-	-
165	SLX1_RAT	Structure-specific endonuclease subunit SLX1	30.7	215.2	8	12.5	-	-
166	SPRY7_RAT	SPRY domain-containing protein 7	21.7	200.8	6	48.0	-	-
167	SRBP2_RAT	Sterol regulatory element-binding protein 2	122.9	232	9	8.6	-	-
168	SRP54_RAT	Signal recognition particle 54 kDa protein	55.7	2840.8	257	39.5	yes	yes
169	SYT3_RAT	Synaptotagmin-3	63.3	254.4	9	20.2	yes	yes
170	TANC1_RAT	Protein TANC1	200.4	346.8	18	9.2	-	yes
171	TAXB1_RAT	Tax1-binding protein 1 homolog	93.1	182.4	8	9.7	-	-
172	TCPA_RAT	T-complex protein 1 subunit alpha	60.3	399.4	13	40.6	yes	yes
173	TDRD7_RAT	Tudor domain-containing protein 7	125.2	370.8	14	16.9	-	-
174	TEP1_RAT	Telomerase protein component 1	291.5	1791.2	131	23.7	-	-
175	TMM33_RAT	Transmembrane protein 33	28.0	88.5	7	27.9	yes	-
176	TNF15_RAT	Tumor necrosis factor ligand superfamily member 15	28.0	213.9	15	41.7	-	-
177	TN13K_RAT	Serine/threonine-protein kinase TNN13K	92.7	302.4	18	17.8	-	-
178	TOR3A_RAT	Torsin-3A	45.1	97	4	8.4	-	-
179	TRPA1_RAT	Transient receptor potential cation channel subfamily A member 1	128.5	501.8	33	20.4	-	-
180	TRPM1_RAT	Transient receptor potential cation channel subfamily M member 1	184.2	317.2	20	9.3	-	-
181	TSHR_RAT	Thyrotropin receptor	86.4	125.3	7	14.0	-	-
182	TBA1A_RAT	Tubulin alpha-1A chain	50.1	472.4	11	28.4	yes	yes
183	TBB2A_RAT	Tubulin beta-2A chain	49.9	482.3	14	44.5	yes	yes
184	UBR4_RAT	E3 ubiquitin-protein ligase UBR4	573.4	2780.5	190	20.9	yes	yes
185	UBR5_RAT	E3 ubiquitin-protein ligase UBR5	103.9	463.1	32	21.1	-	-
186	ULK3_RAT	Serine/threonine-protein kinase ULK3	53.4	215	10	19.3	-	-
187	UN45A_RAT	Protein unc-45 homolog A	103.2	1125.8	61	35.4	-	yes
188	WDR70_RAT	WD repeat-containing protein 70	72.8	137.1	6	9.8	-	-
189	T184A_RAT	Transmembrane protein 184A	46.8	94.7	4	16.7	-	-
190	SERA_RAT	D-3-phosphoglycerate dehydrogenase	56.5	587.9	43	29.5	-	-
191	SUIS_RAT	Sucrase-isomaltase, intestinal	210.2	409.5	13	12.4	-	-
192	SC31A_RAT	Protein transport protein Sec31A	135.2	409.1	19	19.5	-	yes

Listed are all proteins with identified AHA, d10Leu or both modifications. The number and specific modification identified in each protein could not be determined since ProteinScape software was not available any longer at the end of my thesis.

Accession–Database accession number

Protein–Common name of the protein

MW–Molecular weight in Daltons

Scores–Protein score (Mascot score)

#Peptides–Number of peptides identified

SC%–Sequence coverage

Synprot–Synaptic protein database (Pielot et al., 2012)

Transcriptome–Neuropil transcriptome database (Cajigas et al., 2012)

Supplementary Table 8. Newly synthesized proteins identified in synaptosomes isolated from cortical primary cultures at DIV17

Nr.	Accession	Protein	MW [kDa]	Scores	#Peptides	SC [%]	Synprot	Transcriptome
1	ABCA5_RAT	ATP-binding cassette sub-family A member 5	185.7	566.4	42	16.1	-	-
2	ABCB8_RAT	ATP-binding cassette sub-family B member 8, mitochondrial	77.7	906	66	10.2	yes	-
3	ABCB8_RAT	Bile salt export pump	146.2	478.4	26	20.1	-	-
4	ABCC9_RAT	ATP-binding cassette sub-family C member 9	174.0	419.4	29	15.1	-	-
5	ACADS_RAT	Short-chain specific acyl-CoA dehydrogenase, mitochondrial	44.7	373.7	16	26.0	yes	-
6	ACADV_RAT	Very long-chain specific acyl-CoA dehydrogenase, mitochondrial	70.7	679.5	44	40.8	-	-
7	ACSF2_RAT	Acyl-CoA synthetase family member 2, mitochondrial	67.8	209.1	12	17.9	-	-
8	ACSL4_RAT	Long-chain-fatty-acid--CoA ligase 4	74.3	184.9	11	16.4	-	-
9	ACTB_RAT	Actin, cytoplasmic 1	41.7	550.1	13	45.6	yes	yes
10	ACTG_RAT	Actin, cytoplasmic 2	41.8	389.4	16	41.3	yes	yes
11	ACV1C_RAT	Activin receptor type-1C	54.8	256.2	13	33.3	-	-
12	ADCY3_RAT	Adenylate cyclase type 3	128.9	559.9	42	32.2	-	yes
13	ADCYA_RAT	Adenylate cyclase type 10	185.7	773.2	50	32.4	-	-
14	AGTRB_RAT	Type-1B angiotensin II receptor	40.9	131.9	7	17.8	-	-
15	AKAP1_RAT	A-kinase anchor protein 1, mitochondrial	91.7	225.4	10	17.0	-	-
16	AKAP5_RAT	A-kinase anchor protein 5	75.9	185.1	9	12.9	yes	yes
17	AL3A2_RAT	Fatty aldehyde dehydrogenase	54.0	107	5	11.2	-	-
18	AMPD1_RAT	AMP deaminase 1	86.4	249.2	14	14.7	-	-
19	ANKL2_RAT	Ankyrin repeat and LEM domain-containing protein 2	103.3	777.5	56	22.8	-	-
20	APOB_RAT	Apolipoprotein B-100	535.7	1644.2	107	17.2	yes	-
21	ARL2_RAT	ADP-ribosylation factor-like protein 2	20.8	154.3	7	12.0	-	-
22	ARL5A_RAT	ADP-ribosylation factor-like protein 5A	20.7	96.5	5	31.8	-	-
23	ARMC5_RAT	Armadillo repeat-containing protein 5	96.5	416.1	30	28.4	-	-
24	ARMX1_RAT	Armadillo repeat-containing X-linked protein 1	51.0	257.2	10	24.7	-	yes
25	ASNS_RAT	Asparagine synthetase [glutamine-hydrolyzing]	64.2	454.6	25	23.0	-	yes
26	AT1A2_RAT	Sodium/potassium-transporting ATPase subunit alpha-2	112.1	406	18	20.2	yes	-
27	AT1A3_RAT	Sodium/potassium-transporting ATPase subunit alpha-3	111.6	337.9	10	11.4	yes	-
28	AT1A4_RAT	Sodium/potassium-transporting ATPase subunit alpha-4	113.9	350.7	21	21.3	yes	-
29	AT2A3_RAT	Sarcoplasmic/endoplasmic reticulum calcium ATPase 3	109.3	260.1	15	14.0	yes	-
30	BPI_RAT	Bactericidal permeability-increasing protein	53.7	316.3	12	23.9	-	-
31	BTD_RAT	Biotinidase	58.0	300.7	13	15.9	-	-
32	CABIN_RAT	Calcineurin-binding protein cabin-1	242.7	1178.3	120	18.7	-	yes
33	CAC1B_RAT	Voltage-dependent N-type calcium channel subunit alpha-1B	262.1	890.2	46	24.0	yes	yes
34	CAC1D_RAT	Voltage-dependent L-type calcium channel subunit alpha-1D	250.0	2003.8	204	12.8	-	yes
35	CAC1I_RAT	Voltage-dependent T-type calcium channel subunit alpha-1I	243.5	355.3	24	11.6	-	yes
36	CAC1S_RAT	Voltage-dependent L-type calcium channel subunit alpha-1S	130.1	126.8	6	9.3	-	-
37	CCKN_RAT	Cholecystokinin	12.8	157.9	9	60.9	-	yes
38	CELF1_RAT	CUGBP Elav-like family member 1	52.2	228	7	23.4	-	yes
39	CHD8_RAT	Chromodomain-helicase-DNA-binding protein 8	290.5	649.4	38	11.9	-	-
40	CLIP4_RAT	CAP-Gly domain-containing linker protein 4	64.6	475.9	22	29.2	-	-
41	CMA1_RAT	Chymase	27.6	265.9	12	36.4	-	-
42	CNTN1_RAT	Contactin-1	113.4	292.7	8	12.4	yes	-
43	CTGF_RAT	Connective tissue growth factor	37.7	183.6	7	21.6	-	-
44	DISC1_RAT	Disrupted in schizophrenia 1 homolog	92.5	428.3	25	27.9	-	-
45	DPEP1_RAT	Dipeptidase 1	45.5	435.8	27	35.1	-	-
46	DYH12_RAT	Dynein heavy chain 12, axonemal	357.0	780.3	49	17.6	-	-
47	ENPP1_RAT	Ectonucleotide pyrophosphatase/phosphodiesterase family member 1	102.9	234.6	13	10.0	-	-
48	EPHA6_RAT	Ephrin type-A receptor 6	116.1	289.5	20	15.7	-	yes
49	ESR1_RAT	Estrogen receptor	67.0	413.8	27	30.8	-	-
50	FAM5C_RAT	Protein FAM5C	88.4	229.4	7	11.0	-	-
51	FZD1_RAT	Frizzled-1	71.0	203.2	9	16.5	-	-
52	GIPC1_RAT	PDZ domain-containing protein GIPC1	36.1	185.9	7	32.1	yes	-
53	GLRA1_RAT	Glycine receptor subunit alpha-1	52.6	214.4	11	24.7	-	-
54	GLRB_RAT	Glycine receptor subunit beta	55.9	254.4	11	21.2	-	yes
55	GLSL_RAT	Glutaminase liver isoform, mitochondrial	66.2	289.1	22	33.2	-	-
56	GNAO_RAT	Guanine nucleotide-binding protein G(o) subunit alpha	40.0	284.9	6	23.4	-	-
57	GNP3_RAT	GPN-loop GTPase 3	32.8	223.4	10	40.1	-	-
58	GRM8_RAT	Metabotropic glutamate receptor 8	101.8	462.8	24	19.6	-	-
59	GSK3A_RAT	Glycogen synthase kinase-3 alpha	51.0	130.2	5	13.7	yes	-
60	GSHR_RAT	Glutathione reductase (Fragment)	46.3	151.6	9	17.7	yes	-
61	HCN4_RAT	Potassium/sodium hyperpolarization-activated cyclic nucleotide-gated channel 4	128.7	366.2	19	20.1	-	-
62	HDAC8_RAT	Histone deacetylase 8	41.7	132	5	28.4	-	-

63	HMDH_RAT	3-hydroxy-3-methylglutaryl-coenzyme A reductase	96.6	922.2	68	35.6	-	yes
64	HMOX1_RAT	Heme oxygenase 1	33.0	263.2	12	39.8	-	-
65	HD_RAT	Huntingtin	343.5	1544.5	112	19.4	yes	yes
66	HYAL2_RAT	Hyaluronidase-2	54.0	185.6	20	25.8	-	-
67	IDHG1_RAT	Isocitrate dehydrogenase [NAD] subunit gamma 1, mitochondrial	42.8	154.6	15	21.9	yes	-
68	IF172_RAT	Intraflagellar transport protein 172 homolog	197.5	737.7	38	21.8	-	-
69	IL17F_RAT	Interleukin-17F	17.7	146	16	40.4	-	-
70	IMPA1_RAT	Inositol monophosphatase 1	30.5	112.7	4	21.7	yes	-
71	IQUB_RAT	IQ and ubiquitin-like domain-containing protein	91.8	234.5	10	12.2	-	-
72	JAG1_RAT	Protein jagged-1	134.2	474.2	23	14.4	-	-
73	JAK3_RAT	Tyrosine-protein kinase JAK3	122.5	542.5	35	22.7	-	-
74	KCNN4_RAT	Intermediate conductance calcium-activated potassium channel protein 4	47.7	672.5	58	44.7	-	-
75	KCTD5_RAT	BTB/POZ domain-containing protein KCTD5	26.1	247.6	11	25.2	-	-
76	KHDR1_RAT	KH domain-containing, RNA-binding, signal transduction-associated protein 1	48.3	121.7	4	13.5	-	-
77	KDIS_RAT	Kinase D-interacting substrate of 220 kDa	195.6	581.2	33	16.2	yes	-
78	KIF15_RAT	Kinesin-like protein KIF15	159.4	585.2	30	18.2	-	-
79	KLC1_RAT	Kinesin light chain 1	63.7	321.3	18	21.4	yes	-
80	KLK8_RAT	Kallikrein-8	28.5	194.2	20	22.7	-	yes
81	LCAP_RAT	Leucyl-cystinyl aminopeptidase	117.1	400.7	22	15.6	-	-
82	LRAT_RAT	Lecithin retinol acyltransferase	25.8	217.7	16	35.1	-	-
83	LRFN4_RAT	Leucine-rich repeat and fibronectin type-III domain-containing protein 4	67.2	129.8	4	15.1	-	-
84	LRRT2_RAT	Leucine-rich repeat transmembrane neuronal protein 2	58.8	779.5	54	31.1	-	-
85	MAGI2_RAT	Membrane-associated guanylate kinase, WW and PDZ domain-containing protein	141.0	326.2	16	9.6	yes	-
86	ALS_RAT	Insulin-like growth factor-binding protein complex acid labile subunit	66.8	258.1	11	28.0	-	-
87	DHE3_RAT	Glutamate dehydrogenase 1, mitochondrial	61.4	213.1	9	13.4	yes	-
88	GBB5_RAT	Guanine nucleotide-binding protein subunit beta-5	38.7	83.2	4	10.5	-	yes
89	ACHG_RAT	Acetylcholine receptor subunit gamma	58.6	113.2	5	15.0	-	-
90	CJ046_RAT	Uncharacterized protein C10orf46 homolog	38.8	633.8	49	27.1	-	-
91	CO044_RAT	UPF0464 protein C15orf44 homolog	57.1	328.5	19	35.0	-	-
92	CO8B_RAT	Complement component C8 beta chain	66.6	192.3	19	17.0	-	-
93	CP24A_RAT	1,25-dihydroxyvitamin D(3) 24-hydroxylase, mitochondrial	59.4	473.9	30	29.0	-	-
94	5HT3A_RAT	5-hydroxytryptamine receptor 3A	55.4	184.4	8	18.4	-	yes
95	CXB3_RAT	Gap junction beta-3 protein	30.9	142	5	27.4	-	-
96	DCE2_RAT	Glutamate decarboxylase 2	65.4	397.6	20	33.5	yes	-
97	HYES_RAT	Epoxide hydrolase 2	62.3	188.2	9	27.3	-	-
98	K0319_RAT	Dyslexia-associated protein KIAA0319 homolog	117.9	263.2	17	11.4	-	-
99	IMB1_RAT	Importin subunit beta-1	97.1	210	11	15.9	yes	-
100	IRK16_RAT	Inward rectifier potassium channel 16	47.9	205.1	9	16.0	-	-
101	1433B_RAT	14-3-3 protein beta/alpha	28.0	153.6	4	27.6	-	-
102	DH12_RAT	Corticosteroid 11-beta-dehydrogenase isozyme 2	43.7	313.8	19	40.5	-	-
103	DCHS_RAT	Histidine decarboxylase	73.6	295.2	22	10.8	-	-
104	RB612_RAT	ELKS/Rab6-interacting/CAST family member 1	108.8	521.8	27	25.3	yes	-
105	GTR8_RAT	Solute carrier family 2, facilitated glucose transporter member 8	51.4	329.9	25	25.1	-	-
106	NMDE2_RAT	Glutamate [NMDA] receptor subunit epsilon-2	166.0	357.5	18	18.4	yes	yes
107	SYAM_RAT	Alanyl-tRNA synthetase, mitochondrial	107.7	418.1	21	20.3	-	-
108	TACT_RAT	T-cell surface protein tactile	67.2	234.9	15	13.6	-	-
109	PGS1_RAT	Biglycan	41.7	208.7	9	34.1	-	-
110	MKS3_RAT	Meckelin	111.7	361.7	17	10.9	-	yes
111	ZPI_RAT	Protein Z-dependent protease inhibitor	50.2	137.5	5	12.2	-	-
112	CGT_RAT	2-hydroxyacyl sphingosine 1-beta-galactosyltransferase	61.1	183.2	9	16.8	-	yes
113	KCC2G_RAT	Calcium/calmodulin-dependent protein kinase type II subunit gamma	59.0	253.1	6	21.3	yes	-
114	MPIP2_RAT	M-phase inducer phosphatase 2	64.2	88.1	5	9.6	-	-
115	ODBB_RAT	2-oxoisovalerate dehydrogenase subunit beta, mitochondrial	42.8	137.3	8	13.1	-	-
116	VGFR1_RAT	Vascular endothelial growth factor receptor 1	150.2	271.3	15	14.7	-	-
117	RED1_RAT	Double-stranded RNA-specific editase 1	77.9	145.4	6	9.1	-	-
118	ACCN2_RAT	Amiloride-sensitive cation channel 2, neuronal	59.6	230.7	7	28.5	-	-
119	WHRN_RAT	Whirlin	98.3	409.8	24	23.4	-	-
120	KBP_RAT	KIF1-binding protein	71.3	272.6	13	23.3	-	-
121	PO210_RAT	Nuclear pore membrane glycoprotein 210	204.0	319.1	13	12.2	-	-
122	CP2A3_RAT	Cytochrome P450 2A3	56.5	279.4	16	20.4	-	-
123	CP2B3_RAT	Cytochrome P450 2B3	56.3	263.2	12	17.7	-	-
124	GUC2E_RAT	Guanylyl cyclase GC-E	120.7	476.2	24	23.7	-	-
125	SG1C1_RAT	Secretoglobin family 1C member 1	10.4	120.8	12	29.8	-	-
126	REXON_RAT	Putative RNA exonuclease NEF-sp	86.0	264.5	14	19.1	-	-
127	ADT2_RAT	ADP/ATP translocase 2	32.9	316.4	12	40.6	yes	-
128	SUH3_RAT	Alcohol sulfotransferase	33.5	325.3	14	31.9	-	-
129	ABEC1_RAT	C->U-editing enzyme APOBEC-1	27.3	82.5	2	15.7	-	-
130	ALG13_RAT	UDP-N-acetylglucosamine transferase subunit ALG13 homolog	18.3	184	11	21.8	-	-
131	ARMX6_RAT	Protein ARMX6	33.4	1360.9	137	44.2	-	yes

132	CTP5A_RAT	Contactin-associated protein like 5-1	145.4	372.6	15	18.4	-	-
133	CTP5D_RAT	Contactin-associated protein like 5-4	145.8	379.3	16	15.6	-	-
134	H4_RAT	Histone H4	11.4	165.2	4	29.1	yes	-
135	HORM1_RAT	HORMA domain-containing protein 1	44.9	160.2	10	17.1	-	-
136	IGS10_RAT	Immunoglobulin superfamily member 10	284.6	568.1	27	11.9	-	-
137	JMJD8_RAT	JmjC domain-containing protein 8	32.9	164.8	7	24.1	-	-
138	KCNH4_RAT	Potassium voltage-gated channel subfamily H member 4	111.3	275.7	15	14.3	-	-
139	MYST3_RAT	Histone acetyltransferase MYST3	223.2	465.9	24	11.1	-	-
140	PRS54_RAT	Inactive serine protease 54	42.9	102.3	6	14.1	-	-
141	SO1A3_RAT	Solute carrier organic anion transporter family member 1A3	73.8	376.7	18	24.6	-	-
142	TBB2C_RAT	Tubulin beta-2C chain	49.8	866.1	1	43.8	yes	yes
143	TBCC1_RAT	TBCC domain-containing protein 1	64.7	211.1	8	14.9	-	-
144	TDRD9_RAT	Putative ATP-dependent RNA helicase TDRD9	156.1	976.5	54	25.6	-	-
145	TM175_RAT	Transmembrane protein 175	55.7	96.8	4	10.4	-	yes
146	TM232_RAT	Transmembrane protein 232	71.9	289.1	12	9.9	-	-
147	MAP1A_RAT	Microtubule-associated protein 1A	299.3	464.4	20	8.8	yes	yes
148	MBP_RAT	Myelin basic protein S	21.5	214.8	4	34.9	yes	yes
149	MDC1_RAT	Mediator of DNA damage checkpoint protein 1	136.9	302.3	16	12.1	-	-
150	MFN2_RAT	Mitofusin-2	86.1	376.5	19	30.5	yes	-
151	MGAT1_RAT	Alpha-1,3-mannosyl-glycoprotein 2-beta-N-acetylglucosaminyltransferase	51.6	111.8	6	9.4	-	-
152	MPI_RAT	Mannose-6-phosphate isomerase	46.4	438.7	25	20.1	-	yes
153	MTOR_RAT	Serine/threonine-protein kinase mTOR	288.6	1615	112	26.8	-	yes
154	MVP_RAT	Major vault protein	95.7	410.3	19	16.4	-	-
155	MYO9A_RAT	Myosin-IXa	301.2	1050.7	57	19.4	yes	-
156	MYO9B_RAT	Myosin-IXb	224.9	576.4	33	16.7	-	yes
157	MYOC_RAT	Myocilin	56.4	479.4	34	31.1	-	-
158	NALCN_RAT	Sodium leak channel non-selective protein	200.4	315	15	10.0	-	yes
159	NCAM1_RAT	Neural cell adhesion molecule 1	94.6	394.7	15	18.4	yes	-
160	NCKP1_RAT	Nck-associated protein 1	128.8	870.6	45	35.7	yes	yes
161	NF1_RAT	Neurofibromin	316.9	1152.8	68	26.7	-	-
162	NKX61_RAT	Homeobox protein Nkx-6.1	37.7	262	19	13.4	-	-
163	NALP6_RAT	NACHT, LRR and PYD domains-containing protein 6	98.1	457	21	28.1	-	-
164	NOXA1_RAT	NADPH oxidase activator 1	49.2	342	17	18.4	-	-
165	OPN4_RAT	Melanopsin	52.4	90.2	4	13.9	-	-
166	OXR1_RAT	Oxidation resistance protein 1	92.8	181.8	5	8.7	-	-
167	P4HA3_RAT	Prolyl 4-hydroxylase subunit alpha-3	61.1	243.1	16	10.8	-	-
168	PANX3_RAT	Pannexin-3	44.9	163.2	10	11.5	-	-
169	PAX6_RAT	Paired box protein Pax-6	46.7	136.2	5	15.2	-	-
170	PBAS_RAT	Probasin	20.8	359.1	42	19.8	-	-
171	PCLO_RAT	Protein piccolo	552.4	1085.7	59	13.1	yes	-
172	PDE11_RAT	Dual 3',5'-cyclic-AMP and -GMP phosphodiesterase 11A	104.5	365.4	18	23.4	yes	-
173	PDK4_RAT	[Pyruvate dehydrogenase [lipoamide]] kinase isozyme 4, mitochondrial	46.6	272.5	12	32.8	-	-
174	PDS5A_RAT	Sister chromatid cohesion protein PDS5 homolog A	150.2	610.5	38	18.6	-	yes
175	P3C2G_RAT	Phosphatidylinositol-4-phosphate 3-kinase C2 domain-containing subunit gamma	170.9	349	22	11.0	-	-
176	P13R4_RAT	Phosphoinositide 3-kinase regulatory subunit 4	152.4	424.3	15	16.3	-	yes
177	PLD1_RAT	Phospholipase D1	123.7	207.2	11	10.9	-	-
178	PLVAP_RAT	Plasmalemma vesicle-associated protein	50.0	179	5	18.7	-	-
179	PLXA3_RAT	Plexin-A3	207.8	571.7	34	19.7	-	yes
180	PO5F2_RAT	POU domain, class 5, transcription factor 2	37.0	197	9	31.6	-	-
181	PP1RA_RAT	Serine/threonine-protein phosphatase 1 regulatory subunit 10	92.8	338.4	17	17.2	-	-
182	PRRP_RAT	Prolactin-releasing peptide	9.2	127.3	5	51.8	-	-
183	PRAX_RAT	Periaxin	146.3	391.8	17	16.2	-	-
184	PSB4_RAT	Proteasome subunit beta type-4	29.2	96.2	4	24.3	-	-
185	PTGIS_RAT	Prostacyclin synthase	57.1	526.4	28	23.4	-	-
186	PRVA_RAT	Parvalbumin alpha	11.9	104.3	5	20.0	-	-
187	PYC_RAT	Pyruvate carboxylase, mitochondrial	129.7	670.5	42	15.8	yes	-
188	RAB1B_RAT	Ras-related protein Rab-1B	22.1	136	5	22.4	yes	-
189	RAD50_RAT	DNA repair protein RAD50	153.7	720.7	37	17.8	-	-
190	RASA2_RAT	Ras GTPase-activating protein 2	96.3	279.2	10	14.2	-	-
191	RDH7_RAT	Retinol dehydrogenase 7	35.7	421.1	28	44.5	-	-
192	RFIP1_RAT	Rab11 family-interacting protein 1	71.1	362.5	15	23.6	-	-
193	RGNEF_RAT	Rho-guanine nucleotide exchange factor	190.6	327.1	17	11.7	-	yes
194	ROCK2_RAT	Rho-associated protein kinase 2	160.3	409.1	16	17.9	yes	yes
195	RL7A_RAT	60S ribosomal protein L7a	30.0	115.5	5	16.2	yes	yes
196	RRAGB_RAT	Ras-related GTP-binding protein B	43.2	148.7	5	11.2	-	-
197	SBNO1_RAT	Protein strawberry notch homolog 1	140.7	403.6	20	14.1	-	-
198	SCN2A_RAT	Sodium channel protein type 2 subunit alpha	227.7	715.5	47	16.4	yes	-
199	SCN9A_RAT	Sodium channel protein type 9 subunit alpha	225.9	547.7	28	15.0	-	-
200	SEM4F_RAT	Semaphorin-4F	84.2	103.5	5	11.7	-	-

201	SEPT3_RAT	Neuronal-specific septin-3	40.6	88.5	6	22.6	yes	-
202	SH3B4_RAT	SH3 domain-binding protein 4	107.4	227.6	6	12.6	-	-
203	S12A1_RAT	Solute carrier family 12 member 1	120.5	364.7	19	12.9	-	-
204	S22A3_RAT	Solute carrier family 22 member 3	61.0	106.6	3	13.4	-	-
205	S23A2_RAT	Solute carrier family 23 member 2	70.0	269.6	13	9.9	yes	-
206	S2539_RAT	Solute carrier family 25 member 39	39.2	91.1	2	17.8	-	-
207	S4A8_RAT	Electroneutral sodium bicarbonate exchanger 1	119.5	479.7	34	13.4	-	yes
208	SLIT2_RAT	Slit homolog 2 protein (Fragment)	86.0	352.4	17	29.5	-	yes
209	SLIT3_RAT	Slit homolog 3 protein	167.7	399.2	19	16.9	-	-
210	SMG9_RAT	Protein SMG9	57.6	347.9	21	26.0	-	-
211	SNPH_RAT	Syntrophin	54.5	237.4	11	14.3	yes	yes
212	SNX27_RAT	Sorting nexin-27	61.0	152.6	5	10.6	yes	yes
213	SO1A5_RAT	Solute carrier organic anion transporter family member 1A5	74.5	529.1	41	22.8	-	-
214	SPICE_RAT	Spindle and centriole-associated protein 1	96.3	496.2	33	31.9	-	-
215	SPRE2_RAT	Sprouty-related, EVH1 domain-containing protein 2	46.8	413.9	31	15.9	-	-
216	SPRY7_RAT	SPRY domain-containing protein 7	21.7	190.7	6	31.1	-	-
217	SPTA2_RAT	Spectrin alpha chain, brain	284.5	735.7	41	14.6	-	-
218	SRA1_RAT	Steroid receptor RNA activator 1	25.2	90.6	3	13.0	-	-
219	STAU2_RAT	Double-stranded RNA-binding protein Staufen homolog 2	62.6	401.3	17	42.2	-	yes
220	SYNPR_RAT	Synaptoporin	29.1	83.4	6	18.9	-	-
221	TECR_RAT	Trans-2,3-enoyl-CoA reductase	36.1	209.1	12	29.5	yes	yes
222	TEKT4_RAT	Tektin-4	52.1	176.4	7	18.1	-	-
223	TEP1_RAT	Telomerase protein component 1	291.5	1570.7	123	24.5	-	-
224	TM111_RAT	Transmembrane protein 111	30.0	567.8	57	15.7	-	-
225	TPM1_RAT	Tropomyosin alpha-1 chain	32.7	112.3	4	19.7	yes	yes
226	TRFR_RAT	Thyrotropin-releasing hormone receptor	46.6	220.8	13	11.2	-	-
227	TIF1B_RAT	Transcription intermediary factor 1-beta	88.9	227.6	9	13.9	yes	-
228	TRPV1_RAT	Transient receptor potential cation channel subfamily V member 1	94.9	247.1	15	23.6	-	-
229	TTC19_RAT	Tetratricopeptide repeat protein 19, mitochondrial	41.3	288	13	34.5	-	-
230	TBA1A_RAT	Tubulin alpha-1A chain	50.1	800.4	13	44.1	yes	yes
231	TBA1C_RAT	Tubulin alpha-1C chain	49.9	679.8	1	36.5	yes	-
232	TBB5_RAT	Tubulin beta-5 chain	49.6	1112.2	26	56.3	-	-
233	TBB2A_RAT	Tubulin beta-2A chain	49.9	379.6	16	33.5	yes	yes
234	TBB2B_RAT	Tubulin beta-2B chain	49.9	1042.7	12	52.1	yes	-
235	XYLT1_RAT	Xylosyltransferase 1 (Fragment)	93.8	253.7	16	13.0	-	-
236	ZCCHV_RAT	Zinc finger CCCH-type antiviral protein 1	86.7	435.5	21	21.5	-	-
237	ZN830_RAT	Zinc finger protein 830	41.6	134.9	5	14.3	-	-
238	RT15_RAT	28S ribosomal protein S15, mitochondrial	29.7	94.6	3	16.0	-	-
239	SCO2A_RAT	Succinyl-CoA:3-ketoacid-coenzyme A transferase 2A, mitochondrial	56.9	584.7	27	34.4	-	-
240	NDC1_RAT	Nucleoporin NDC1	75.7	100.3	8	4.8	-	-
241	SUIS_RAT	Sucrase-isomaltase, intestinal	210.2	298.6	12	7.5	-	-
242	SIA8B_RAT	Alpha-2,8-sialyltransferase 8B	42.4	102.2	5	10.9	-	-
243	SPF30_RAT	Survival of motor neuron-related-splicing factor 30	26.8	131.3	6	32.8	-	-
244	PERT_RAT	Thyroid peroxidase	101.4	755.7	52	27.4	-	-
245	RX_RAT	Retinal homeobox protein Rx	36.3	310.2	22	14.6	-	-
246	PAI2_RAT	Plasminogen activator inhibitor 2 type A	47.2	245.1	16	7.7	-	-
247	PERI_RAT	Peripherin	53.5	106.7	4	10.5	yes	-
248	VIP1_RAT	Inositol hexakisphosphate and diphosphoinositol-pentakisphosphate kinase 1	159.5	529.7	26	18.3	-	yes
249	P5CR3_RAT	Pyroline-5-carboxylate reductase 3	28.9	151.2	8	31.8	-	-

Listed are all proteins with identified AHA, d10Leu or both modifications. The number and specific modification identified in each protein could not be determined since ProteinScape software was not available any longer at the end of my thesis.

Accession–Database accession number

Protein–Common name of the protein

MW–Molecular weight in Daltons

Scores–Protein score (Mascot score)

#Peptides–Number of peptides identified

SC%–Sequence coverage

Synprot–Synaptic protein database (Pielot et al., 2012)

Transcriptome–Neuropil transcriptome database (Cajigas et al., 2012)

Supplementary Table 9. Newly synthesized proteins identified in synaptosomes isolated from cortical primary cultures at DIV19

Nr.	Accession	Protein	MW [kDa]	Scores	#Peptides	SC [%]	Synprot	Transcriptome
1	ABCB8_RAT	ATP-binding cassette sub-family B member 8, mitochondrial	77.7	1431.7	112	24.1	yes	-
2	ABCD3_RAT	ATP-binding cassette sub-family D member 3	75.3	427.2	22	26.9	yes	-
3	ABTB2_RAT	Ankyrin repeat and BTB/POZ domain-containing protein 2	111.5	729.1	44	25.6	-	-
4	ACOX1_RAT	Peroxisomal acyl-coenzyme A oxidase 1	74.6	135.3	6	7.6	-	-
5	ACSM3_RAT	Acyl-coenzyme A synthetase ACSM3, mitochondrial	65.7	212.3	9	21.4	-	-
6	ACSM5_RAT	Acyl-coenzyme A synthetase ACSM5, mitochondrial	64.6	214.7	12	14.9	-	-
7	ACTB_RAT	Actin, cytoplasmic 1	41.7	327.6	8	23.5	yes	yes
8	ACL7A_RAT	Actin-like protein 7A	49.5	951	62	30.7	-	-
9	ACVR1_RAT	Activin receptor type-1	57.2	500.5	45	16.9	-	-
10	ADCY3_RAT	Adenylate cyclase type 3	128.9	1004	78	35.1	-	yes
11	ADDG_RAT	Gamma-adducin	78.8	291.8	9	19.6	-	-
12	AGRN_RAT	Agrin	208.5	525.7	33	19.4	yes	-
13	AL3A2_RAT	Fatty aldehyde dehydrogenase	54.0	171.4	13	15.1	-	-
14	ANKL2_RAT	Ankyrin repeat and LEM domain-containing protein 2	103.3	642.7	33	29.5	-	-
15	AP2A2_RAT	AP-2 complex subunit alpha-2	104.0	255.9	10	12.4	yes	yes
16	APOB_RAT	Apolipoprotein B-100	535.7	1569.4	91	13.9	yes	-
17	A4_RAT	Amyloid beta A4 protein	86.6	270	22	17.1	yes	yes
18	ARL2_RAT	ADP-ribosylation factor-like protein 2	20.8	155.4	10	14.7	-	-
19	ARLY_RAT	Argininosuccinate lyase	51.5	382.4	16	34.1	-	-
20	ATAD1_RAT	ATPase family AAA domain-containing protein 1	40.7	174.1	17	36.8	yes	-
21	AT12A_RAT	Potassium-transporting ATPase alpha chain 2	114.9	241.6	8	11.0	-	-
22	ATP7B_RAT	Copper-transporting ATPase 2	155.9	455.4	18	17.2	-	-
23	ATS1_RAT	A disintegrin and metalloproteinase with thrombospondin motifs 1	105.6	366.9	17	17.7	-	-
24	ATX3_RAT	Ataxin-3	40.4	148.6	8	24.2	-	-
25	B4GN1_RAT	Beta-1,4 N-acetylgalactosaminyltransferase 1	59.2	176.2	4	18.0	-	-
26	BIN1_RAT	Myc box-dependent-interacting protein 1	64.5	170.9	9	12.4	yes	-
27	BKRB2_RAT	B2 bradykinin receptor	44.9	541.9	43	30.8	-	-
28	BST1_RAT	ADP-ribosyl cyclase 2	35.1	371.6	17	41.1	-	-
29	CA2D3_RAT	Voltage-dependent calcium channel subunit alpha-2/delta-3	122.1	271.6	17	14.3	yes	yes
30	CALB1_RAT	Calbindin	30.0	131.5	6	23.4	-	yes
31	CAND1_RAT	Cullin-associated NEDD8-dissociated protein 1	136.3	625.8	29	26.2	yes	-
32	CD81_RAT	CD81 antigen	25.9	205	8	39.0	yes	-
33	CDYL_RAT	Chromodomain Y-like protein	65.0	325	17	22.6	-	-
34	CENPN_RAT	Centromere protein N	39.4	201.4	9	25.6	-	-
35	CHD8_RAT	Chromodomain-helicase-DNA-binding protein 8	290.5	1070.3	75	15.0	-	-
36	CLCN2_RAT	Chloride channel protein 2	99.3	455.9	21	21.7	-	yes
37	COPB_RAT	Coatomer subunit beta	106.9	536.6	28	26.7	-	yes
38	CTF8A_RAT	Chromosome transmission fidelity protein 8 homolog isoform 2	52.1	358	16	34.1	-	-
39	CTBL1_RAT	Beta-catenin-like protein 1	64.9	497.4	24	21.7	-	yes
40	CYLD_RAT	Ubiquitin carboxyl-terminal hydrolase CYLD	106.6	410.6	18	15.6	yes	-
41	DCXR_RAT	L-xylulose reductase	25.7	241.7	10	32.0	-	-
42	DLG1_RAT	Disks large homolog 1	100.5	206.3	10	7.4	yes	yes
43	DRD5_RAT	D(1B) dopamine receptor	52.8	169.2	10	16.4	-	-
44	DRP2_RAT	Dystrophin-related protein 2	108.0	212.8	14	14.2	yes	-
45	DUS1_RAT	Dual specificity protein phosphatase 1	39.5	252.4	10	27.2	-	-
46	DUT_RAT	Deoxyuridine 5'-triphosphate nucleotidohydrolase	22.0	174	9	25.4	-	-
47	DYH12_RAT	Dynein heavy chain 12, axonemal	357.0	886.2	48	18.6	-	-
48	DYH7_RAT	Dynein heavy chain 7, axonemal	464.3	1309.6	76	18.1	-	-
49	DYN2_RAT	Dynamin-2	98.2	278.5	13	11.8	yes	-
50	EF1A1_RAT	Elongation factor 1-alpha 1	50.1	142.2	8	21.4	-	yes
51	EF2_RAT	Elongation factor 2	95.2	309.9	11	15.3	yes	yes
52	EPHA3_RAT	Ephrin type-A receptor 3	110.2	612.6	36	20.7	yes	-
53	EPHA6_RAT	Ephrin type-A receptor 6	116.1	269.7	9	13.9	-	yes
54	F13A_RAT	Coagulation factor XIII A chain	82.6	285.5	13	19.1	-	-
55	FAAH1_RAT	Fatty-acid amide hydrolase 1	63.3	380.8	19	33.5	-	yes
56	FAS_RAT	Fatty acid synthase	272.5	959.2	53	20.2	yes	-
57	FBRL_RAT	rRNA 2'-O-methyltransferase fibrillar	34.2	146.5	4	19.6	yes	-
58	FCERA_RAT	High affinity immunoglobulin epsilon receptor subunit alpha	27.8	150.1	6	13.1	-	-
59	FDFT_RAT	Squalene synthase	48.1	217	8	17.1	-	-
60	ADRO_RAT	NADPH:adrenodoxin oxidoreductase, mitochondrial	54.3	133	5	15.6	-	-
61	FNDC1_RAT	Fibronectin type III domain-containing protein 1	193.9	360	14	8.6	-	-
62	FUMH_RAT	Fumarate hydratase, mitochondrial	54.4	349.3	19	24.7	-	-

63	FUT2_RAT	Galactoside 2-alpha-L-fucosyltransferase 2	40.0	400.6	23	35.3	-	-
64	GBRR2_RAT	Gamma-aminobutyric acid receptor subunit rho-2	57.0	393.2	18	26.3	-	-
65	GLRA2_RAT	Glycine receptor subunit alpha-2	52.0	140	5	14.8	-	yes
66	GNAQ_RAT	Guanine nucleotide-binding protein G(q) subunit alpha	42.1	397.3	20	16.7	yes	yes
67	GON4L_RAT	GON-4-like protein	247.7	455.2	23	12.7	-	-
68	GP173_RAT	Probable G-protein coupled receptor 173	41.5	388.2	23	45.6	-	-
69	GRM3_RAT	Metabotropic glutamate receptor 3	98.9	263	8	10.0	yes	-
70	GSTA1_RAT	Glutathione S-transferase alpha-1	25.6	120.9	7	23.9	-	-
71	GUC2E_RAT	Guanylyl cyclase GC-E	120.7	561.6	24	27.3	-	-
72	HMDH_RAT	3-hydroxy-3-methylglutaryl-coenzyme A reductase	96.6	740.8	56	31.1	-	yes
73	HNRPD_RAT	Heterogeneous nuclear ribonucleoprotein D0	38.2	113.3	5	11.0	-	-
74	CH60_RAT	60 kDa heat shock protein, mitochondrial	60.9	2739.9	227	36.0	-	-
75	HXK1_RAT	Hexokinase-1	102.3	443	20	21.2	-	-
76	I22R2_RAT	Interleukin-22 receptor subunit alpha-2	26.7	92	3	19.7	-	-
77	IPO13_RAT	Importin-13	108.1	923.5	82	20.5	-	-
78	ITB4_RAT	Integrin beta-4	200.5	697.6	43	14.7	-	-
79	KALRN_RAT	Kalirin	336.4	631.8	33	13.0	yes	yes
80	KCNQ2_RAT	Potassium voltage-gated channel subfamily KQT member 2	93.9	152.2	7	8.6	yes	-
81	KDIS_RAT	Kinase D-interacting substrate of 220 kDa	195.6	597	29	18.5	yes	-
82	KIF15_RAT	Kinesin-like protein KIF15	159.4	536	25	21.5	-	-
83	KIF1C_RAT	Kinesin-like protein KIF1C	122.3	603.6	35	18.9	-	-
84	KLHL7_RAT	Kelch-like protein 7	65.9	621.2	42	26.8	-	yes
85	IMA5_RAT	Importin subunit alpha-6	60.3	191.8	14	27.6	yes	-
86	K1C10_RAT	Keratin, type I cytoskeletal 10	56.5	208	8	19.4	-	-
87	KYNU_RAT	Kynureninase	52.4	177.3	6	19.8	-	-
88	LDLR_RAT	Low-density lipoprotein receptor	96.6	291.4	13	14.9	-	-
89	LEG1_RAT	Galectin-1	14.8	259	9	30.4	-	-
90	LHX2_RAT	LIM/homeobox protein Lhx2	47.4	320	16	18.3	-	-
91	LHX9_RAT	LIM/homeobox protein Lhx9	42.9	502.4	35	29.9	-	-
92	LRP2_RAT	Low-density lipoprotein receptor-related protein 2	518.9	853.6	46	12.3	-	-
93	LRRC7_RAT	Leucine-rich repeat-containing protein 7	167.4	544.1	29	15.0	yes	-
94	LUZP1_RAT	Leucine zipper protein 1	117.1	334.1	15	16.7	yes	-
95	MANF_RAT	Mesencephalic astrocyte-derived neurotrophic factor	20.4	214.8	7	39.1	-	-
96	MAP1A_RAT	Microtubule-associated protein 1A	299.3	443.1	19	9.9	yes	yes
97	MAP2_RAT	Microtubule-associated protein 2	202.3	539	29	12.7	yes	yes
98	GABT_RAT	4-aminobutyrate aminotransferase, mitochondrial	56.4	307.8	19	14.4	-	-
99	KCY_RAT	UMP-CMP kinase	22.2	109.8	5	33.2	yes	yes
100	IF2G_RAT	Eukaryotic translation initiation factor 2 subunit 3	51.0	180	7	14.2	-	yes
101	IF4H_RAT	Eukaryotic translation initiation factor 4H	27.3	115.7	5	18.1	yes	-
102	1433F_RAT	14-3-3 protein eta	28.2	250	5	42.7	-	-
103	MMSA_RAT	Methylmalonate-semialdehyde dehydrogenase [acylating], mitochondrial	57.8	344.8	20	37.6	-	-
104	CSPG2_RAT	Versican core protein (Fragments)	299.8	582.4	28	8.5	yes	-
105	CTR1_RAT	High affinity cationic amino acid transporter 1	67.2	442.7	18	41.3	-	-
106	EAA1_RAT	Excitatory amino acid transporter 1	59.7	471.3	34	21.9	yes	-
107	LYRIC_RAT	Protein LYRIC	63.9	162.7	5	14.5	-	-
108	DPOG1_RAT	DNA polymerase subunit gamma-1	136.8	516.3	39	11.7	-	-
109	RB62_RAT	ELKS/Rab6-interacting/CAST family member 1	108.8	416.6	19	23.1	yes	-
110	RRMJ3_RAT	Putative rRNA methyltransferase 3	94.7	266.7	11	12.8	-	-
111	GRP4_RAT	RAS guanyl-releasing protein 4	75.4	285.7	17	24.2	-	-
112	VGFR2_RAT	Vascular endothelial growth factor receptor 2	150.3	517	27	13.9	-	-
113	SIAT9_RAT	Lactosylceramide alpha-2,3-sialyltransferase	44.6	89.6	3	10.3	-	yes
114	ZEP2_RAT	Human immunodeficiency virus type I enhancer-binding protein 2 homolog	267.3	689.9	36	17.4	-	-
115	FAK1_RAT	Focal adhesion kinase 1	119.6	457.7	24	15.4	-	yes
116	TCPG_RAT	T-complex protein 1 subunit gamma	60.6	651	47	27.2	yes	yes
117	CP062_RAT	UPF0505 protein C16orf62 homolog	106.1	390.1	21	24.4	-	-
118	RNZ2_RAT	Zinc phosphodiesterase ELAC protein 2	92.3	359.1	17	20.0	-	-
119	MOSC2_RAT	MOSC domain-containing protein 2, mitochondrial	38.2	104	5	18.3	yes	-
120	KLK6_RAT	Prostatic glandular kallikrein-6	29.0	176.5	6	29.1	-	-
121	CI041_RAT	UPF0586 protein C9orf41 homolog	46.4	118.4	2	6.0	-	-
122	CF211_RAT	UPF0364 protein C6orf211 homolog	50.2	139.5	10	18.2	-	-
123	OSPT_RAT	Protein osteopotencia homolog	139.2	1522.6	113	17.6	-	-
124	NBL1_RAT	Neuroblastoma suppressor of tumorigenicity 1	19.2	145.5	11	16.9	-	yes
125	ABHGB_RAT	Abhydrolase domain-containing protein 16B	53.3	150.9	5	17.7	-	-
126	ARMX6_RAT	Protein ARMX6	33.4	2057.6	198	35.5	-	yes
127	CC105_RAT	Coiled-coil domain-containing protein 105	57.4	603.2	36	27.0	-	-
128	CF186_RAT	UPF0624 protein C6orf186 homolog	40.9	336.7	17	24.0	-	-
129	CH082_RAT	UPF0598 protein C8orf82 homolog	24.4	227.5	14	16.1	-	-
130	EMAL5_RAT	Echinoderm microtubule-associated protein-like 5	219.7	749.7	47	18.2	-	-
131	HIPK4_RAT	Homeodomain-interacting protein kinase 4	69.3	254.1	11	17.4	-	-

132	HUWE1_RAT	E3 ubiquitin-protein ligase HUWE1 (Fragment)	37.3	114.3	7	19.3	-	-
133	IGS10_RAT	Immunoglobulin superfamily member 10	284.6	999.6	56	14.3	-	-
134	JMJD8_RAT	JmjC domain-containing protein 8	32.9	249.5	9	16.5	-	-
135	K1C24_RAT	Keratin, type I cytoskeletal 24	52.3	439.1	19	22.4	-	-
136	KCNH4_RAT	Potassium voltage-gated channel subfamily H member 4	111.3	223.9	11	14.1	-	-
137	MDGA2_RAT	MAM domain-containing glycosylphosphatidylinositol anchor protein 2	106.7	170.7	6	11.0	-	-
138	OTOP1_RAT	Otopetrin-1	65.9	237.4	11	27.8	-	-
139	PRS27_RAT	Serine protease 27	35.8	145	10	22.0	-	-
140	SO1A3_RAT	Solute carrier organic anion transporter family member 1A3	73.8	475.4	27	34.2	-	-
141	TA2R3_RAT	Taste receptor type 2 member 3	36.2	218.7	12	31.0	-	-
142	TBB2C_RAT	Tubulin beta-2C chain	49.8	580.2	16	31.0	yes	yes
143	TMM22_RAT	Transmembrane protein 22	46.6	152.9	8	15.5	-	-
144	YPEL4_RAT	Protein yippee-like 4	14.3	119.4	4	25.2	-	yes
145	CL2DB_RAT	C-type lectin domain family 2 member D11	23.5	150.4	10	40.6	-	-
146	CLC9A_RAT	C-type lectin domain family 9 member A	27.4	111.1	5	23.7	-	-
147	KRBBB_RAT	Killer cell lectin-like receptor subfamily B member 1B allele B	24.9	163.1	7	21.5	-	-
148	MATR3_RAT	Matrin-3	94.4	301.8	17	18.8	yes	yes
149	MBP_RAT	Myelin basic protein	21.5	230.4	5	25.6	yes	yes
150	MEGF8_RAT	Multiple epidermal growth factor-like domains protein 8	297.4	773.4	42	15.6	-	-
151	MIMP_RAT	Migration and invasion-inhibitory protein	43.3	125.1	4	17.7	-	-
152	MPRIIP_RAT	Myosin phosphatase Rho-interacting protein	117.0	337.2	21	16.3	yes	-
153	MUC2_RAT	Mucin-2 (Fragment)	165.9	401.4	21	10.9	-	-
154	MUC4_RAT	Mucin-4	247.9	374.3	15	9.4	-	-
155	MYH4_RAT	Myosin-4	222.7	877.6	45	21.0	-	-
156	MYH7_RAT	Myosin-7	222.9	684	35	17.6	-	-
157	NAA11_RAT	N-alpha-acetyltransferase 11, NatA catalytic subunit	27.6	260.1	13	30.1	-	-
158	NAA35_RAT	N-alpha-acetyltransferase 35, NatC auxiliary subunit	83.2	619.7	45	29.0	-	yes
159	NAGAB_RAT	Alpha-N-acetylgalactosaminidase	46.8	534.3	27	30.1	-	-
160	NALCN_RAT	Sodium leak channel non-selective protein	200.4	595.6	34	14.3	-	yes
161	NCKP1_RAT	Nck-associated protein 1	128.8	453.8	25	31.5	yes	yes
162	NCOA2_RAT	Nuclear receptor coactivator 2	159.3	812	47	23.4	-	-
163	NLGN2_RAT	Neurologin-2	90.9	283	15	10.3	yes	yes
164	NOTC1_RAT	Neurogenic locus notch homolog protein 1	270.8	465.9	19	9.2	-	-
165	NOTC2_RAT	Neurogenic locus notch homolog protein 2	265.2	797	45	14.0	-	-
166	NR1D2_RAT	Nuclear receptor subfamily 1 group D member 2	64.2	484.8	22	38.4	-	-
167	NRX2A_RAT	Neurexin-2-alpha	185.1	853	42	23.2	-	-
168	NTRK2_RAT	BDNF/NT-3 growth factors receptor	92.1	169.1	5	13.2	yes	yes
169	NUCL_RAT	Nucleolin	77.1	205.7	7	10.1	yes	-
170	NUP85_RAT	Nuclear pore complex protein Nup85	74.8	620.6	37	37.2	-	-
171	NUP98_RAT	Nuclear pore complex protein Nup98-Nup96	197.2	442	25	9.1	yes	-
172	OLA1_RAT	Obg-like ATPase 1	44.5	142.6	7	18.7	yes	yes
173	OLFL1_RAT	Olfactomedin-like protein 1	45.6	273.4	13	22.4	-	-
174	P4HA3_RAT	Prolyl 4-hydroxylase subunit alpha-3	61.1	126.4	8	9.6	-	-
175	PARD3_RAT	Partitioning defective 3 homolog	149.4	384.2	16	9.3	yes	-
176	PDS5B_RAT	Sister chromatid cohesion protein PDS5 homolog B	164.4	692.1	42	22.0	yes	-
177	P20L1_RAT	PHD finger protein 20-like protein 1	114.0	302	16	17.8	-	-
178	PWIL4_RAT	Piwi-like protein 4	95.9	695.1	50	24.9	-	-
179	PJA2_RAT	E3 ubiquitin-protein ligase Praja-2	77.9	111.9	4	10.7	-	-
180	PLAP_RAT	Phospholipase A-2-activating protein	87.0	473.8	28	17.4	-	yes
181	PLCB2_RAT	1-phosphatidylinositol-4,5-bisphosphate phosphodiesterase beta-2	134.8	623.6	41	26.8	-	-
182	PLEC_RAT	Plectin	533.2	1588.2	103	17.3	yes	-
183	MYPR_RAT	Myelin proteolipid protein	30.1	145.2	5	15.2	-	-
184	PLXA3_RAT	Plexin-A3	207.8	654.3	33	16.4	-	yes
185	PP1RA_RAT	Serine/threonine-protein phosphatase 1 regulatory subunit 10	92.8	277.2	13	17.2	-	-
186	PERF_RAT	Perforin-1	61.5	167	6	11.2	-	-
187	PRAX_RAT	Periaxin	146.3	491	25	22.2	-	-
188	PSB1_RAT	Proteasome subunit beta type-1	26.5	196.5	9	29.2	-	-
189	PSRC1_RAT	Proline/serine-rich coiled-coil protein 1	34.6	129.6	3	23.1	-	-
190	PTHY_RAT	Parathyroid hormone	12.7	620.8	53	57.4	yes	-
191	PTPRS_RAT	Receptor-type tyrosine-protein phosphatase S	211.8	327.1	13	12.0	yes	-
192	PYC_RAT	Pyruvate carboxylase, mitochondrial	129.7	792.2	50	21.7	yes	-
193	RASF5_RAT	Ras association domain-containing protein 5	46.7	161.6	5	16.2	-	-
194	RBGPR_RAT	Rab3 GTPase-activating protein non-catalytic subunit	154.3	797.7	54	26.8	-	yes
195	RIC8A_RAT	Synembryn-A	59.8	407.1	22	39.9	-	-
196	RIMS1_RAT	Regulating synaptic membrane exocytosis protein 1	179.5	618.9	29	18.6	yes	yes
197	RIMS2_RAT	Regulating synaptic membrane exocytosis protein 2	175.8	923	59	20.8	yes	yes
198	ROBO4_RAT	Roundabout homolog 4	102.5	541.1	28	18.8	-	-
199	ROCK2_RAT	Rho-associated protein kinase 2	160.3	418.8	18	15.0	yes	yes
200	RPAP1_RAT	RNA polymerase II-associated protein 1	154.7	296.1	15	12.4	-	-

201	RPH3L_RAT	Rab effector Noc2	33.4	445.6	29	40.1	-	-
202	SCN5A_RAT	Sodium channel protein type 5 subunit alpha	227.2	547.1	35	17.0	-	-
203	SCNNA_RAT	Amiloride-sensitive sodium channel subunit alpha	78.8	201.6	7	10.6	-	-
204	PAI2_RAT	Plasminogen activator inhibitor 2 type A	47.2	312	16	16.8	-	-
205	SFTPD_RAT	Pulmonary surfactant-associated protein D	37.5	640.1	37	30.5	-	-
206	SFXN1_RAT	Sideroflexin-1	35.5	851.1	75	28.6	yes	-
207	SG196_RAT	Protein kinase-like protein SgK196	40.0	337.4	30	25.8	-	yes
208	SIGIR_RAT	Single Ig L-1-related receptor	46.1	144.7	7	15.2	-	-
209	S22AC_RAT	Solute carrier family 22 member 12	60.2	400	22	35.8	-	-
210	S40A1_RAT	Solute carrier family 40 member 1	62.5	119.2	5	16.8	-	-
211	SLIT3_RAT	Slit homolog 3 protein	167.7	461.5	24	15.4	-	-
212	SPRE2_RAT	Sprouty-related, EVH1 domain-containing protein 2	46.8	763.7	62	34.4	-	-
213	SPT20_RAT	Spermatogenesis-associated protein 20	88.1	411.9	21	26.7	-	-
214	SRBP1_RAT	Sterol regulatory element-binding protein 1	120.4	616.1	34	19.6	-	-
215	SRBP2_RAT	Sterol regulatory element-binding protein 2	122.9	308.3	13	18.1	-	-
216	SSPO_RAT	SCO-spondin	550.3	631.4	33	9.8	-	-
217	STAU2_RAT	Double-stranded RNA-binding protein Staufen homolog 2	62.6	411.8	22	38.9	-	yes
218	SUGP1_RAT	SURP and G-patch domain-containing protein 1	72.5	392.1	20	24.5	-	-
219	SYCN_RAT	Syncollin	14.6	322.6	11	34.3	-	-
220	SYNRG_RAT	Synergisin gamma	141.3	393.2	20	20.5	-	-
221	SYT13_RAT	Synaptotagmin-13	46.9	223.3	14	12.7	-	yes
222	TAOK3_RAT	Serine/threonine-protein kinase TAO3	105.4	169.1	5	7.0	-	-
223	TAXB1_RAT	Tax1-binding protein 1 homolog	93.1	291	12	15.7	-	-
224	TCPA_RAT	T-complex protein 1 subunit alpha	60.3	241	11	30.2	-	-
225	TINAL_RAT	Tubulointerstitial nephritis antigen-like	52.8	371.3	21	20.3	-	-
226	TMM43_RAT	Transmembrane protein 43	44.7	622.2	55	7.2	-	-
227	TMM79_RAT	Transmembrane protein 79	43.3	202.4	11	21.2	-	-
228	TOP1M_RAT	DNA topoisomerase I, mitochondrial	69.0	250.5	10	13.8	yes	-
229	TRAP1_RAT	Heat shock protein 75 kDa, mitochondrial	80.4	313.1	13	21.1	-	-
230	TR139_RAT	Tripartite motif-containing protein 39	56.4	171.9	6	17.4	-	-
231	TRPA1_RAT	Transient receptor potential cation channel subfamily A member 1	128.5	1492.3	134	37.5	-	-
232	TRPC1_RAT	Short transient receptor potential channel 1	87.6	397.8	23	32.3	yes	-
233	TRPC2_RAT	Short transient receptor potential channel 2	130.4	514.9	35	21.1	-	-
234	TRPC4_RAT	Short transient receptor potential channel 4	111.8	190.9	6	8.5	-	yes
235	TRPM1_RAT	Transient receptor potential cation channel subfamily M member 1	184.2	747	64	22.7	-	-
236	TRPM4_RAT	Transient receptor potential cation channel subfamily M member 4	135.3	466.9	21	19.8	-	-
237	TSH3_RAT	Teashirt homolog 3	117.4	588.9	39	27.1	-	-
238	TTHY_RAT	Transthyretin	15.7	94.8	5	34.7	-	-
239	TTYH1_RAT	Protein tweety homolog 1	49.0	118.5	5	13.3	yes	-
240	TBA1A_RAT	Tubulin alpha-1A chain	50.1	696.2	12	34.8	yes	yes
241	TBB5_RAT	Tubulin beta-5 chain	49.6	553.2	2	30.2	-	-
242	TBB2A_RAT	Tubulin beta-2A chain	49.9	560.1	3	31.7	yes	yes
243	STPAP_RAT	Speckle targeted PIP5K1A-regulated poly(A) polymerase	94.3	255	14	19.9	-	-
244	TYPH_RAT	Thymidine phosphorylase	49.9	683.3	37	38.2	-	-
245	TYRO3_RAT	Tyrosine-protein kinase receptor TYRO3	95.9	528.7	27	18.8	-	yes
246	VINC_RAT	Vinculin	116.5	1004.9	66	28.9	-	-
247	VLDLR_RAT	Very low-density lipoprotein receptor	96.5	271.6	14	20.8	-	-
248	ZDH12_RAT	Probable palmitoyltransferase ZDHHC12	31.0	142.8	9	13.5	-	-
249	ZN667_RAT	Zinc finger protein 667	70.0	412.3	19	20.6	-	-
250	MIPPEP_RAT	Mitochondrial intermediate peptidase	80.6	992.5	99	17.9	-	-
251	SERA_RAT	D-3-phosphoglycerate dehydrogenase	56.5	1034.1	102	25.3	-	-
252	MKS3_RAT	Meckelin	111.7	551.5	31	30.6	-	yes
253	SCO2A_RAT	Succinyl-CoA:3-ketoacid-coenzyme A transferase 2A, mitochondrial	56.9	488.7	25	39.4	-	-
254	RM02_RAT	39S ribosomal protein L2, mitochondrial	33.0	161.4	9	15.1	-	-
255	PR57_RAT	26S protease regulatory subunit 7	48.5	233.9	12	29.1	-	-
256	MPCP_RAT	Phosphate carrier protein, mitochondrial	39.4	128.9	6	23.9	yes	-
257	VGLU3_RAT	Vesicular glutamate transporter 3	64.7	384.6	15	31.1	-	-

Listed are all proteins with identified AHA, d10Leu or both modifications. The number and specific modification identified in each protein could not be determined since ProteinScape software was not available any longer at the end of my thesis.

Accession–Database accession number

Protein–Common name of the protein

MW–Molecular weight in Daltons

Scores–Protein score (Mascot score)

#Peptides–Number of peptides identified

SC%–Sequence coverage

Synprot–Synaptic protein database (Pielot et al., 2012)

Transcriptome–Neuropil transcriptome database (Cajigas et al., 2012)

Supplementary Table 10. GO analysis (GoMiner) of the identified newly synthesized proteins

Biological Process							
	%						
GO Term	DIV7	DIV9	DIV11	DIV15	DIV17	DIV17Local	DIV19
cellular process	13.08	13.90	14.06	13.10	13.21	12.38	14.00
biological regulation	7.76	7.75	8.26	8.55	8.52	7.45	7.99
regulation of biological process	6.92	6.95	7.37	7.59	7.53	6.44	7.26
developmental process	5.91	5.26	5.92	5.16	5.11	5.52	5.28
localization	5.91	6.65	5.92	5.73	5.82	6.28	6.01
establishment of localization	4.73	5.96	5.19	4.82	5.04	5.69	5.13
signaling	4.30	5.36	4.69	4.77	6.11	6.11	4.99
signaling process	3.46	3.97	3.40	3.47	4.55	4.69	3.67
negative regulation of biological process	3.38	3.18	3.29	3.34	3.84	3.01	3.01
positive regulation of biological process	3.29	2.98	3.01	3.21	2.91	3.01	3.37
locomotion	1.43	1.09	1.23	1.26	1.35	1.00	1.25
biological adhesion	1.10	0.60	1.17	1.30	0.57	1.17	1.17
growth	0.76	0.89	0.67	1.13	1.07	0.75	0.81
others	37.97	35.45	35.83	36.57	34.38	36.49	36.07
sum	100	100	100	100	100	100	100

Cellular Component							
	%						
GO Term	DIV7	DIV9	DIV11	DIV15	DIV17	DIV17Local	DIV19
cell	25.00	24.73	25.22	24.57	24.97	25.76	24.58
cell part	25.00	24.73	25.22	24.57	24.97	25.76	24.58
organelle	17.41	18.36	17.54	17.27	16.41	16.25	17.67
organelle part	11.16	12.44	11.08	11.27	11.61	11.02	11.55
macromolecular complex	7.89	6.83	6.81	7.80	8.32	6.20	7.81
membrane-enclosed lumen	3.87	3.49	4.45	4.41	4.57	4.41	3.96
extracellular region	3.72	3.03	3.40	3.32	2.81	3.03	3.85
extracellular region part	2.83	2.43	2.71	2.60	1.99	2.75	2.49
synapse	2.08	2.12	2.18	2.53	2.46	2.75	2.04
synapse part	1.04	1.82	1.40	1.66	1.88	2.07	1.47
sum	100	100	100	100	100	100	100

Molecular Function							
	%						
GO Term	DIV7	DIV9	DIV11	DIV15	DIV17	DIV17Local	DIV19
binding	43.03	46.90	45.26	44.88	43.86	42.26	44.53
catalytic activity	26.01	25.52	26.69	23.60	25.33	26.19	22.66
enzyme regulator activity	6.81	3.10	2.51	3.57	3.13	4.76	3.91
molecular transducer activity	6.81	7.93	7.93	8.54	7.05	9.82	9.64
transporter activity	6.19	8.97	7.54	6.83	9.66	7.44	8.85
structural molecule activity	4.33	2.07	3.68	2.80	3.13	2.68	3.91
transcription regulator activity	2.79	1.72	2.13	4.04	2.35	1.49	2.86
nucleic acid binding transcription factor activity	1.55	1.03	1.55	2.64	1.57	1.49	1.82
protein binding transcription factor activity	1.24	0.69	0.58	1.09	0.78	0.30	0.26
receptor regulator activity	0.62	0.34	0.39	0.16	0.26	0.00	0.78
others	0.62	1.72	1.74	0.00	2.87	3.57	0.78
sum	100	100	100	100	100	100	100

Supplementary Table 11. Enrichment analyses of over-represented annotations (GO terms) from the biological processes domain

Biological Processes (DAVID)	DIV 7		DIV 9		DIV 11		DIV 15		DIV 17		DIV 19	
GO Term	PValue	Count										
Aging	--	--	--	--	--	--	1.9E-02	(10)	--	--	--	--
Axonogenesis	3.3E-02	(7)	--	--	2.0E-02	(10)	4.0E-03	(13)	7.4E-02	(7)	1.1E-02	(9)
Calcium ion transport	--	--	--	--	--	--	3.0E-04	(12)	2.7E-03	(8)	4.3E-02	(6)
Cell adhesion	--	--	--	--	--	--	6.1E-03	(23)	--	--	--	--
Endocytosis	4.8E-02	(6)	1.1E-02	(7)	--	--	--	--	--	--	1.3E-02	(8)
Exocytosis	--	--	--	--	3.8E-03	(9)	3.5E-02	(8)	--	--	--	--
Forebrain development	6.5E-02	(6)	--	--	3.0E-02	(9)	1.4E-02	(11)	5.0E-02	(7)	--	--
Intracellular protein transport	--	--	--	--	2.3E-02	(13)	--	--	--	--	4.3E-02	(10)
Learning	6.5E-02	(4)	--	--	7.2E-02	(5)	4.2E-02	(6)	5.6E-03	(6)	--	--
Microtubule-based movement	6.5E-03	(6)	2.5E-02	(5)	--	--	3.6E-02	(7)	1.0E-04	(9)	7.2E-04	(8)
Microtubule-based process	4.0E-02	(7)	8.5E-02	(6)	--	--	1.5E-02	(12)	3.8E-03	(10)	1.3E-03	(11)
Neuron projection development	2.7E-03	(11)	--	--	9.4E-04	(16)	1.3E-05	(22)	3.0E-02	(10)	5.0E-03	(12)
Neuron projection morphogenesis	5.8E-02	(7)	--	--	1.9E-02	(11)	6.0E-05	(18)	5.4E-02	(8)	8.4E-03	(10)
Neurotransmitter transport	4.0E-02	(5)	--	--	1.5E-03	(9)	1.7E-02	(8)	7.4E-02	(5)	2.3E-02	(6)
Receptor clustering	--	--	--	--	--	--	4.5E-02	(3)	--	--	--	--
Regulation of membrane potential	--	--	--	--	--	--	2.1E-02	(10)	1.6E-04	(11)	--	--
Regulation of neuronal synaptic plasticity	--	--	--	--	4.1E-03	(6)	--	--	4.2E-02	(4)	--	--
Regulation of synaptic plasticity	--	--	--	--	8.3E-03	(7)	6.4E-02	(6)	9.1E-03	(6)	--	--
Response to calcium ion	--	--	7.2E-03	(5)	--	--	--	--	--	--	--	--
Response to cAMP	4.9E-02	(4)	--	--	--	--	2.7E-02	(6)	--	--	8.5E-02	(4)
Sodium ion transport	5.1E-02	(5)	--	--	--	--	--	--	3.3E-04	(9)	--	--
Spinal cord development	--	--	--	--	--	--	--	--	3.2E-02	(4)	--	--
Synapse organization	--	--	--	--	9.9E-02	(4)	4.6E-02	(5)	--	--	1.4E-03	(6)
Synaptic transmission	--	--	--	--	8.5E-03	(12)	2.5E-04	(17)	7.1E-04	(12)	--	--
Vesicle-mediated transport	--	--	2.4E-04	(16)	3.3E-03	(20)	6.5E-03	(22)	--	--	7.7E-04	(18)

Biological Processes (GeneCodis)	DIV 7		DIV 9		DIV 11		DIV 15		DIV 17		DIV 19	
Term	PValue	Count										
aging	--	--	5.0E-02	(4)	--	--	2.3E-03	(9)	--	--	4.8E-03	(7)
axonogenesis	3.6E-03	(5)	--	--	--	--	1.9E-02	(5)	4.9E-03	(5)	7.2E-03	(5)
calcium ion transport	--	--	--	--	--	--	5.3E-03	(6)	1.5E-04	(7)	3.2E-02	(4)
cell adhesion	1.6E-02	(7)	--	--	2.2E-02	(10)	1.2E-06	(18)	--	--	1.9E-03	(10)
endocytosis	--	--	1.9E-03	(5)	--	--	--	--	--	--	9.2E-04	(6)
exocytosis	2.3E-02	(3)	--	--	--	--	1.7E-02	(4)	--	--	4.3E-02	(3)
forebrain development	--	--	--	--	--	--	3.7E-03	(6)	--	--	--	--
intracellular protein transport	--	--	--	--	--	--	1.7E-02	(7)	--	--	4.4E-02	(5)
learning	--	--	--	--	--	--	4.1E-02	(3)	--	--	--	--
microtubule-based movement	6.1E-03	(4)	5.9E-04	(5)	--	--	2.2E-02	(4)	1.3E-04	(6)	2.0E-03	(5)
microtubule-based process	--	--	--	--	--	--	--	--	3.8E-02	(2)	9.1E-03	(3)
neuron projection development	1.5E-02	(4)	--	--	--	--	--	--	--	--	--	--
neuron projection morphogenesis	--	--	--	--	--	--	8.7E-05	(6)	1.5E-02	(3)	--	--
neurotransmitter transport	1.7E-02	(3)	--	--	--	--	--	--	--	--	--	--
receptor clustering	--	--	--	--	--	--	1.1E-02	(3)	4.7E-02	(2)	--	--
regulation of membrane potential	--	--	--	--	--	--	1.6E-02	(4)	3.0E-02	(3)	--	--
regulation of neuronal synaptic plasticity	--	--	--	--	--	--	1.7E-02	(3)	--	--	--	--
regulation of synaptic plasticity	--	--	--	--	--	--	7.5E-03	(4)	1.7E-02	(3)	--	--
response to calcium ion	4.8E-02	(3)	--	--	--	--	--	--	4.8E-02	(3)	--	--
response to cAMP	--	--	--	--	--	--	2.6E-03	(6)	--	--	4.6E-02	(3)
sodium ion transport	2.2E-02	(4)	--	--	--	--	--	--	3.6E-02	(4)	--	--
spinal cord development	4.7E-02	(2)	--	--	--	--	1.7E-02	(3)	7.4E-03	(3)	4.2E-02	(2)
synapse organization	--	--	--	--	--	--	5.0E-02	(2)	--	--	4.8E-02	(2)
synaptic transmission	--	--	--	--	--	--	8.0E-03	(6)	2.7E-04	(7)	--	--
vesicle-mediated transport	--	--	--	--	--	--	4.3E-03	(8)	--	--	--	--

Supplementary Table 12. Enrichment analyses of over-represented annotations (GO terms) from the cellular components domain

Cellular Components (DAVID)	DIV 7		DIV 9		DIV 11		DIV 15		DIV 17		DIV 19	
Term	PValue	Count										
axon	1.6E-03	(10)	--	--	--	--	5.1E-04	(16)	3.0E-06	(16)	--	--
cell junction	3.9E-02	(12)	6.5E-03	(14)	9.2E-04	(23)	5.3E-05	(29)	--	--	9.9E-03	(17)
cell projection	9.2E-04	(22)	--	--	1.4E-03	(32)	1.2E-08	(50)	9.1E-08	(36)	3.0E-03	(26)
cell surface	4.4E-02	(10)	4.1E-02	(10)	--	--	--	--	--	--	--	--
cytoskeleton	1.7E-04	(28)	7.9E-04	(26)	3.6E-03	(37)	2.2E-06	(53)	3.3E-03	(30)	6.8E-06	(39)
dendrite	4.2E-02	(8)	--	--	--	--	1.3E-04	(19)	1.0E-02	(11)	--	--
dendritic spine	--	--	--	--	--	--	3.7E-02	(6)	--	--	--	--
endoplasmic reticulum	4.4E-03	(21)	--	--	3.5E-03	(32)	2.1E-02	(33)	4.2E-02	(22)	--	--
extracellular space	3.8E-02	(13)	--	--	3.9E-03	(23)	7.2E-03	(25)	--	--	--	--
Golgi apparatus	--	--	2.5E-04	(22)	2.9E-03	(29)	--	--	--	--	3.0E-02	(21)
growth cone	--	--	--	--	--	--	2.9E-03	(8)	--	--	--	--
membrane raft	--	--	2.2E-02	(7)	4.0E-02	(9)	3.9E-02	(10)	--	--	--	--
microtubule	8.5E-05	(11)	6.9E-03	(8)	--	--	4.2E-06	(18)	2.0E-04	(12)	7.1E-05	(13)
mitochondrion	--	--	2.9E-02	(26)	--	--	--	--	--	--	--	--
neuron projection	9.5E-04	(16)	--	--	9.3E-03	(20)	8.2E-07	(33)	1.2E-06	(25)	--	--
postsynaptic density	--	--	--	--	--	--	5.7E-04	(10)	--	--	--	--
postsynaptic membrane	--	--	1.1E-02	(7)	--	--	--	--	1.3E-02	(8)	4.8E-02	(7)
presynaptic active zone	--	--	--	--	1.5E-02	(3)	--	--	--	--	--	--
synapse	3.6E-02	(11)	3.3E-02	(11)	4.8E-03	(19)	3.7E-06	(29)	1.5E-03	(17)	6.2E-03	(16)
synaptosome	--	--	--	--	--	--	--	--	3.2E-03	(8)	--	--
vesicle membrane	--	--	--	--	--	--	1.7E-02	(10)	4.0E-02	(7)	1.7E-02	(8)
voltage-gated calcium channel complex	--	--	--	--	--	--	--	--	3.3E-03	(4)	--	--

Cellular Components (GeneCodis)	DIV 7		DIV 9		DIV 11		DIV 15		DIV 17		DIV 19	
Term	PValue	Count										
axon	1.4E-05	(9)	--	--	9.4E-03	(7)	1.3E-09	(17)	9.8E-10	(14)	8.5E-03	(6)
cell junction	1.0E-04	(10)	5.1E-05	(10)	4.5E-08	(18)	7.8E-11	(23)	5.9E-07	(14)	6.1E-06	(13)
cell projection	2.8E-03	(5)	1.7E-03	(5)	4.7E-03	(6)	2.1E-03	(7)	--	--	2.6E-02	(4)
cell surface	1.0E-04	(10)	5.1E-05	(10)	6.1E-06	(15)	1.3E-02	(10)	5.9E-03	(8)	6.1E-06	(13)
cytoskeleton	2.8E-08	(16)	4.1E-09	(16)	3.0E-08	(20)	2.1E-11	(26)	6.9E-10	(19)	2.4E-12	(22)
dendrite	3.4E-04	(8)	--	--	5.6E-06	(13)	7.5E-07	(15)	2.0E-04	(9)	5.7E-03	(7)
dendritic spine	5.8E-04	(5)	2.2E-02	(3)	--	--	3.4E-02	(4)	8.7E-03	(4)	1.7E-03	(5)
endoplasmic reticulum	3.2E-06	(17)	1.6E-05	(15)	1.7E-11	(31)	5.9E-05	(22)	7.3E-08	(21)	1.6E-04	(16)
extracellular space	4.9E-05	(14)	3.4E-03	(10)	1.5E-08	(25)	4.7E-08	(26)	3.1E-04	(14)	5.1E-04	(14)
Golgi apparatus	4.9E-04	(13)	7.4E-12	(23)	2.7E-10	(29)	3.5E-07	(26)	7.7E-05	(16)	1.9E-10	(25)
growth cone	3.2E-02	(3)	2.1E-02	(3)	4.6E-03	(5)	2.5E-06	(9)	4.4E-02	(3)	--	--
membrane raft	6.3E-03	(5)	2.0E-02	(4)	1.2E-02	(6)	3.4E-04	(9)	--	--	1.3E-02	(5)
microtubule	2.9E-05	(8)	1.5E-06	(9)	4.4E-02	(5)	1.5E-05	(11)	8.3E-05	(8)	2.4E-07	(11)
mitochondrion	1.2E-03	(18)	1.7E-05	(21)	2.8E-04	(28)	1.7E-08	(41)	7.1E-09	(31)	3.8E-06	(27)
neuron projection	5.7E-04	(6)	--	--	1.7E-03	(7)	3.4E-03	(7)	2.0E-04	(7)	2.7E-04	(7)
postsynaptic density	--	--	1.7E-03	(5)	9.5E-04	(7)	1.5E-09	(14)	--	--	1.5E-04	(7)
postsynaptic membrane	--	--	6.2E-04	(6)	1.3E-04	(9)	5.4E-05	(10)	8.0E-07	(10)	3.3E-03	(6)
presynaptic active zone	--	--	4.7E-03	(2)	8.3E-04	(3)	--	--	--	--	9.4E-03	(2)
synapse	2.5E-05	(10)	6.1E-05	(9)	5.7E-07	(15)	3.0E-09	(19)	6.6E-09	(15)	5.3E-06	(12)
synaptosome	--	--	2.3E-03	(5)	--	--	3.3E-03	(7)	2.9E-05	(8)	8.5E-03	(5)
vesicle membrane	--	--	--	--	--	--	7.9E-03	(3)	2.1E-03	(3)	--	--
voltage-gated calcium channel complex	--	--	--	--	2.9E-02	(2)	3.4E-02	(2)	9.1E-04	(3)	--	--

Supplementary Table 13. Enrichment analyses of over-represented annotations (GO terms) from the molecular functions domain

Molecular Functions (DAVID)		DIV 7		DIV 9		DIV 11		DIV 15		DIV 17		DIV 19	
Term	PValue	Count	PValue	Count	PValue	Count	PValue	Count	PValue	Count	PValue	Count	
Actin binding	--	--	--	--	6.4E-04	(15)	--	--	--	--	3.7E-02	(9)	
ATP binding	5.8E-05	(33)	3.2E-04	(30)	7.3E-05	(49)	1.6E-04	(53)	2.5E-07	(44)	9.9E-05	(39)	
ATPase activity	6.8E-03	(10)	9.1E-05	(13)	2.5E-03	(15)	5.0E-05	(20)	3.0E-03	(12)	3.2E-02	(10)	
Calcium channel activity	--	--	--	--	3.7E-03	(7)	2.8E-02	(6)	3.9E-03	(6)	5.0E-03	(6)	
Calmodulin binding	1.9E-03	(7)	--	--	8.0E-03	(8)	1.2E-03	(10)	5.3E-03	(7)	7.0E-03	(7)	
Cation channel activity	--	--	--	--	9.0E-03	(13)	--	--	6.8E-06	(16)	7.7E-03	(11)	
GTP binding	--	--	3.4E-02	(9)	--	--	--	--	1.1E-03	(14)	1.3E-02	(12)	
GTPase activity	--	--	3.0E-02	(5)	--	--	--	--	1.8E-02	(6)	5.3E-03	(7)	
Protein tyrosine kinase activity	--	--	--	--	4.7E-03	(9)	--	--	--	--	1.3E-02	(7)	
SH3 domain binding	--	--	--	--	5.3E-03	(7)	1.0E-02	(7)	--	--	--	--	
Transmembrane receptor protein tyrosine kinase activity	--	--	--	--	5.1E-03	(6)	--	--	--	--	9.4E-03	(5)	

Molecular Functions (GeneCodis)		DIV 7		DIV 9		DIV 11		DIV 15		DIV 17		DIV 19	
Term	PValue	Count	PValue	Count	PValue	Count	PValue	Count	PValue	Count	PValue	Count	
Actin binding	4.3E-02	(4)	--	--	6.0E-05	(11)	7.2E-04	(10)	1.3E-02	(6)	9.4E-04	(8)	
ATP binding	7.6E-11	(29)	4.0E-06	(21)	9.1E-11	(39)	8.8E-10	(41)	1.3E-14	(37)	1.3E-11	(34)	
ATPase activity	3.7E-02	(4)	6.7E-06	(8)	1.6E-02	(6)	1.9E-02	(6)	--	--	3.8E-02	(4)	
Calcium channel activity	--	--	3.8E-02	(2)	--	--	4.0E-02	(3)	--	--	2.5E-03	(4)	
Calmodulin binding	4.6E-03	(5)	4.2E-02	(3)	5.1E-03	(6)	4.5E-07	(11)	9.1E-05	(7)	7.5E-03	(5)	
Cation channel activity	--	--	--	--	--	--	2.2E-02	(3)	--	--	--	--	
GTP binding	--	--	3.9E-04	(9)	--	--	3.6E-02	(9)	7.9E-06	(13)	1.2E-03	(10)	
GTPase activity	3.3E-02	(4)	2.2E-04	(7)	--	--	--	--	1.7E-04	(8)	2.8E-04	(8)	
Protein tyrosine kinase activity	--	--	--	--	1.5E-02	(5)	--	--	--	--	--	--	
SH3 domain binding	--	--	--	--	5.1E-03	(6)	1.6E-03	(7)	--	--	--	--	
Transmembrane receptor protein tyrosine kinase activity	--	--	--	--	--	--	--	--	--	--	4.4E-02	(2)	

8. ABBREVIATIONS

aa	Amino acid(s)
AHA	Azidohomoalanine
Amp	Ampicillin
AMPA	Alpha-amino-3-hydroxy-5-methyl-isoxasole-4-propionic acid
ANL	Azidonorleucine
AZ	Active zone
BDNF	Brain derived neurotrophic factor
bp	Base pairs
BONCAT	Bio-orthogonal non-canonical amino acid tagging
BSA	Bovine serum albumin
C	Celsius
Ca ²⁺	Calcium ion
CAMKII	Ca ²⁺ - Calmodulin dependent kinase II
CAZ	Cytomatrix of the active zone
cDNA	Complementary DNA
CNS	Central nervous system
CREB	Cyclic-AMP response element binding protein
CTRL	Control
C-terminus	Carboxy terminus
c-myc	Epitope EQKLISEEDL
DIV	Day in vitro
DMEM	Dulbecco's Modified Eagle Medium
DNA	Deoxyribonucleic acid
dNTPs	Deoxy-nucleotide-triphosphates
DST	Disulfide-Tag
Erc2	ELKS/RAB6-Interacting/CAST Family Member 2
ERK1/2	Extracellular signal-regulated protein kinases 1/2
<i>E.coli</i>	<i>Escherichia coli</i>
EDTA	Ethylenediamine-N,N,N',N' -tetraacetic acid
EGFP	Enhanced Green fluorescent protein

E-LTP	Early long-time potentiation
et al.	Et alia
FCS	Fetal calf serum
FUNCAT	Fluorescence non-canonical amino acid tagging
GFAP	Glial fibrillary acidic protein
GINCAT	Genetically introduced non-canonical amino acid tagging
GluR1	Glutamate receptor 1
GluR2	Glutamate receptor 2
h	Hour(s)
HBS	HEPES-buffered solution
HDACs	Histone deacetylases
Hib	Hibernate
IB	Immunoblots
IF	Immunofluorescence
kDa	Kilo Dalton
LTD	Long-term depression
LTP	Long-term potentiation
M	Molar
MAP2	Microtubule-associated protein 2
MAPK	Mitogen-Activated Protein Kinase
Met	Methionine
MetRS	Methionyl-tRNA-Synthetase
mEPSC	Miniature excitatory postsynaptic current
min	Minutes
mRNA	Messenger RNA
n	Number of scored cells/samples
NCAM	Neural cell adhesion molecule 1
NMDA	N-methyl-D-aspartate
NMDARs	N-methyl D-aspartate receptors
NR1	N-methyl-D-aspartate receptor subunit NR1
NR2B	N-methyl D-aspartate receptor subtype 2B
N-terminus	Amino terminus

ORF	Open reading frame
PBS	Phosphate-buffered saline
PC12	Cell line derived from pheochromocytoma of the rat adrenal medulla
Pclo	Piccolo
PCR	Polymerase chain reaction
PFA	Paraformaldehyde
PI	Protease Inhibitor
ProSAP	Proline-rich synapse associated protein
PSD	Postsynaptic density
RGC	Retinal ganglion cell
RNA	Ribonucleic acid
RT	Room temperature
SDS-PAGE	Sodium dodecyl sulfate polyacrylamide gel electrophoresis
SEM	Standard error of the mean
TBS	Tris buffered saline
tRNA	Transfer ribonucleic acid
VGLUT	Vesicular glutamate transporter
WB	Western Blot
WT	Wild-type

9. CURRICULUM VITAE

Name: Elmer Rodrigo
Family Name: Antileo Ibarra
Date of Birth: 28.01.1981
Nationality: Chilean
Parents: Oscar Antileo
Berta Ibarra

EDUCATION

2009–2016 Doctoral Thesis. Otto-von-Guericke-University-Leibniz
Institute for Neurobiology (LIN) and Institute for
Pharmacology and Toxicology (IPT), Magdeburg,
Germany.

2007–2008 Master of Science. University of Chile, Santiago, Chile

2005–2006 Undergraduate Thesis Institute for Nutrition and Foods
Technology (INTA)-University of Chile, Santiago, Chile

2000–2005 Molecular Biotechnology Engineering.
University of Chile. Santiago, Chile.

1994–1998 High School. Liceo de Hombre A-59,
Los Ángeles. Región VIII, Chile.

September 22, 2016. Magdeburg, Germany

10. SCIENTIFIC PUBLICATIONS

Peter Landgraf, **Elmer R. Antileo**, Erin M. Schuman, and Daniela C. Dieterich. Chapter 14. BONCAT: Metabolic Labeling, Click Chemistry, and Affinity Purification of Newly Synthesized Proteomes. Site-Specific Protein Labeling Book. Methods Mol Biol. 2015; 1266:199-215.

Endocytic pathway of exogenous iron-loaded ferritin in intestinal epithelial (Caco-2) cells. **Antileo E**, Garri C, Tapia V, Muñoz JP, Chiong M, Nualart F, Lavandero S, Fernández J, Núñez MT. Am J Physiol Gastrointest Liver Physiol. 2013 Apr 1; 304(7): G655-61.

A cyclic peptide derived from alpha-fetoprotein inhibits the proliferative effects of the epidermal growth factor and estradiol in MCF7 cells. Torres C, **Antileo E**, Epuñán MJ, Pino AM, Valladares LE, Sierralta WD. Oncol Rep. 2008 Jun; 19(6):1597-603.

Erklärung

Hiermit erkläre ich, dass ich die von mir eingereichte Dissertation zum dem Thema

“Developmental-dependent changes in the synaptic proteome”

selbständig verfasst, nicht schon als Dissertation verwendet habe und die benutzten Hilfsmittel und Quellen vollständig angegeben wurden.

Weiterhin erkläre ich, dass ich weder diese noch eine andere Arbeit zur Erlangung des akademischen Grades doctor rerum naturalium (Dr. rer. nat.) an anderen Einrichtungen eingereicht habe.

Magdeburg 22.09.16

(Ort, Datum)

(Elmer Antileo)